RESEARCH

UDOT Keeping Utah Moving

Utah Department of Transportation - Research Division
4501 South 2700 West - P.O. Box 148410 - SLC,UT 84114-8410

Report No. UT-18.21

RELIABILITY OF FEQDRAIN FOR MODELING PERFORMANCE OF SAND TREATED WITH LARGE DIAMETER PREFABRICATED VERTICAL DRAINS FOR LIQUEFACTION MITIGATION

Prepared For:

Utah Department of Transportation/
Research Division

Submitted By:

Brigham Young University
Department of Civil and Environmental Engineering

Authored By:

Kyle M. Rollins
Travis H. Meservy

Final Report
August 2018

DISCLAIMER

The authors alone are responsible for the preparation and accuracy of the information, data, analysis, discussions, recommendations, and conclusions presented herein. The contents do not necessarily reflect the views, opinions, endorsements, or policies of the Utah Department of Transportation, the U.S. Department of Transportation, or other agencies that provided funding for the project. The Utah Department of Transportation makes no representation or warranty of any kind, and assumes no liability therefore.

ACKNOWLEDGMENTS

Funding for this study was provided by an FHWA pooled fund study TPF-5(244) "Shaking Table Testing to Evaluate Effectiveness of Vertical Drains for Liquefaction Mitigation" supported by Departments of Transportation from the states of Alaska, California, New York and Utah. Utah DOT served as the lead agency with David Stevens as the project manager and Jim Higbee as the geotechnical champion. In addition, the National Science Foundation (NSF) provided funding for the testing portion of the study under grant CMMI-1052645 "EAGER: Evaluation of effectiveness of Vertical Drains for Liquefaction Mitigation." Furthermore, HB-Drains provided the slotted drain pipes and filter sleeves for the drains in this study. This support is gratefully acknowledged; however, the opinions, conclusions and recommendations in this report do not necessarily represent those of the sponsoring organizations.

TECHNICAL REPORT ABSTRACT

1. Report No.	2. Government Accession No.	3. Recipient's Catalog No.
UT-18.21	N/A	N/A

4. Title and Subtitle	5. Report Date
RELIABILITY OF FEQDRAIN FOR MODELING PERFORMANCE OF SAND TREATED WITH LARGE DIAMETER PREFABRICATED VERTICAL DRAINS FOR LIQUEFACTION MITIGATION	August 2018
	6. Performing Organization Code: N/A
7. Author(s): Kyle M. Rollins, Travis H. Meservy	8. Performing Organization Report No.: N/A
9. Performing Organization Name and Address: Brigham Young University, Department of Civil and Environmental Engineering, 368 Clyde Building, Provo, UT 84602	10. Work Unit No.: 4204615D
	11. Contract or Grant No.: 13-8731
12. Sponsoring Agency Name and Address: Utah Department of Transportation, 4501 South 2700 West, P.O. Box 148410, Salt Lake City, UT 84114-8410	13. Type of Report & Period Covered: Final Report, May 2013 to August 2018
	14. Sponsoring Agency Code: PIC No. UT07.708

15. Supplementary Notes

Prepared in cooperation with the Utah Department of Transportation, other partner state DOTs, and the U.S. Department of Transportation, Federal Highway Administration, for the TPF-5(244) pooled fund study.

16. Abstract

The objective of the modeling in this study was to evaluate the reliability of the axisymmetric finite element computer program FEQDrain for computing excess pore pressure ratios (R_u) and settlement at sand sites treated with prefabricated vertical drains (PVDs). FEQDrain was found to be capable of successfully modeling measured excess pore pressure ratio time histories from the laminar shear box experiment, as long as an appropriate combination of 'number of equivalent cycles' and 'shaking duration' was chosen, and sensitive soil parameters were in the range of measured values. Hydraulic conductivity, soil compressibility, and cycles to liquefaction are sensitive parameters and govern the computed R_u values. Computed R_u values decreased as hydraulic conductivity increased and compressibility decreased. Computed settlement was somewhat overestimated relative to measured values.

Modeling shows that the loading rate in the laminar shear box (15 cycles at 2 Hz) likely induced higher R_u values than would be expected in a typical earthquake event with a longer duration.

Results from models in this study compare favorably with those from computer modeling performed by Howell et al. (2014) in connection with centrifuge tests. In both cases, the drains were more effective at decreasing pore pressures at greater depths than at shallow depths presumably owing to upward fluid flow. Similar R_u values can be modeled with different combinations of hydraulic conductivity and compressibility.

Based on computer analyses, wick drains and 2" diameter PVDs were found to be relatively ineffective for preventing liquefaction. However, 3" diameter PVDs are fairly effective but can be overwhelmed during intense shaking. In contrast, 4" diameter and larger PVDs are significantly more effective.

17. Key Words	18. Distribution Statement	23. Registrant's Seal
Computer modeling, shaking table, earthquake, liquefaction, vertical drains, mitigation, settlement	Not restricted. Available through: UDOT Research Division, 4501 South 2700 West, P.O. Box 148410, Salt Lake City, UT 84114-8410, www.udot.utah.gov/go/research	N/A

19. Security Classification (of this report)	20. Security Classification (of this page)	21. No. of Pages	22. Price
Unclassified	Unclassified	184	N/A

TABLE OF CONTENTS

LIST OF TABLES

LIST OF FIGURES

UNIT CONVERSION FACTORS

SI* (MODERN METRIC) CONVERSION FACTORS

APPROXIMATE CONVERSIONS TO SI UNITS

Symbol	When You Know	Multiply By	To Find	Symbol
		LENGTH		
in	inches	25.4	millimeters	mm
ft	feet	0.305	meters	m
yd	yards	0.914	meters	m
mi	miles	1.61	kilometers	km
		AREA		
in^2	square inches	645.2	square millimeters	mm^2
ft^2	square feet	0.093	square meters	m^2
yd^2	square yard	0.836	square meters	m^2
ac	acres	0.405	hectares	ha
mi^2	square miles	2.59	square kilometers	km^2
		VOLUME		
fl oz	fluid ounces	29.57	milliliters	mL
gal	gallons	3.785	liters	L
ft^3	cubic feet	0.028	cubic meters	m^3
yd^3	cubic yards	0.765	cubic meters	m^3
		NOTE: volumes greater than 1000 L shall be shown in m^3		
		MASS		
oz	ounces	28.35	grams	g
lb	pounds	0.454	kilograms	kg
T	short tons (2000 lb)	0.907	megagrams (or "metric ton")	Mg (or "t")
		TEMPERATURE (exact degrees)		
°F	Fahrenheit	5 (F-32)/9 or (F-32)/1.8	Celsius	°C
		ILLUMINATION		
fc	foot-candles	10.76	lux	lx
fl	foot-Lamberts	3.426	$candela/m^2$	cd/m^2
		FORCE and PRESSURE or STRESS		
lbf	poundforce	4.45	newtons	N
lbf/in^2	poundforce per square inch	6.89	kilopascals	kPa

APPROXIMATE CONVERSIONS FROM SI UNITS

Symbol	When You Know	Multiply By	To Find	Symbol
		LENGTH		
mm	millimeters	0.039	inches	in
m	meters	3.28	feet	ft
m	meters	1.09	yards	yd
km	kilometers	0.621	miles	mi
		AREA		
mm^2	square millimeters	0.0016	square inches	in^2
m^2	square meters	10.764	square feet	ft^2
m^2	square meters	1.195	square yards	yd^2
ha	hectares	2.47	acres	ac
km^2	square kilometers	0.386	square miles	mi^2
		VOLUME		
mL	milliliters	0.034	fluid ounces	fl oz
L	liters	0.264	gallons	gal
m^3	cubic meters	35.314	cubic feet	ft^3
m^3	cubic meters	1.307	cubic yards	yd^3
		MASS		
g	grams	0.035	ounces	oz
kg	kilograms	2.202	pounds	lb
Mg (or "t")	megagrams (or "metric ton")	1.103	short tons (2000 lb)	T
		TEMPERATURE (exact degrees)		
°C	Celsius	1.8C+32	Fahrenheit	°F
		ILLUMINATION		
lx	lux	0.0929	foot-candles	fc
cd/m^2	$candela/m^2$	0.2919	foot-Lamberts	fl
		FORCE and PRESSURE or STRESS		
N	newtons	0.225	poundforce	lbf
kPa	kilopascals	0.145	poundforce per square inch	lbf/in^2

*SI is the symbol for the International System of Units. (Adapted from FHWA report template, Revised March 2003)

EXECUTIVE SUMMARY

The objective of the modeling in this study was to evaluate the reliability of the axisymmetric finite element computer program FEQDrain for computing excess pore pressure ratios (R_u) and settlement at sand sites treated with prefabricated vertical drains (PVDs). FEQDrain was found to be capable of successfully modeling measured excess pore pressure ratio time histories from the laminar shear box experiment, as long as an appropriate combination of 'number of equivalent cycles' and 'shaking duration' was chosen, and sensitive soil parameters were in the range of measured values. Hydraulic conductivity, soil compressibility, and cycles to liquefaction are sensitive parameters and govern the computed R_u values. Computed R_u values decreased as hydraulic conductivity increased and compressibility decreased. Computed settlement was somewhat overestimated relative to measured values.

Modeling shows that the loading rate in the laminar shear box (15 cycles at 2 Hz) likely induced higher R_u values than would be expected in a typical earthquake event with a longer duration. The longer duration allows the drains to dissipate pore pressures and prevent liquefaction. The number of equivalent cycles and duration of shaking combinations recommended for various moment magnitudes in the FEQDrain user manual predict lower, but similar R_u versus time curves. Thus, suggesting that PVDs would be equally effective for any size earthquake. However, drains are most effective at preventing liquefaction when earthquake ground motions are long and uniform, rather than short and intense.

Results from models in this study compare favorably with those from computer modeling performed by Howell et al. (2014) in connection with centrifuge tests. In both cases, the drains were more effective at decreasing pore pressures at greater depths than at shallow depths presumably owing to upward fluid flow. Similar R_u values can be modeled with different combinations of hydraulic conductivity and compressibility.

Based on computer analyses, wick drains and 2" diameter PVDs were found to be relatively ineffective for preventing liquefaction. However, 3" diameter PVDs are fairly effective but can be overwhelmed during intense shaking. In contrast, 4" diameter and larger PVDs are significantly more effective.

1 INTRODUCTION

1.1 Background

Earthquakes occur all over the world each year and cause substantial damage. Much of the damage caused by earthquakes is from soil liquefaction rather than strong ground motions. Lateral spreading caused by liquefaction led to the collapse of the Showa Bridge in the 1964 Niigata, Japan earthquake (NRC, 1985). Figure 1-1 shows sections of the bridge deck that fell into the river when the piers were pulled apart by lateral spreading of the soil. In the 1964 Alaska, USA earthquake liquefaction triggered massive landslides. The largest slide in Anchorage was two miles long and 900 feet wide. This slide destroyed about 75 houses and severed utility and telephone lines. (Stover and Coffman, 1993). Figure 1-2 Shows a portion of the downtown area which experienced flow deformations caused by liquefied soil slumping towards the harbor. More recently the 1995 Kobe, Japan earthquake caused $12 billion in damage to the city's port facilities (EQE, 1995).

The 2011 Christchurch, New Zealand earthquakes caused widespread and severe liquefaction of the central business district. Over a third of buildings in this area had to be demolished because of damage caused by liquefaction, not shaking. Tens of thousands of residential homes were affected or destroyed by liquefaction or associated slope failure and instability (Cubrinovski et al. 2011).

Liquefaction occurs when loose, saturated sand, experiences ground motions. The loose soil particles rearrange and densify. As the soil compacts, water attempts to leave the voids. But if drainage cannot occur, the tendency to decrease in volume will cause an increase in pore pressure. If pore pressure becomes equal to the overburden pressure the effective stress is null and the soil behaves like a viscous fluid, thus the term "liquefaction". It should be noted that pore pressures don't have to rise high enough to reduce effective stress to zero to cause failure of

the soil. Flow deformations can occur once the resisting forces in the soil are less than the driving forces.

Liquefied soil loses shear strength and becomes prone to lateral movement, even on mild slopes. Excessive settlement also occurs in liquefied soils because they cannot support concentrated loads such as structures or embankments. Underground structures with low density such as tunnels or sewer lines can even float to the surface of the liquefied soil. Non-structural signs of liquefaction include sand boils, subsidence, ground fracturing, and horizontal sliding.

Figure 1-1 Lateral Spread Collapsed the Showa Bridge, Niigata, Japan. The City Suffered Slight Damage from Shaking, But Heavy Damage from Liquefaction (NRC, 1985).

Figure 1-2 Downtown Anchorage, AK Experienced Flow Deformation and Lateral Spreading Which Caused Downhill Slumping Towards the Harbor as a Result of Liquefaction Caused by M_w 9.2 Earthquake of 1964.

1.2 Liquefaction Mitigation

Preventing liquefaction is usually accomplished by densification of soil to prevent seismic compaction. In-situ densification can be accomplished by techniques such as vibro-compaction, vibro-replacement, deep soil cement mixing, compaction grouting, and dynamic compaction (shown in Figure 1-3). These methods densify the loose soil layer which prevents seismic compaction during an earthquake. Although these techniques are usually less expensive than deep foundations or switching sites, they are still costly and slow.

Using deep foundations to bypass the liquefiable layer is another option, but it is more costly if not otherwise needed. In addition to vertical loads, these foundation members must be designed to withstand lateral spreading and downdrag, both of which are liquefaction effects on deep foundations. Drilled concrete shafts are better suited for this application because they have greater flexural resistance and a lower surface area to cross section ratio. Another foundation

style is a thick concrete mat foundation which is designed to float like a raft. These mat foundations must be capable of withstanding the differential and total settlements that may occur (Lew and Hudson, 2004). A full discussion of foundation types, however, is outside the scope of this report, which is concerned only with using drains to mitigate liquefaction.

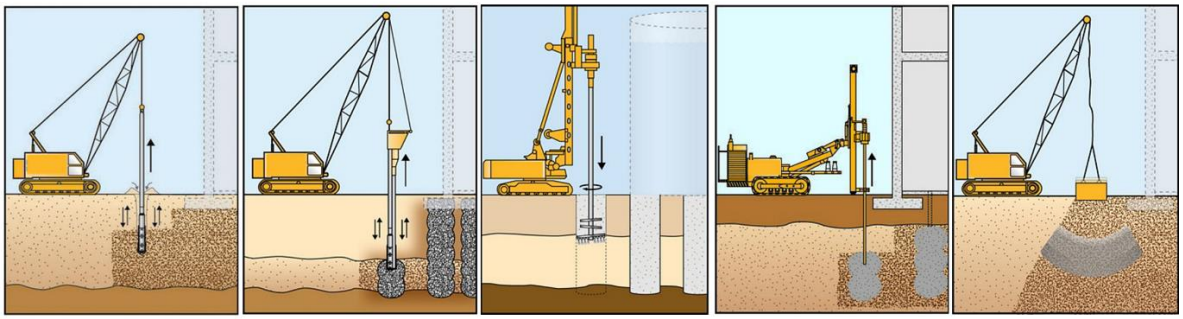

Figure 1-3 In-situ Densification Methods, from L-R: Vibro-compaction, Vibro-replacement, Soil Mixing, Compaction Grouting, and Dynamic Compaction. (Pictures from haywardbaker.com)

Soil improvements may be avoided if pore pressures can be quickly dissipated as they are being generated. Vertical drains made of gravel, which allow horizontal drainage of soil, were introduced by Seed and Booker (1977). These vertical drains reduce the drainage path distance, and are particularly effective if horizontal layers of impermeable silt or clay block vertical flow. Having these drains closely spaced, or made larger increases their effectiveness.

Vertical gravel drains have been use for decades, but the design engineer often relies upon the soil densification that occurs during installation, not the drainage (Rollins and Anderson, 2004). Whether the gravel drains would be effective in preventing the buildup of excess pore pressures from drainage alone is questionable. Some designers worry that drainage alone would still allow unacceptable settlement to occur. Settlement is related to soil compressibility, and soil compressibility increases with pore pressure ratio (shown in Figure 1-4). If the soil compressibility can be kept low, excessive settlement can be prevented. For example, by keeping excess pore pressures ratios below, $R_u = 0.40$ the increase in soil compressibility is negligible, from 0.4-0.6 the compressibility increases about 40%. For R_u above 0.6 the compressibility may increase by 10-12 times (Seed et al., 1975a).

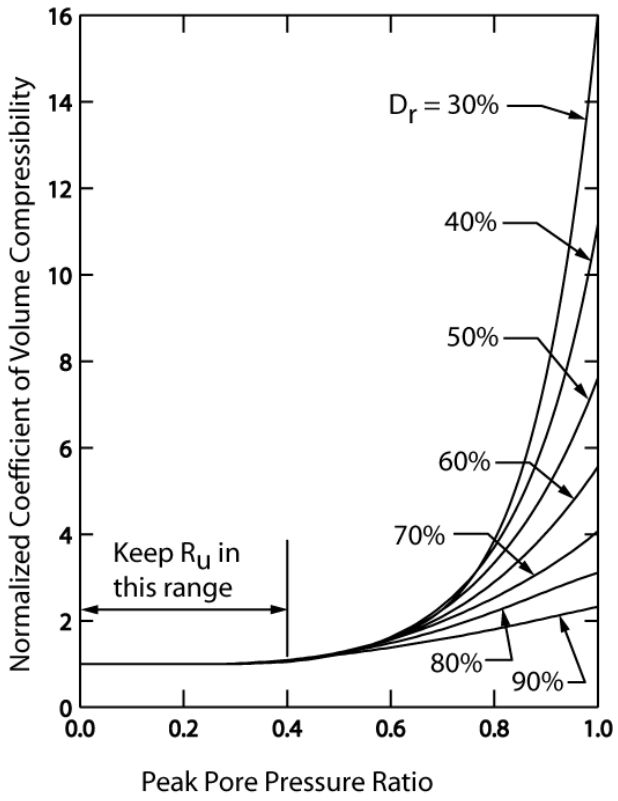

Figure 1-4 Normalized Coefficient of Volumetric Compressibility (m_v) Versus Excess Pore Pressure Ratio (R_u). Above R_u=0.40 the Soil Will Experience Settlement

Large diameter prefabricated vertical drains (PVDs) are designed to rapidly dissipate pore pressures, and are quick and inexpensive to install. When earthquake induced shear stresses cause excess pore water pressure, the water can flow horizontally to the drains and then up and out the large diameter drain, as illustrated in Figure 1-5. Prefabricated drains are made from a 75-150mm diameter corrugated plastic pipe, perforated with short slits or small holes. The pipe is sleeved in a geosynthetic filter fabric to prevent infiltration of soil. PVDs are installed vertically into the soil by a vibrating mandrel, which has fins to increase the area of soil densified by the installation process, although this is a secondary effect only. The installation process is similar to that for “wick drains” for clay consolidation.

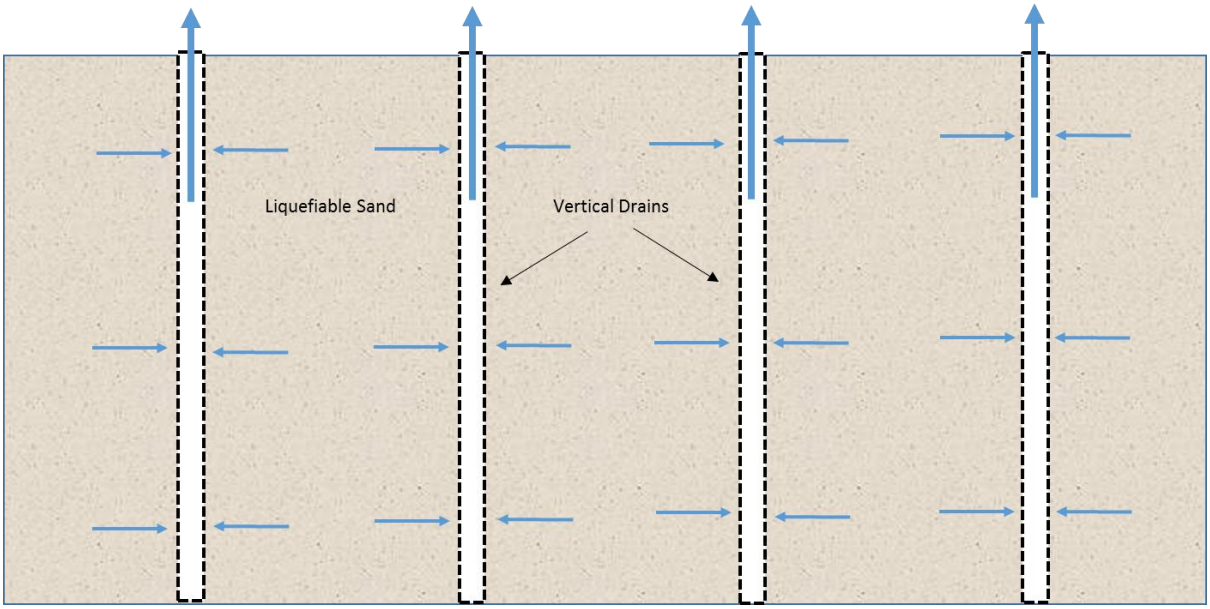

Figure 1-5 Large Diameter Prefabricated Drains in Liquefiable Sand. Pore Water Flows Laterally to Drains, then Escapes

Drains are installed in a triangular pattern to provide the shortest radial drainage path with minimum overlap. This creates nearly cylindrical columns of soil with drains at each center. The spacing is usually 1-2m, depending on the permeability of the soil. Though similar to "wick drains" which have a maximum flow rate of ($2.8x10^{-5}$ m^3/s at hydraulic gradient=0.25), a 100mm diameter prefabricated drain has a much larger flow capacity, (0.093 m^3/s at the same gradient). This is also about 10 times the flow capacity of a 1m diameter gravel drain (Rollins et al. 2003).

Installation time requirements and costs for PVDs are also more favorable than for gravel drains. If a 12m thick layer at the surface needed to be mitigated, the gravel drains (stone columns) might cost about $\$107/m^2$. Vibro-compaction might cost $\$75/m^2$, but PVDs would only cost $\$48/m^2$. The installation time for drains is also about half or one-third of usual methods (Rollins et al. 2003).

1.3 Motivation

Prefabricated drains are of particular interest to geotechnical engineers and specialty contractors because they show promise of being a fast, low cost method to mitigate liquefaction. However, no site at which PVDs have been installed has yet experienced an earthquake,

therefore their performance must be predicted using computer models. This lack of empirical knowledge is a hindrance to the wide spread use of drains for preventing liquefaction. The overall objectives of this research study are to investigate the performance of vertical drains for liquefaction mitigation and to evaluate the ability of a current numerical model for predicting pore pressure dissipation and settlement. Even in the absence of this information, a significant number of project owners have chosen drains as their preferred solution for low rise buildings with a large footprint, linear infrastructure such as roads and pipelines, as well as ports, tanks and other infrastructure because of the cost and time advantages described previously (Ellington Cross, 2008), (Hayward Baker, 2015).

1.4 Prefabricated Drains Research Program

This report is focused on evaluating a finite-element program, FEQDrain, developed by Pestana et al. (1997) for modeling the performance of vertical drains in liquefiable sand based on full-scale shake table experiment data (Oakes, 2015). The results from the computer model will be compared against the experimental results to determine the accuracy and realism of outputs produced by the computer program. The end goal, which is beyond the scope of this report, is to develop a tool or design procedure that engineers can confidently use to predict the behavior of PVDs during seismic events.

The earthquake drain testing and data collection was conducted in August 2014 at the University at Buffalo, New York, by a previous graduate student, Caleb Oakes and is reported in his thesis (Oakes, 2015). Tests were performed within a 20-ft high laminar shear box. The first set of tests used PVDs on a 4ft triangular grid. The soil was then placed around the drains by hydraulic pluviation. Three rounds of shake tests were conducted at different accelerations, for a total of nine tests. This experiment was then reconstructed and repeated with drains on 3ft spacing. The results for both spacing were similar. A more complete description is found in Section 2.3.

1.5 Objective

The main objective of this part of the research is to examine the reliability of an existing computer modeling program designed for use with prefabricated drains. All tests from Oakes

(2015) experiments will be modeled through iteration until the theoretical curve matches the measured pore pressure curve. Every computer model makes assumptions and generalizations, and has limitations in terms of accuracy and reliability. But, if it can be shown that our calibrated model parameters are similar to the measured soil values, then the computer model becomes a valuable tool. By showing that FEQDrain can reliably predict excess pore pressure ratios and settlements for a controlled full-scale shake table experiment, then we are one step closer to being able to trust it for predicting the effects of prefabricated drains, in natural soil, under natural conditions.

1.6 Report Outline

The rest of this report is organized as follows:

- Chapter 2 presents a literature review, including an in-depth review of the parent study (Oakes, 2015).
- Chapter 3 explains the methods that were used to generate and analyze the finite element models.
- Chapter 4 presents the calibrated excess pore pressure ratios (R_u) from the finite element model which were matched to Oakes's experiment. This chapter analyzes model input values and discusses the accuracy of the modeling software. In addition, results from a parametric sensitivity study are presented.
- Chapter 5 explains the conclusions which were reached as a result of this study, and possibilities for future research.

2 LITERATURE REVIEW

Soil drainage has long been proposed for liquefaction mitigation, starting with vertical gravel drains (Seed and Booker, 1997). Later it was found that gravel columns are less effective at conducting water than early studies assumed (Onoue ,1988). Prefabricated drains can conduct more water out of the soil, but studies are ongoing to prove their efficacy.

2.1 Behavior of Gravel Drains

Although this report is interested in PVDs, it is helpful to understand the behavior of gravel drains. Their behavior may provide insights into how PVDs may be used most effectively.

2.1.1 The Original Idea

It is well known that loose, saturated sands tend to liquefy when pore pressures cannot escape. Seed & Booker (1977) suggest using vertical columns of gravel installed down through the liquefaction susceptible soil layer, to dissipate excess pore pressure. The higher hydraulic conductivity of gravel will create a preferential drainage path laterally to the drain, instead of vertically to the soil surface. Also, soil is generally more permeable in the horizontal direction, so lateral flow is again favored, especially if there are interspersed lenses of impermeable silt or clay which inhibit vertical flow.

Seed & Booker (1977) expanded on the pore pressure generation and dissipation equations previously developed by Seed, Martin & Lysmer (1976) to model a system with radial symmetry and purely radial drainage.

Seed & Booker (1977) used these equations and wrote a finite element program to perform liquefaction analysis for radial flow. They varied the sand permeability, drain spacing, and the intensity and duration of the cyclic accelerations in the model. They equated the irregular

motions of an earthquake to an equivalent number of cyclic loadings. They found that a small drain delayed liquefaction, but a large drain might entirely prevent liquefaction. They plotted their results and constructed curves for design that show peak pore pressure ratio vs. spacing ratio. A second set of curves plotted the greatest average pore pressure ratio vs. spacing ratio.

The results of their theoretical model were insensitive to the coefficient of volumetric compressibility, but sensitive to the coefficient of permeability. Thus in-situ permeability should be measured carefully. The model also assumes zero head loss through the gravel, which they specify as permeability of the drain at least 200 times that of the sand. Thus for most sands a medium-to-fine gravel would suffice. Also, vertical drainage through the sand is considered negligible, which may be true for sand inter-bedded with impermeable silt or clay layers.

Seed & Booker (1977) suggest that having a drainage system of some type is an economical way to reduce liquefaction potential in loose sands.

2.1.2 Well Resistance of Gravel Drains

For many years, gravel drains have been used to reduce liquefaction potential of loose, saturated sands, but these methods did not account for well resistance, which a number of researchers found to be significant, Tokimatsu and Yoshimi (1980), Ishihara (1982), Okita et al. (1986), Onoue et al. (1987a). Therefore, a simple method to account for it was needed. Onoue (1988) expanded on the work of Tanaka et al. (1983, 1984, and 1986) to create simple design charts.

Onoue (1988) applies the finite difference model to the same pore pressure generation and dissipation equations as used by Seed & Booker (1977), along with well resistance equations created by him and other researchers to produce new design charts that accounted for well resistance. These charts are usable over a range of values for the design pore pressure ratios, cycle ratios, and coefficients of well resistance, not just one resistance as others had done. A design excess pore pressure ratio (R_u) of below 0.6 is used.

The diagrams, which included well resistance, were compared against in-situ liquefaction experiment values. A 120cm steel pipe was driven into the ground, isolating a cylinder of soil in which a 30, 40, or 50cm gravel column was formed at the center. This is a practical replica of the

geometry of the finite difference model. Cyclic accelerations were generated by vibrations applied to the head of the steel cylinder with a vibratory hammer.

The measured pore pressure ratios were compared to the analytical charts previously developed by Seed and Booker (1977) and more recently by Onoue (1988). When plotted, these values agree well with the computed analytical values that accounted for well resistance, thus validating the usefulness of the structured analysis model including well resistance. It was found that resulting pore pressure ratios were not affected by whether water flowed vertically through the sand, or through the drain only. Finally, it was determined that the required drain spacing was about four times closer when well resistance is accounted for. Even very low well coefficients affected the calculated pore pressure ratio significantly. Thus, well resistance should always be considered.

2.1.3 Centrifuge Modeling of Flow to a Gravel Drain

Brennan & Madabhushi (2002) performed high quality centrifuge testing to analyze the behavior of vertical gravel drains and the flow patterns they cause within the soil. It was found that when pore pressures are generated they immediately attempt to flow upward, however because the drain has higher permeability a zone of horizontal gradient begins to develop. The drain's zone of influence expands with time, progressively slower, and reaches a limit. The study also found that shallow soil layers liquefied sooner than deep layers, in fact the deepest soil did not liquefy. Equally important, it was discovered that pressure at deep layers dissipates first, and shallow layers stay liquefied the longest. Deep layers drain quickly, and shallow layers drain later and longer likely owing to upward flow of water from deeper layers to the surface.

2.1.4 Centrifuge Modeling of Partial Depth Gravel Drains

Brennan & Madabhushi (2006) also explored the behavior of partial depth gravel drains via centrifuge testing as a method to facilitate drainage of shallow soils, which had been previously found to drain only after pore pressures have dissipated from deep soils. Two experiments were conducted. In the first experiment all drains penetrated the full depth of the liquefiable layer, while the second experiment had only half of the drains penetrated the full depth while the remainder only penetrated the upper half of the liquefiable zone. Results showed that no water flowed into or out of the partial drains until the entire lower half had finished

dissipating its excess pore pressure. From this it was concluded that partial drains are completely ineffective, and that the only way to improve drainage of the shallow soils is to quickly drain the lower layers first. Thus, all drains should be installed to the full depth of the liquefiable soil strata.

2.2 Behavior of Prefabricated Drains

Large diameter prefabricated vertical drains (PVDs) are a newer method of allowing dissipation of elevated pore pressures to escape from cyclically loaded soil. These drains have a diameter of 75-150mm and are hollow which allows greater flow than through gravel. Theoretically, a 100mm PVD can convey 10 times the flow of a 1m diameter gravel column (Rollins et al. 2003). They are placed vertically into the soil by a vibrating mandrel, which gives the added benefit of densifying the surrounding soil during installation. The PVD is made of a corrugated tube with perforated walls and sleeved in filter fabric. Although PVDs have been installed in several places, no treated site has experienced an earthquake.

2.2.1 FEQDrain Computer Model

Pestana et al. (1997) developed the axi-symmetric finite element computer program FEQDrain, working in collaboration with industry experts. FEQDrain computes the generation and dissipation of excess pore pressure ratios in the soil, with or without prefabricated drains, due to a specified number of uniform cycles of loading. In addition, the computer program computes the settlement of the profile resulting from the dissipation of the excess pore pressure. FEQDrain uses the pore pressure generation and pore pressure dissipation equations from Seed and Booker (1977). These are the same equations that had been used to create the design charts in the original 1977 journal article on gravel drains.

2.2.2 Behavior of PVD Drains from Controlled Blasting Field Tests

Rollins et al. (2004) and Rollins & Anderson (2004) describe research investigations to investigate the performance of PVD drains at two geotechnical field test sites (Treasure Island, CA and Vancouver, BC). The performance of treated and untreated sites were compared at both sites to assess drain performance.

Immediate settlement caused by the installation process of PVDs was measured and reported, since this was also a matter of interest. The use of high vibration during drain installation increased the relative density of the soil by 10% and produced volumetric strains of 2.5% which is similar liquefaction-induced settlements observed in earthquakes. The use of PVDs typically decreased the settlement in treated sites to only 60% of that measured at the untreated sites.

The soil profile was instrumented and rigged with explosive charges at various depths and locations. The charges were fired in sequence, with a very small pause between each. This rapid cyclic loading produced liquefaction very quickly. The treated and control areas both liquefied. This was attributed to the extremely fast cyclic loading caused by the explosives (about 3seconds) instead of an earthquake (about 10-60seconds). During an earthquake the drains would likely work more effectively since they would have more time to expel water from the soil, thus preventing liquefaction. Also, despite the drain fabric meeting filter requirements, sand still infiltrated some of the drains. Still, the excess pore pressures dissipated more quickly from the treated areas.

The soil parameters measured at each site were used to model the pore pressure response using the computer program FEQDrain. The modeled and the measured pore pressure ratios agreed well, despite the accidental sand infiltration which affected the field test. The model was next adjusted by the equivalent cycles method to simulate earthquake loadings with longer durations. The adjusted model indicated that the maximum excess pore pressure would have been kept low enough to have prevented liquefaction. Table 2-1 compares blast testing to other earthquakes based on a combination of duration, and ratio of equivalent cycles to cycles before liquefaction.

Table 2-1 Summary of Computed Maximum R_u and Settlement for Various Earthquake Events and Drain Spacings at the Vancouver Site (Rollins and Anderson 2004).

Magnitude	Duration (sec)	N_q/N_l	Drain Spacing (m)	Maximum. R_u	Settlement (mm)
Blast	8	4.0	1.22	1.0	310
6.0	8	2.0	0.91	0.40	31
6.75	17	2.0	0.91	0.47	35
6.75	17	3.0	0.91	0.61	48
7.5	35	2.0	0.91	0.65	53

2.2.3 Localized Vibration

Rathje et al. (2004) performed field tests on a volume of reconstituted, saturated sand measuring 1.2 m x 1.2 m x 1.2 m, surrounded by an impervious membrane. Tests were conducted with and without a PVD in the center of the test volume. The relative density of the sand for both tests was approximately 35 percent. Stress cycles were applied using a large Vibroseis oil-prospecting truck, with pore pressure and acceleration measured at several points within the test volume.

Plots of the measured excess pore pressure ratio with and without a drain from this test are presented in Figure 2-1. Without a drain, liquefaction was produced during the application of 60 stress cycles (3 second total duration), while the excess pore pressure ratio did not exceed 25% for the test volume with a drain subjected to the same vibrations. Volumetric strain decreased from 2.1% without a drain to less than 0.5% with a drain in place.

While PVDs successfully prevented liquefaction for this shallow deposit, questions remain about their performance for deeper soil deposits. Of particular concern is the observation made by Brennan and Madabhushi (2002, 2006) that shallower soils drain after deeper soils. In a liquefiable soil only 1.2 m thick, this phenomenon may not fully develop or indeed may not occur at all.

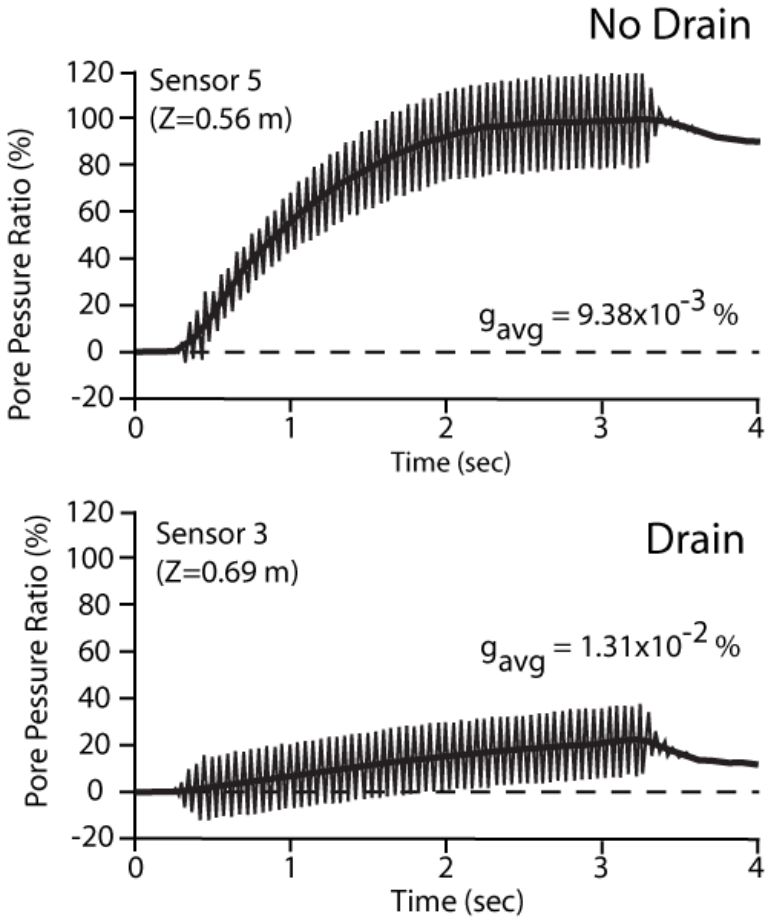

Figure 2-1 Excess Pore Pressure Ratio Time Histories Induced by Vibroseis Oil-Prospecting Truck for Sand Volume with and Without PVD. (Reproduced from Rathje et al., 2004).

2.2.4 Centrifuge Testing to Evaluate Performance of PVD Drains

As part of the NEES Grand Challenge project for Seismic Risk Management of Port Systems, a series of three dynamic centrifuge tests was conducted. Each test had a gently sloping liquefiable soil profile that included zones treated with prefabricated drains and zones left untreated. The goal was to determine the effects of PVDs in preventing lateral spreading and slope failures. Design methods for drains have previously only focused on keeping seismically-induced pore pressures below a certain level, rather than controlling soil deformations.

Testing was performed on the 9m radius centrifuge of NEES at UC Davis. Three separate models of liquefiable, sloping ground were spun at 15g: SSK01 (Kamai et al. 2007, Marinucci et

al. 2008, Howell et al 2009b, Marinucci 2010), RNK01 (Kamai et al. 2008, Howell 2009a), and RLH01, (Rathje et al. 2012).

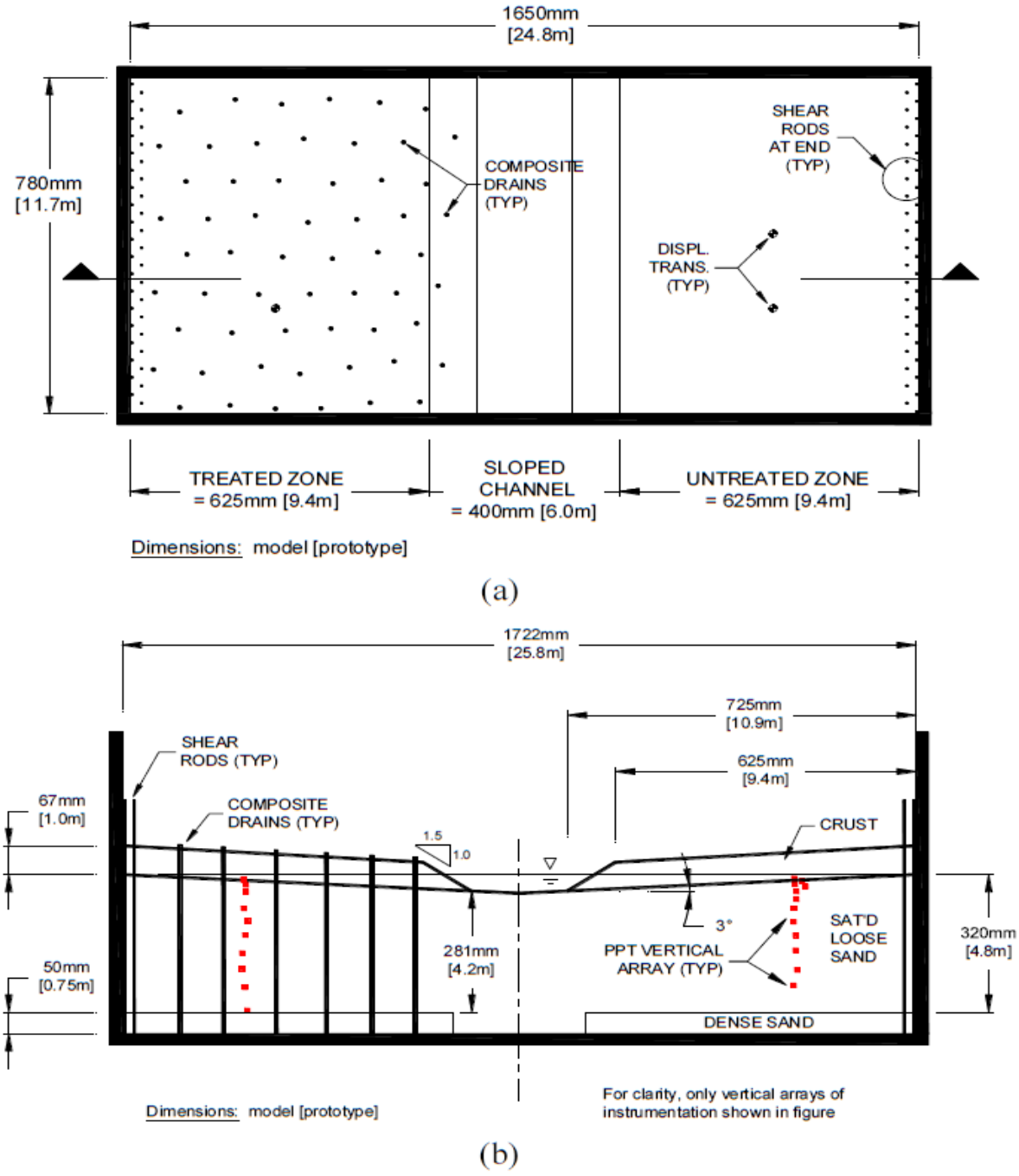

Figure 2-2 Layout of Centrifuge Test SSK01. (a) Plan View of Centrifuge Model and (b) Cross-Section. (Reproduced from Marinucci et al 2008).

The first test (SSK01) used two zones, treated and untreated, sloping towards a central channel. Saturated loose sand was placed with a 3 degree surface slope, and a clay crust over the two zones, but not over the channel. Figure 2-2 shows the experiment setup. No-drain/drain-treated zones in plan view (a), and soil profile and slope in side view (b). The results of the experiment are shown in the following two figures. The measured pore pressure ratios Figure 2-3, and horizontal and vertical displacements for the treated and untreated zones are shown, Figure 2-4.

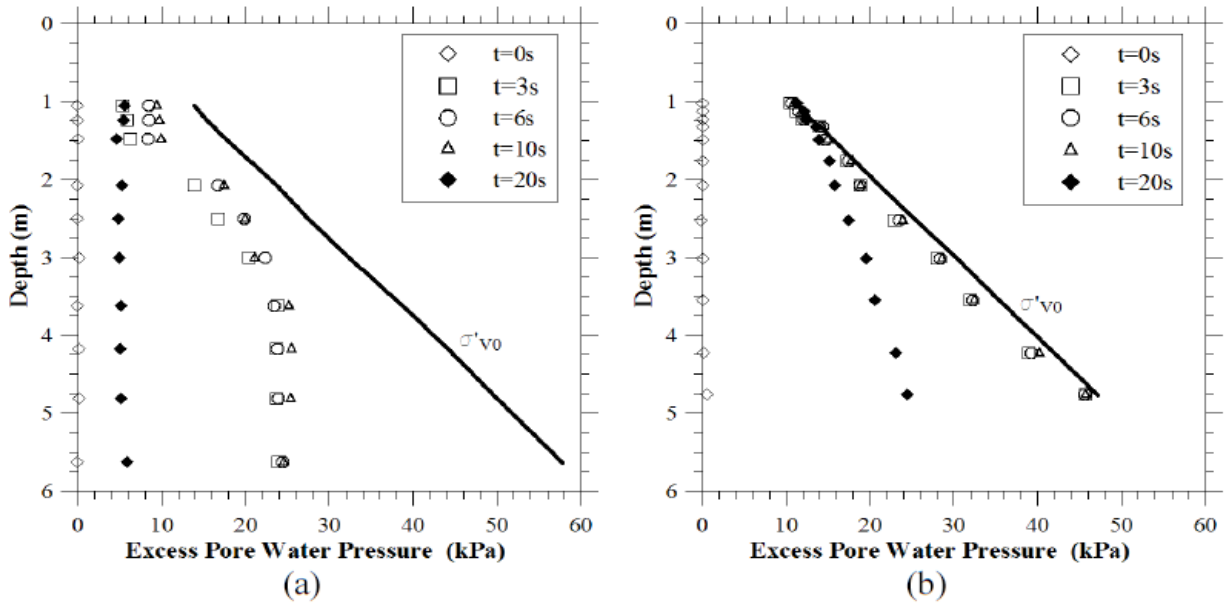

Figure 2-3 Measured Data from Centrifuge Experiment SSK01. Excess Pore Pressure Profile for Varying Times for PGA=0.28g for (a) Treated and (b) Untreated Sides. (Reproduced from Marinucci et al 2008).

These plots show lower excess pore pressures and smaller deformations for the zone that was treated with drains. This means the drains were effective in preventing or reducing liquefaction. This second test (RNK01), (not shown) used the same geometry as SSK01, but the untreated area had non-draining tubes to rule out the possibility of the shear strength of the drains preventing lateral deformations of the soil, called 'soil pinning'. Results again showed that drainage was effective, but also demonstrated that soil pinning was negligible.

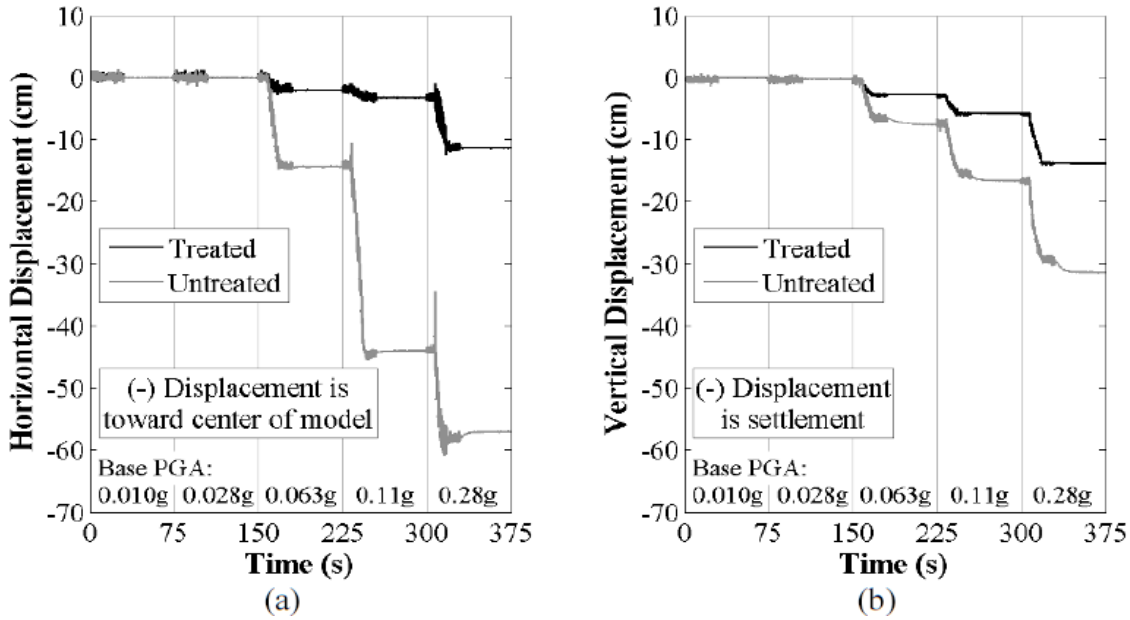

Figure 2-4 Shaking Induced Deformation: (a) Horizontal and (b) Vertical Directions. (Reproduced from Marinucci et al 2008).

This third test (RLH01) re-examined the same factors as both the first two, but with slight changes. It was designed as a stand-alone test, even though it was part of a series. This model used a single, wide incline, divided into three zones; treated, untreated, and non-draining tube zones, as illustrated in Figure 2-5. It also had a steeper slope of 10 degrees, with all zones oriented in parallel towards a common channel. Earthquake time histories were applied as the cyclic motion scheme, also one sinusoidal shake was applied. The results from the previous test were confirmed again, with the addition of observing the effect of different ground motion types.

The untreated area and non-draining tube area had similar pore pressure ratios, Figure 2-6, and equal deformations, Figure 2-7, both of which were significantly higher than the treated zone. Thus it was clear that drainage was causing the improvement in performance and soil pinning was insignificant. Also, the impact of drains was shown to be sensitive to the characteristics of the input motion. They found that the characteristics of the shaking are more significant than the peak ground acceleration.

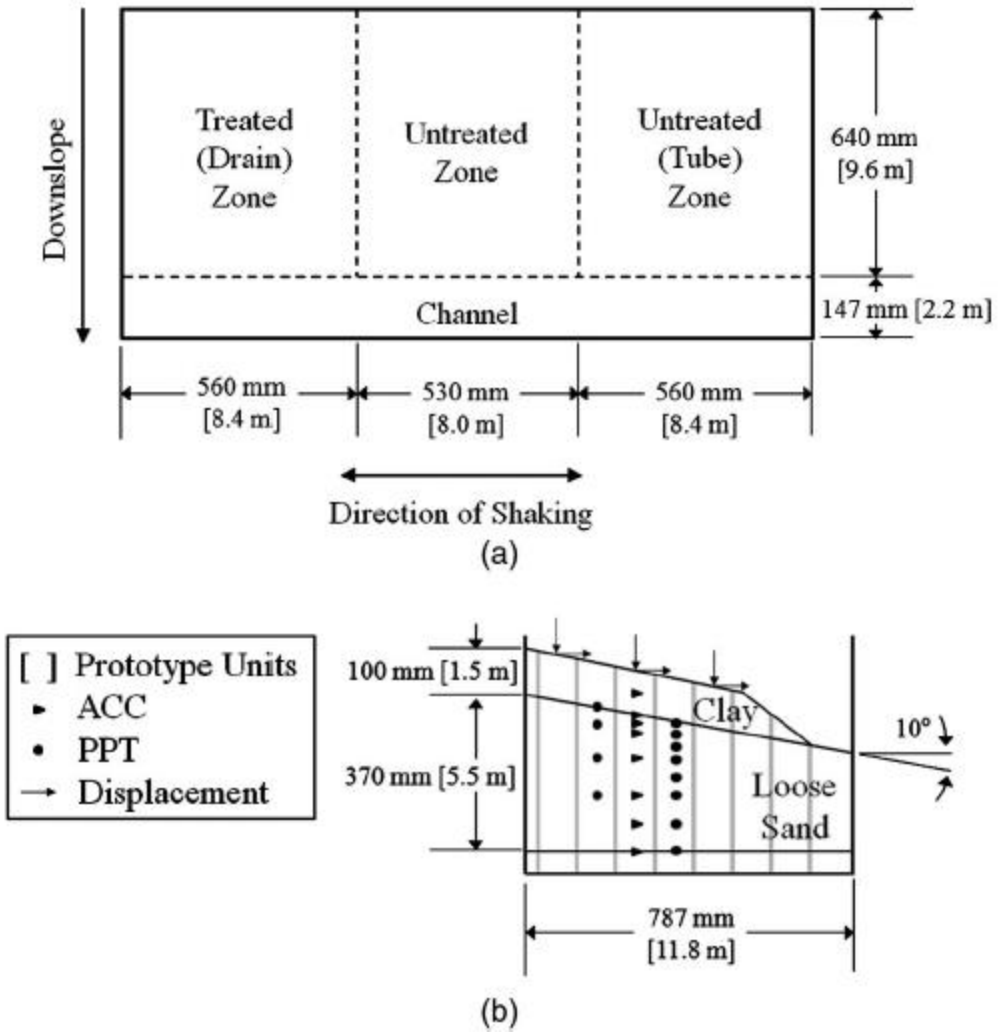

Figure 2-5 Views of Model Geometry for Centrifuge Test RLH01. (a) Plan View, (b) Cross-Section. (Reproduced from Howell et al. 2012).

For example, earthquakes with high intensity at the beginning caused elevated pore pressures that eventually subsided when the drains caught up with the generation of pore pressures. Ground motion time histories that slowly increased in intensity were better controlled by the drains. However, the sinusoidal shake quickly overwhelmed the drains because there was no interval of low intensity for the rate of drainage to catch up with the induced pore pressures. When the drains are overwhelmed, their full impact was not noticed until the shaking stopped, at which time the pore pressures dissipated significantly faster than untreated areas. Ground settlement were reduced by 30 to 60% while lateral spread displacements were also reduced by 30 to 60%.

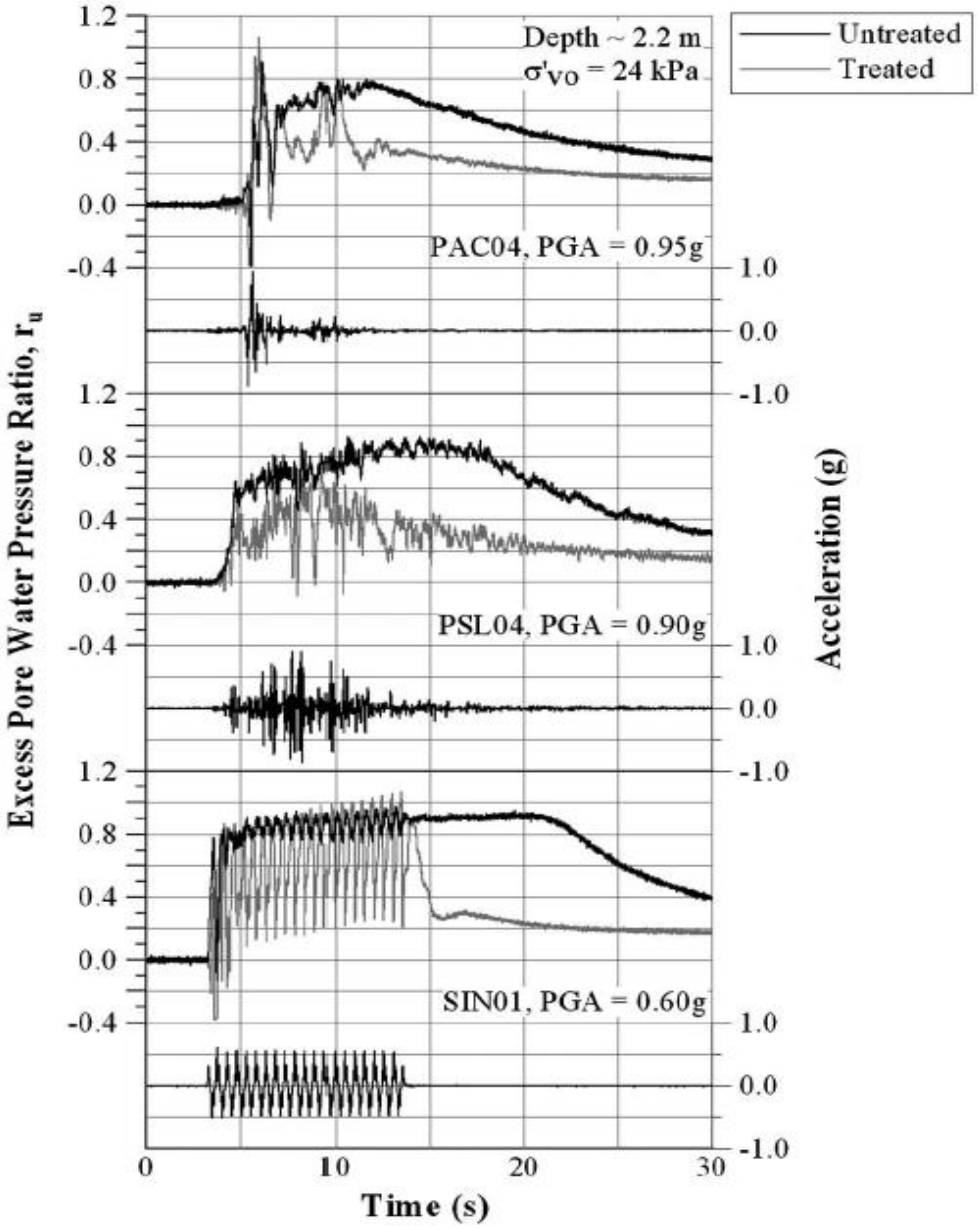

Figure 2-6 Measured Data from Centrifuge Experiment RLH01. Pore Pressure Ratio Curves Versus Time for Treated and Untreated Cases. The Corresponding Acceleration Time History is Plotted Immediately Beneath Each. (Reproduced from Howell et al. 2012).

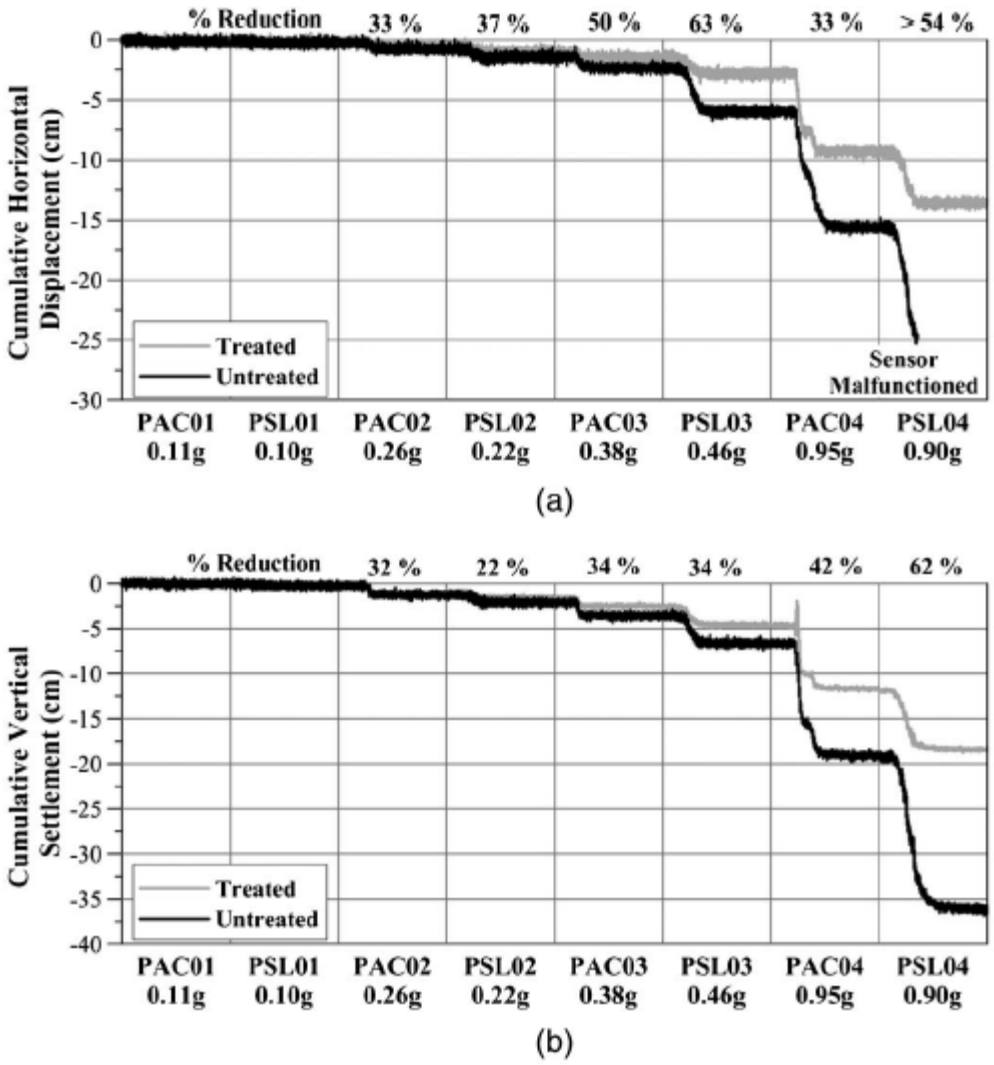

Figure 2-7 Measured Data from Centrifuge Experiment RLH01, Cumulative (a) Horizontal and (b) Vertical Displacements at Mid-Slope in Treated and Untreated Areas for All Shaking Events. (Reproduced from Howell et al. 2012).

2.2.5 Numerical Modeling of Peformance of PVD Drains

Howell, Rathje, and Boulanger (2014) conducted 2D and 3D numerical modeling of the centrifuge experiments described in the previous section. The finite element program *OpenSees* was used to create: a 2D model of the full centrifuge test, and 2D and 3D unit-cell models. It was discovered that the geometry of the soil surface and mode of deformation affected which model type produced a more accurate representation. Horizontal and vertical deformations were modeled fairly well, Figure 2-8, as were pore pressure ratios, Figure 2-9.

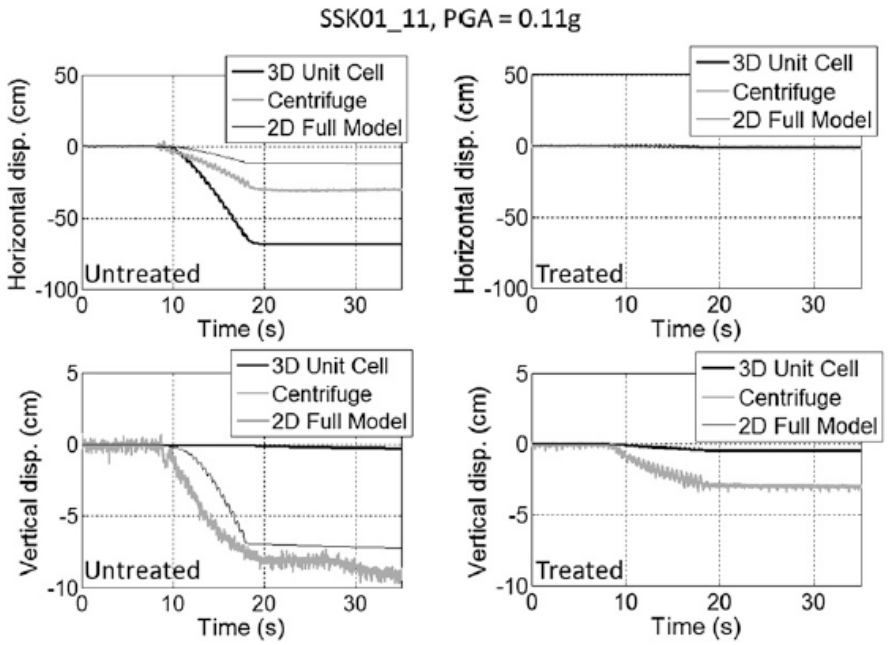

Figure 2-8 Deformation Responses From Centrifuge Tests and Numerical Simulations for SSK01_11. (Reproduced from Howell et al. 2014).

The hydraulic conductivity (*k*), scaled down to prototype scale from 15g, was *k*=0.03 cm/s. Numerical modeling showed that for a set value of hydraulic conductivity, the rate of pore pressure dissipation is controlled by soil compressibility. The numerical simulations also showed that constitutive models over-predicted the volumetric stiffness, Figure 2-10, thus either hydraulic conductivity or soil compressibility must be modified to achieve accurate modeling. This study chose to adjust the conductivity, within a range, until a best fit value was obtained; rather than deviate from suggested values of soil compressibility. This under prediction of volumetric compressibility inherent in the constitutive model produced an under-prediction of settlement.

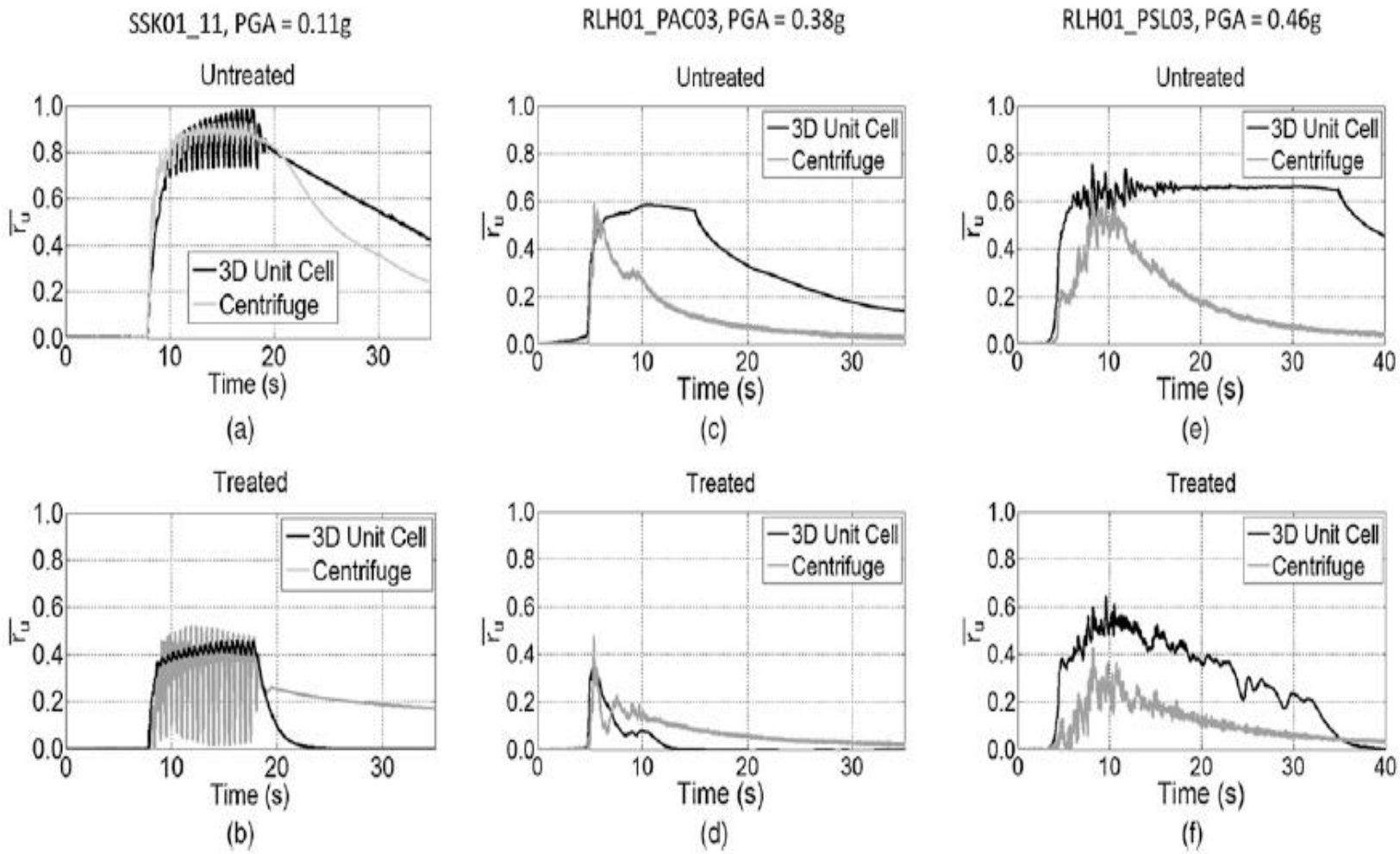

Figure 2-9 Excess Pore Pressure Responses from Centrifuge Tests and Numerical Simulations. Plots of the Untreated Cases (a, c, and e) are Positioned Above the Plots of the Corresponding Drain-Treated Case (b, d, f). Each Plot Has a Measured Curve and a Modeled Curve. (Reproduced from Howell et al. 2014).

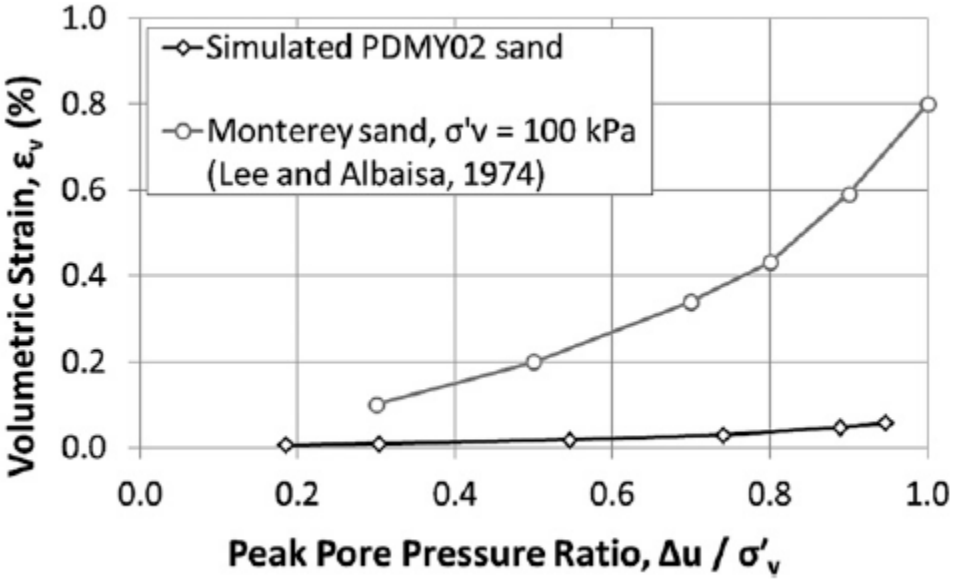

Figure 2-10 Measured and Simulated Volumetric Strain Response for Liquefiable Sand. Excessively High Stiffness Necessitated Adjustment of Hydraulic Conductivity (Howell et al. 2014).

Numerical modeling by Vytiniotis et al. (2013), using *OpenSees*, compared slope deformations of a partially-submerged sandy slope, for drain-treated and untreated cases. Model geometry is shown in Figure 2-11, and is similar to some facilities at U.S. ports. Boundary conditions, ground motions, pore water pressures, and soil deformations were modeled. Soil was modeled with an elasto-plastic effective stress soil model (Dafalias & Manzari, 2004). A total of 58 seismic ground motions were used as input ground motions, all having a minimum moment magnitude of M_w=5.5 and duration of less than or equal to 33.10sec.

The results of the simulations showed that drained systems are effective in reducing earthquake-induced permanent lateral deformations by a factor of 1.2 to 3.5, for 1m drain spacing. Though the drains are behind the crest of the partially submerged slope rather than directly within it, they reduce slope deformations by prohibiting diffusion of excess pore pressures from far afield to the slope.

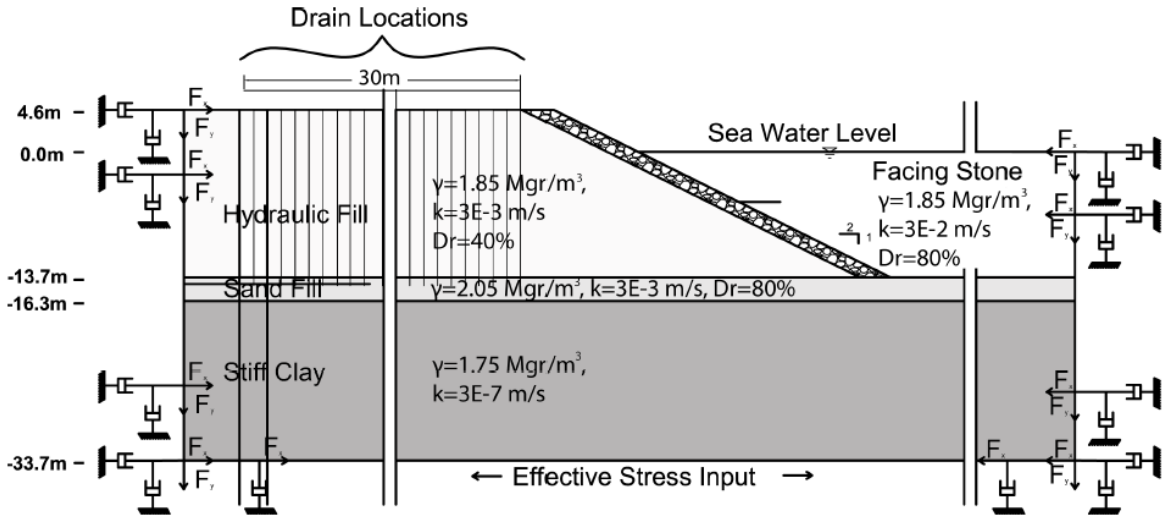

Figure 2-11 Diagram of Partially-Submerged Sandy Slope, with Details, Analyzed by Finite-Element Numerical Modeling (Vytiniotis et al. 2013).

It was also found that computed permanent slope deformations were well correlated with peak ground accelerations (PGA) and especially Arias Intensity. The Arias Intensity being the integral of the square of the acceleration time-history. However, there was no correlation found between the improvement ratio and the Arias Intensity. From this, Vytiniotis (2013) asserted that the effectiveness of drained systems is largely independent of the characteristics of the ground motions.

2.2.6 Previous Laminar Shear Box Testing Without Drains

Large-scale testing of liquefiable soils without prefabricated drains was performed using the NEES@Buffalo site laminar shear box. Tests included a Level Ground Test, LG0, (Bethapudi, 2008), Level Ground Test, LG1 (Dobry & Thevanayagam, 2013) and Induced Partial Saturation Test IPS-1 (Yegian, 2015). The soil was comprised of loosely placed saturated sand with a relative density of about 40%. Input motions were provided by high speed hydraulic actuators at the base of the laminar box. LG0 used sinusoidal inputs of progressively higher acceleration, in a single continuously shaking test as illustrated in Figure 2-12. Accelerations ranged from 0.001g to 0.30g. Profiles of excess pore pressures and excess pore pressure ratios (R_u) from this test are provided in Figure 2-13.

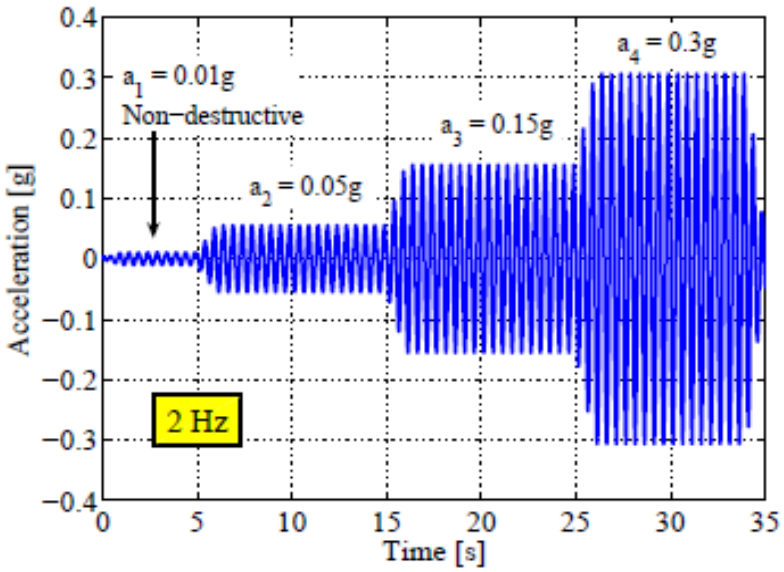

Figure 2-12 Input Motions for Level Ground Test LG0. (Bethapudi 2008).

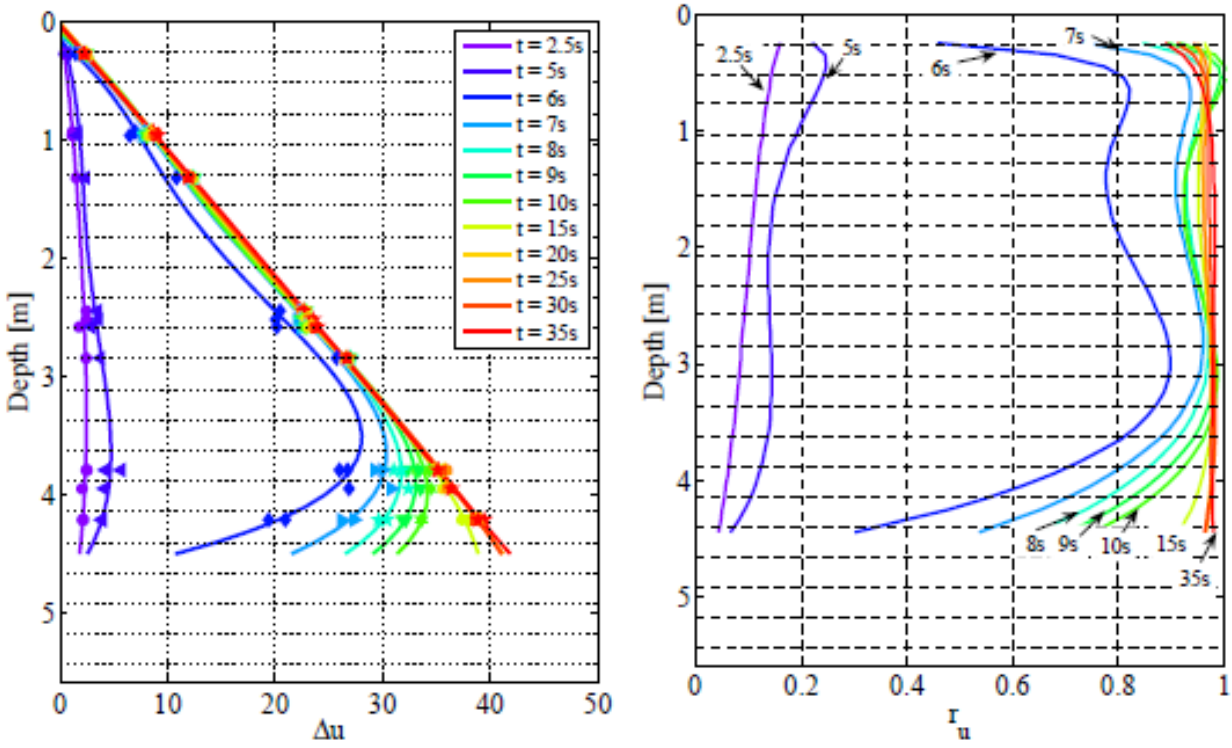

(a) Excess pore pressure (b) Excess pore pressure ratio

Figure 2-13 Excess Pore Pressure Profiles for LG0 (Bethapudi 2008).

Tests on LG1 (Dobry and Thevanayagam, 2013) used seven distinct series of shaking, so that an increase in liquefaction resistance could be observed with increasing numbers of shaking events. The soil conditions were the same as LG0. Accelerations ranged from 0.03g to 0.1g with 15 uniform shaking cycles per test. The cumulative settlement versus the number of shaking tests is plotted in Figure 2-14.Settlement decreased for each successive shake as the soil densified.

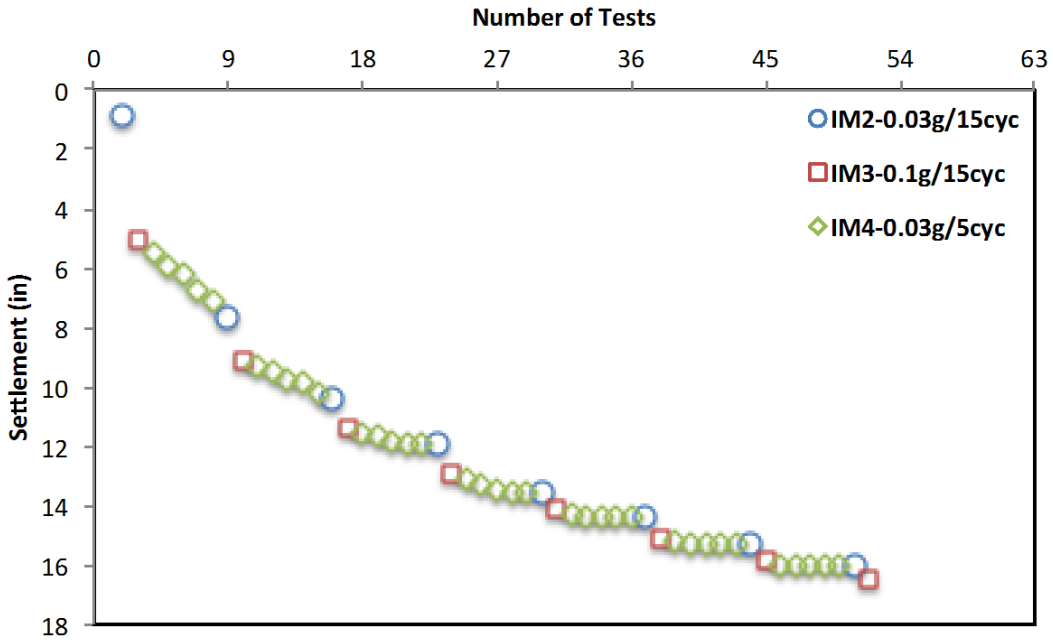

Figure 2-14 Settlement Due to Number of Cycles (Dobry and Thevanayagam, 2013).

The IPS1 tests investigated whether a partially saturated condition, would increase the liquefaction resistance of the soil. This was done by injecting a chemical compound into the ground, to create bubbles that would entrain in the pore water. The top 10ft of the total 16ft of soil in the box were treated.

Shake testing consisted of six 0.1g tests with 15 cycles, followed by two 0.2g tests with 15 cycles. This is similar to LG1 for all but the last two shakes, as the many 0.03g shakes in LG1 are less significant than the 0.1g shakes that separate them. Instrumentation of IPS1 showed that the untreated layer experienced the majority of settlement. To provide a comparison with settlement from LG1, the settlement of the untreated layer was then scaled up by the ratio of the full soil thickness divided by the thickness of the untreated layer. Cumulative settlement from both tests after

this adjustment are plotted in Figure 2-15 The cumulative settlement is remarkably consistent for the 0.1g shake tests but increases substantially for the 0.2g shake tests.

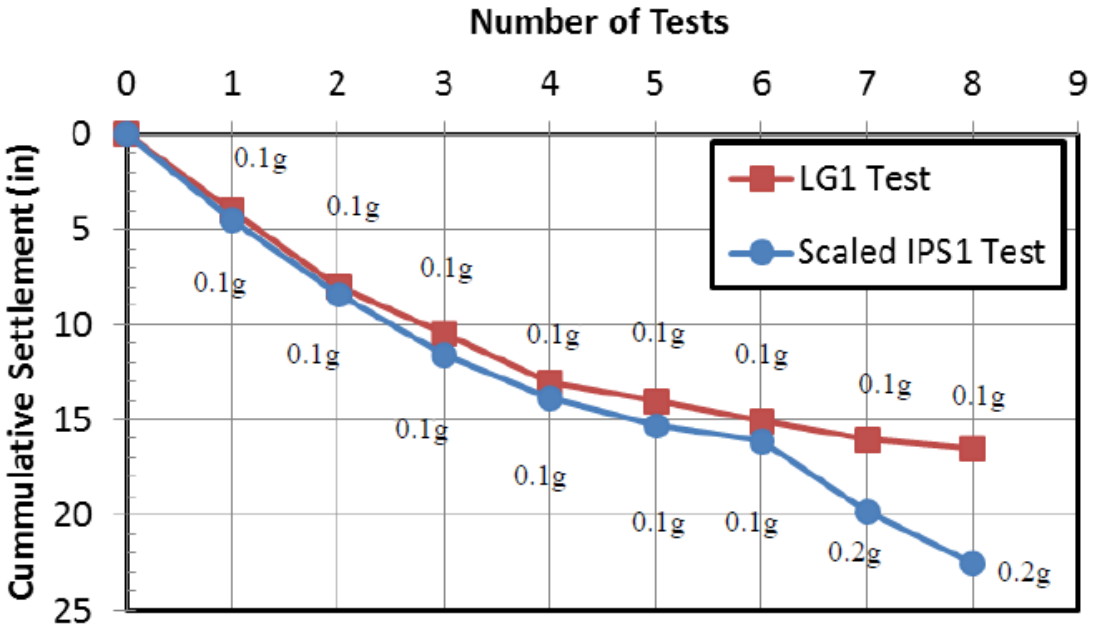

Figure 2-15 Settlement vs Number of Tests for IPS with Scaled Settlement (Yegian, 2015)

2.3 Laminar Box Shaking Tests with Drains (Oakes, 2015)

A previous graduate student working under Dr. Rollins, Caleb Oakes, conducted full-scale laminar shear box shaking tests on loose sand, prepared with large diameter prefabricated drains (PVDs). The experimental data from Oakes (2015) was used as the basis for the numerical modeling conducted in this report. The accelerations, excess pore pressure ratios, and settlement data, were presented by Oakes (2015). Prefabricated vertical drains, and several arrays of instruments were installed. After this, sand was pumped into the tank. The measured accelerations, excess pore pressure ratios, and settlement data were presented by Oakes (2015). A detailed description of the shake table, instrumentation scheme, soil characteristics, shake strength, and recorded measurements are provided subsequently in the respective sub-sections.

2.3.1 Laminar Shear Box Shake Table

Equipment and technical support for the NEES laboratory laminar shear box were provided by the University at Buffalo, New York. The shear box is 20ft tall and has plan view dimensions of 9ft and 16.4ft. It has 40 horizontal rectangular layers called ‘rings’ which, being

separated by ball bearings, are free to slide relative to each other. The rings are made of wide flange steel beams turned on their side, with the web horizontal, and attached at the corners to form a rectangle. A double-layer flexible rubber membrane contains the saturated soil within the box and prevents drainage on the sides and bottom.

Accelerations are imposed at the base of the box by high-speed hydraulic actuators. Because the mass of the soil is large relative to that of the rings and interface friction is minimal, shear waves transfer through the soil as they might during an earthquake under field conditions. Photographs in Figure 2-16 show the laminar box in the UB@NEES laboratory and the actuators at the base of the laminar box. The box and its dimensions are depicted in Figure 2-17, Figure 2-18, and Figure 2-19.

Figure 2-16 Laminar Shear Box and Hydraulic Actuators at the Base (Oakes, 2015)

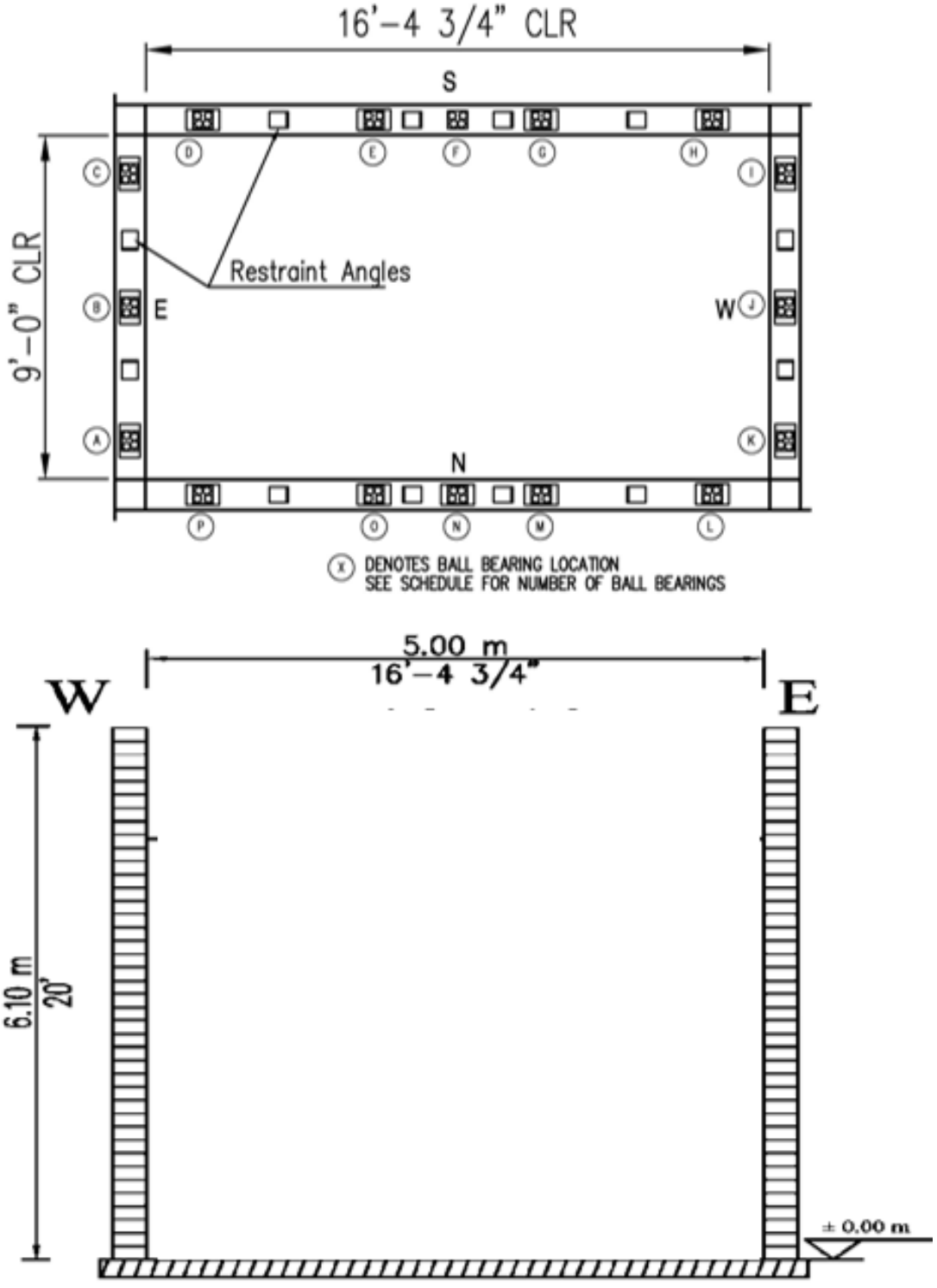

Figure 2-17 Profile and Plan View of Laminar Shear Box. (Oakes, 2015)

2.3.2 Instrumentation and Drain Scheme

Drains were hung vertically in the box on a triangular grid, and columns of instruments were hung at various distances from drains before the sand was placed. This was done to eliminate the densification caused by pushing/vibrating drains into place from the soil surface, but also it was not feasible to drive them in with a mandrel while indoors. Plan and profile drawings showing the locations of the drains and instrumentation arrays are provided in, Figure 2-18, Figure 2-19, Figure 2-21, and Figure 2-22. As shown in Figure 2-18 and Figure 2-19, the instrumentation attached to the rings consisted of horizontal accelerometers (AE1X-AE35X) and LDVTs (H0X-H31X) to record acceleration time histories and displacement time histories, respectively during the tests.

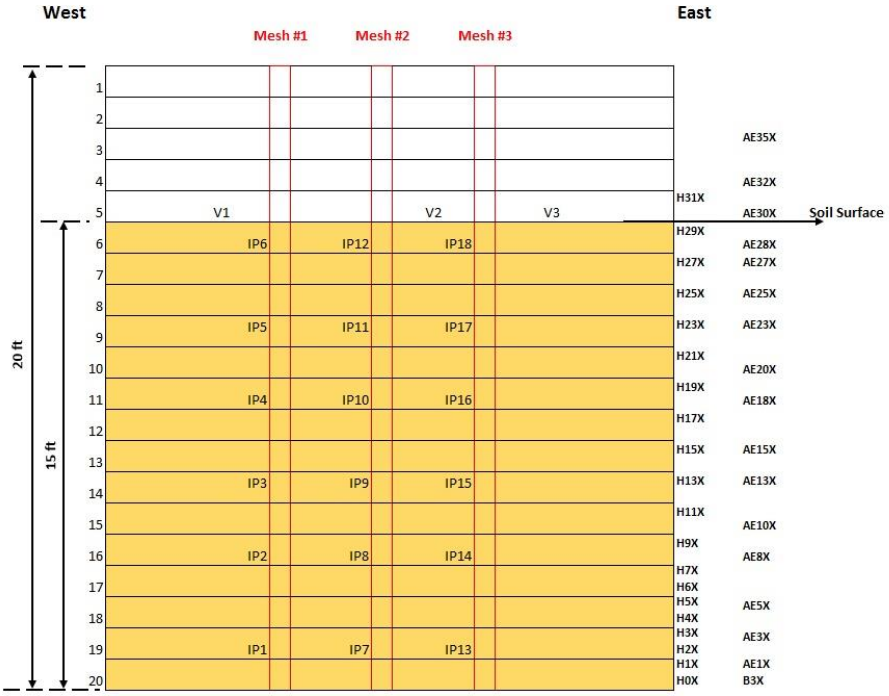

Figure 2-18 Profile View of Pore Pressure Transducers (IP1-IP118), Horizontal LVDTs (H0-H31) and Horizontal Accelerometers (AE1X-AE35X) (4 ft drain spacing, Oakes, 2015).

The instrumentation within the sand inside the laminar box consisted of three vertical arrays of pore pressure transducers, two Sondex settlement profilometers, slotted pipes for measuring horizontal soil permeability, and three string potentiometers attached to surface

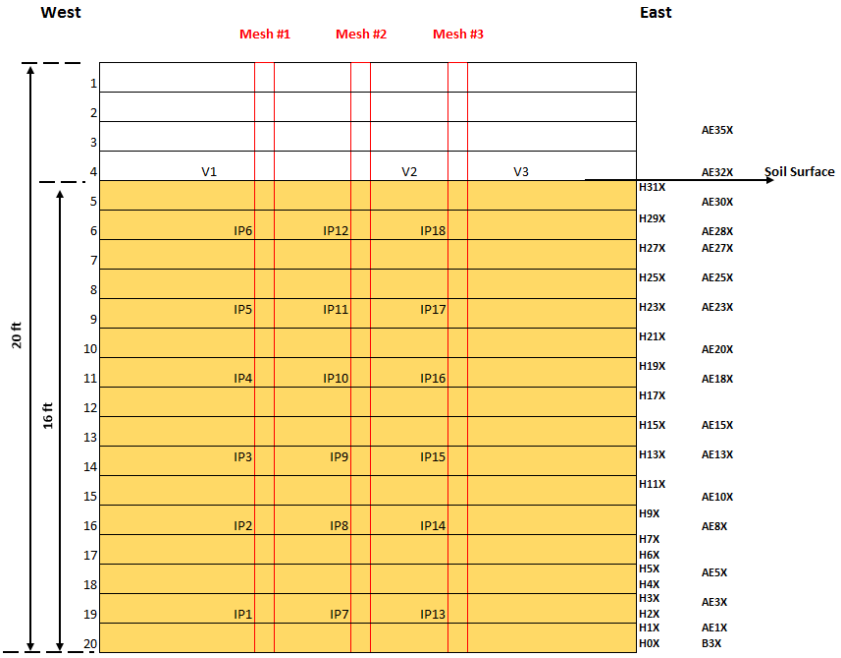

Figure 2-19 Profile View of Pore Pressure Transducers (IP1-IP118), Horizontal LVDTs (H0-H31) and Horizontal Accelerometers (AE1X-AE35X) (3 ft drain spacing, Oakes, 2015).

settlement plates (Figure 2-21 and Figure 2-22). While the surface plates provided continuous settlement versus time, the Sondex profilometers, only gave settlement at 2ft intervals at the conclusion of each test. Each column of piezometers were attached to a vertical mesh to maintain position during sand filling. The instruments and drains for the 4ft spacing tests were held in place at the base, but not the top; so they were moved slightly as the sand was deposited.

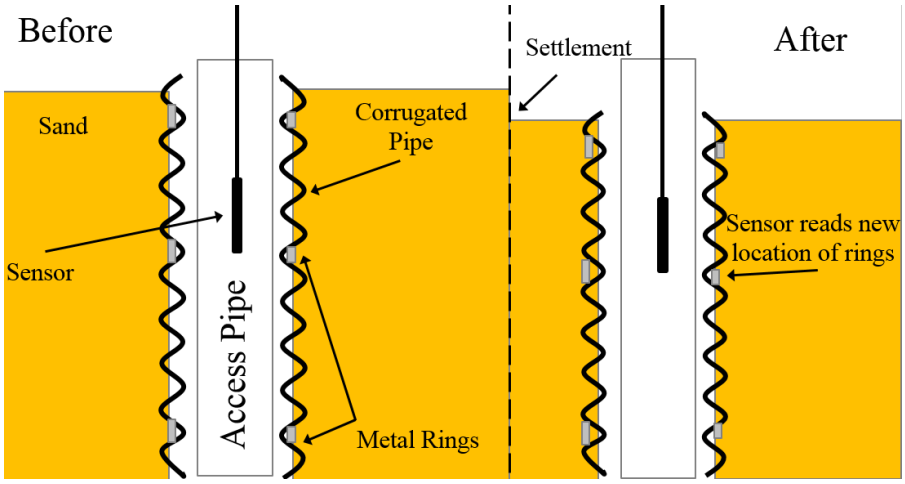

Figure 2-20 Profile View of Sondex Settlement Profilometer (Oakes, 2015

Thus they were close, but not in exactly the right places during the testing. Error in positioning increased with height above the base. For the 3ft spacing, the instrument columns and drains were held in place at the bottom and top, so the spacing was much more consistent and reliable.

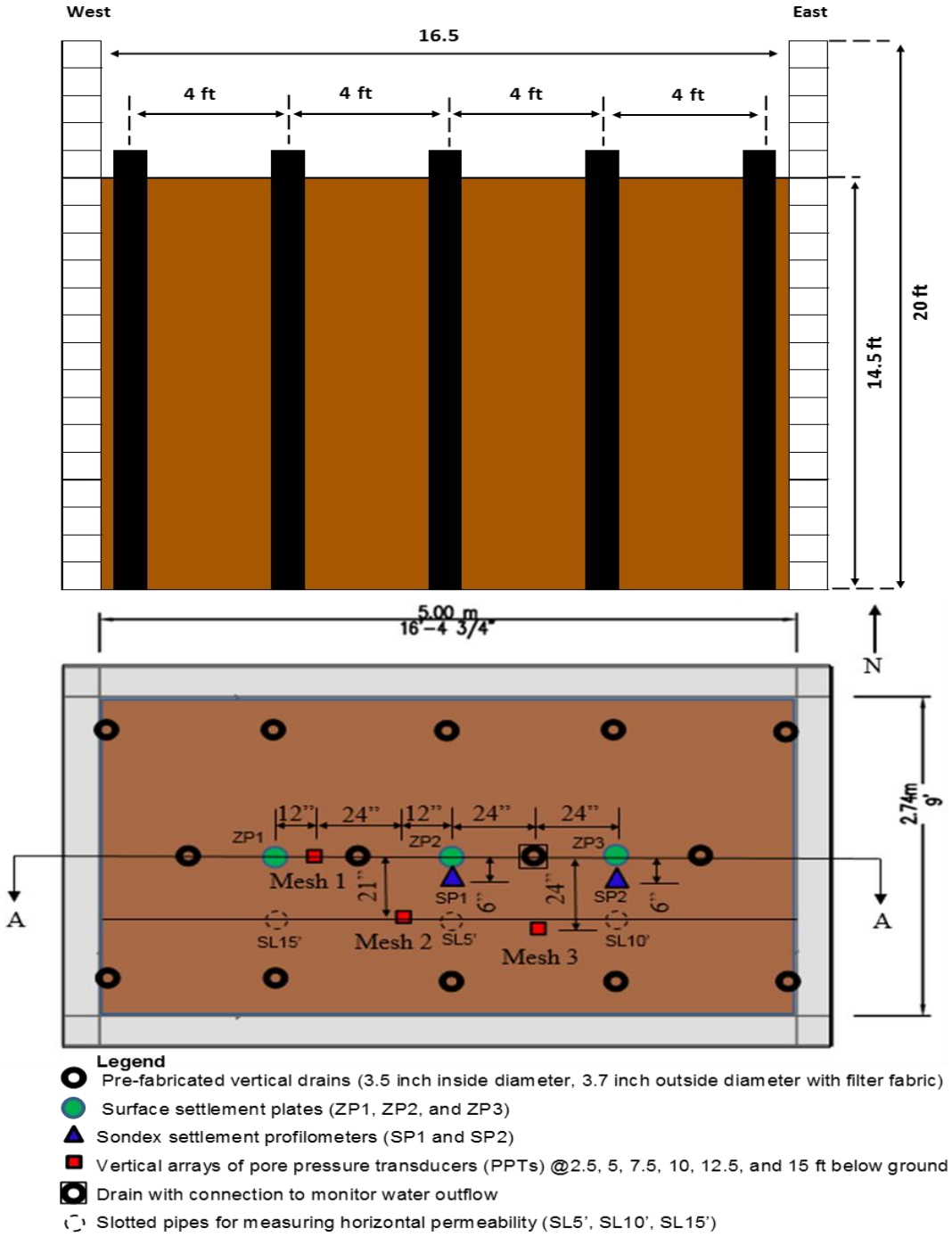

Figure 2-21 Elevation View of Drains and Plan View of Sensors for the Tests With Drains at 4ft Triangular Spacing (Oakes, 2015)

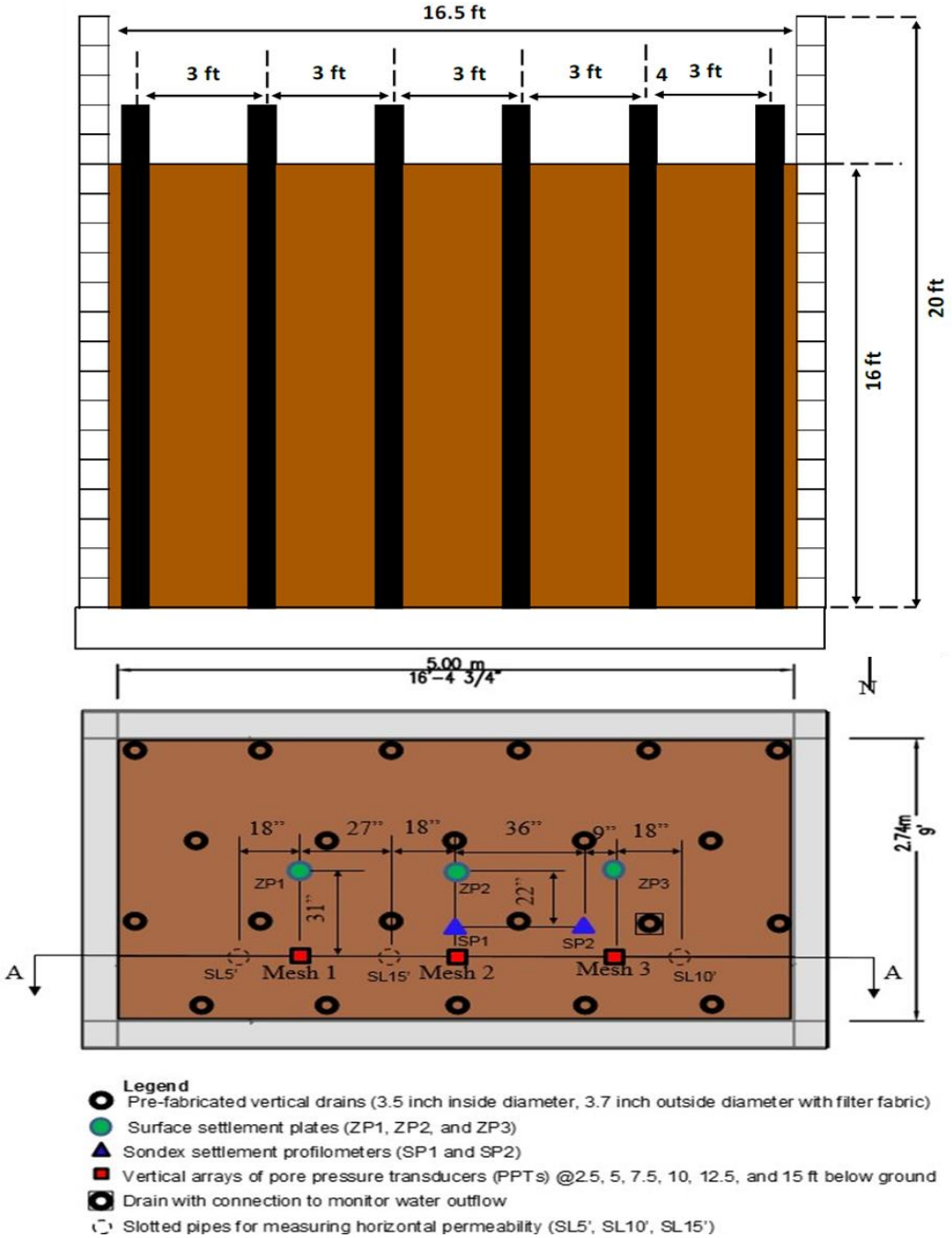

Figure 2-22 Elevation View of Drains and Plan View of Sensors for the Tests With Drains at 3ft Triangular Spacing (Oakes, 2015)

2.3.3 Soil Characteristics

The sand in the box was a commercially obtained Ottawa F55 sand that was used because of its consistent and well-known properties. The sand is a poorly graded clean sand with a mean

grain size (D50) of 0.23 mm. The sand classifies as SP material according to the Unified Soil Classification System and A-3 according to the AASHTO system. Minimum and maximum void ratios along with grain size characteristics are summarized in Table 2-2.

Sand was pumped into the box as a slurry, then it passes through a diffuser and falls into standing water before being deposited. This deposition method, called wet pluviation and illustrated by a photo in Figure 2-23, ensured that the sand was deposited loosely and somewhat uniformly. Filling the box took about 5 days.

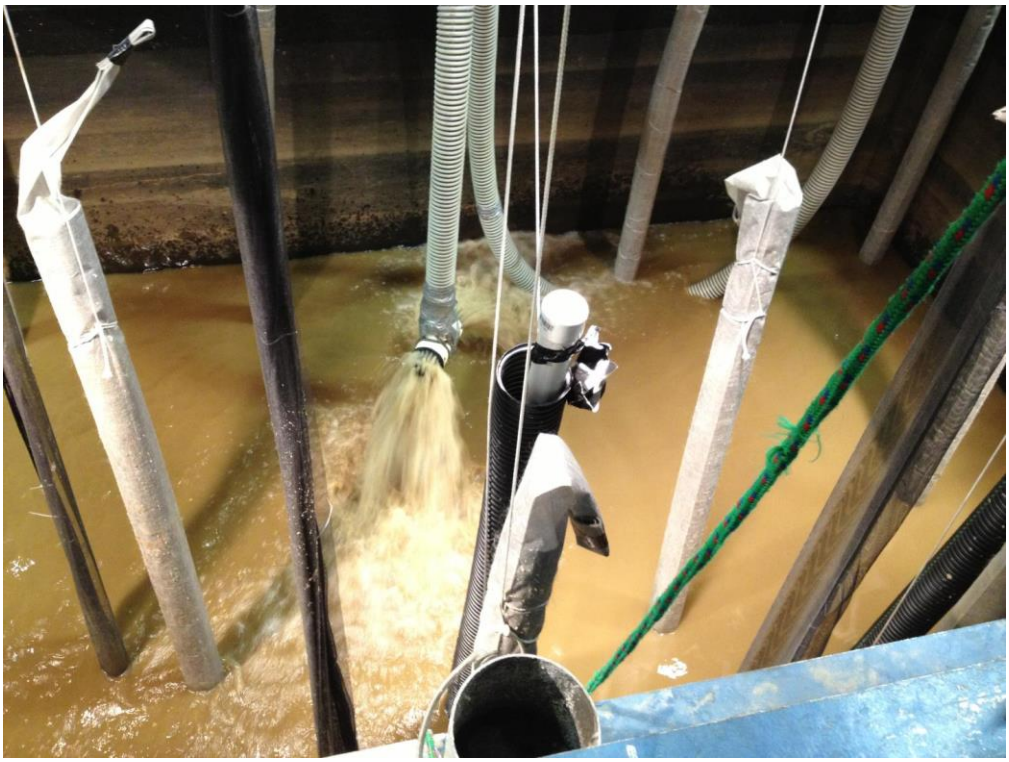

Figure 2-23 Sand Being Deposited in Laminar Shear Box by Pluviation (Oakes, 2015)

Prior to filling for the tests with the 4 ft drain spacing, NEES@UBuffalo staff apparently left about 2.5ft of sand in the bottom of the box from previous testing because of difficulty in removing it with the sand extraction system. This sand was denser than newly placed sand. However, prior to subsequent tests with the 3 ft drain spacing, this lower sand layer was excavated by hand so that the entire profile consisted of more uniform loose sand. In addition, for the 4 ft tests the sand only extended to a height of 14.5 ft while for the 3 ft tests the sand extended to a height of 16 ft.

The relative density of the new sand was measured at different depths while filling the tank. This was done by lowering a bucket on a rope and allowing the bucket to fill with sand as it was deposited. The collector of the sample then had to be careful to pull up the bucket without letting it bump into anything, or else the vibration would compact the loose sand and give an incorrect density. Measured average relative density profiles for the 4ft and 3ft drain spacings are plotted versus depth in Figure 2-24.

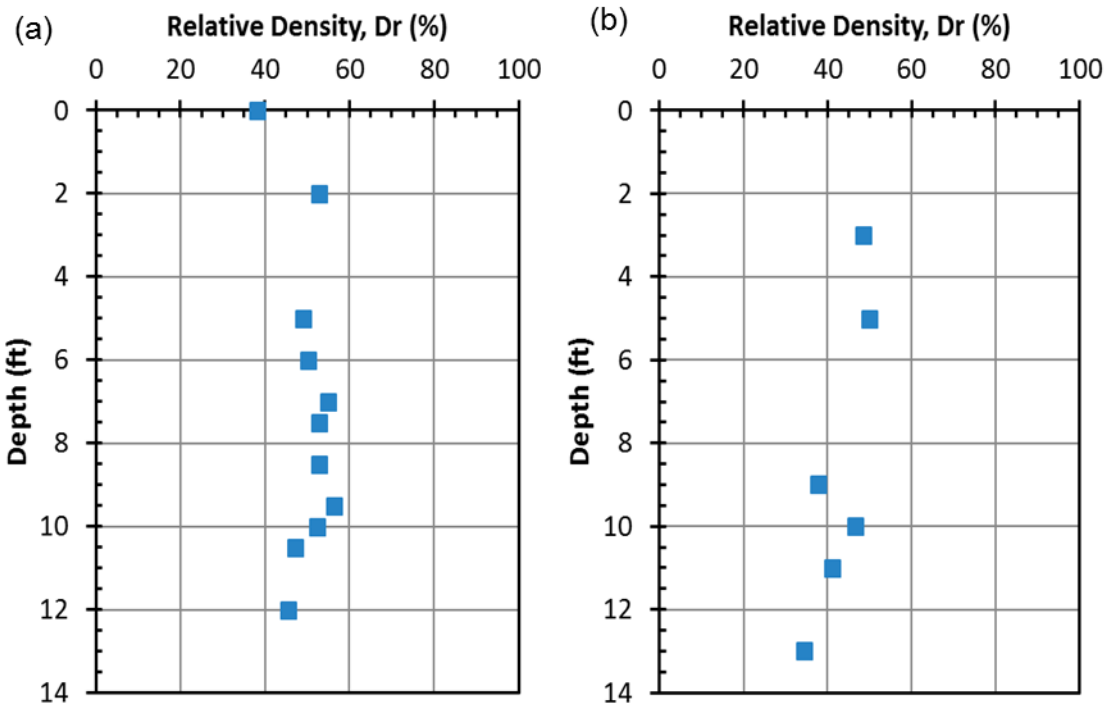

Figure 2-24 Relative Density Measurements for (a) 4ft and (b) 3ft-Drain Spacing From Bucket Samples Taken During Filling (Oakes, 2015).

The relative density was typically between 40 and 50% based on the reported minimum and maximum void ratios; however, investigations indicate that this density is likely lower as will be discussed subsequently, in section 3.4.2. Before each of the three rounds of testing a Cone Penetration (CPT) test was conducted to define the soil properties and document potential densification, Figure 2-25 and Figure 2-26. A pulley system above the box provided the force to drive the CPT.

Table 2-2 Properties of F55 Ottawa Sand Used in the Laminar Shear Box (Oakes, 2015)

Parameters	Values
FC (%)	0
[1] e_{max}	0.800
[2] e_{min}	0.608
D_{10} (mm)	0.161
D_{30} (mm)	0.201
D_{50} (mm)	0.230
D_{60} (mm)	0.245
[3] C_u	1.522
[4] C_c	1.024

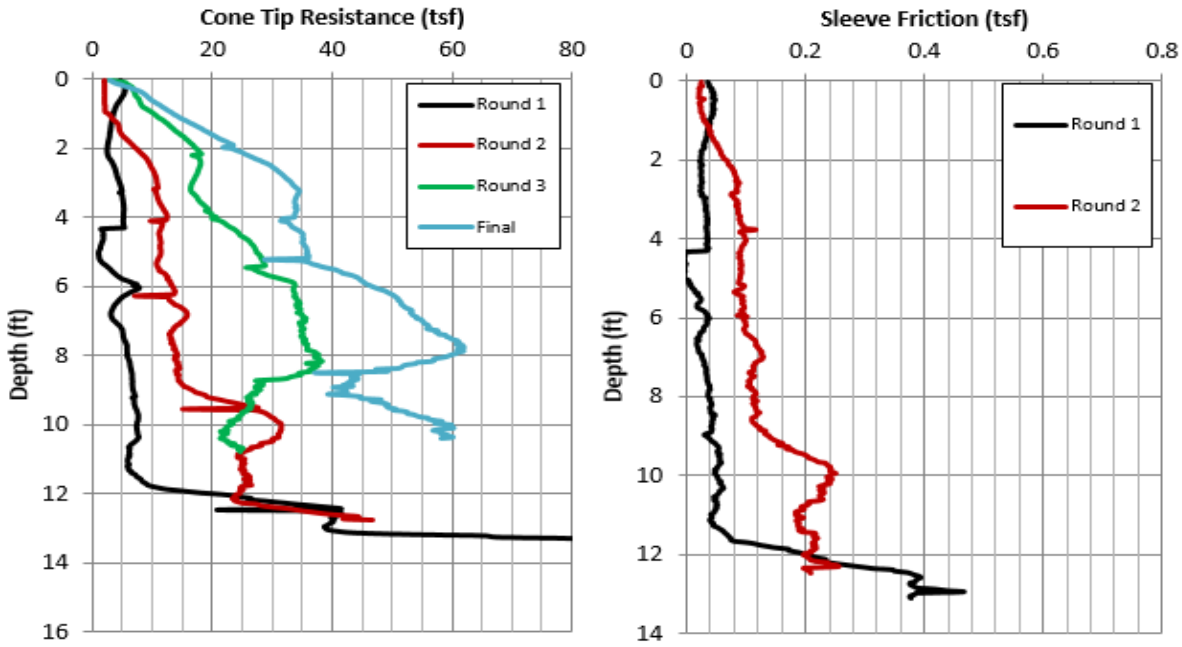

Figure 2-25 CPT Cone Tip Resistance Values for 4ft Test (Oakes 2015).

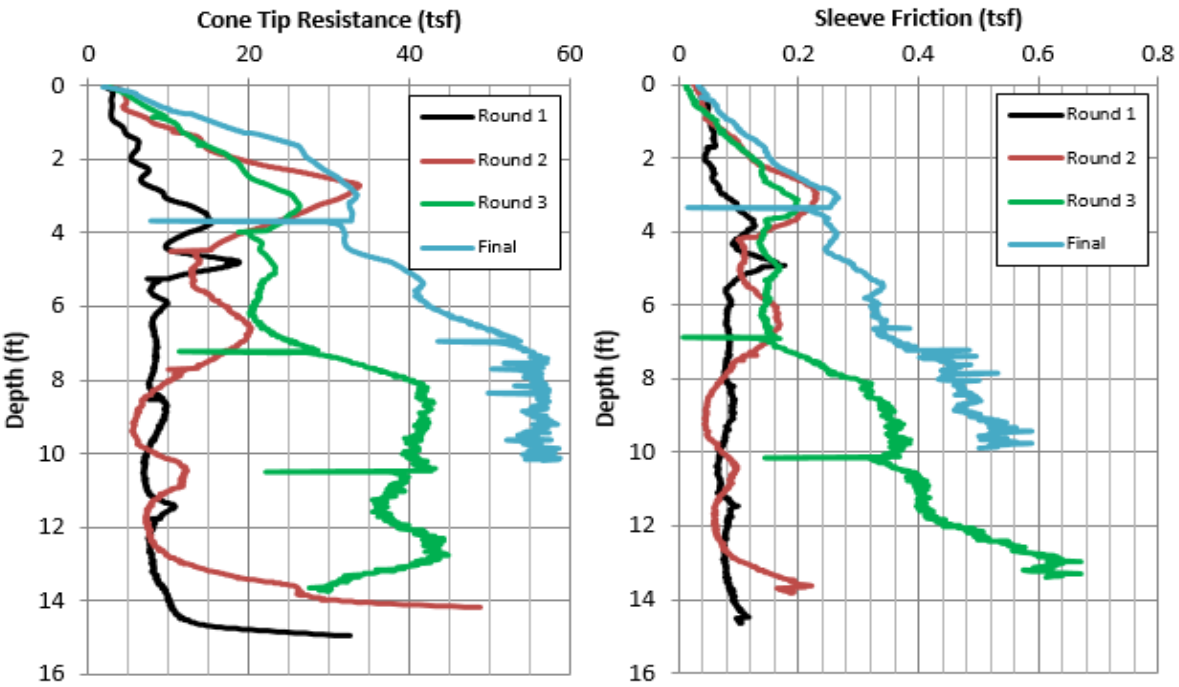

Figure 2-26 CPT Cone Tip Resistance for 3ft Test (Oakes 2015).

Hydraulic conductivity was measured, using the slotted pipes illustrated in Figure 2-27 and Figure 2-28. Horizontal hydraulic conductivity was calculated from a constant head horizontal borehole permeability test. The flow rate necessary to keep the water level at the top of the pipe was measured and hydraulic conductivity was computed for each segment of slotted pipe. For the 4 ft drain spacing, measurements were only made before the shaking tests started and at two depth intervals, 4.5 to 9.5 ft and 9.5 to 14.5 ft. The measured permeability was 0.07cm/s for the upper level and 0.05cm/s for the lower level. For the 3 ft drain spacing, measurements were made before and after each round of shaking, at three depth intervals 0-5ft, 5-10ft, and 10-15ft.

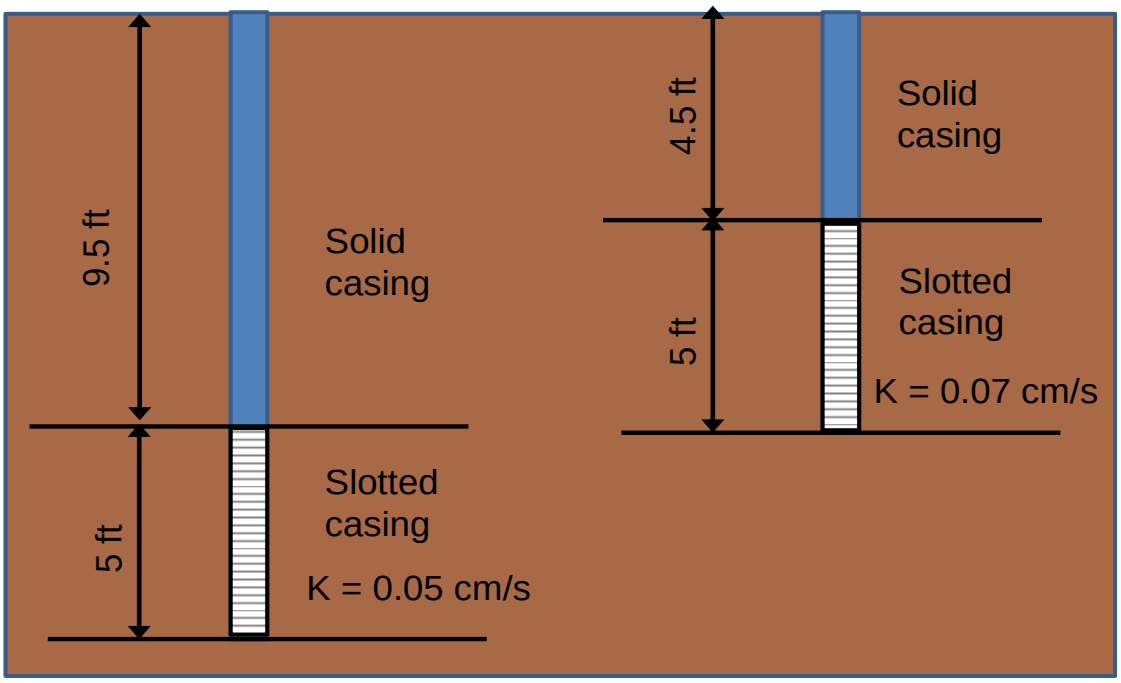

Figure 2-27 Layout of Slotted Casing for Hydraulic Conductivity Test, (4ft Drain Spacing) (Oakes, 2015).

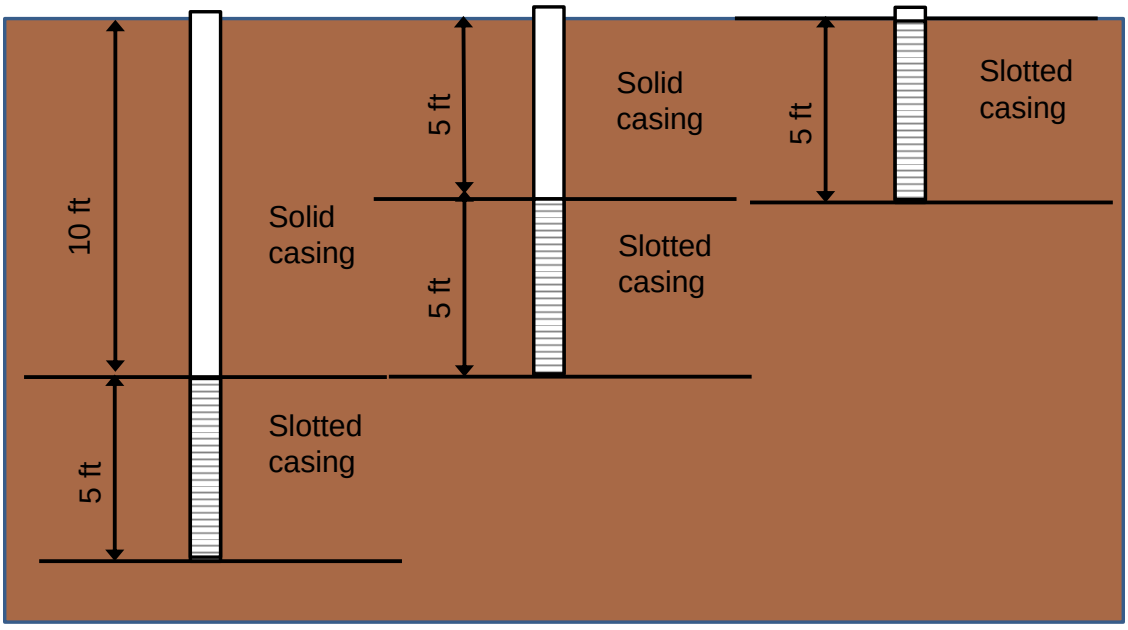

Figure 2-28 Layout of Slotted Casing for Hydraulic Conductivity Test (3ft Drain Spacing). (Oakes, 2015).

For the 3 ft drain tests, hydraulic conductivity was measured at three depth intervals and measurements were taken before each round of testing to evaluate potential changes with densification. As shaking progressed, the soil became denser, and less prone to liquefaction. This reduced the hydraulic conductivity, as shown by the borehole permeability tests conducted between subsequent rounds of shaking for the 3ft spacing experiment, Table 2-3.

Table 2-3 Hydraulic Conductivity Measurements of 3ft Test

	Horizontal Hydraulic Conductivity (cm/sec)			
Depth Interval (ft)	Round 1	Round 2	Round 3	Average
0-5	0.064	0.043	0.036	0.0477
5-10	0.045	0.032	0.029	0.0353
10-15	0.039	0.032	0.028	0.0330
Average	0.049	0.036	0.031	0.0387

2.3.4 Shake Accelerations and Load Rate

The shake tests imposed acceleration cycles at a frequency of 2 cycles per second for 7.5 seconds, equaling 15 cycles at the base of the laminar shear box. This frequency was used because all tests by previous researchers using the facility used this frequency. It was desirable for Oakes (2015) to be able to compare his results to these other studies. A frequency of 2 cycles/second is more rapid than many earthquakes, when counting only large shear motions. Rapidly recurring cycles with a medium acceleration places more demand on the drains than an earthquake with a few strong accelerations, as indicated previously in Figure 2-6. Also, 15 uniform cycles correspond to a M_w7.5 quake, according to the table produced by Seed et al. (1975). Each of the three rounds of testing had shake tests with peak accelerations of 0.05g, 0.1g, and 0.2g at the base of the box, as shown in Figure 2-29.

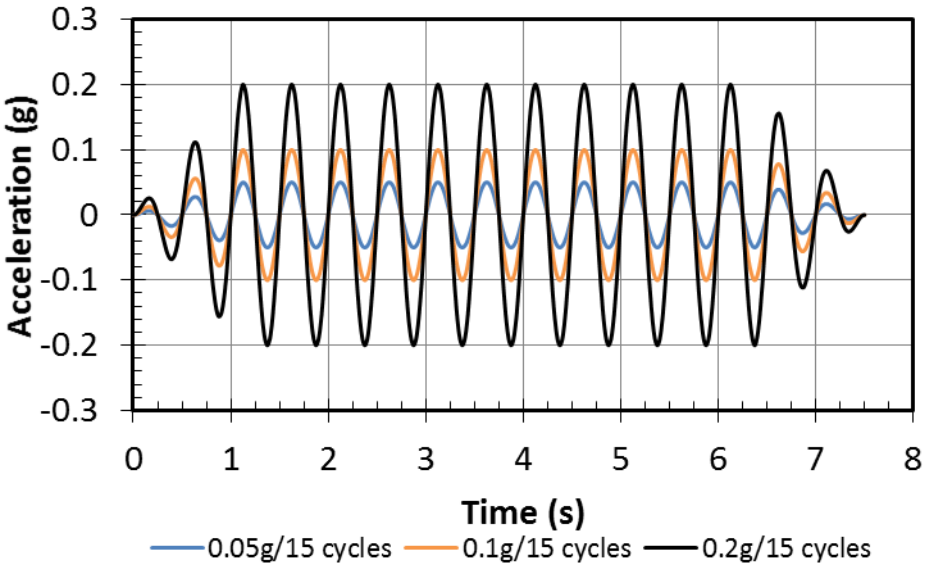

Figure 2-29 Idealized Plot of Shake Table Acceleration Levels.

2.3.5 Test Results and Conclusions

In his thesis Oakes (2015) presents plots of the excess pore pressure ratio (PPR) or (R_u), and acceleration plots at various depths of the laminar shear box experiment. Figure 2-30, Figure 2-31, and Figure 2-32, show the acceleration plots on the left, and R_u on the right. The horizontal lines running across the page correspond to the labeled depths. The centerline of each acceleration plot is aligned with the base of a R_u vs. time plot. The base of each R_u plot is at the depth of the piezometer that made the reading. There are 18 such plots, 9 each for the 4ft and 3ft spacing tests, respectively. Only 3 plots are shown in this section, the remainder are in Appendix C. Parent Study R_u Plots.

Several trends were identified from the results. Pore pressures dissipate rapidly after shaking stops at 7 seconds. The R_u values are higher in the shallow layers and lower in the deeper layers. This agrees with centrifuge test results (Brennan & Madabushi, 2002) which found that deeper layers must drain before upper layers can drain. Looking at successive rounds of testing, it can be seen that pore pressures are lower for each new shake test at a particular acceleration. This indicates that the soil is densifying, and thus becoming more resistant to

liquefaction. Another observable behavior is the oscillation of R_u in the later rounds. This is evidence that the soil has become dense enough that the sand is dilating at larger strain levels, not continually contracting. High shear forces in a denser soil at low confining pressure tend to force the particles apart towards a less dense arrangement. This induces a negative pore pressure for undrained conditions, and increases the effective stress for a moment which increases shear strength, before the soil contracts again and induces a high R_u value. This is the behavior that is evident in the later rounds of testing.

Curves showing the measured settlement vs. test number for the tests with drains are shown in Figure 2-34. The PVD-1 and PVD-2 curves are for the 3ft and 4ft drain spacing test, respectively. The plot indicates greater settlement for higher accelerations, but less settlement for each successive round. The LG1 and IPS1 curves in Figure 2-34 represent settlement for tests performed without drains. The settlement with drains is about 30 to 40% lower than without drains. This result is consistent with results from centrifuge tests reported in Section 2.2.4.

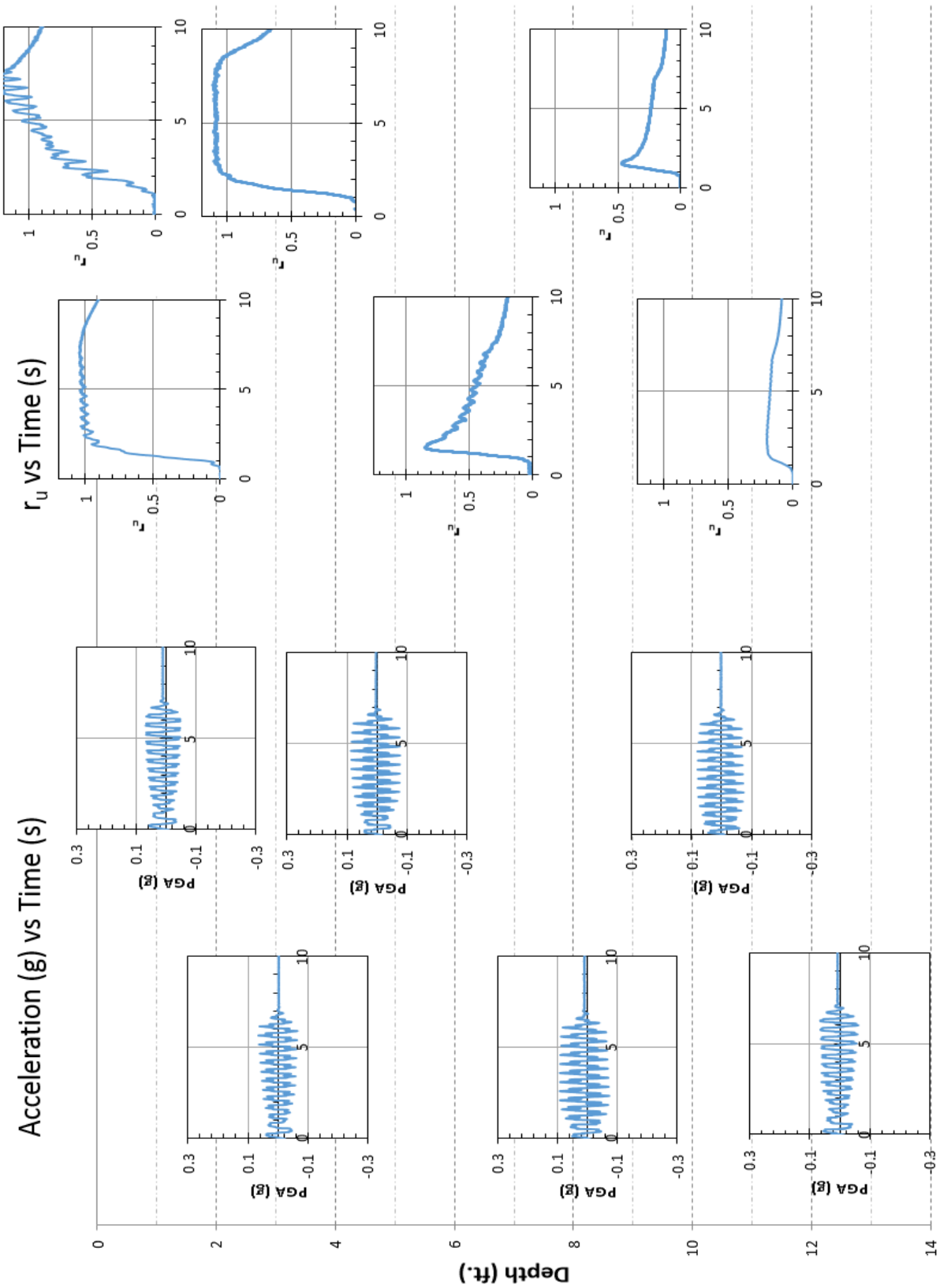

Figure 2-30 Acceleration vs. Time Paired with Excess Pore Pressure Ratio vs. Time for Round 1, a_{max} = 0.05

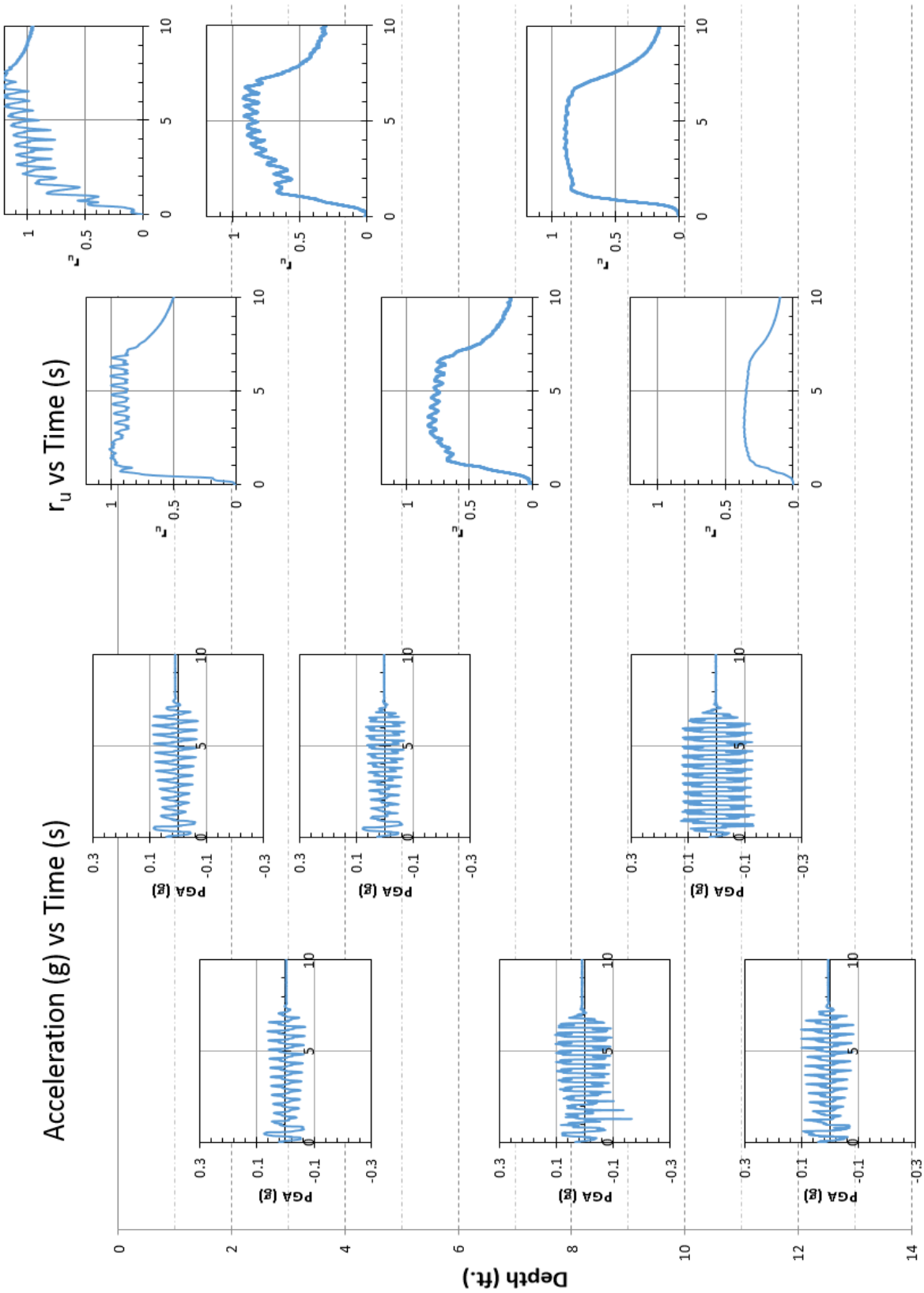

Figure 2-31 Acceleration vs. Time Paired with Excess Pore Pressure Ratio vs. Time for Round 1, a_{max} = 0.1g

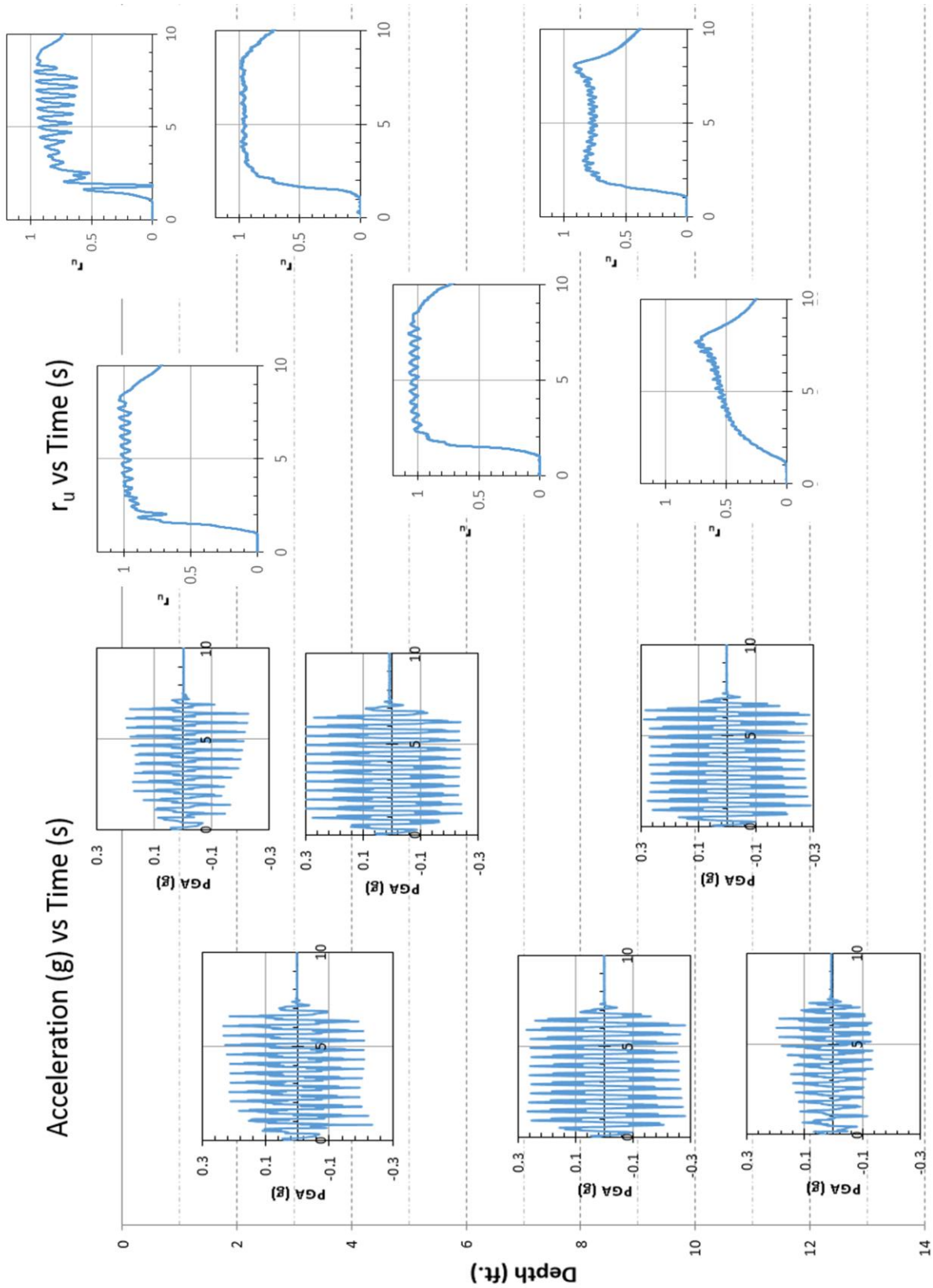

Figure 2-32 Acceleration vs. Time Paired with Excess Pore Pressure Ratio vs. Time for Round 1, a_{max} = 0.2g

For each shake of the laminar shear box, the settlement was measured by each of three methods. These values represent the total settlement for each shake, and are shown in Table 2-4 and Table 2-5. The column on the left edge of the table shows which round of testing and the acceleration level for each shake tests in descending order, there were nine tests.

Table 2-4 Settlement Measured by Different Methods for 4ft Test (Oakes, 2015).

		Average Sondex (in)	Average string pot (in)	Water volume (in)
Round 1	0.05	1.32	1.89	#N/A
	0.1	1.80	2.03	1.94
	0.2	1.68	2.64	2.88
Round 2	0.05	0.72	0.90	0.94
	0.1	0.84	1.22	1.36
	0.2	1.56	1.39	1.83
Round 3	0.05	0.36	0.46	0.47
	0.1	0.60	0.67	0.65
	0.2	1.08	1.19	1.02

Table 2-5 Settlement Measured by Different Methods for 3ft Test (Oakes, 2015).

		Average Sondex (in)	Average string pot (in)	Water volume (in)
Round 1	0.05	1.74	1.83	2.14
	0.1	1.92	2.78	2.52
	0.2	3.36	3.20	3.18
Round 2	0.05	0.84	0.88	0.88
	0.1	1.02	1.63	1.48
	0.2	1.74	2.30	2.08
Round 3	0.05	0.36	0.58	0.49
	0.1	0.66	1.10	0.66
	0.2	0.78	1.29	1.15

The “Average Sondex” column gives the values measured by the lowering an instrument down a special tube. This accordion style tube has evenly spaced metal rings along its length, that compress vertically with the sand as it settles during shaking. The “Average String Pot” column gives the average of the values measured by each of three string potentiometers attached to a settlement plate on the soil surface. The “Water Volume” column is total settlement back-calculated from the volume of water collected from the soil surface after it came up from the drains during each shake test. Settlement values presented here will be used later on to back calculate the initial soil compressibility for use in modeling, in Section 3.4.3.

Measurements from the Sondex tube made it possible to measure how much each layer of the soil had changed in thickness. Knowing this allowed the vertical strain at various depths to be computed, and in turn the volumetric stain too, since changes in size and shape were constrained by the box. Strain is later used to back calculate soil compressibility, in Section 3.2.2. The percent of volumetric strain vs. depth is shown in Figure 2-33 for Round 1 of the 4ft spacing experiment. Additional plots of strain vs. depth are available in Oakes’s (2015) thesis.

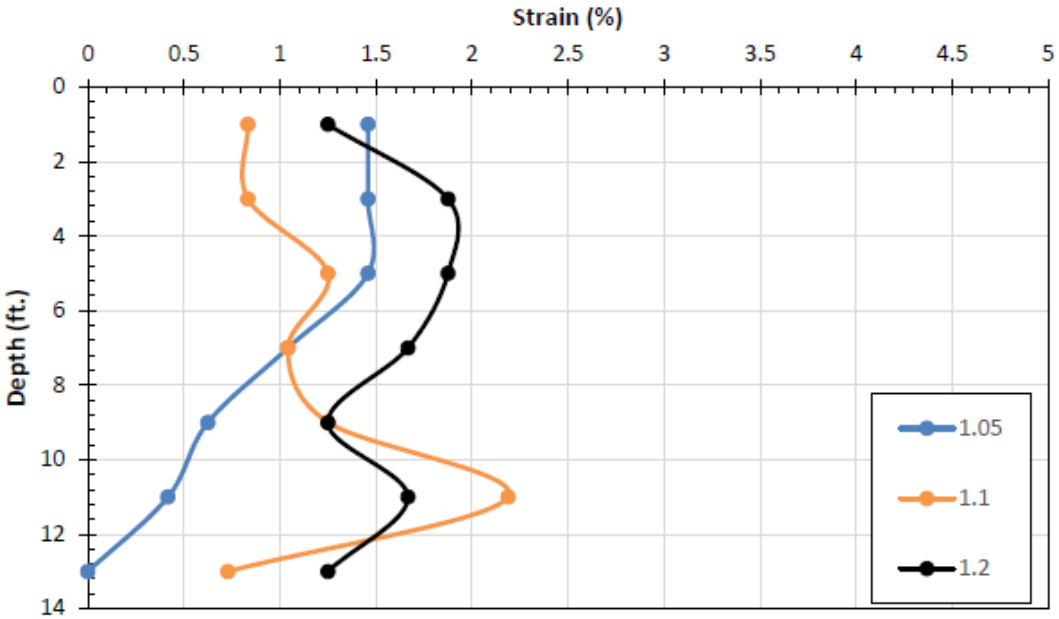

Figure 2-33 Profiles of Strain vs. Depth Using Smoothed Sondex Measurements for Round 1. (4ft Drain Spacing).

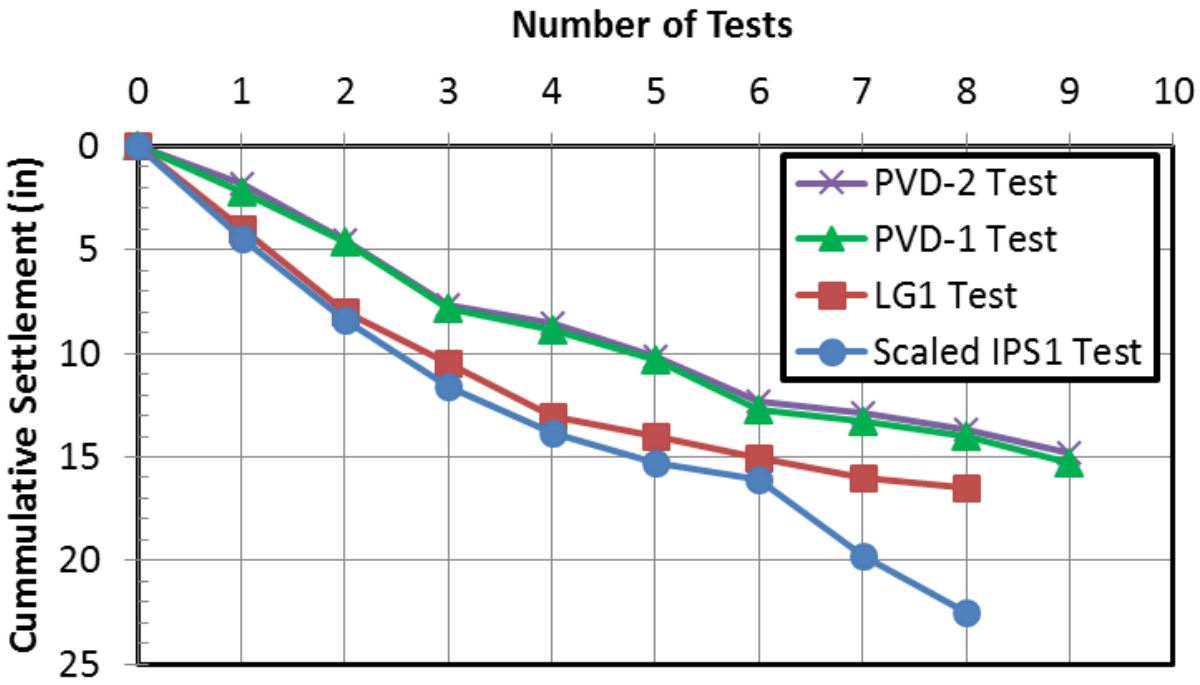

Figure 2-34 Settlement with Drains: PVD-1, PVD-2 (Oakes, 2015), and without Drains: LG1, Scaled IPS1 (Yegian, 2015; Thevanayagam, personal communication 2015).

Based on the testing and analysis of the laminar shear box test with drains, Oakes (2015) drew several conclusions.

1. Excess pore pressures dissipated rapidly after shaking, with higher density in later rounds of testing increasing the rate of dissipation

2. Excess pore pressures dissipated significantly faster than previous laminar shear box testing without drains, taking seconds rather than minutes for pore pressures to fully dissipate.

3. Higher acceleration caused more settlement and caused settlement deeper in the soil profile.

4. Settlement was reduced by 20-64% when compared to previous laminar shear box testing without drains. This is consistent with previous results from centrifuge testing.

5. Drains spaced closer together are more effective at reducing excess pore pressures.

3 METHODS OF INVESTIGATION

As described previously, this report evaluates the ability of the computer program FEQDrain (Pestana et al., 1997) to model the behavior observed in the shaking tests with prefabricated drains performed with the laminar shear box at the University at Buffalo. The behavior includes pore pressure generation, pore pressure dissipation, and resulting ground settlement. In this chapter, Section 3.1 gives an overview of how the FEQDrain modeling program works. Section 3.2 explains the most important variables and their mathematical formulation. Section 3.3 describes how the soil profile was divided into finite elements. Section 3.4 explains how values were chosen for these variables. Section 3.5 and 3.6 provides all other needed input values. Section 3.7 explains how data processing was done.

3.1 Finite Element Model Overview

The performance of potentially liquefiable layers with prefabricated vertical drains is commonly analyzed using the computer program FEQDrain. FEQDrain uses an axi-symmetric finite element model of the soil profile and composite drain system. The program models an individual drain within a grid of drains using a "radius of influence" or concept based on the drain spacing, also called a "unit-cell" model. The program computes the excess pore pressure ratio for each soil layer within the radius of influence. It does this by computing how much pressure is generated by the earthquake shaking in a given time interval and then subtracting how much pressure has dissipated from water flowing to the drain in the same time interval.

The program is able to compute head loss in the drain and also considers storage volume of the drain. Also, it can account for the non-linear increases in modulus of soil compressibility resulting from elevated pore pressure, which it can factor into its analysis. Besides calculating

pore pressure response, the program can calculate settlement associated with drainage and dissipation of pore pressure.

3.2 Mathematical Formulation

The reaction of the soil to seismic motions is modeled by FEQDrain using the solution to the following equation

$$\left(\nabla \mathbf{k} \frac{\nabla u}{\gamma_w}\right) = m_v \left(\frac{\partial u}{\partial t} - \frac{\partial u_g}{\partial t}\right) \quad (1)$$

Where: k = hydraulic conductivity

u = pore pressure

∇= space gradient operator

γ_w = unit weight of water

m_v = coefficient of volumetric compressibility

u_g = excess pore pressure generated by cyclic loading

t = time

The derivation of Equation 1 is explained in Pestana et al. (1997) and will be omitted here. But several supporting assumptions must be met for Equation 1 to be valid. These assumptions are (1) continuity of flow and that flow is governed by Darcy's law, (2) the soil is completely saturated, and (3) the change in porosity due to seismically induced compression is equivalent to the change in volumetric strain.

Naturally deposited soils often contain thin layers of finer-grained material intermixed with coarser-grained material, causing the soil to exhibit anisotropic flow characteristics in the

vertical and horizontal directions. Flow through anisotropic soils involves different horizontal and vertical hydraulic conductivities, k_h and k_v. For an axi-symmetric case, as assumed by the program, Equation (1) becomes

$$\frac{\partial}{\partial r}\left(\frac{k_h}{\gamma_w}\cdot\frac{1}{r}\frac{\partial u}{\partial r}\right)+\frac{\partial}{\partial z}\left(\frac{k_v}{\gamma_w}\cdot\frac{\partial u}{\partial z}\right)=m_v\left(\frac{\partial u}{\partial t}-\frac{\partial u_g}{\partial t}\right) \tag{2}$$

To solve Equation (2), values for m_v and u_g must be calculated for each time step of the simulation.

3.2.1 Pore Pressure Generation

Pore pressure generation is modeled in FEQDrain by transforming irregular seismic loading into an equivalent number of uniform cycles occurring within a specified length of time, as described by Seed et al. (1975a)

$$\frac{\partial u_g}{\partial t}=\frac{\partial u_g}{\partial N}\cdot\frac{\partial N}{\partial t} \tag{3}$$

$$\frac{\partial N}{\partial t}=\begin{cases}N_{eq}/t_d & (0<t\le t_d)\\ 0 & (t>t_d)\end{cases} \tag{4}$$

where: N = the accumulated number of cycles at time t

N_{eq} = equivalent number of uniform cycles

t_d = time period of shaking (typically equivalent to time of strong motion)

Extensive laboratory testing using cyclic triaxial and simple shear tests has shown that the relationship between u_g and N can be expressed by

$$r_u = \frac{u_g}{\sigma_o'} = \frac{2}{\pi}\arcsin\left(\frac{N}{N_l}\right)^{\frac{1}{2\theta}} \quad (5)$$

where: R_u = excess pore pressure ratio
σ'_o = initial mean effective stress under triaxial conditions or the initial vertical stress for simple shear conditions
N_l = number of uniform stress cycles causing liquefaction in a cyclic undrained test
θ = an empirical constant, typically equal to 0.7

As shown in Figure 3-1 this equation can be represented graphically by a plot with N/N_l on the horizontal axis, a generation function curve, and the resulting excess pore pressure ratio R_u, on the vertical axis.

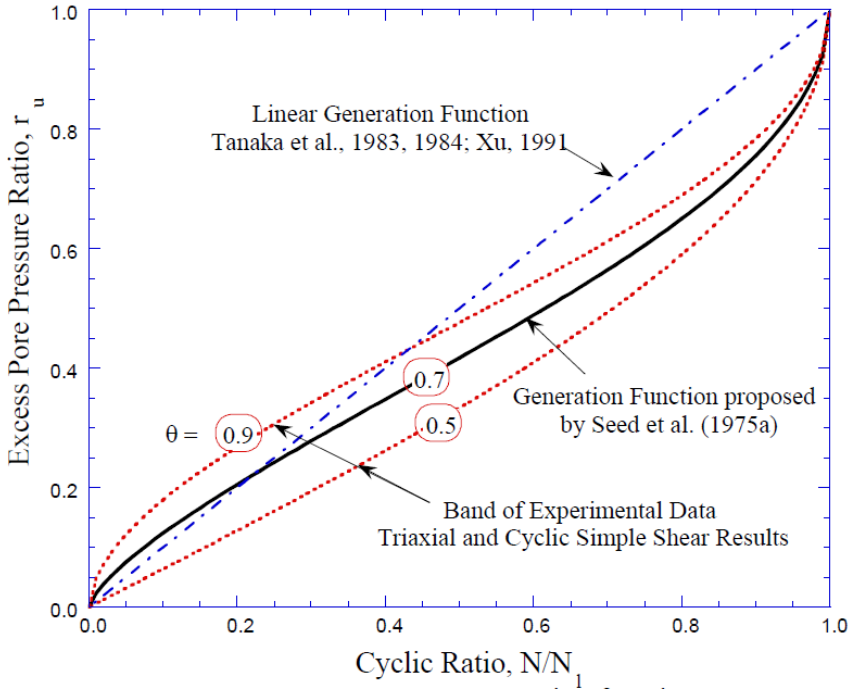

Figure 3-1 Rate of Pore Water Pressure Build-up after N Cycles Relative to the Number of Cycles Required to Induce Liquefaction (N_L) from Cyclic Tests.

Taking the derivative of Equation (5) we obtain

$$\frac{\partial u_g}{\partial N} = \frac{\sigma_o'}{\theta \cdot \pi \cdot N_l} \cdot \frac{\tan(\pi \cdot r_u/2)}{\sin^{2\theta}(\pi \cdot r_u/2)} \quad (6)$$

Substituting Equation (4) and Equation (6) back into Equation (3), the rate of excess pore pressure generation becomes

$$\frac{\partial u_g}{\partial t} = \frac{\sigma_o'}{\theta \cdot \pi} \cdot \left(\frac{N_{eq}}{N_l \cdot t_d}\right) \cdot \frac{\tan(\pi \cdot r_u/2)}{\sin^{2\theta}(\pi \cdot r_u/2)} \quad (7)$$

The rate of excess pore pressure generation, $\partial u_g/\partial t$, depends on the previous cyclic loading history represented by the current value of pore pressure ratio, r_u.

3.2.2 Soil Compressibility

FEQDrain computes the change in volumetric compressibility, m_v, caused by increases in R_u, using the equation developed by Seed et al. (1975a).

$$\frac{m_v}{m_{vo}} = \frac{\exp(y)}{1 + y + y^2/2} \geq 1 \quad (8)$$

where: $y = a \bullet r_u^b$

$a = 5(1.5\text{-}Dr)$

$b = 3(4)^{-Dr}$

Dr = initial relative density

m_{vo} = initial value of volumetric compressibility = $\Delta\varepsilon/\Delta\sigma'$

The relationship formed by Equation (8) is charted in Figure 3-2 for different values of relative density. Before an earthquake, the soil has some relative density, and an excess pore water pressure ratio of zero, (r_u= 0). When seismic motions cause pore pressures to rise, the soil becomes more compressible. For low values of pore pressure ratio, r_u, it has been found that compressibility, m_v is essentially constant. But, for pore pressure ratios larger than 50-60%, m_v is found to increase significantly with increases in the pore pressure ratio as shown in Figure 3-2. During post-earthquake analysis, the value of m_v does not decrease from the highest value obtained, as suggested by Seed et al. (1975a).

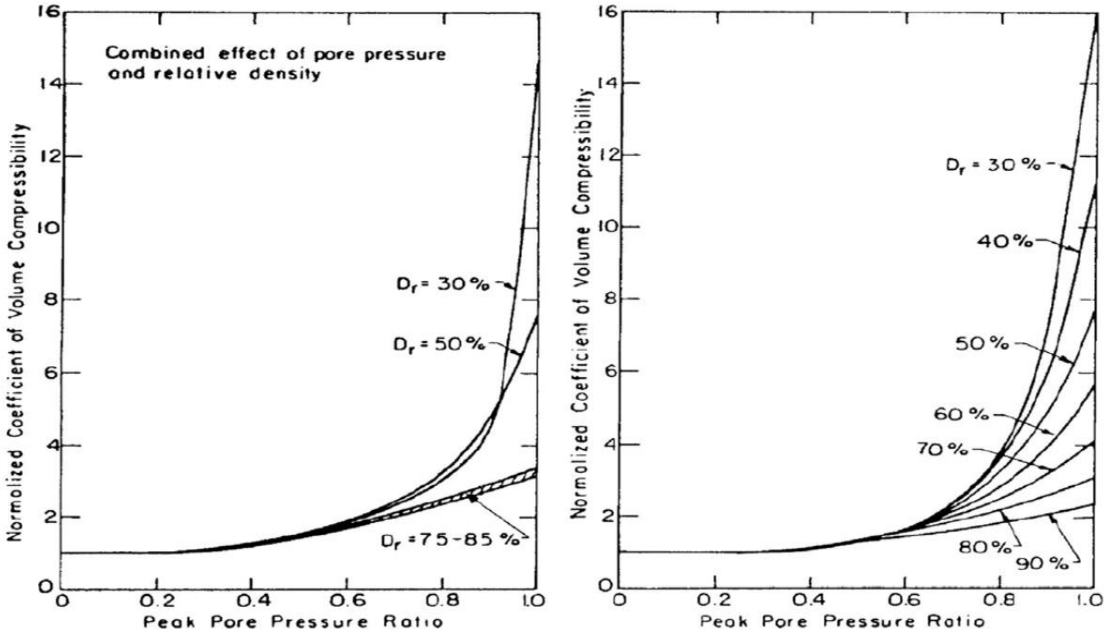

(a): Measured compressibility of saturated sands following pore pressure build-up (after Lee & Albaisa, 1974)

(b): Theoretical relationships between compressibility of sands and pore pressure build-up (after Seed et al.,1975a)

Figure 3-2 Increase in Soil Compressibility with Increased Pore Pressure Ratio.
(a) Measured Change in Compressibility (Lee & Albaisa, 1974),
(b) Theoretical Change in Compressibility (Seed et al., 1974)

3.2.3 Boundary Conditions

Figure 3-3 shows the typical configuration of a vertical drain installed in a potentially liquefiable layered soil profile. The soil profile is composed of *n* soil layers with individual properties up to a depth *H*. A single vertical drain reaches the full depth of the soil layer. Since

FEQDrain cannot model partially penetrating drains, the soil profile modeled by FEQDrain must not extend below the bottom of the drain. It is assumed that the soil layers below the bottom of the drain make no contribution to the drain, thus FEQDrain models the bottom of the drain and soil profile as a no-flow boundary.

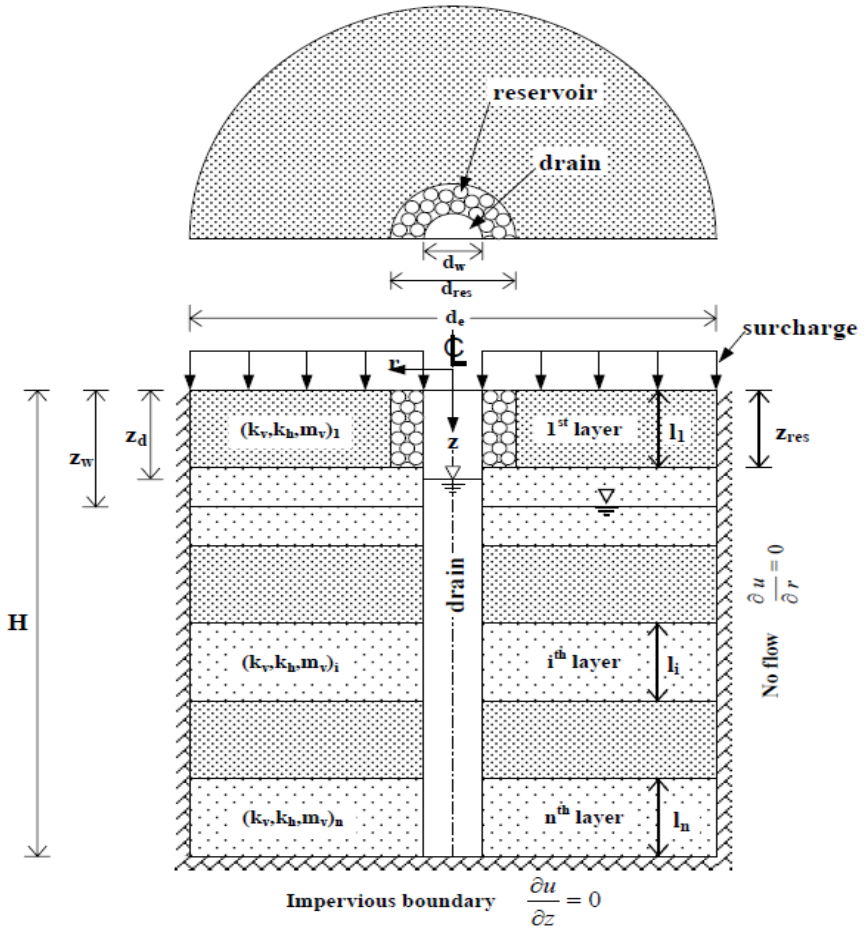

Figure 3-3 Typical Geometry and Boundary Conditions for Analysis by FEQDrain (Pestana et al., 1997).

Seismic motions cause hydraulic gradients to form towards drains as excess pore pressures build-up in the soil away from the drain. This gradient causes flow towards the drain and dissipation of pressure. The radial extent of this gradient is called the zone of influence, or effective diameter (d_e) in Figure 3-3. The drain capacity is limited by the hydraulic conductivity of the surrounding soil, and the strength and time duration of the shaking. As the zone of

influence reaches outward, it will eventually intersect with the zones of adjacent drains. At this intersection boundary, there will be no additional flow from outside, and so the radial limit of the zone of influence can be modeled as a no-flow boundary.

In many soil profiles the ground water level is lower than the drain height. As water enters the drain and the water level within the drain rises, some water can enter the unsaturated soil. This reservoir slows the rise of water in the drain and slows the associated increase in static pressure in the drain. The volume of water entering the drain equals the volume of water expelled from the saturated soil. When this volume exceeds the combined volume of the drain and reservoir, the water will overflow from the top of the drain.

3.2.4 Assumptions and Limitations

A number of simplifying assumptions and limitations are inherent in the finite element models generated.

Assumptions of the modeling process:

- Drains are surrounded by other drains.
- Pore pressure ratios continue increasing until shaking stops or equilibrium is reached.
- Variable soil compressibility, since pore pressure ratios may exceed r_u =0.6
- Sand infiltration is not significant, but head loss at the drain is accounted for.
- To better match laminar box test conditions, unit weight and relative density are adjusted for each subsequent shake, to account for the increasing soil density. This is done by volumetric analysis, using settlement data and CPT measurements.

Limitations inherent in the modeling process:

- Soil properties are assumed to be constant and uniform within and across a layer.

- Coefficient of Soil Compressibility calculations are based on settlement measurements, which may have been affected by proximity to sides of the laminar box and inaccuracies in measurement.

3.3 Discretization of Flow Region

The sand in the laminar box was 14.5 feet thick for the test with the 4 ft drain spacing and 16 ft thick for the test with the 3 ft drain spacing. For analysis purposes, the relatively uniform sand in the laminar box was typically divided into six or seven horizontal layers. Each layer was typically 2.5 ft thick and had 5 vertical sub-layers 0.5 ft thick. This arrangement allowed soil properties to be varied by layer for each piezometer. Ten radial increments were used beyond the edge of the drain out to the mid-point between drains for the 4 ft and 3 ft drain spacing tests. Plots of the finite element grids for both tests used in the FEQDrain program are provided in Figure 3-4.

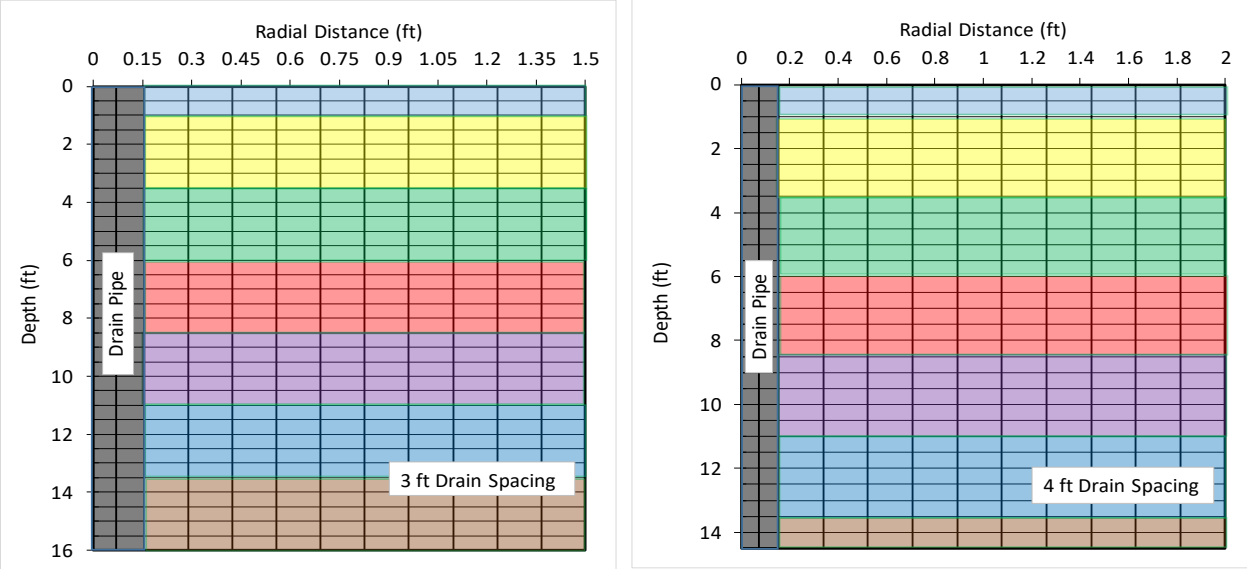

Figure 3-4 Finite Element Models of the Drain and Sand Profile in FEQDrain for the 3 ft and 4 ft Drain Spacing Tests.

3.4 Selection of Soil Input Parameters

Soil input values used in the modeling for this report are generally based on measured values from the laminar shear box testing done by Oakes (2015). In cases where measured values

were not available, estimates were made based on engineering principles. Where measurements were expressed as SI units, they have been converted to Imperial units.

The most important soil parameters for modeling are horizontal hydraulic conductivity (k_x), vertical hydraulic conductivity (k_y), soil compressibility (m_v), relative density (D_r), and number of cycles to liquefaction (*N-Liq*) for a given acceleration level. These properties are described in the following sections along with the procedures applied for selecting appropriate input values.

As described previously, the sand in the laminar box was a clean uniform fine sand which classifies as a poorly graded sand (SP) according to the Unified Soil Classification System.

Figure 3-5 provides a plot showing the grain size distribution curve for the sand.

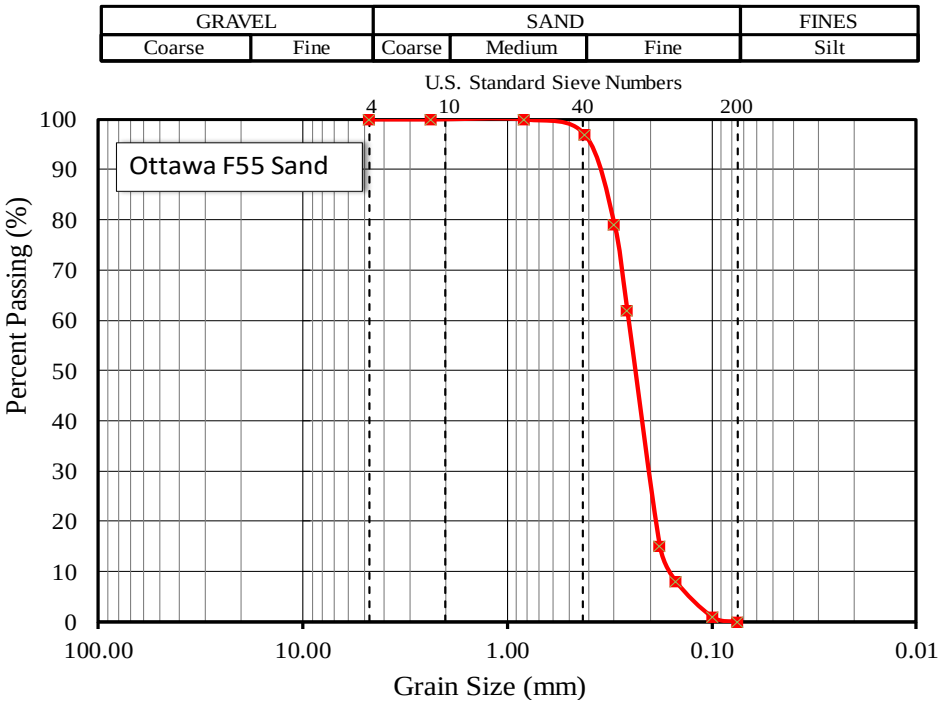

Figure 3-5 Grain-Size Distribution Curve for Ottawa F55 Sand in the Laminar Shear Box.

The sand is an Ottawa sand with a designation of F55. Ottawa sand is a silica sand composed of well-rounded quartzite particles. Useful grain size parameter data obtained from the gradation curve are summarized in Table 3-1 along with minimum and maximum void ratios.

Table 3-1 Properties of F55 Ottawa Sand Used in the Laminar Shear Box.

Parameters	Values
FC (%)	0
[1] e_{max}	0.800
[2] e_{min}	0.608
D_{10} (mm)	0.161
D_{30} (mm)	0.201
D_{50} (mm)	0.230
D_{60} (mm)	0.245
[3] C_u	1.522
[4] C_c	1.024

3.4.1 Hydraulic Conductivity

Hydraulic conductivity desribes the average rate or speed at which water flows through soil for a unit hydraulic gradient. The hydraulic conductivity of the sand in the laminar shear box was calculated from constant head horizontal borehole permeability tests. These tests were performed using slotted vertical PVC pipes, embedded in the sand prior to sand placement specifically for this purpose. For the 4 ft drain spacing, measurements were made at two depth intervals, 4.5 to 9.5 ft and 9.5 to 14.5 ft, before the shake tests started and were not repeated. The measured permeability was 0.07 cm/s for the upper level and 0.05 cm/s for the lower level. For the tests with a 3 ft drain spacing, measurements were made at three depth intervals 0-5 ft, 5-10 ft, and 10-15 ft, before and after each round of shaking.

The values of hydraulic conductivity measured prior to each round of shaking are shown in Table 3-2. Measured conductivity from the 3ft experiment is shown in the upper half of the table while values for the 4ft experiment are shown in the lower half of the table. Considering that the hydraulic conductivity of a clean sand can vary over two orders of magnitude, the agreement between hydraulic conductivity for the 3 ft and the 4 ft tests is quite good. The values are also similar to the range of hydraulic conductivity (0.05 to 0.07 cm/sec) measured by Yegian and his students while injecting water into the laminar box (Yegian, 2013, personal communication). The measured hydraulic conductivity in the 3 ft tests decreased with each round of shaking. Relative to the initial values, the hydraulic conductivity decreased about 30% after the first round and 40% after the second round. The reduction in hydraulic conductivity was

somewhat higher at shallow depths than at deeper depths. Because similar test data was not available for the 4 ft tests, the same relative reduction in hydraulic conductivity was assumed in the analyses that were performed.

Table 3-2 Measurements of Hydraulic Conductivity

		Horizontal Hydraulic Conductivity (cm/sec)		
3ft Test	Depth Interval (ft)	Round 1	Round 2	Round 3
	0-5	0.064	0.043	0.036
	5-10	0.045	0.032	0.029
	10-15	0.039	0.032	0.028
4ft Test	Depth Interval (ft)	Round 1	Round 2	Round 3
	4.5-9.5	0.07	No Measurements	
	10-13	0.05		

Based on measured hydraulic conductivity, the Terzaghi and Peck (1948) soil properties chart (Table 3-3), characterizes the laminar shear box sand as medium grained sand. However, the particle size is actually in the range of fine sand. This somewhat higher hydraulic conductivity is likely attributable to the fact that the fines content of the sand is zero and the sand was initially in a loose condition. Figure 3-6 is a plot of hydraulic conductivity (k_h) in logrithmic scale versus depth, prior to any shaking. Each conductivity measurement is plotted at its average depth with a red diamond for 3ft values, or an orange square for 4ft values. The particle size ranges of fine and medium sand, from Terzaghi and Peck (1948), are shown by the black arrows. The measured values plot within a relatively narrow band.

Table 3-3 Coefficient of Hydraulic Conductivity for Granular Soils (Terzaghi & Peck, 1948).

Soil type	Particle size (mm)	Coefficient of hydraulic conductivity (cm/s)
Very fine sand	0.05~0.10	0.001~0.005
Fine sand	0.10~0.25	0.005~0.01
Medium sand	0.25~0.50	0.01~0.1
Coarse sand	0.50~1.00	0.1~1.0
Small pebbles	1.00~5.00	1.0~5.0

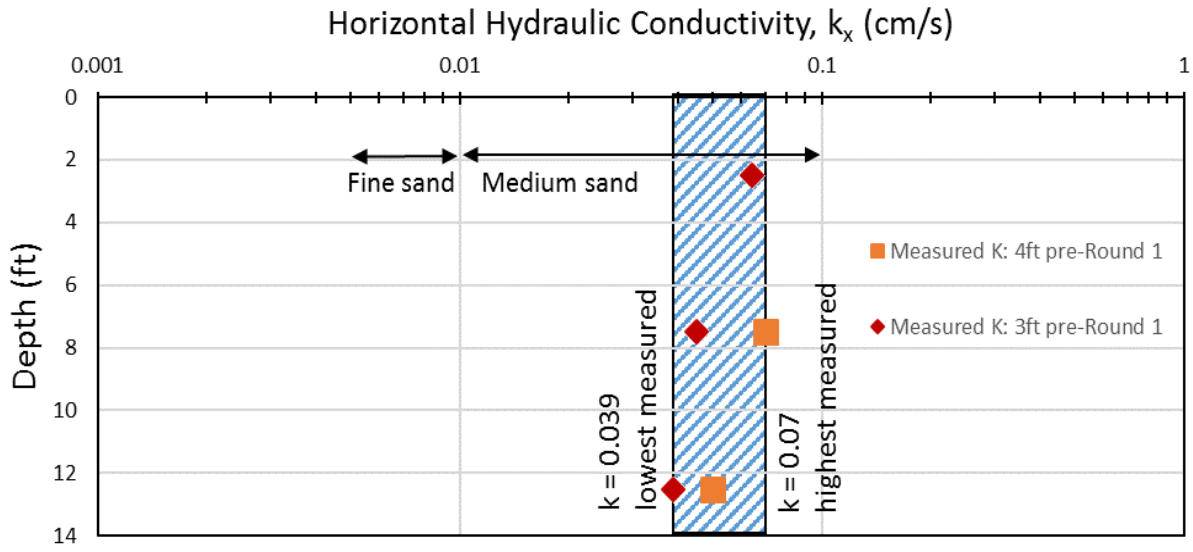

Figure 3-6 Depth Vs. Measured Hydraulic Conductivity, Prior to Shaking. Red Diamonds (3ft) and Orange Squares (4ft) are Plotted at Average Depth of the Slotted Pipe Used to Make the Measurement. Particle Size of Sands (Terzaghi & Peck, 1948) are Shown by Black Arrows.

The ratio of horizontal and vertical hydraulic conductivity was not measured in the laminar box experiment. Table 3-4 shows typical ratios of horizontal to vertical conductivity. Three types of sand are shown, along with a their typical k_h/k_v ratio. Uniform, clean sands have a ratio as low as 1.5 for natural soils.

Table 3-4 Typical Values of k_h/k_v for Sand Deposits

Description	k_h/k_v
Uniform (clean sands)	1.5~2
Moderately anisotropic (silt seams)	4~5
Highly anisotropic	10~100

For modeling purposes we assumed equal horizontal and vertical conductivity, so k_h/k_v equaled 1.0. This was an acceptible simplification because our sand had a small range of particle size and was newly deposited. Also, potential inaccuracy of vertical conductivity would have only slight effect on the numerical model. The horizontal hydraulic conductivity has a much stronger effect, than vertical conductivity, on pore pressures computed by FEQDrain when vertical drains are present (Pestana, 1997).

For modeling purposes we interpolated trends in hydraulic conductivity from Table 3-2, to create a matrix of assumed hydraulic conductivity for all shakes of the 3ft and 4ft drain spacings. Table 3-5 shows the assumed hydraulic conductivity for each shake. The upper half of the table contains values for the 3 ft experiment, the lower half of the table contains values for the 4 ft experiment. The first column of the table indicates the general horizontal soil layer. The remaining three columns correspond to Round 1, Round 2, and Round 3 of shaking. The 'shake' sub-column specifies the order and acceleration level of the specific shake. The 'k_x' sub-column specifies the interpolated conductivity value. Numbers shown in bold are measured values. Adjustments were made after each shake, based on the strength of the acceleration. The sum of past acceleration levels within that round, (0.05g, 0.15g, and 0.35g) were divided by the total sum of accelerations, 0.35g. Thus the 0.05g shake accounts for 14% of the total change of that round, and by the end of the 0.1g shake there has been 43% of the change for the round. After the 0.2g shake there has been 100% of the change in conductivity for that round. Values were assumed for the end of Round 3, in order to compute the incremental change in Round 3. Values were also assumed for Round 2 and 3 of the 4 ft expereiment based on the results from the 3 ft experiment. All values were rounded to three decimals.

Thus for numerical modeling in FEQDrain, there will be a slightly different set of hydraulic conductivity values used for each shake.

Table 3-5 Assumed Hydraulic Conductivity

3ft Test	Round 1		Round 2		Round 3	
	Shake	k_x	Shake	k_x	Shake	k_x
Top	1.05	**0.064**	2.05	**0.043**	3.05	**0.036**
	1.1	0.061	2.1	0.042	3.1	0.036
	1.2	0.052	2.2	0.039	3.2	0.035
Middle	1.05	**0.045**	2.05	**0.032**	3.05	**0.029**
	1.1	0.043	2.1	0.032	3.1	0.029
	1.2	0.038	2.2	0.030	3.2	0.028
Bottom	1.05	**0.039**	2.05	**0.032**	3.05	**0.028**
	1.1	0.038	2.1	0.031	3.1	0.028
	1.2	0.035	2.2	0.030	3.2	0.027

4ft Test	Round 1		Round 2		Round 3	
	Shake	k_x	Shake	k_x	Shake	k_x
Top	1.05	**0.070**	2.05	**0.043**	3.05	**0.036**
	1.1	0.066	2.1	0.042	3.1	0.036
	1.2	0.055	2.2	0.039	3.2	0.035
Bottom	1.05	**0.050**	2.05	**0.032**	3.05	**0.029**
	1.1	0.047	2.1	0.032	3.1	0.029
	1.2	0.040	2.2	0.030	3.2	0.028

3.4.2 Relative Density

Relative density (D_r) expresses the density state of a granular soil in relation to its loosest (D_r=0%) and densest (D_r=100%) possible states. Relative density is defined by the equation

$$D_r = (e_{max} - e) / (e_{max} - e_{min}) \quad (9)$$

where e_{max} and e_{min} are the maximum and minimum void ratios obtained according to ASTM standards and e is the in-place void ratio of the sand. Relative density has a strong effect on the liquefaction potential and compressibility of sand, and this effect is incorporated in FEQDrain.

Oakes (2013) obtained sand density data during sand placement by extracting small buckets of sand and determining the in-place void ratio. The relative density was then computed using Equation (9) based on minimum and maximum void ratios supplied by the University at Buffalo as indicated in Table 3-1. However, this approach produced D_r values which were inconsistent with the relative density from the cone penetration tests. In addition, the difference

between e_{max} and e_{min} was much smaller than suggested by several correlations. Furthermore, when the change in void ratio due to settlement was tracked throughout the testing process, the relative density eventually increased above 100% which is not reasonable. During this investigation, both e_{min} and e_{max} were re-tested using sand obtained from the laminar box during Oakes original tests. The e_{max} value was in good agreement with the value in Table 2-2, but the e_{min} value was found to be 0.48 which was considerably lower than the given value. Researchers at the University at Buffalo indicate that they have observed a change in the sand gradation and e_{min} value as the sand has been repeatedly used for shaking test during previous tests at the site (Prof. Anthony Tessari, Personal communication, 2016).

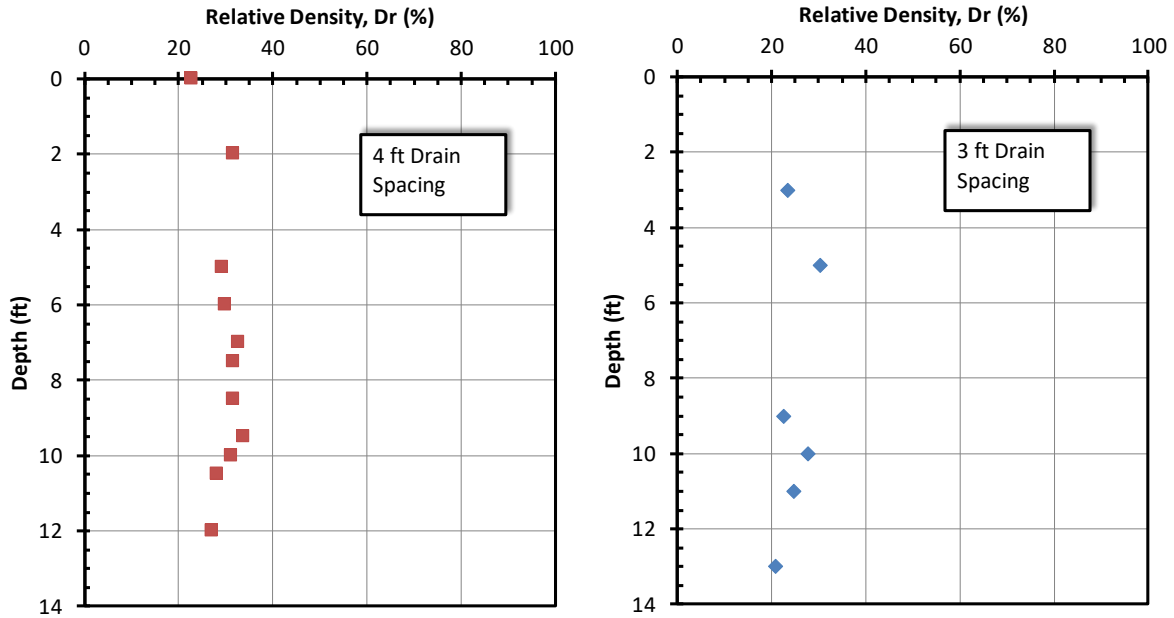

Figure 3-7 Relative Density Measurements for 4 ft and 3 ft-Drain Spacing from Bucket Samples Taken During Filling with Corrected e_{min} of 0.48.

In this study, the corrected e_{min} value has been used to compute the relative density. Relative density profiles for the tests with the 4-foot and 3-foot drain spacings are presented in Figure 3-7. Relative density is typically between 25-30% and is relatively consistent with depth.

Relative density was also estimated from the CPT cone tip resistance using correlations developed by Kulhawy and Mayne (1990). Relative density profiles are presented in Figure 3-8 for the 4-foot and Figure 3-9 for the 3-foot drain spacing tests at the start of each round of testing and at the conclusion of testing. The relative density profiles from the CPT generally indicate the relative density for each round of testing is progressively increasing as expected based on

reconsolidation settlement measurements. The relative density obtained from the CPT soundings predict somewhat lower values of relative density than what was measured from the density buckets. It is unclear if this is attributable to failure of the CPT to account for the very compressible nature of the sand structure after deposition or potential arching across the sand box which may have reduced the vertical effective stress and hence the cone tip resistance.

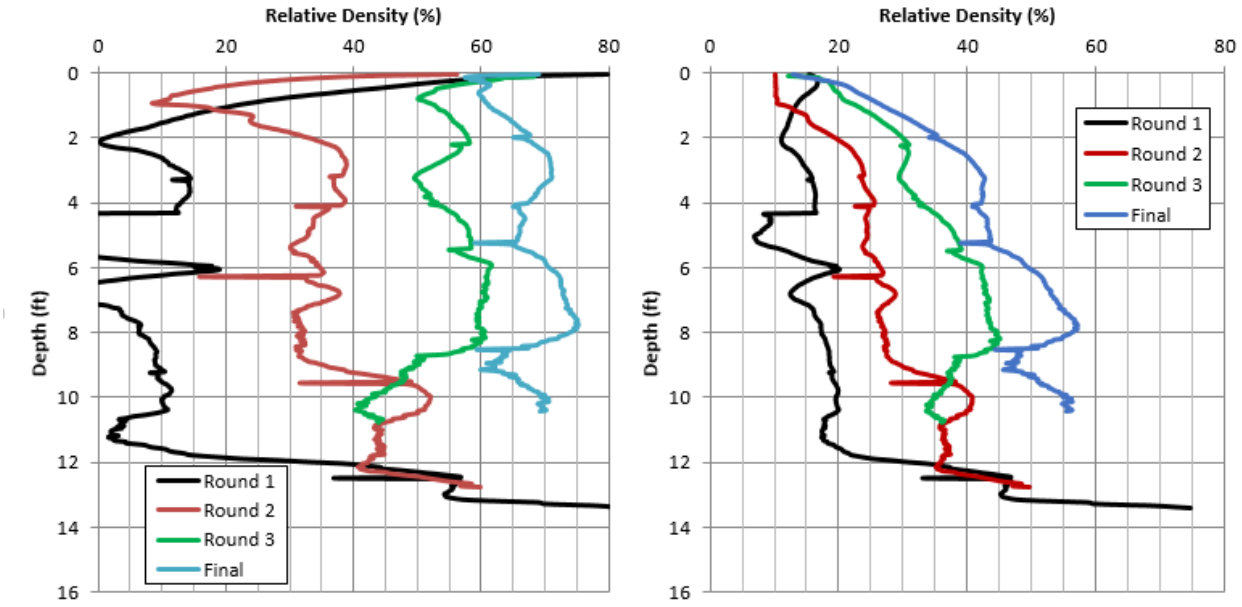

Figure 3-8 (Oakes, 2015) (4ft) Relative Density from CPT Correlation, Jamiolkowsky, et al. (1985), Left, and Kulhawy and Mayne (1990), Right.

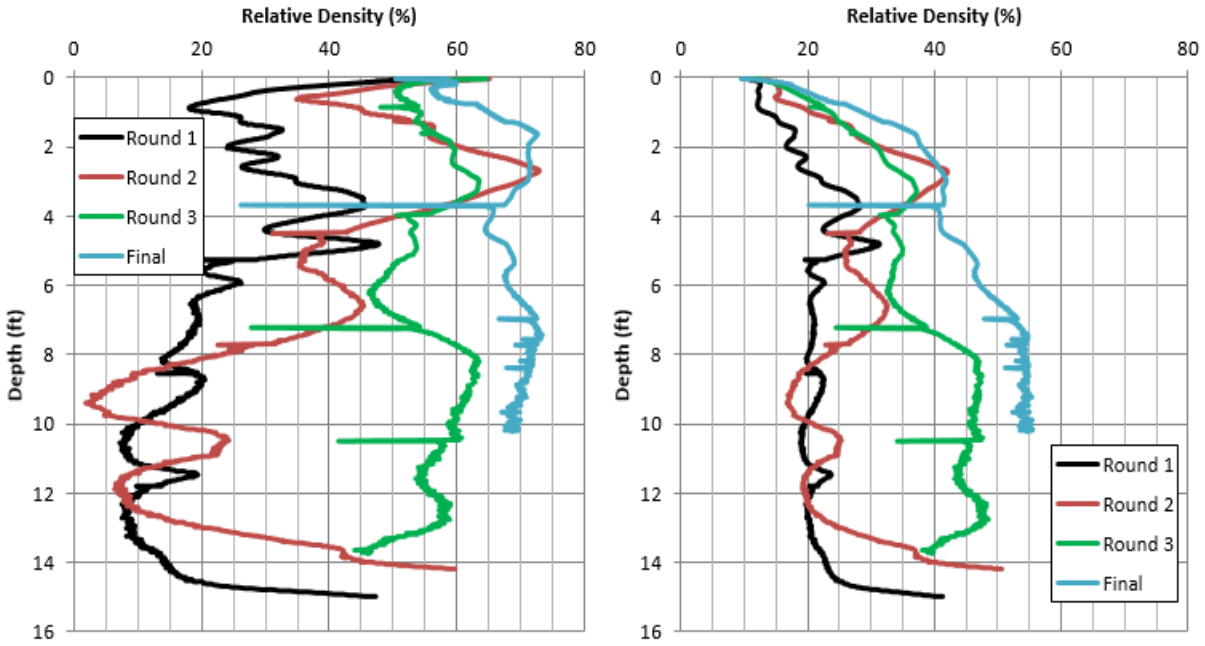

Figure 3-9 (Oakes, 2015) (3ft) Relative Density from CPT Correlation, Jamiolkowsky, et al. (1985), Left, and Kulhawy and Mayne (1990), Right.

Although the relative density prior to any shaking tests was measured, the relative density is increasing with each shaking test as the void ratio decreases. To determine the relative density for each shake test, the average change in void ratio was computed based on the settlement for each shake test. First, the initial void ratio must be found. The initial void ratio can be found using the equation

$$\gamma_{sat} = \frac{(G_s + e)\,\gamma_w}{1 + e} \tag{10}$$

where γ_{sat} = saturated unit weight of soil

G_s = specific gravity of sand

γ_w = unit weight of water

e = void ratio

For soil having a saturated unit weight of 122.5 lb/ft^3 (average value after initial depositions) assuming a specific gravity of 2.6, and 62.4 lb/ft^3 for the unit weight of water,

Equation (10) yields a void ratio of 0.713. This can then be simplified to a height of voids and a height of solids, using the equation

$$H_v = \frac{V_v}{V} = \frac{e}{1+e} \tag{11}$$

where H_v = height of voids in the soil

V_v = volume of voids

V = total volume

e = void ratio

Solving for the height of the voids gives 0.4164 as the portion of the total height. This value is then multiplied by the height of the sand in the laminar box, to give the initial height of the voids. A new height of voids ($H._{v.new}$) is found by subtracting the prior total settlement ($H._{total.prior\ settlement}$) from the initial height of voids ($H._{v.initial}$).

$$H_{v\ new} = H_{v\ initial} - H_{\ total\ prior\ settlement} \tag{12}$$

The new void ratio ($e_{\ new}$) is then found by dividing the new height of voids ($H_{v\ new}$) by the height of solids ($H_{\ solids}$) using the equation

$$e_{\ new} = H_{v\ new} / H_{\ solids} \tag{13}$$

From this new void ratio, a new relative density (D_r) is found using Equation (9). Also, a new saturated unit weight is found by substituting the new void ratio back into Equation (10).

A summary of the relative densities calculated at the beginning of each shaking test is provided in Table 3-6. The results indicate a gradual increase in D_r within each round of testing; however, the rate appears to decrease with each round of testing. Once again, the computed D_r values are somewhat higher than predicted by the correlations with the CPT but they are not

unreasonable. Because the computed values are based on the measured average settlement from the tests themselves, they have been preferred for use with the FEQDrain program.

Table 3-6 Computed D_r at the Start of each Shaking Test for the 4 ft and 3 ft Drain Spacings.

4 ft Drain Sapcing				3 ft Drain Spacing			
Base Acceleration	Round 1	Round 2	Round 3	Base Acceleration	Round 1	Round 2	Round 3
0.05g	27	47	58	0.05g	27	49	62
0.1g	33	50	59	0.1g	32	51	64
0.2g	39	54	61	0.2g	40	56	67

3.4.3 Modulus of Compressibility

The volumetric compressibility, m_v, is also referred to as coefficient of volumetric compressibility or modulus of compressibility, in other technical literature. This parameter defines the change in vertical soil strain relative to the change in vertical stress. For low values of pore pressure ratio, r_u, it has been found that m_v is essentially constant. However, for pore pressure ratios larger than 50-60%, m_v increases significantly with increases in the pore pressure ratio as described previously in Figure 3-2.

A cyclic triaxial compression test is the typical method for measuring the compressibility of a soil sample, but values are often selected from a table of typical values in practice. However, because of the instrumentation in the laminar box, there is sufficient data (r_u and ε_v) to back-calculate the volumetric compressibility of the sand, using Equation (8). Because of the confinement provided by the walls of the laminar shear box, it may be assumed that all volumetric strain can be attributed to the change in height of the soil, also known as the vertical settlement.

FEQDrain uses the initial modulus of compressibility m_{vo}, and relative density, D_r, as input values, and determines the appropriate adjusted m_v value as a function of r_u for use in iterative calculations. From the data collected by Oakes (2015), the m_v, was calculated and then m_{vo} was back-calculated using Equation (8). The procedure used in computing m_{vo} values is described in the following section. To compute m_{vo} from m_v using Equation (8) the relative density at the start of each shake test must be known. The procedure used to compute the

relative density has been described in the previous section. The change is strain ($\Delta\varepsilon$) for each shake test was determined within each depth interval by taking the change in settlement (Δs) from the Sondex Tube profilometer measurements and dividing by the length between the two points (ΔL) according to the equation

$$\Delta\varepsilon = \Delta s / \Delta L \tag{14}$$

The change in vertical effective stress ($\Delta\sigma'$) was then computed using the equation

$$\Delta\sigma' = z\,(\gamma_{new} - \gamma_w)\; r_u \tag{15}$$

where depth, z, corresponds to the depth of the transducer that measured pore pressure ratio and γ_{new} is the unit weight of the sand. The modulus of compressibility (m_v) is then obtained using the equation

$$m_v = \Delta\varepsilon / \Delta\sigma' \tag{16}$$

Remember, this is the elevated (m_v) with compressibility increased from the excess pore pressures. The initial compressibility (m_{vo}) value can then be back-calculated using a revised version of Equation **(8)**.

$$m_{vo} = m_v\,(1 + Y + 0.5\,Y^2) / e^Y \tag{17}$$

where Y was defined previously. There is a different r_u value and thus a different Y value for each depth at which a piezometer measured pore pressures.

The computed values of m_{vo} for all shakes and all depths for the 3 ft and 4 ft drain spacing experiments are shown in Table 3-7 and Table 3-8, respectively. These tables show the initial soil modulus values in units of ft^2/lb, at various depths. Each column represents the m_{vo} values in the soil profile for each shake. An average of these m_{vo} values is listed in a separate row at the bottom of each table. The top row of each table shows the shake test number, from 1 to 9.

The second row indicates the peak acceleration of each shake. These rows are directly above their corresponding columns of m_{vo} data in the main area of the table. The computed modulus of compressibility values range from $2x10^{-6}$ to $2x10^{-5}$ ft^2/lb.

Table 3-7 Computed m_{vo} Values at Each Depth for Each Shake of the 3ft Test

Shake #	1	2	3	4	5	6	7	8	9
Acceleration (g)	0.05	0.1	0.2	0.05	0.1	0.2	0.05	0.1	0.2
Depth (ft)	3ft Data -- M_{vo} Values (ft^2/ lb)								
3.2	3.9E-06	2.5E-05	2.0E-05	3.1E-05	2.2E-05	3.6E-05	4.6E-06	6.4E-06	3.3E-05
5.6	1.0E-05	1.9E-05	7.2E-06	2.7E-05	1.1E-05	2.3E-05	2.6E-05	7.9E-06	8.9E-06
8	3.5E-05	7.6E-06	7.1E-06	8.5E-06	1.8E-05	9.0E-06	1.0E-05	3.7E-06	2.0E-05
10.5	3.0E-05	1.7E-05	1.2E-05	5.3E-05	1.2E-05	6.2E-06	7.7E-06	2.1E-05	1.4E-05
13	2.9E-05	1.6E-05	2.5E-05	1.9E-05	1.8E-05	7.5E-06	5.1E-05	5.0E-05	5.3E-06
15.5	#N/A	2.5E-05	2.1E-05	3.7E-05	2.4E-05	1.1E-05	#N/A	3.3E-05	8.2E-06
Avg M_{vo}	**2.2E-05**	**1.8E-05**	**1.5E-05**	**2.9E-05**	**1.7E-05**	**1.6E-05**	**2.8E-05**	**2.0E-05**	**1.5E-05**

Table 3-8 Computed m_{vo} Values at Each Depth for Each Shake of the 4ft Test

Shake #	1	2	3	4	5	6	7	8	9
Acceleration (g)	0.05	0.1	0.2	0.05	0.1	0.2	0.05	0.1	0.2
Depth (ft)	4ft Data -- M_{vo} Values (ft^2/ lb)								
2.5	5.4E-06	3.6E-06	9.7E-06	5.4E-06	8.3E-06	1.8E-06	5.0E-06	4.0E-06	6.8E-06
4.5	3.0E-06	1.5E-05	2.0E-05	2.0E-06	3.7E-06	2.0E-06	4.2E-06	4.8E-06	4.1E-06
7.5	3.5E-06	2.9E-05	4.7E-06	2.3E-06	3.9E-06	7.4E-07	8.2E-06	7.8E-06	5.7E-06
10	1.5E-05	2.1E-05	3.9E-06	7.8E-06	2.5E-06	3.3E-06	3.0E-06	8.4E-06	9.8E-06
12.5	2.0E-05	#N/A	2.2E-05	1.0E-05	5.0E-06	8.4E-06	2.0E-05	1.0E-05	1.1E-05
Avg M_{vo}	**9.3E-06**	**1.7E-05**	**1.2E-05**	**5.5E-06**	**4.7E-06**	**3.2E-06**	**8.1E-06**	**7.0E-06**	**7.5E-06**

As a comparison to the back-calculated values, typical compressibility's of natural sands are shown in Table 3-9 (Pestana et al. 1997). Several types of sands are listed, with compressibility shown in both imperial and metric units. The mean particle size of each sand is also listed. The compressibility values range from $1x10^{-6}$ to $5x10^{-6}$ ft^2/lb.

Table 3-9 Typical Values of Volumetric Compressibility of Sand (After Pestana et al. 1997)

Type of sand	Coefficient of volumetric compressibility		Mean particle size, D_{50} (mm)
	(ft^2/lb)*	(m^2/kN)*	
Sacramento River Sand	1×10^{-6}	2×10^{-5}	~0.2
El Monte Sand (D)	1×10^{-6}	2×10^{-5}	~0.22
El Monte Sand (E)	1×10^{-6}	2×10^{-5}	~0.1
Akita Port Sand	$1.5 \sim 2 \times 10^{-6}$	$3 \sim 4 \times 10^{-5}$	0.15
El Monte Sand (C)	2×10^{-6}	4×10^{-5}	0.65
Monterey Sand	2×10^{-6}	4×10^{-5}	0.6
Fuji River Sand	3×10^{-6}	6×10^{-5}	0.4
El Monte Sand (B)	4×10^{-6}	8×10^{-5}	3.0
Ogishima Sand	5×10^{-6}	10×10^{-5}	0.32
* Measured at $u/\sigma_c' < 0.5$, $\sigma_c' = 2048$ ft^2/lb = 98.1 kN/m^2			

For a more direct comparison, the back-calculated and the typical values of compressibility from Pestana et al. (1997) are shown in Figure 3-10 and Figure 3-11. The horizontal axis is modulus of soil compressibility (ft^2/lb) plotted in logarithmic scale, and the vertical axis is depth (ft) on a linear scale. The thick vertical black lines mark the upper and lower limits of the computed values. The gray hatched area in the background of the chart is the range of compressibility reported in literature (Pestana, 1997). Markers plotted on the chart represent the compressibility of the soil in the laminar box at that depth. Each of the markers for a single shake is connected by a colored curve. The blue curves with diamond shaped markers are Round 1. The orange curves with triangular markers are Round 2. And the green curves with square markers are Round 3. Within each range the stronger shakes are darker shades of the same color. In the chart legend, the series title indicates the round and acceleration level of each shake. Thus 1.05 represents the 0.05g shake of Round 1, and 3.2 represents the 0.2g shake of Round 3. The series titles are listed in sequential order from top to bottom.

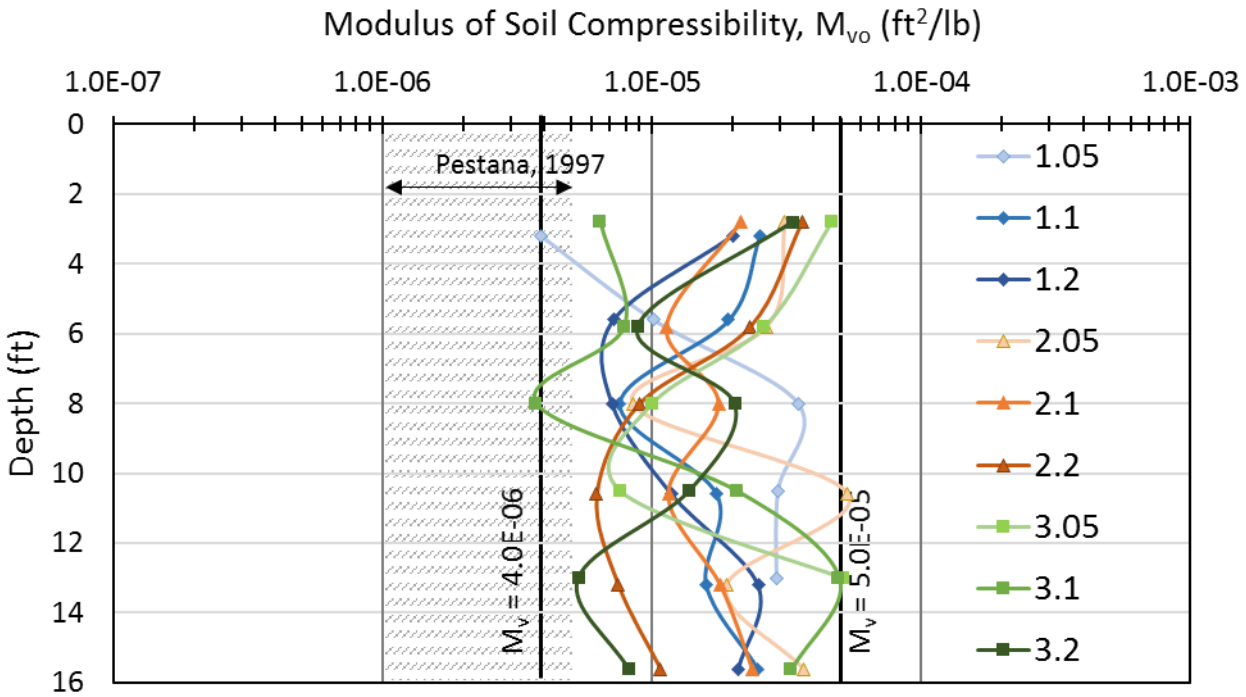

Figure 3-10 Modulus of Soil Compressibility for 3ft Experiment, Upper and Lower Limits Marked by Black Lines. Back Calculated from Data Measured by Oakes (2015). Gray Hatched Area is Range of Compressibility Reported in Literature (Pestana, 1997).

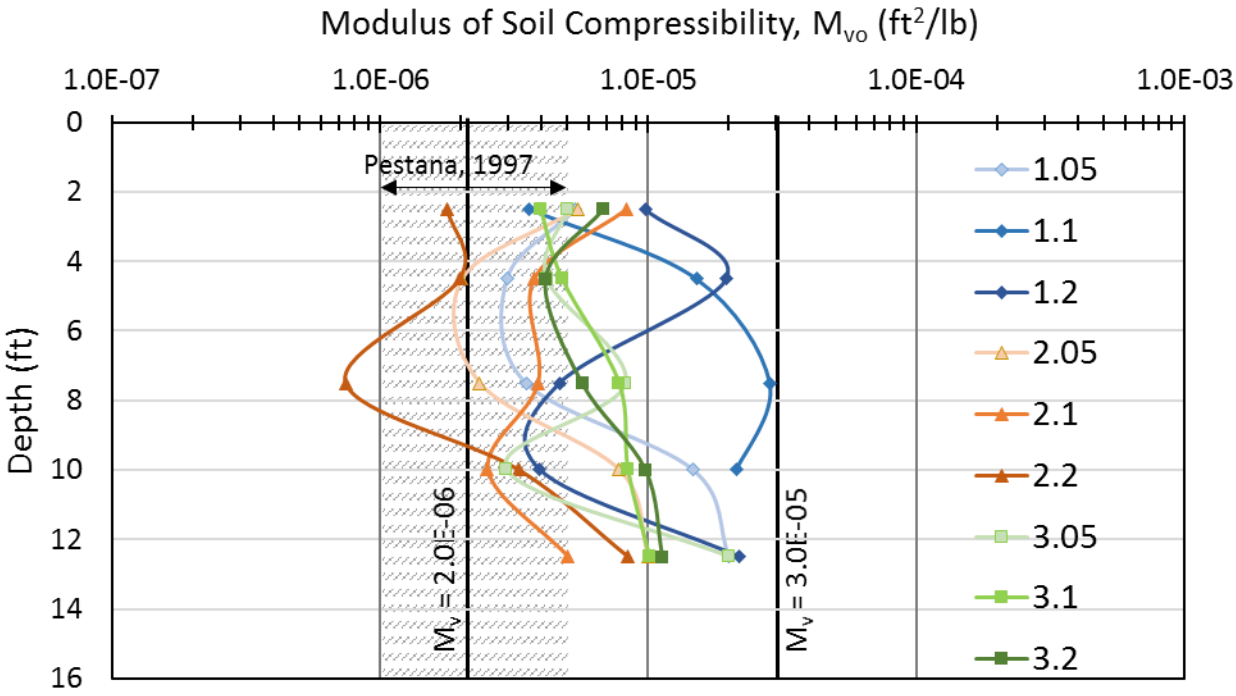

Figure 3-11 Modulus of Soil Compressibility for 4ft Experiment, Upper and Lower Limits Marked by Black Lines. Back Calculated from Data Measured by Oakes (2015). Gray Hatched Area is Range of Compressibility Reported in Literature (Pestana, 1997).

The modulus of compressibility back-calculated for the laminar shear box test sand had an average of about $8x10^{-6}$ ft^2/lb.; which is higher than the typical values suggested by Pestana et al (1997). However, this sand was very young (7 to 10 days old) and deposited by water pluviation. Therefore, any "micro-structure" that would increase the stiffness of an older natural soil would not be present. For modeling of native soils, a value within the typical compressibility range would likely be more appropriate.

3.4.4 Number of Cycles to Liquefaction

The number of cycles to liquefaction (N-Liq) is an indicator of the liquefaction resistance of a soil. It is dependent on the relative density and micro-structure of the soil, as well the cyclic stress ratio (CSR) induced in the soil by the sinusoidal accelerations applied at the base of the model. A smaller number indicates a soil layer more prone to liquefaction, and a high number indicates greater resistance to liquefaction.

Previous laminar shear box testing, with freshly deposited sand but without drains, showed that the sand would liquefy within three to four cycles of loading with a peak acceleration of 0.05 g (Bethapudi, 2008). However, as the peak acceleration of the input motion is increased, the number of cycles to liquefaction would be expected to decrease. Unfortunately, the selection of the number of cycles to liquefaction for each shake test is problematic because as the sand densifies with each shake, the liquefaction resistance increases leading to an increase in the number of cycles to liquefaction. Lastly, correlations between number of cycles to liquefaction and penetration resistance developed for natural soils are unlikely to be applicable for the newly deposited sand in the box with little micro-structure.

Parametric studies suggest that number of cycles to liquefaction primarily controls the rate of excess pore pressure generation in the first few seconds of shaking but subsequent results are not strongly influenced by this parameter. Generally, using about three cycles to liquefaction produced acceptable results. As a simplification for the initial numerical evaluations, it was decided to use the same number of cycles to liquefaction (N-Liq=3) for all tests, all accelerations, and all rounds.

For the 4ft spacing test, there was sand remaining in the shear box from previous experiments by previous users. This sand was assumed to be dense and thus make no significant contribution to excess pore pressures. Therefore, one hundred cycles to liquefaction was used.

3.5 Drain Parameters

The outside radius of the drain was 0.1542 ft which corresponds to a drain area of 0.0491 ft^2. The radius of the area of influence was 1.5 ft and 2 ft which represents a drain spacing of 3ft and 4 ft in a triangular grid. The area of openings per unit length in the perforated pipe was 0.0077 ft^2/ft of length. The constant associated with head loss through the perforations was taken as 1.0, and the geosynthetic had a permittivity of 0.8325 s^{-1}. The constant of head loss due to vertical resistance in the drain was C_1=1.7049 and C_2=2 provided by the manufacturer. Parameters relating to a reservoir were set the same as the drain dimensions, because there was no reservoir. The static groundwater level was at the soil surface

3.6 Other Required Input Parameters

The equivalent number of cycles was set at 15 which corresponds to the number of cycles produced by the shaking table. the time duration of shaking was 7.5 seconds because the cycles were applied at a frequency of 2 Hz. The total time of analysis was set at 100 seconds to capture the full dissipation curve after shaking stopped. The FEQDrain user manual states that the total time of analysis must be double or more than the time of shaking. However, the time of analysis must be far greater than the time of interest. For example, attempting to analyze 15 seconds time interval for 7 seconds of shaking will lead to error messages, and failure of the program to complete calculations. Therefore, the time of analysis must be far greater. The standard value of 0.7 for coefficient of pore pressure generation (θ) was used for all tests.

3.7 Data Processing/File Management

The FEQDrain program uses text file inputs that require the user to place the input values together in comma delimited strings of text as shown in Figure 3-12, with varying lengths and numbers of lines, depending on the soil layer geometry chosen. A full discussion of what each line means can be found in the FEQDrain user manual (Pestana et al., 1997). The process of

creating these input files is tedious and prone to human error, also they are non-intuitive for visualizing the values of the parameters.

```
PPR Matching 1_2_42
7,10,62.4,0,0,1,0
2,1,0.00105,0.000105,0.00002,122.5,1,0.55,0.7
5,2.5,0.00105,0.000105,0.000008,122.5,1,0.55,0.7
5,2.5,0.001,0.0001,0.000007,122.5,1,0.55,0.7
5,2.5,0.001,0.0001,0.000006,122.5,1,0.55,0.7
5,2.5,0.0017,0.00017,0.000008,122.5,1,0.55,0.7
5,2.5,0.0012,0.00012,0.000008,122.5,7,0.55,0.7
5,2.5,0.0002,0.00002,0.000001,122.5,100,0.7,0.7
14,7,1,100
100,1,1
2,2,4,7
0.154166666666667,2,0.0491
1.7049,2,1,0.0077,0.8325
0.0491,0,1.7049,2
end
```

Figure 3-12 Example of Input File Ready for Processing in FEQDrain.

To simplify the creation of these input files, an Excel spreadsheet with VBA macros was used. The input file spreadsheet was originally developed by a previous graduate student, Strand (2008). This spreadsheet is shown in Figure 3-13. Input parameters are grouped by type. The group in the top left corner (General analysis parameters) specifies the dimensions of the finite element node-array, and groundwater level. The group in the top middle (Earthquake loading conditions) specifies the strength of ground motions which are expressed as number of equivalent uniform cycles, duration of shaking, and time extent of the model computation. The group in the top right corner (Drain and reservoir parameters) relates to the type, and presence or absence of drains in the soil. The group in the center (Additional drainage parameters) specifies the geometry of the drain and the head loss into and within the vertical drain. The largest group, located on the lower half of the figure (Soil profile and properties) contains the properties specific to each layer of the soil, (hydraulic conductivity, soil compressibility, relative density, unit weight, etc.). This chart format makes it easy to see the value of each parameter, make changes to input values, and visualize the variations.

The spreadsheet file has two embedded macros. The first macro (activated by click) creates the input file. Next, the user opens FEQDrain and types the title of the macro-generated input file. FEQDrain closes automatically upon running to completion, which takes 2-3 seconds. Then a second macro (activated by click) imports and sorts the output file, and pastes it to a new sheet of the workbook. The second macro also copies and pastes input values from the first page, thus preserving a record of both the input and output on a single sheet.

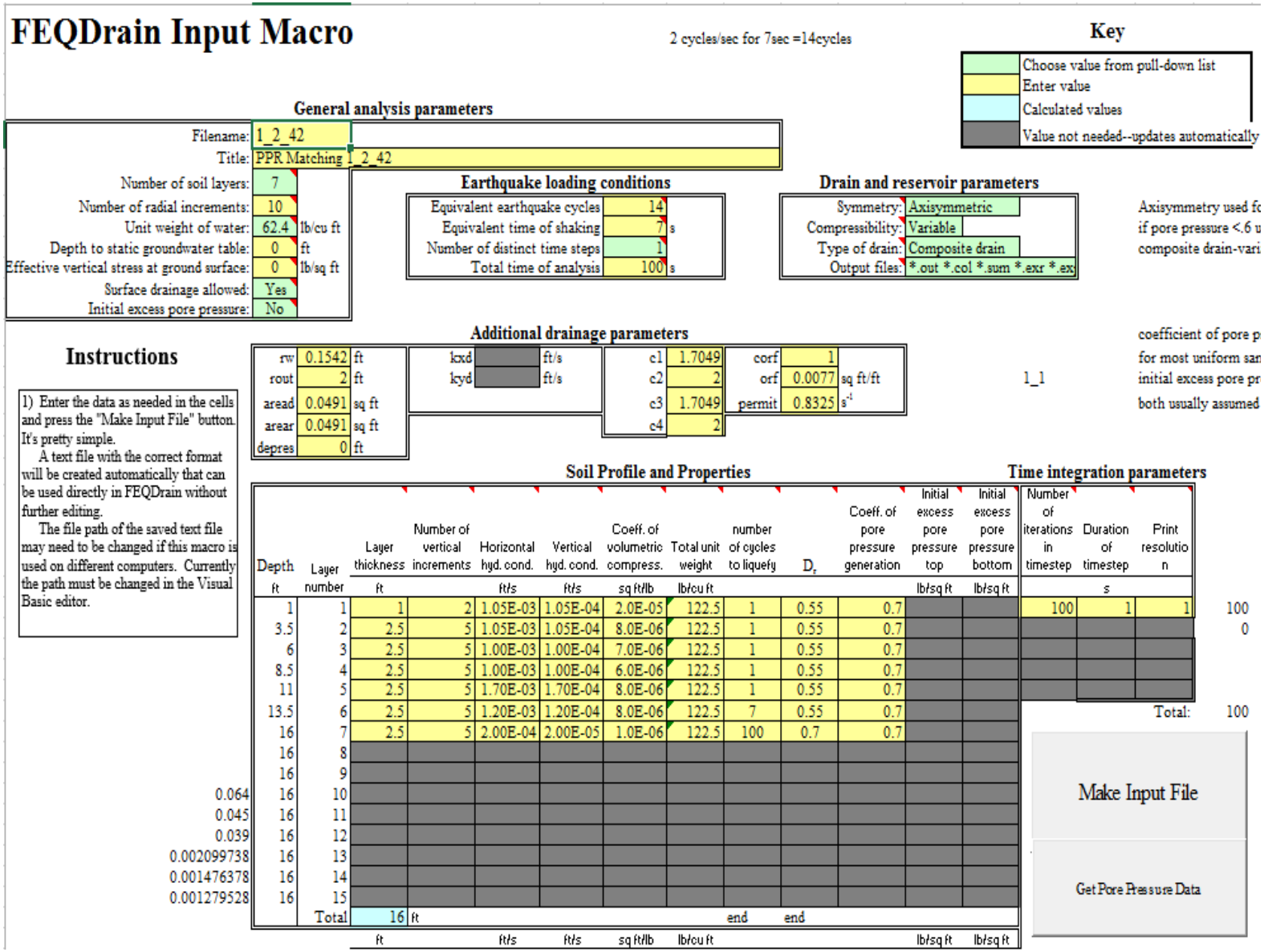

Figure 3-13 FEQDrain Input Macro (Strand, 2008).

The graphing tools that come with FEQDrain when downloading the program from the NISEE e-Library are illustrated in Figure 3-14. These plots show excess pore pressure ratios for the entire profile at a given time. Each colored bar represents a node. The graphic presented are all for the same time.

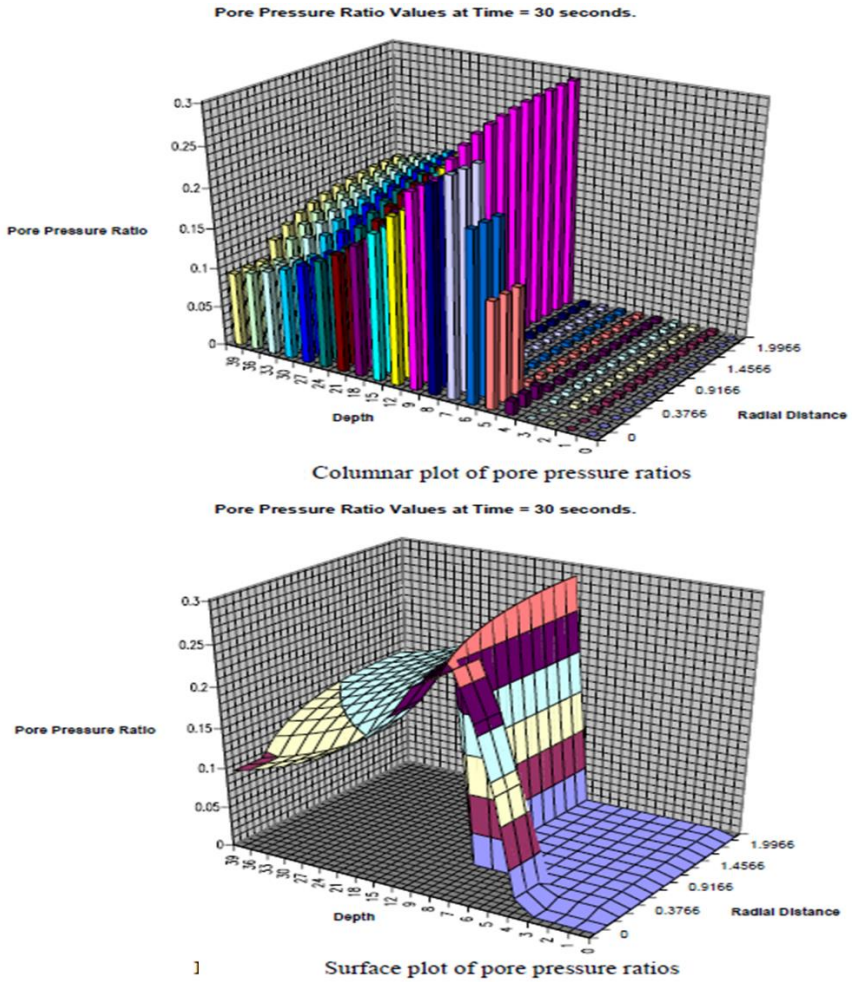

Figure 3-14 Plots Made Using the Graphing Tools Provided with FEQDrain.

Unfortunately, these plots do not allow for computed excess pore pressure ratio (R_u) to be easily compared with measured R_u time histories. Therefore, as part of this study, a separate spreadsheet was used to plot the measured and calculated time histories at selected nodes. This greatly facilitated the evaluation of the effect of various input parameters on the measured response.

Computer models were made for all shake tests done by Oakes (2015), one at each acceleration level for each of three rounds. Thus nine models for 4ft spacing tests and nine more models for 3ft spacing tests. Also a parametric study was done with models to determine the effect of changing the soil property parameters. More modeling was later done to determine the effects of drainage and seismic parameters. Modeling was somewhat of an iterative process to produce a good match with appropriate parameters.

Because so many similar files were created, a naming system was implemented for managing the hundreds of input and output files. The name of each model corresponds to which round (1, 2 or 3), acceleration level (0.05g, 0.1g or 0.2g), and iteration number they represent; generally following a #_#_## format. For example, 2_05_4 is: round 2, acceleration=0.05g, iteration 4. The file name cannot be more than eight characters for FEQDrain to accept it.

4 FINITE ELEMENT RESULTS AND DISCUSSION

This chapter provides comparisons of the measured and computed excess pore pressure ratio time histories at six depths for each shake test. In Section 4.1, plots of measured and modeled pore pressure ratios are presented using modulus of compressibility, relative density and hydraulic conductivity from the experimental data for each shake. This approach did not consistently yield good agreement with measured response over the entire depth of the profile. Therefore, in Section 4.2, similar comparison plots are provided; however, the modulus of compressibility has been back-calculated to provide the best-fit with the measured excess pore pressure ratio time histories. Generally, the modulus was adjusted within the range of measured values to achieve improved agreement with the measured pore pressure response. In addition, plots comparing the measured and computed settlement for reconsolidation after liquefaction are also provided in this section.

A separate model was made for each shake in each section; thus, nine models were developed for each of the 3-foot and 4-foot drain spacing shake tests. However, drain geometries and properties were the same for all drain tests with a given drain spacing. The number of cycles to liquefaction was kept constant at three for every model as indicated in the previous chapter.

Section 4.3 investigates the effects of varying soil input parameters. Section 4.4 illustrates the difference caused by different drain diameters. Section 4.5 Shows and discusses how different earthquake magnitudes are treated by the program. Section 4.6 and 4.7 make comparison between this numerical modeling effort and those of Vytiniotis et al. (2013), and Howell et al. (2014). Section 4.8 makes comparison with the conclusions of the parent study (Oakes, 2015). Section 4.9 provides suggestions on the practical use of FEQDrain.

4.1 Computed Pore Time Histories with Experimental Soil Properties

The computer program FEQDrain (Pestana et al, 2007) was used to compute time histories of excess pore pressure ratios at selected depths corresponding to the locations of the pore pressure transducers in the laminar shear box experiment. Figure 4-1 through Figure 4-3 provide comparisons of measured and computed excess pore pressure ratio (R_u) time histories for the shake tests at 0.1 g for rounds 1, 2, and 3 using the measured hydraulic conductivity, along with the back-calculated relative density and modulus of compressibility obtained from the experimental data. Similar comparison curves were also developed for each shake test for each pore pressure transducer depth.

Results are presented at the depths of the six pore pressure transducers in the profile. Generally, the computed R_u time histories are higher than the measured curves at a given time and the over-prediction becomes worse with depth. The least reliable parameter in the analysis is the modulus of compressibility which is based on strain from the settlement versus depth curves which appeared to be somewhat irregular with depth. A major assumption in back-calculating the static modulus of compressibility (m_{vo}) is that the static compressibility can be interpreted from the compressibility associated with the liquefied sand according to equation 8. Recent experience in the Tohoku earthquake has shown that the compressibility of liquefied sands can vary significantly from average values leading to discrepancies in predicted settlements. Even if the average measured modulus of compressibility is used for each shake test, the disagreement between measured and computed R_u's also increases with depth, with the computed values being higher. Howell et al. (2014) also found that the error in the computed R_u in centrifuge tests was largely attributable to discrepancies in the modulus of compressibility used in the analyses.

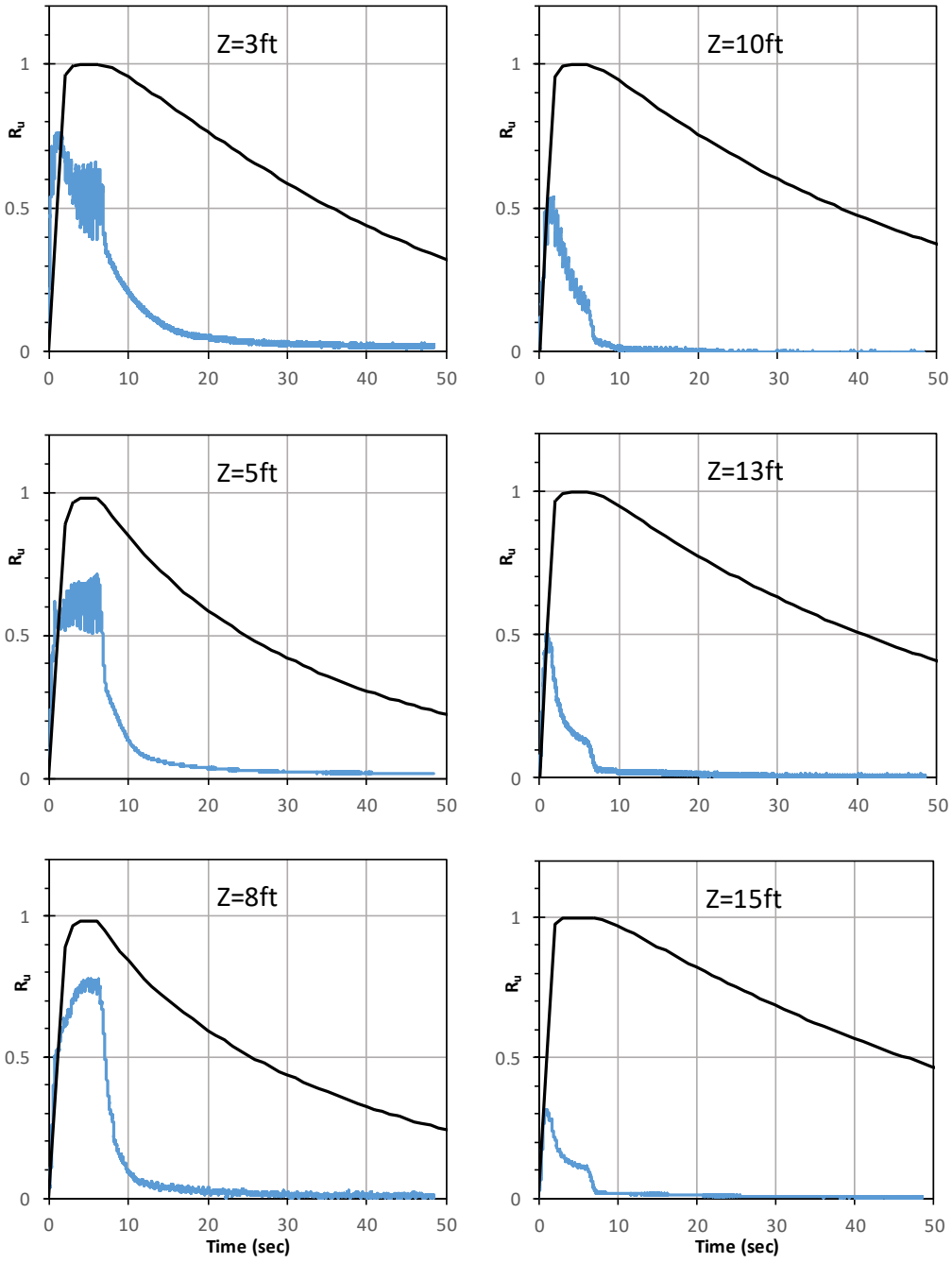

Figure 4-1 Comparison of Measured and Computed Excess Pore Pressure Ratio Time Histories at Six Depths Using m_v from Experimental Data for 3-Foot Drain Spacing, Round 1, A_{max}=0.10g. (Measured-Solid Blue Curve and Computed-Dashed Black Curve)

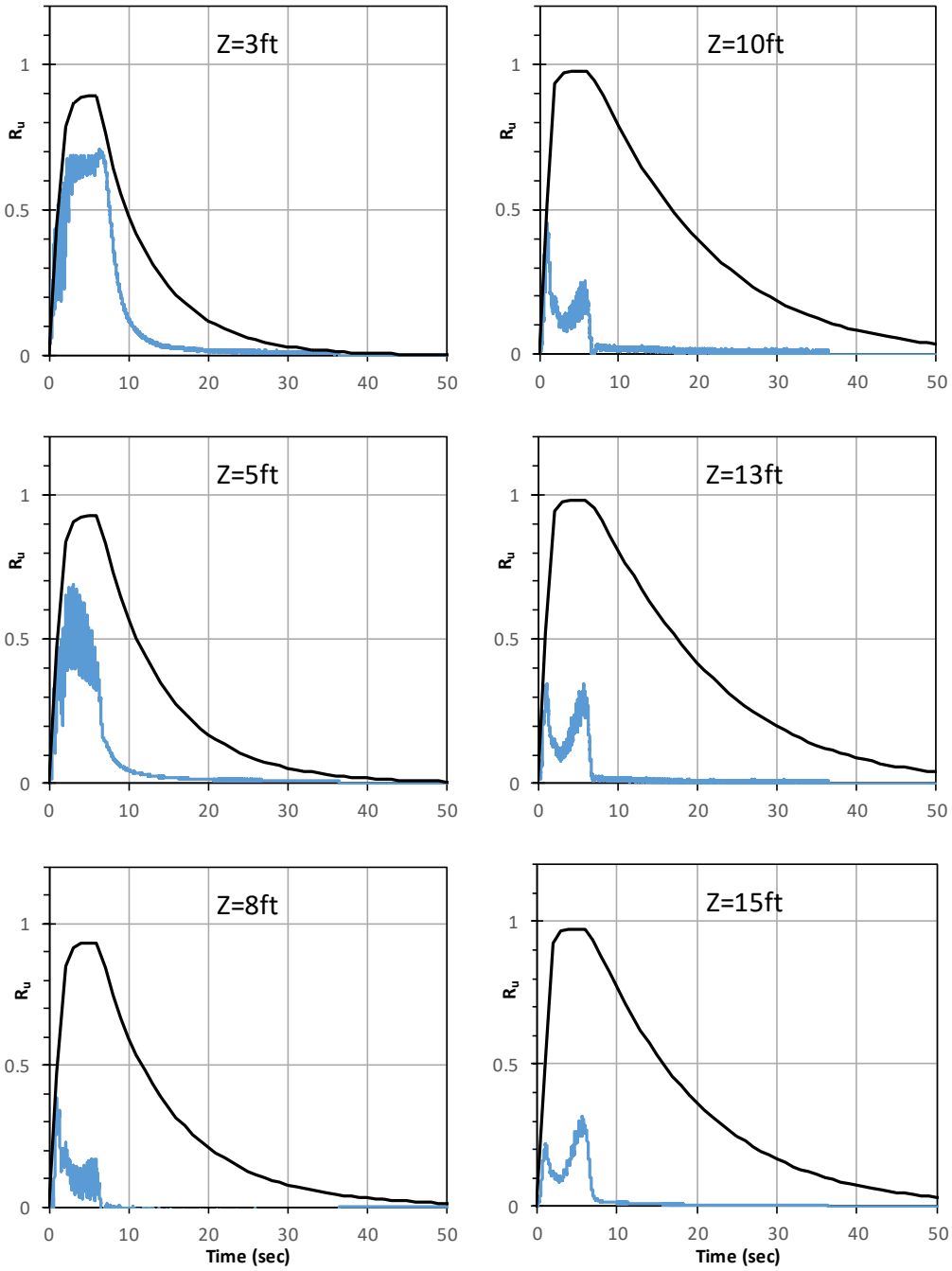

Figure 4-2 Comparison of Measured and Computed Excess Pore Pressure Ratio Time Histories at Six Depths Using m_v from Experimental Data for 3-Foot Drain Spacing, Round 2, A_{max}=0.10g. (Measured-Solid Blue Curve and Computed-Dashed Black Curve)

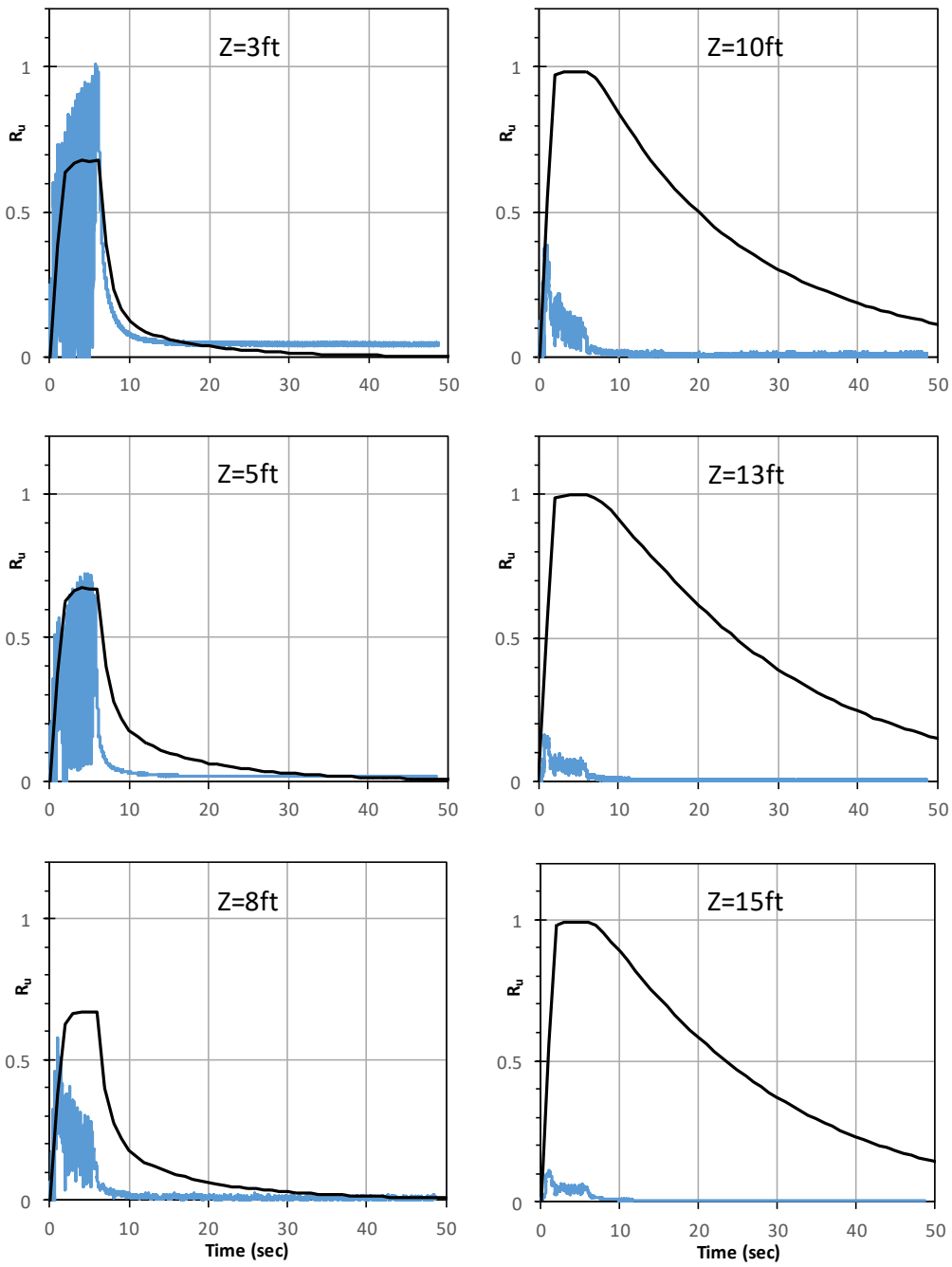

Figure 4-3 Comparison of Measured and Computed Excess Pore Pressure Ratio Time Histories at Six Depths Using m_v from Experimental Data for 3-Foot Drain Spacing, Round 3, A_{max}=0.10g. (Measured-Solid Blue Curve and Computed-Dashed Black Curve)

A spreadsheet containing calculations of the initial soil modulus of compressibility (m_{vo}) is shown in Appendix D. Soil Compressibility. Therein is also shown how the vertical strain divided by the vertical effective stress is used to calculate the post liquefaction soil compressibility (m_v) for each soil layer. From there, the settlement, is used to determine the change in height of total soil voids, via volumetric analysis. From there a new void ratio and relative density is found for the soil profile after subsequent shakes have occurred. This new relative density is then available for computation of the equations for m_{vo} presented earlier in section 3.2.2

4.2 Computed Pore Time Histories with Adjusted Soil Compressibility

To provide increased understanding of the effect of the drains relative to the material properties for the sand in the box, the modulus of compressibility at each depth was adjusted to optimize the agreement between the computed R_u's and the measured results. Typically, this required some decrease in the modulus of compressibility (m_{vo}) with depth. The compressibility has a pronounced effect on the rate of pore pressure generation and dissipation. The relative density and hydraulic conductivity values were kept equal to the measured values from the laminar box experiments because they are fairly well-constrained by the data. Figure 4-4 through

Figure 4-6 provide comparisons of measured and computed excess pore pressure ratio time histories for the shake tests at 0.1 g for rounds 1, 2, and 3. Similar comparison curves were also developed for each shake test for each pore pressure transducer depth. Generally, the computer model is reasonably capturing the basic features of the R_u time histories in Figure 4-4 through

Figure 4-6, such as the peak R_u and the dissipation time, but there are some discrepancies in some instances.

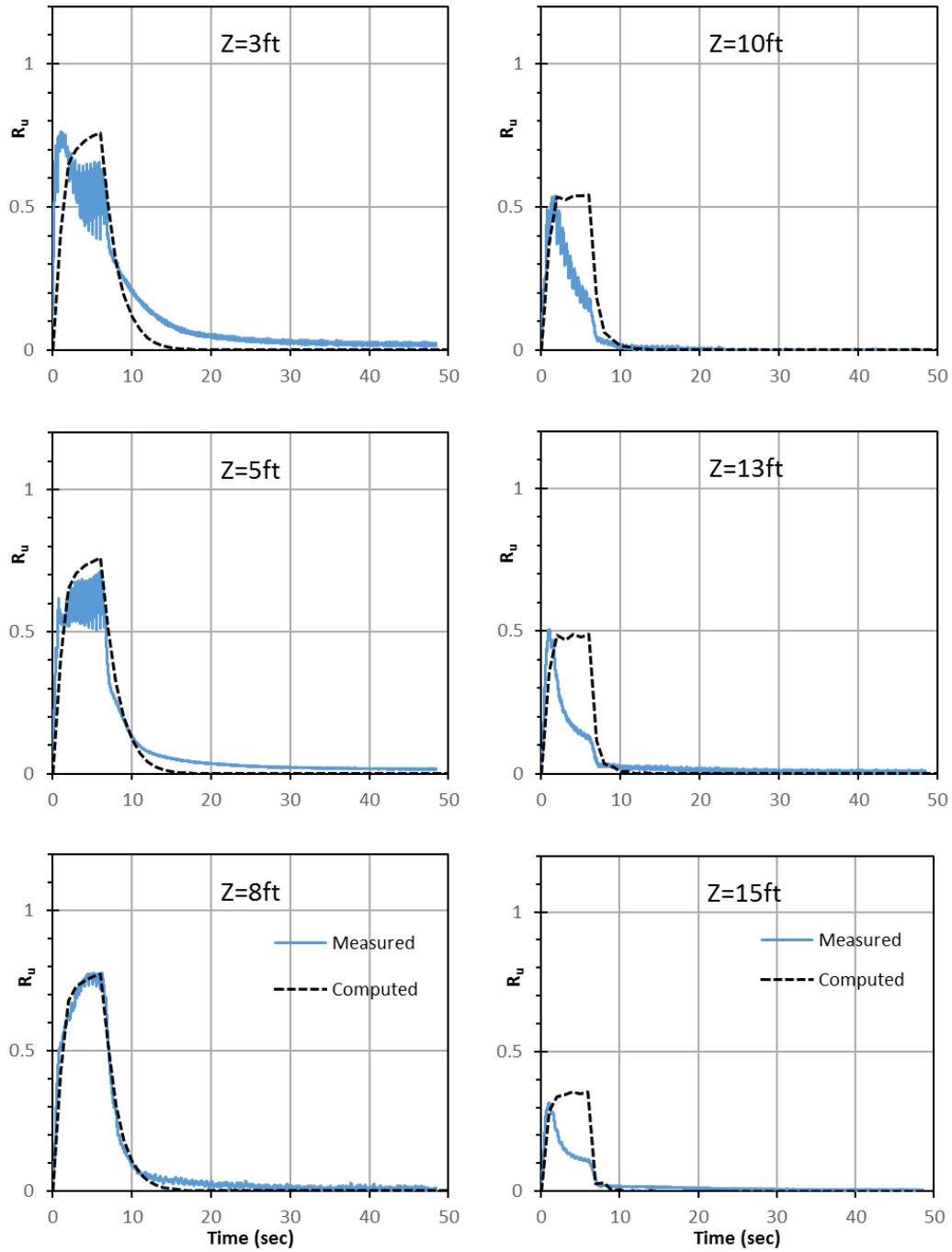

Figure 4-4 Comparison of Measured and Computed Excess Pore Pressure Ratio Time Histories at Six Depths Using Back-Calculated m_v to Fit R_u Time Histories for 3-Foot Drain Spacing, Round 1, A_{max}=0.10g. (Measured-Solid Blue Curve and Computed-Dashed Black Curve)

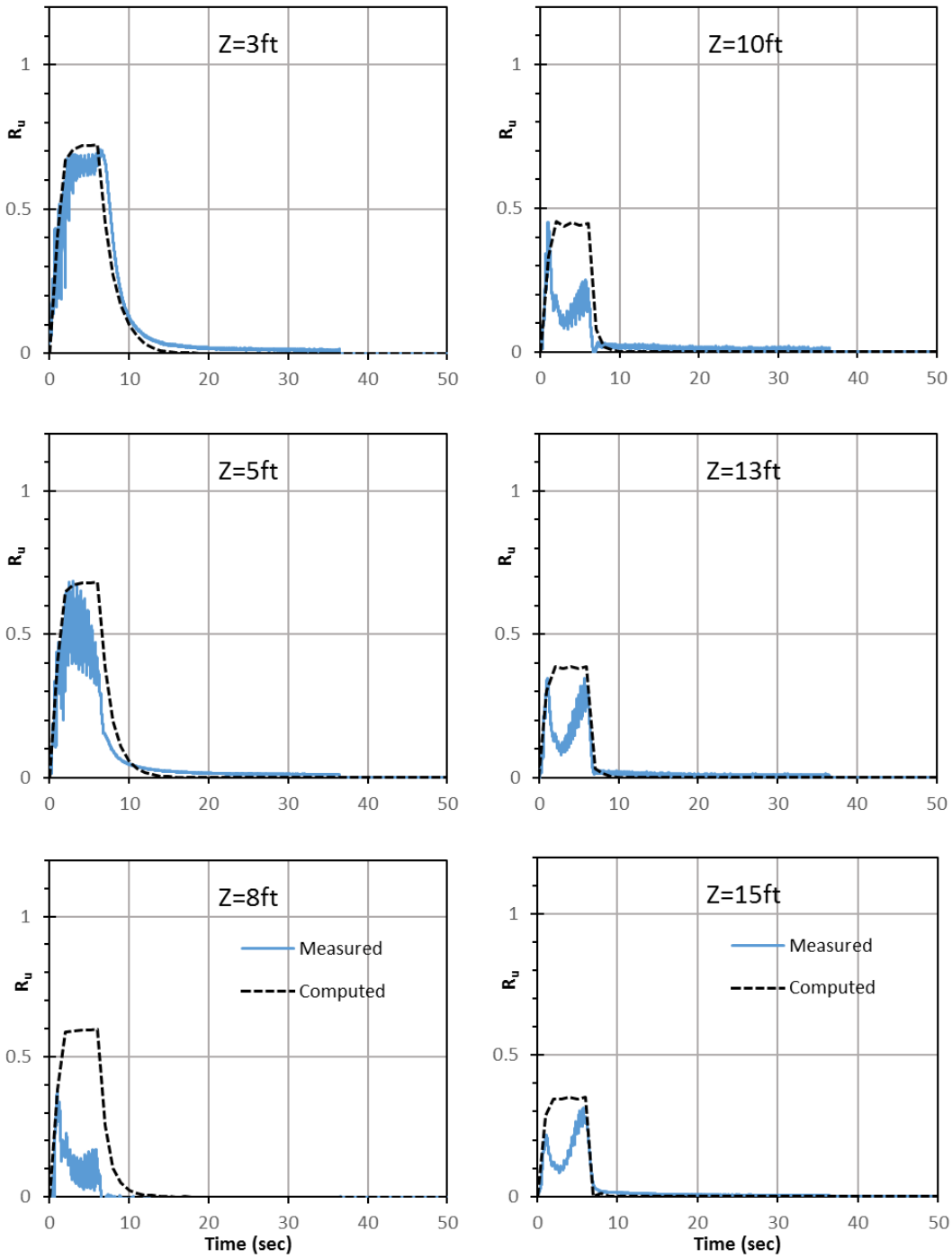

Figure 4-5 Comparison of Measured and Computed Excess Pore Pressure Ratio Time Histories at Six Depths Using Back-Calculated m_v to Fit R_u Time Histories for 3-Foot Drain Spacing, Round 2, A_{max}=0.10g. (Measured-Solid Blue Curve and Computed-Dashed Black Curve)

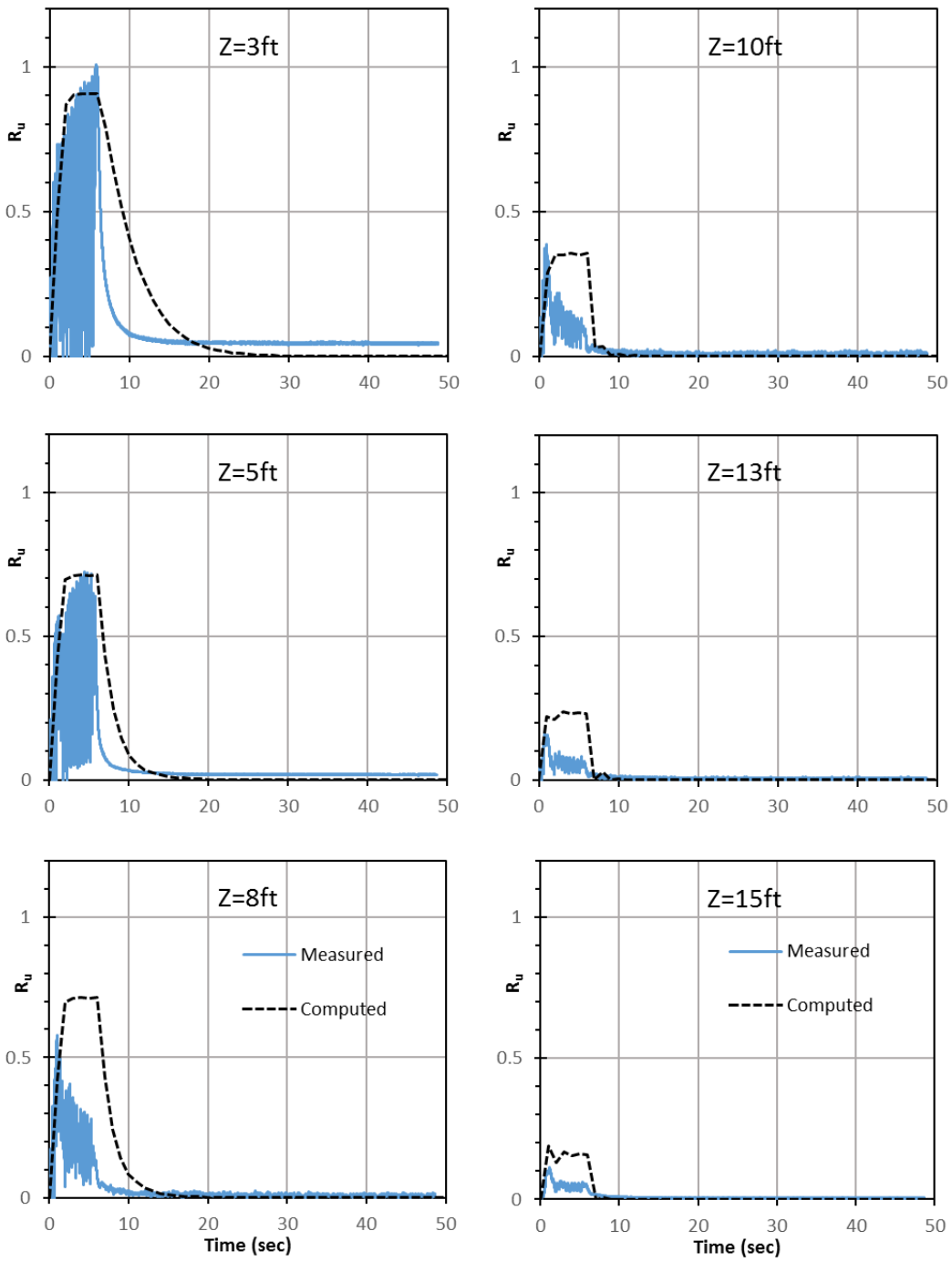

Figure 4-6 Comparison of Measured and Computed Excess Pore Pressure Ratio Time Histories at Six Depths Using Back-Calculated m_v to Fit R_u Time Histories for 3-Foot Drain Spacing, Round 3, A_{max}=0.10g. (Measured-Solid Blue Curve and Computed-Dashed Black Curve)

Figure 4-7 through Figure 4-9 provide comparisons of measured and computed excess pore pressure ratio time histories for the shake tests of Round 1, at 0.05g, 0.1g, and 0.2g. These results illustrate the ability of the computer model to compute the measured R_u time histories for various acceleration levels within a given round of testing.

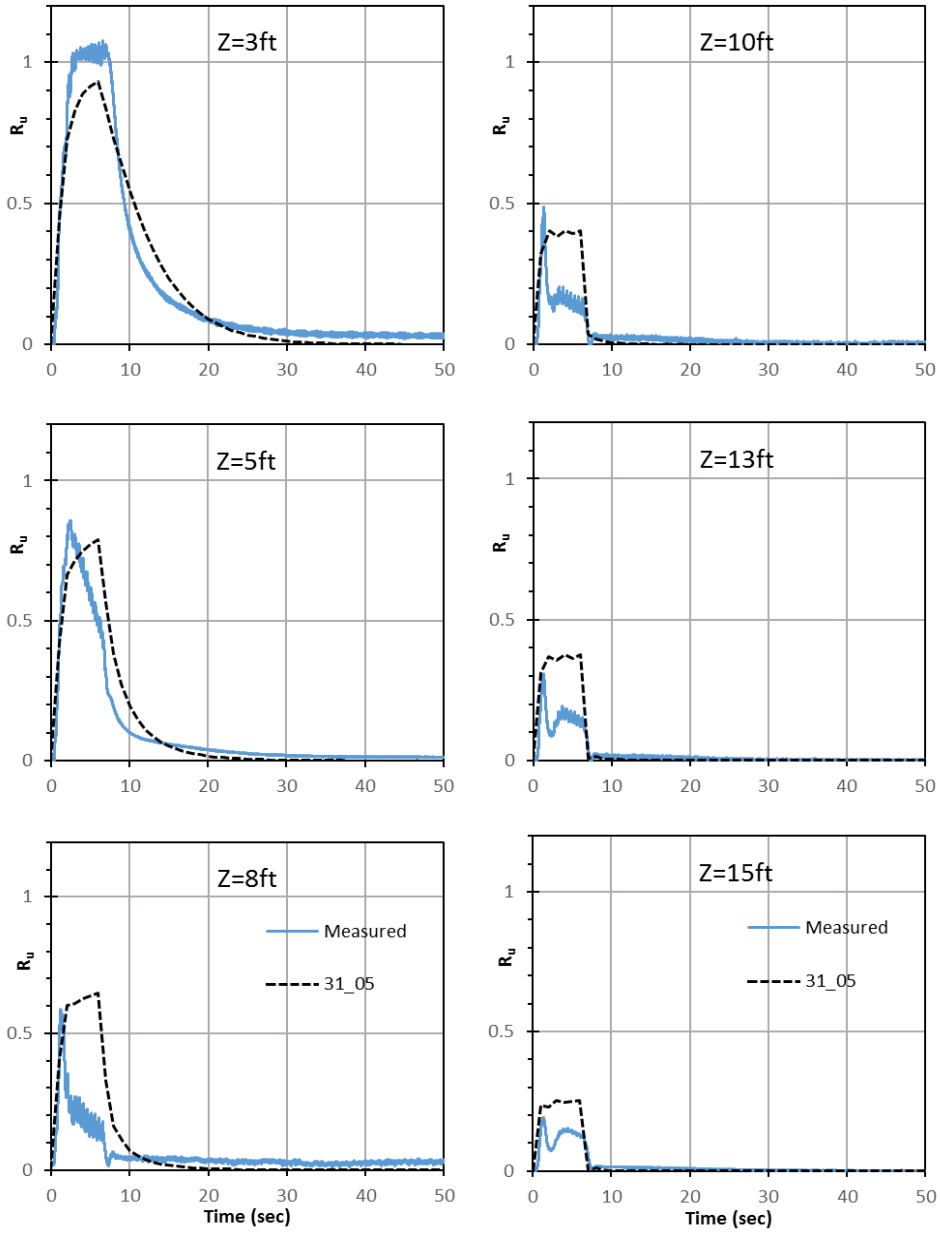

Figure 4-7 Comparison of Measured and Computed Excess Pore Pressure Ratio Time Histories at Six Depths Using Back-Calculated m_v to Fit R_u Time Histories for 3-Foot Drain Spacing, Round 1, A_{max}=0.05g. (Measured-Solid Blue Curve and Computed-Dashed Black Curve)

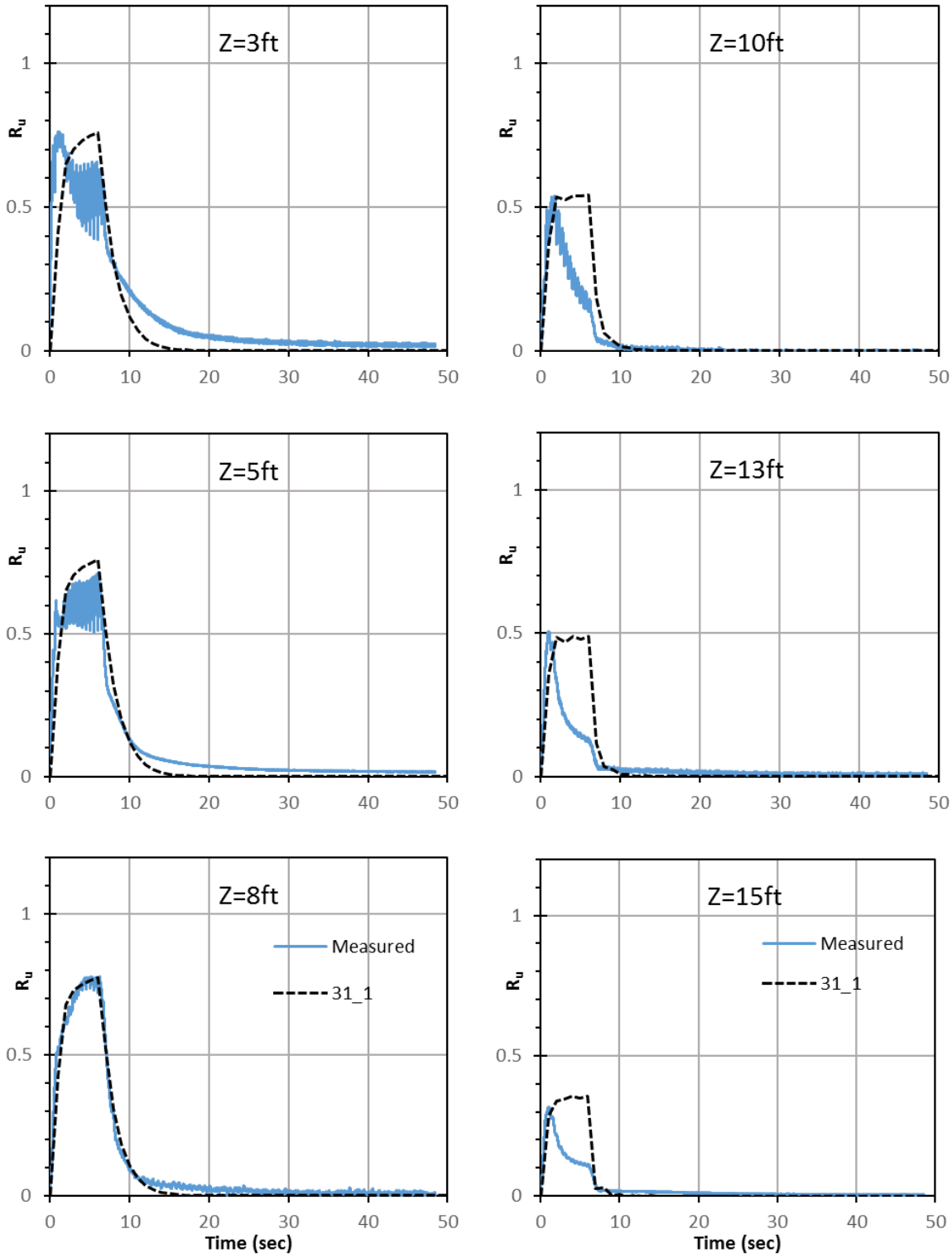

Figure 4-8 Comparison of Measured and Computed Excess Pore Pressure Ratio Time Histories at Six Depths Using Back-Calculated m_v to Fit R_u Time Histories for 3-Foot Drain Spacing, Round 1, A_{max}=0.10g. (Measured-Solid Blue Curve and Computed-Dashed Black Curve)

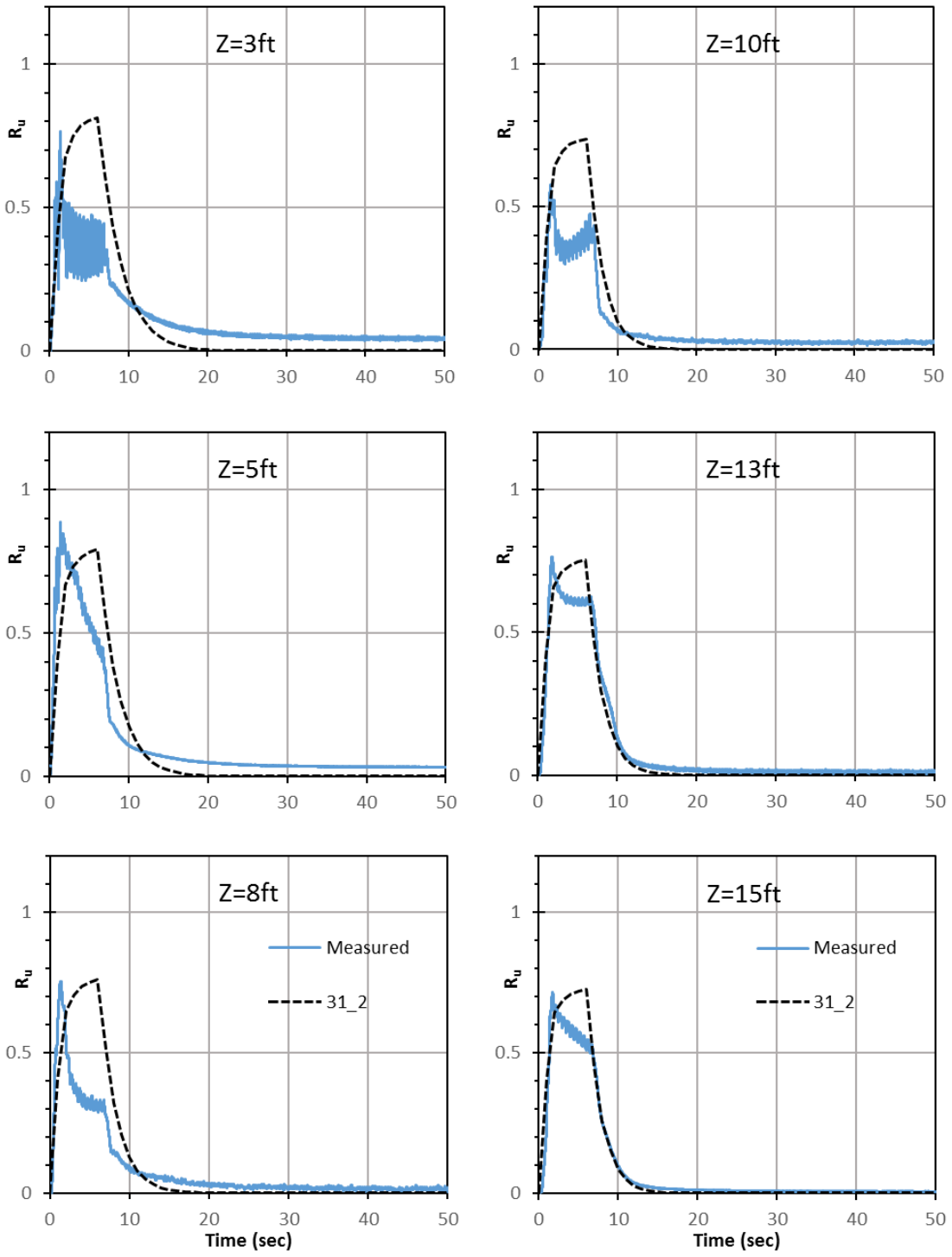

Figure 4-9 Comparison of Measured and Computed Excess Pore Pressure Ratio Time Histories at Six Depths Using Back-Calculated m_v to Fit R_u Time Histories for 3-Foot Drain Spacing, Round 1, A_{max}=0.20g. (Measured-Solid Blue Curve and Computed-Dashed Black Curve)

The back-calculated m_{vo} values are plotted versus depth for each shake test and for each drain spacing in Figure 4-10. Generally, the back-calculated m_{vo} values plot within the center of the range of m_{vo} values obtained experimentally, as illustrated in and decrease with depth.

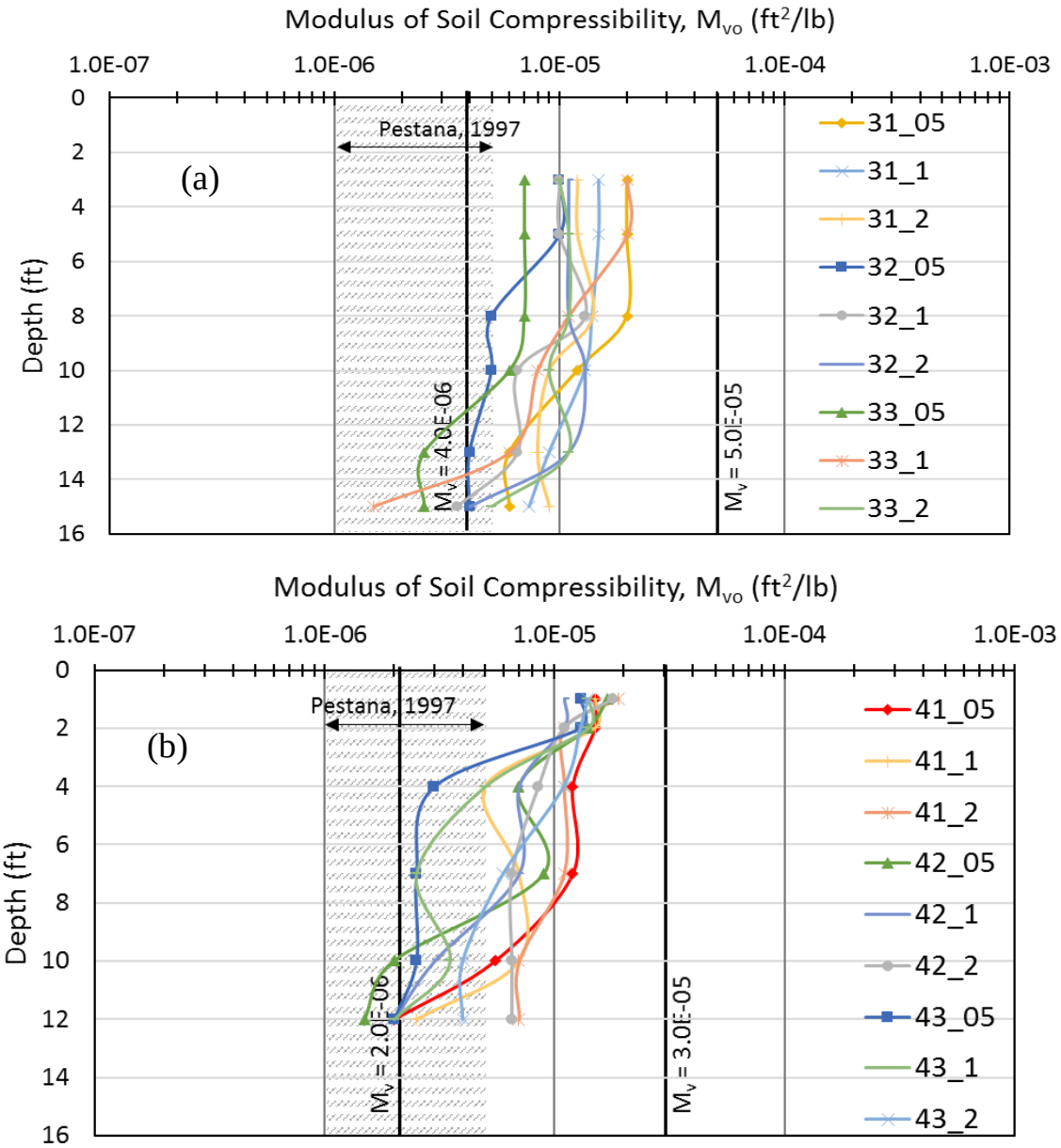

Figure 4-10 Back-Calculated Modulus of Compressibility Values Necessary to Produce Agreement with Pore Pressure Response in Comparison with Range of Experimental Compressibility Values for All Shaking Tests with the (A) 3-Ft. and (B) 4-Ft. Drain Spacings.

This agreement suggests that the back-calculated m_v values are reasonable values considering the potential for local variations in the measured settlement versus depth curves. The back-calculated m_v values are generally higher than those tabulated by Pestana et al (1997) in the user's manual for the FEQDrain program for cyclic triaxial shear specimens. This could be due to the nature of the deposition process in the laminar shear box which appears to produce a loose, unstructured soil deposit which is more compressible than conventional soils.

4.2.1 Settlement Computation

The FEQDrain program also computes the settlement which develops as a result of liquefaction. and reconsolidation. Computed settlements are plotted against the measured settlements for the 3-ft. and 4-ft. drain spacings in Figure 4-11. In all cases of this test, the computed settlements are higher than the measured settlements. For the 3ft drain spacing test, FEQDrain overestimated by 66%, and overestimated by 94% for the 4ft test. It should also be noted that measured settlement values are for pre-placed drains to which the sand was added rather than vibrating mandrel-installed drains. Thus, the measured settlement would conceivably be even lower, thus increasing the disagreement with the settlements predicted by FEQDrain.

However, the large variation in computed and measured settlements is not unexpected since the calculation of liquefaction induced settlement is a challenging undertaking. The range of variation in measured settlement is often two times to one-half of the predicted settlement based on recent comparison with large settlement data bases in New Zealand and Japan. In addition, reconsolidation settlements following cyclic shear testing are known to vary over a considerable range. Therefore, the discrepancies in the measured and computed values are not too surprising. Again, it should also be noted that measured settlement values are for pre-placed drains to which the sand was added rather than vibrating mandrel-installed drains. These results should be limited to this test only.

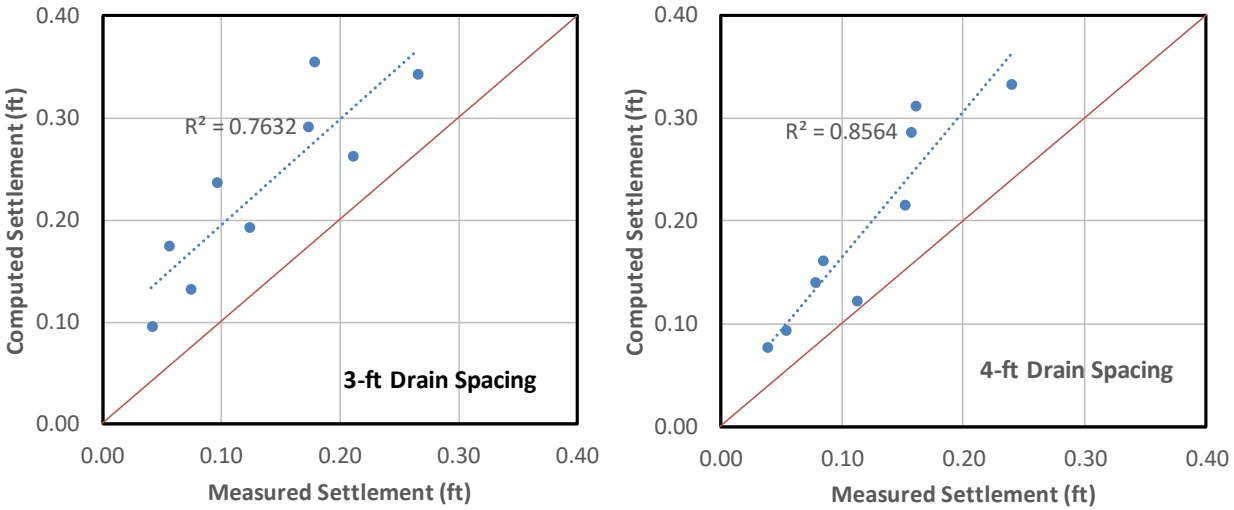

Figure 4-11 Comparison of Measured and Computed Settlement for Each Shaking Test for Both the 3-ft. and 4-ft. Drain Spacings.

4.3 Parametric Sensitivity Study

A parametric study was performed to determine the effect of changing certain model parameters that are related to soil properties, and drain properties. For this investigation, the calibrated model for the 4ft drain spacing during Round1 testing, with a_{max}=0.1g was used as the example. This changing of parameters was done systematically, with all other parameters kept equal, despite the fact that some parameters might be cross-correlated. The resulting excess pore pressure vs. time curves were plotted together on one plot for each depth where a pore pressure transducer was located for comparison. It is assumed that the behavior observed when varying each parameter in this example will have the same or very similar effects on all other models.

It was found that for the initial R_u rise (generation curve), and the peak R_u value attained, the number of cycles to liquefaction and the hydraulic conductivity have the greatest effect. However, the downward slope (dissipation curve) is most influenced by hydraulic conductivity (k) and coefficient of compressibility (m_v), with the latter having particular effect on the initial angel of the dissipation slope.

In the subsequent sections, the effect of variations in hydraulic conductivity, relative density, modulus of soil compressibility, coefficient of soil compressibility, number of cycles to liquefaction, soil unit weight, coefficient of pore pressure generation, drain diameter, and earthquake magnitude will all be examined

4.3.1 Effect of Variations in Hydraulic Conductivity (k)

The hydraulic conductivity of the soil has the strongest effect on the dissipation of pore pressures to drains and the resulting R_u values. It is also the most sensitive property as shown by parametric study. However, conductivity was relatively simple to measure in-situ for these tests, thus reducing the variability in modeling. Intuitively, a higher conductivity value leads to a lower R_u value since water can escape more easily; this is confirmed by the parametric study. In real field applications, the determination of an accurate hydraulic conductivity in the horizontal direction becomes of paramount importance. It should also be noted that the computer model assumes that the hydraulic conductivity remains constant within a single seismic event, regardless of R_u even after liquefaction has begun. This may differ from reality, since a liquefied soil could be expected to have significantly greater conductivity while still liquefied. However, densification of the soil resulting from the seismic event would reduce the void ratio for subsequent seismic events. Thus a slightly lower relative density and conductivity should be chosen for modeling the next event.

Results of the parametric study for hydraulic conductivity are shown in Figure 4-12 and hydraulic conductivity values used in this analysis are summarized in Table 4-1. The dashed black curve is the model prediction of R_u made using the measured hydraulic conductivity while the measured R_u time history is shown in dark blue. Changing the hydraulic conductivity by about 25% (k_{model} x 1.25 and k_{model} x 0.75) typically changed the computed peak R_u values 10 to 25 percentage points. The highest and lowest R_u vs time curves use the overall maximum and minimum k-values (upper bound k, and lower bound k) measured in the laminar shear box, and use the same k at all depths. Peak R_u values change somewhat for the 25% variation case particularly at shallow depth and dissipation times increased markedly for the lowest k values.

Results produced using a wider range of hydraulic conductivity values (Table 4-1) are shown in Figure 4-13, while the type of soils that may correspond to that k value is shown in Table 4-2. Specific examples of soil type are difficult to provide because the property varies widely and can be drastically affected by a small percentage of fines within the gradation. Nevertheless, when the hydraulic conductivity decreased by a factor of 5 to 10 times, the peak R_u values typically increased to near 1.0 while the rate of dissipation increased substantially for the drain spacing and diameter analyzed.

The results of these parametric studies highlight the importance of selecting appropriate k values when designing a mitigation strategy based on drainage. Analyses should always consider the lower range of k values that might be present in the field and in-situ testing data is extremely valuable in this process because variations in particle gradation, fines content, and clay plasticity could have a pronounced effect on the peak R_u values generated and the rate of excess pore pressure dissipation.

Table 4-1 Hydraulic Conductivity Values Used in Sensitivity Analysis

	Horizontal Hydraulic Conductivity (cm/sec)				
	Lowest Measured	Back-Calculated $\mathbf{k_{bc}}$			Highest Measured
Depth Interval (ft)	k_{min}	0.75 x k_{bc}	1.00 x k_{bc}	1.25 x k_{bc}	k_{max}
0-6	0.028	0.046	**0.061**	0.076	0.07
6-11	0.028	0.032	**0.043**	0.054	**0.07**
11-16	**0.028**	0.029	**0.038**	0.048	0.07

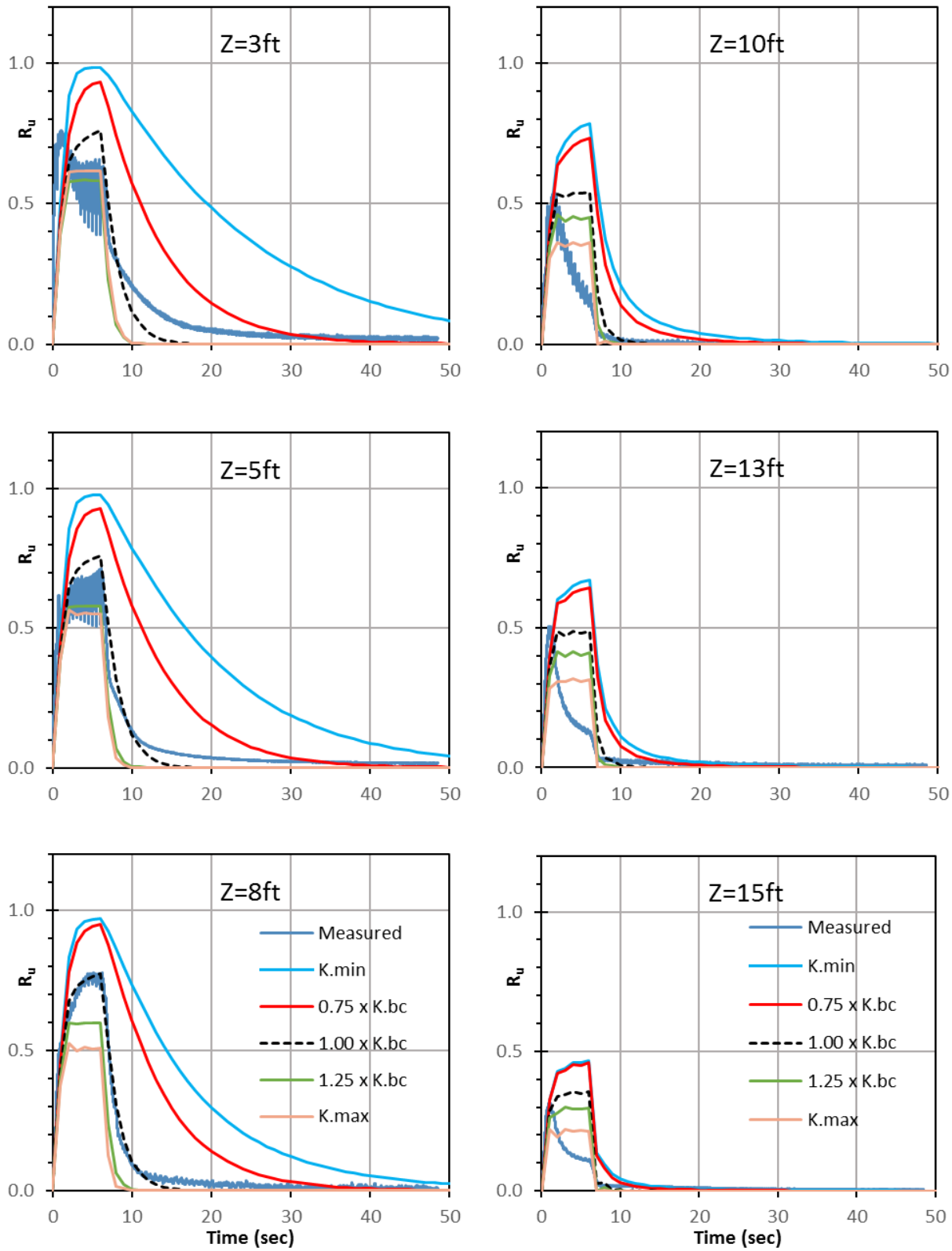

Figure 4-12 Effect of Varying Hydraulic Conductivity (k) at Each Piezometer Level.

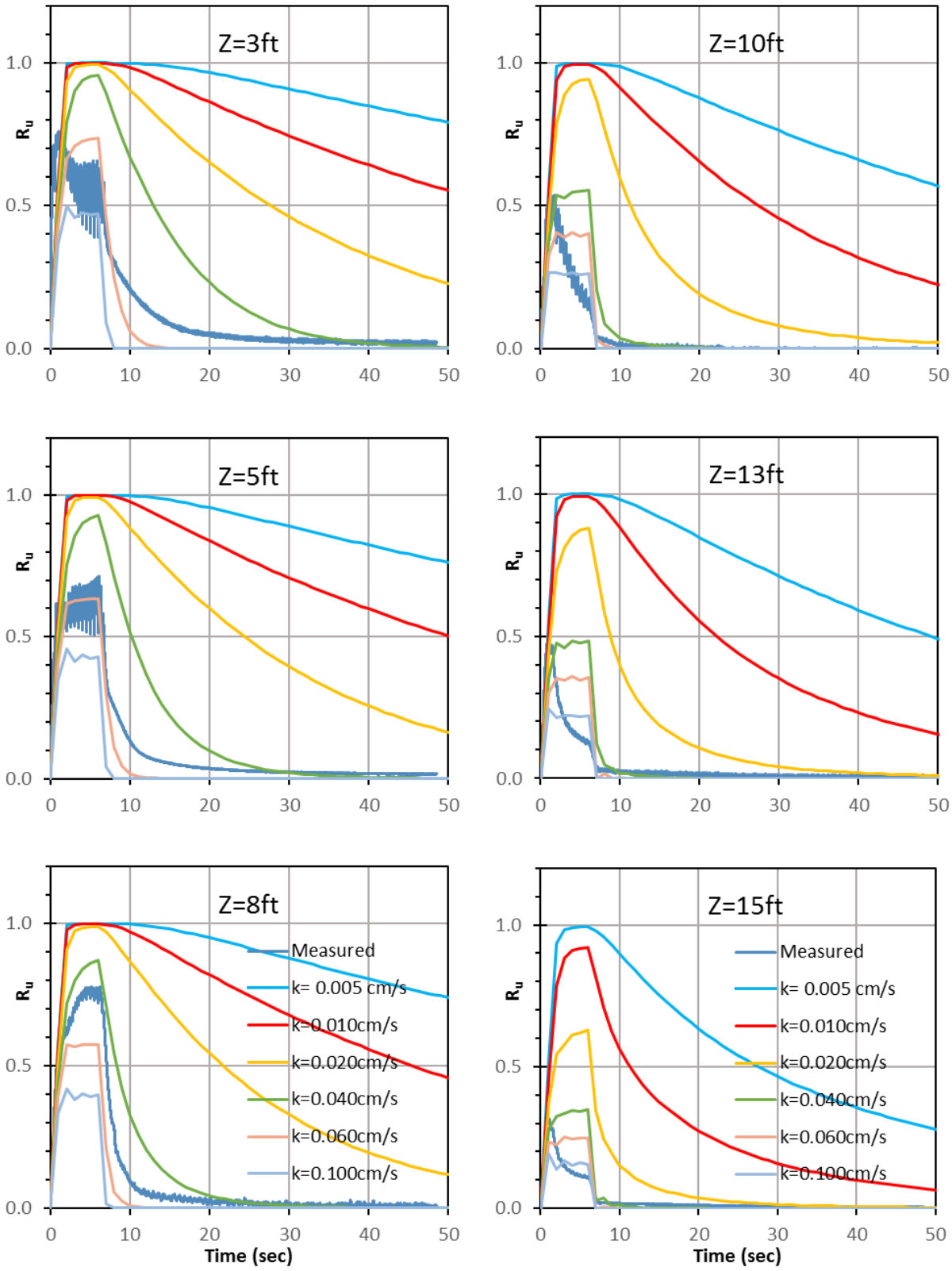

Figure 4-13 Effect of Varying Hydraulic Conductivity at Each Piezometer Level.

Table 4-2 Possible Correlation of Hydraulic Conductivity and Soil Type

Conductivity Range (cm/sec)	Soil Type	Possible Conductivity (cm/sec)	Expected Relative Density (Dr)
Course to Fine Sand 0.1 to 0.001	Sandy gravel	0.100	
	Very loose clean sand	0.060	25%
	Loose clean sand	0.040	50%
	Clean sand	0.020	75%
Fine Sand/ Silty Sand 0.001 to 0.00001	Dense/Fine sand	0.010	
	Well graded/ Very fine sand	0.005	
	Very fine sand/ Silty sand	0.001	

4.3.2 Effect of Variations in Modulus of Soil Compressibility, (m_v)

As previously stated, soil compressibility has a strong effect on the peak values and dissipation rate of the computed R_u curves. The back calculated m_v values for the experimental soil was much higher than those suggested in the FEQDrain manual for natural soils. Most of the back-calculated m_{vo} values were close to $8x10^{-6}$ ft^2/lb, but the suggested values were around $2x10^{-6}$ ft^2/lb. This is likely because the sand in the laminar box was very uniform, newly deposited and did not have any significant structure or bonding between the particles.

Results of the parametric study of the modulus of soil compressibility are shown in Figure 4-14 for each level where pore pressure transducers are located. Comparisons are provided with measured and back-calculated models as was done previously. The results of modeling show a higher coefficient of compressibility produces higher R_u peak values, and slower dissipation. Lower compressibility produces lower pore pressures and faster dissipation. This effect is clearly illustrated in Figure 4-14, which shows several curves produced by increasing or decreasing the m_{vo} by multiplying the back-calculated compressibility for each layer by a factor. The values in the legend and Table 4-3 indicate what factor was applied for each curve.

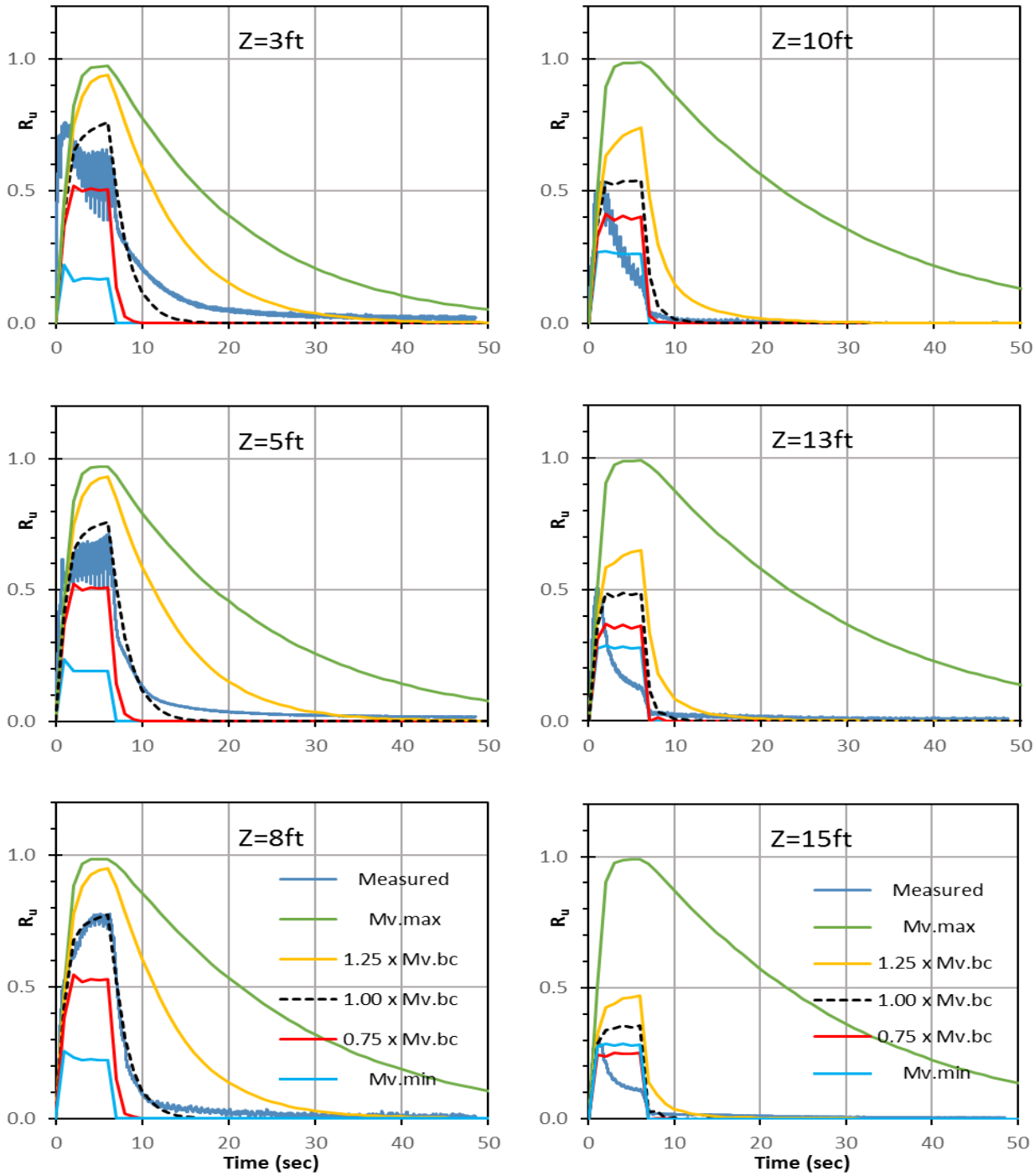

Figure 4-14 Effect of Varying Coefficient of Volumetric Compressibility (m_{vo}) at Each Piezometer Level.

Changing the m_{vo} values by factors of 1.25 and 0.75 changed the peak R_u values by 10 to 25 percent points which is very similar to the sensitivity observed with the hydraulic conductivity. This explains why R_u values observed by Oakes (2015) were similar for all tests; because the progressive reduction in compressibility, caused by successive densification, is

counteracted by the decreasing hydraulic conductivity. R_u vs time curves computed using the maximum and minimum range of m_{vo} values measured in the experiment show a variation in peak R_u values of plus 25% to 50% and minus 20 to 50%.

Table 4-3 Soil Compressibility Values Used in Sensitivity Analysis

	Modulus of Soil Compressibility (ft^2/lb)				
	Lowest Measured	Back-Calculated $\mathbf{M_{v\ (bc)}}$			Highest Measured
Depth Interval (ft)	$M_{v\ min}$	0.75 x $M_{v\ (bc)}$	1.00 x $M_{v\ (bc)}$	1.25 x $M_{v\ (bc)}$	$M_{v\ max}$
0-1	4.00E-06	1.13E-05	**1.50E-05**	1.88E-05	**2.00E-05**
1-3.5	4.00E-06	1.13E-05	**1.50E-05**	1.88E-05	**2.00E-05**
3.5-6	4.00E-06	1.05E-05	**1.40E-05**	1.75E-05	**2.00E-05**
6-8.5	4.00E-06	9.75E-06	**1.30E-05**	1.63E-05	**2.00E-05**
8.5-11	**4.00E-06**	6.75E-06	**9.00E-06**	1.13E-05	2.00E-05
11-13.5	**4.00E-06**	5.50E-06	**7.33E-06**	9.16E-06	2.00E-05
13.5-16	**4.00E-06**	1.50E-06	**2.00E-06**	2.50E-06	2.00E-05

4.3.3 Interaction of Hydraulic Conductivity and Modulus of Compressibility

As discussed in the previous two sections, the hydraulic conductivity and modulus of compressibility are sensitive parameters, and are both related to void ratio and hence related to relative density. Conductivity and compressibility are both inversely correlated to the relative density. As relative density increases, both the conductivity and the compressibility decrease. However, these parameters have opposite effects on the excess pore pressures generated. For example, low conductivity contributes to high pore pressures, but a low compressibility reduces the generation of pore pressures. Because these parameters are inter-related, it is unrealistic to change one of these sensitive parameters in a calibrated soil model without changing the other an appropriate amount.

Best-fit curves defining the hydraulic conductivity (K) and soil compressibility (m_{vo}) as a function of relative density (D_r) are shown in Figure 4-15. These correlations are based on the average K, m_{vo}, and D_r values for nine shaking tests for the 3ft drain spacing. Average K and m_{vo} are plotted on separate y-axes relative to D_r on the x-axis.

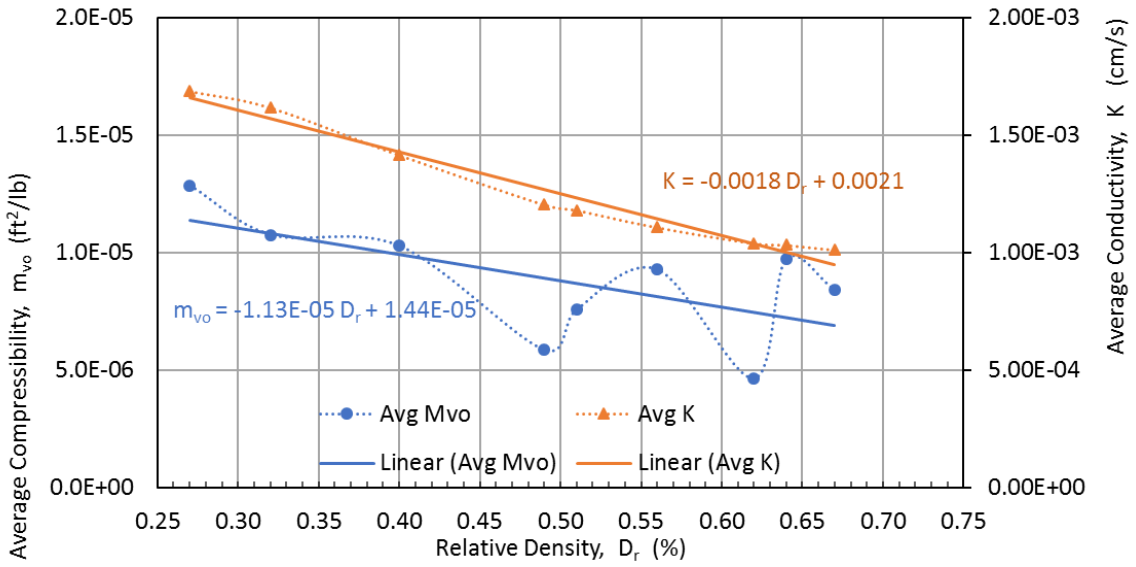

Figure 4-15 Best-fit Correlations of Average Hydraulic Conductivity (K) and Average Soil Compressibility (m_{vo}) with Relative Density (D_r). The Nine Markers of Each Parameter Because of the Nine Shake Tests of the 3ft Drain Spacing Test.

The best-fit curves in Figure 4-15 and the resulting equations were used to mathematically compute a new relative density when one sensitive parameter was adjusted. From this relative density, a new combination of conductivity and compressibility were used to model the expected R_u vs time curves with FEQDrain. To determine the parameters for the analysis, the conductivity was first changed to 1.25 and 0.75 times its measured value, then the relative density and compressibility were adjusted with the best-fit equations in Figure 4-15 to be compatible with these changes. The computed R_u vs. time curve at each piezometer depth is plotted along with the measured curve in Figure 4-16 and Figure 4-17, considering the variation in K and m_{vo}, respectively.

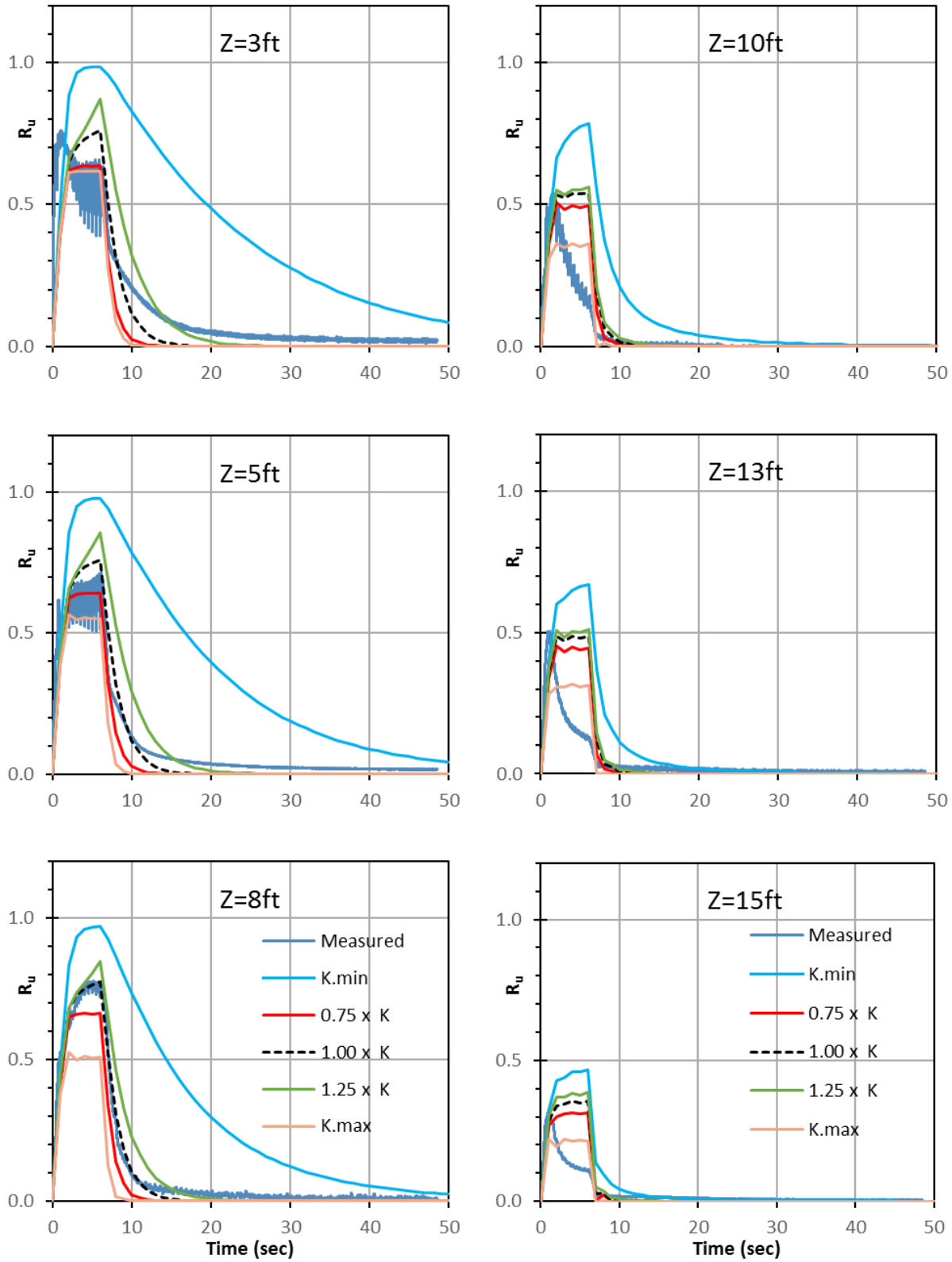

Figure 4-16 Combination Parametric Study, with Changes to Compressibility and Relative Density Following Changes of Conductivity (K).

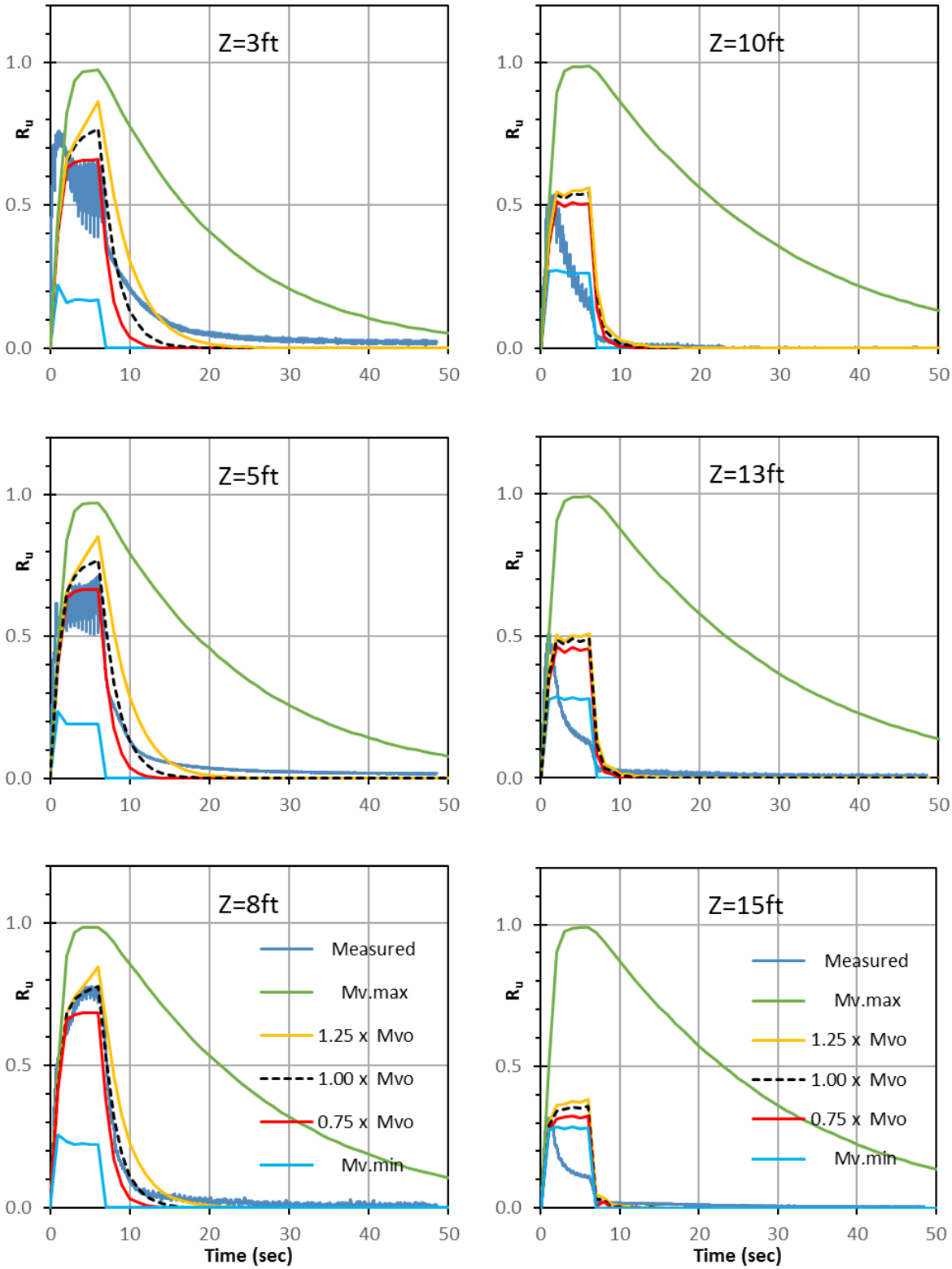

Figure 4-17 Combination Parametric Study, with Changes to Conductivity and Relative Density Following Changes of Compressibility (m_{vo}).

A review of the plots in Figure 4-16 indicates that the peak computed R_u values were only about 10 percentage points higher or lower than the best-fit curve for the shallower three depths and about 5 percentage points higher or lower than the best-fit curve for the deeper three depths This variation in the peak R_u is a reduction of about half relative to the sensitivity curves where K was adjusted without appropriately considering the effect of this variation on the compressibility. This analysis indicates that the sensitivity of the R_u vs time curves to changes in K and m_{vo} are much less pronounced than originally predicted when adjusting either K or m_{vo} without considering the effect on the other parameters. As illustrated in this analysis, the counter-balancing effects of the K and m_{vo} values help to reduce extreme variations in the predicted response.

Similar results, were obtained when the compressibility was first changed by factors of 1.25 and 0.75 times the best-fit values and then relative density and hydraulic conductivity were adjusted to be compatible. The computed R_u vs. time curve at each piezometer depth is plotted along with the measured curve in Figure 4-17 considering the variation in m_{vo}.

4.3.4 Effect of Variations in Relative Density (D_r)

To investigate the effect of relative density on pore pressure response, three values of relative density (D_r) were used, namely 30%, 50%, and 70%. The sand in the laminar box was typically within this density range. This range of relative densities includes loose to dense sands. Results of the parametric study for relative density are shown in Figure 4-18 for each level where pore pressure transducers are located. Comparisons are provided with measured and back-calculated models as was done previously. The computed curves show that relative density by itself has a small effect on pore pressure dissipation when the number of cycles to liquefaction is held constant. However, D_r will affect the number of cycles to liquefaction in most cases.

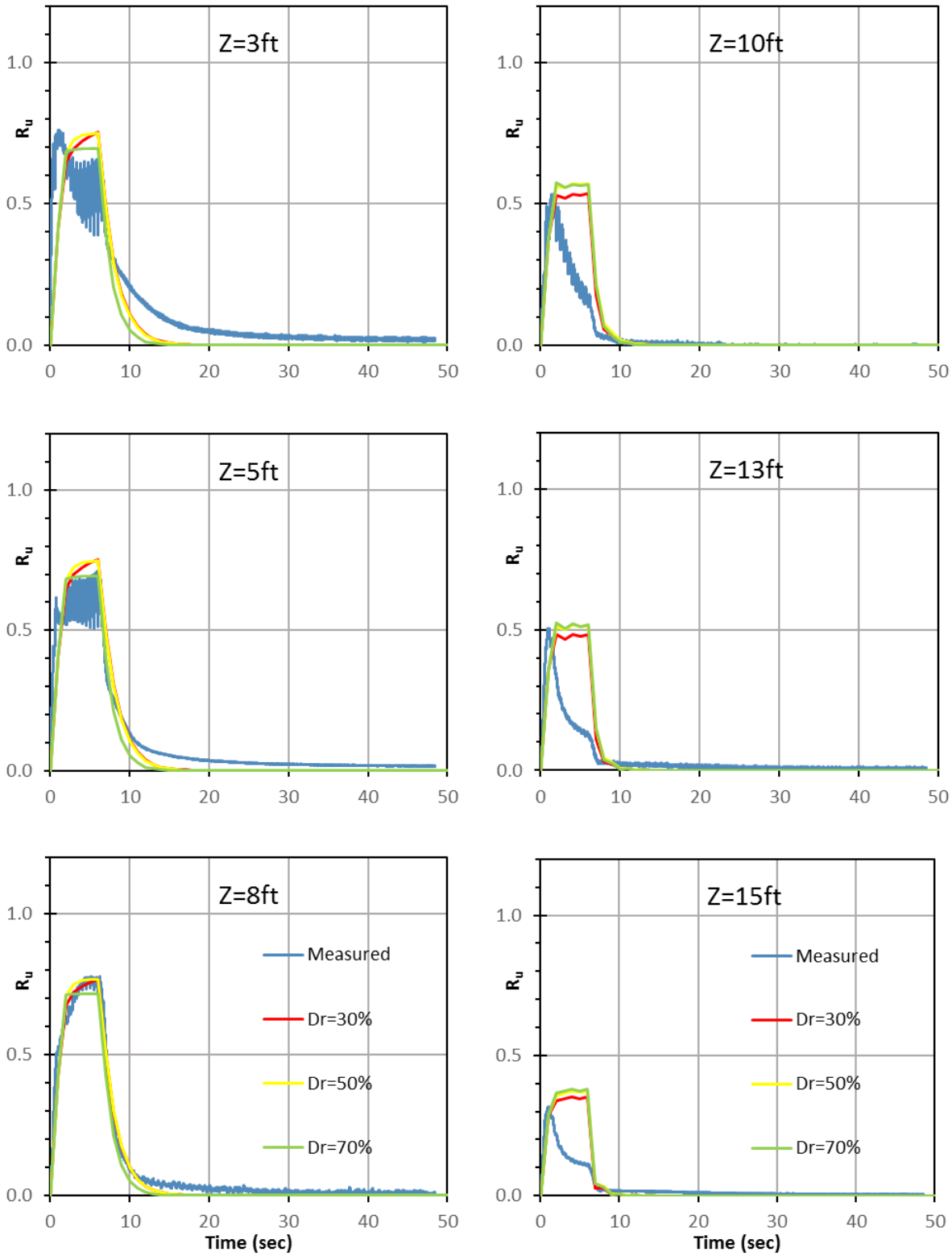

Figure 4-18 Effect of Varying Relative Density (D_r) at Each Piezometer Level.

Although the change in D_r has little effect on the computed R_u, the relative density is cross-correlated with hydraulic conductivity and the modulus of compressibility which both have large effects on pore pressure response. Typically, increasing the relative density decreases the hydraulic conductivity but also decreases the modulus of compressibility. These factors have compensating effects which would tend to reduce the influence on pore pressure response.

However, while performing preliminary modeling and parametric studies, the relative density was found to have a fairly significant effect on R_u when using a higher number of cycles to liquefaction.

4.3.5 Effect of Variation in the Cycles to Liquefaction

The number of cycles to liquefaction (N-Liq) is a property of each soil layer. A lower value indicates greater susceptibility to liquefaction. A method to determine an appropriate value for this parameter is described by Pestana et al., (1997); however, this method is difficult to apply to the laminar shear box testing where multiple shaking events are progressively applied with little time between effects for the sand to redevelop a micro-structure after densification.

To determine the sensitivity of this parameter, the number of cycles to liquefaction was systematically varied to show the general behavior. Results of the parametric study of the number of cycles to liquefaction are shown in Figure 4-19 for each level where pore pressure transducers are located. Comparisons are provided with measured and back-calculated models has been done previously. From Figure 4-19, we observe that lower values correspond to higher pore pressure values. It was found that the range N-Liq=1 to N-Liq=4 generally produce similar R_u vs. time curves. For N-Liq=10 or more cycles there is also a progressive reduction in peak R_u values, but the computed R_u vs time curves grossly under-estimate the measured curves.

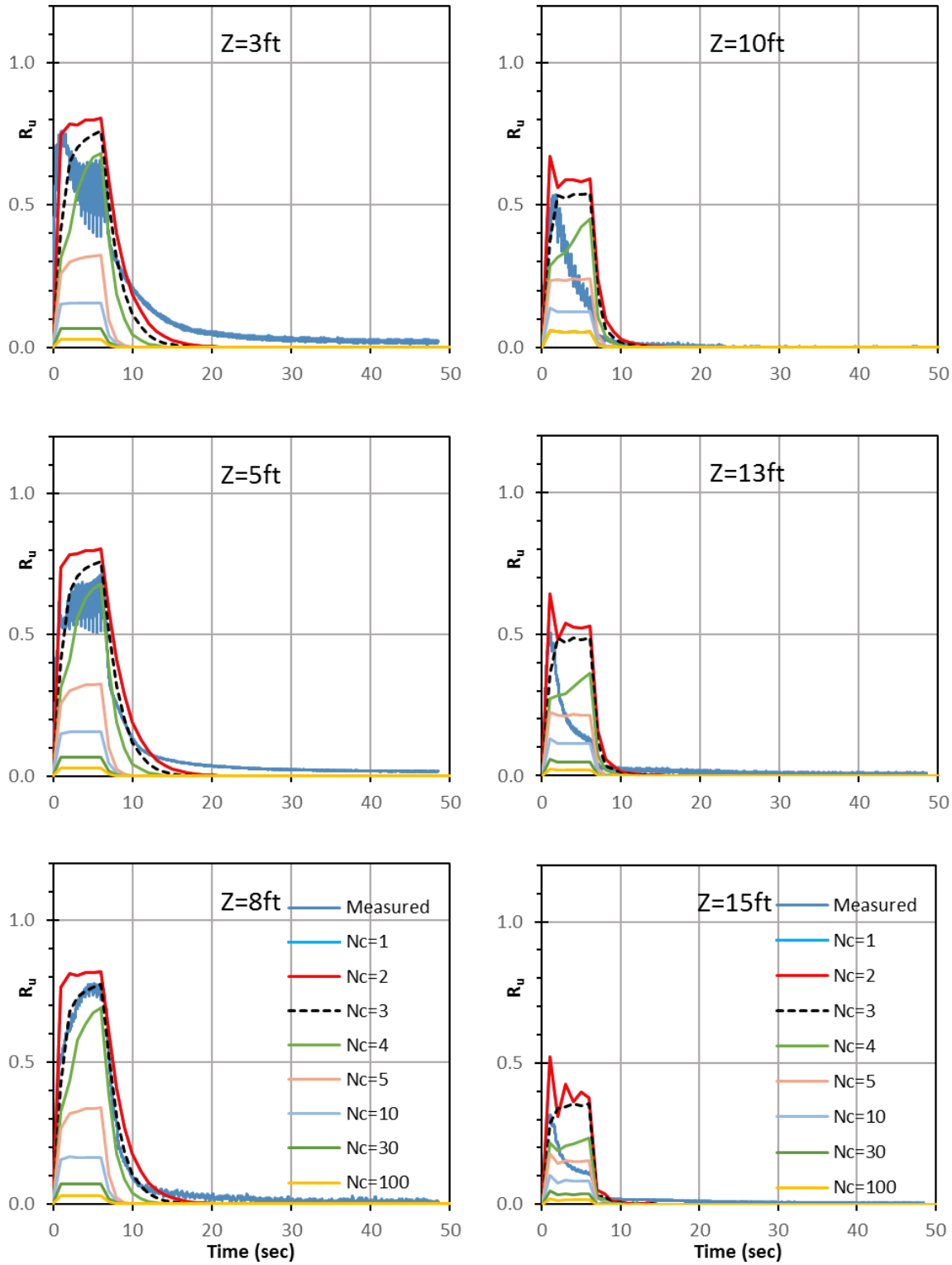

Figure 4-19 Effect of Varying the Number of Cycles to Liquefaction (N-Liq) at Each Piezometer Level.

It should be noted that N-Liq=2 is the effective lower limit for this value, because N-Liq=1 produces the same computed R_u vs time curves. These results indicate that the drains perform much better when the sand becomes denser and develops a greater number of cycles to liquefaction.

Experience also showed that the number of cycles to liquefaction must be an integer value. Non-integers will be rounded by the program before computations are performed. This can be seen by viewing the parameter values shown in the '.OUT' output file.

4.3.6 Effect of Variation in the Coefficient of Pore Pressure Generation (θ)

The coefficient of pore pressure generation (θ) controls the shape of the curve defining the generation of excess pore pressure with the number of cycles as illustrated in Figure 3-1. While θ is typically assumed to be 0.7, but the variable commonly ranges from 0.5 to 1.0. For the parametric study θ values from 0.3 to 1.1 were used. Results of the parametric study for the coefficient of pore pressure generation number of cycles to liquefaction are shown in Figure 4-20 for each level where pore pressure transducers are located. Comparisons are provided with measured and back-calculated models has been done previously. A review of the data in Figure 4-20 indicates that the coefficient of pore pressure generation appears to have little effect on the computed R_u, vs. time cures, thus it seems best to use the recommended value ($\theta = 0.7$), from the FEQDrain manual, for all soil types (Pestana et al., 1997).

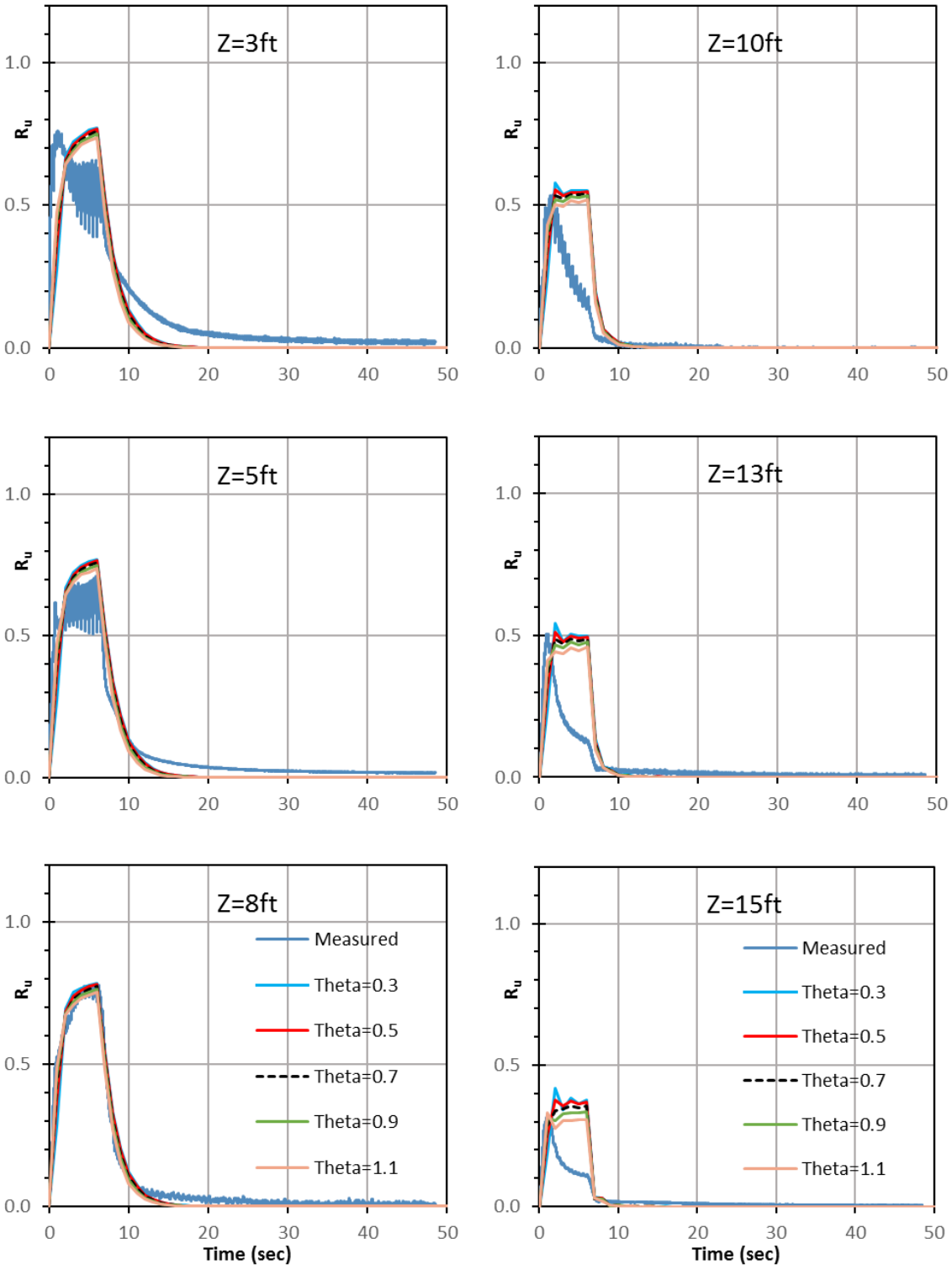

Figure 4-20 Effect of Varying Coefficient of Pore Pressure Generation (θ) at Each Piezometer Level.

4.3.7 Effect of Variation in the Soil Unit Weight (γ)

The soil unit weight (γ) is directly related to the vertical effective stress versus depth profile. While the average γ in the profile was approximately 122.5 lb/ft^3, variation could occur in this parameter. Therefore, analyses were performed with γ ranging from 115 lbs/ft^3 to 135 lbs/ft^3.which represent lower and upper bounds, respectively.

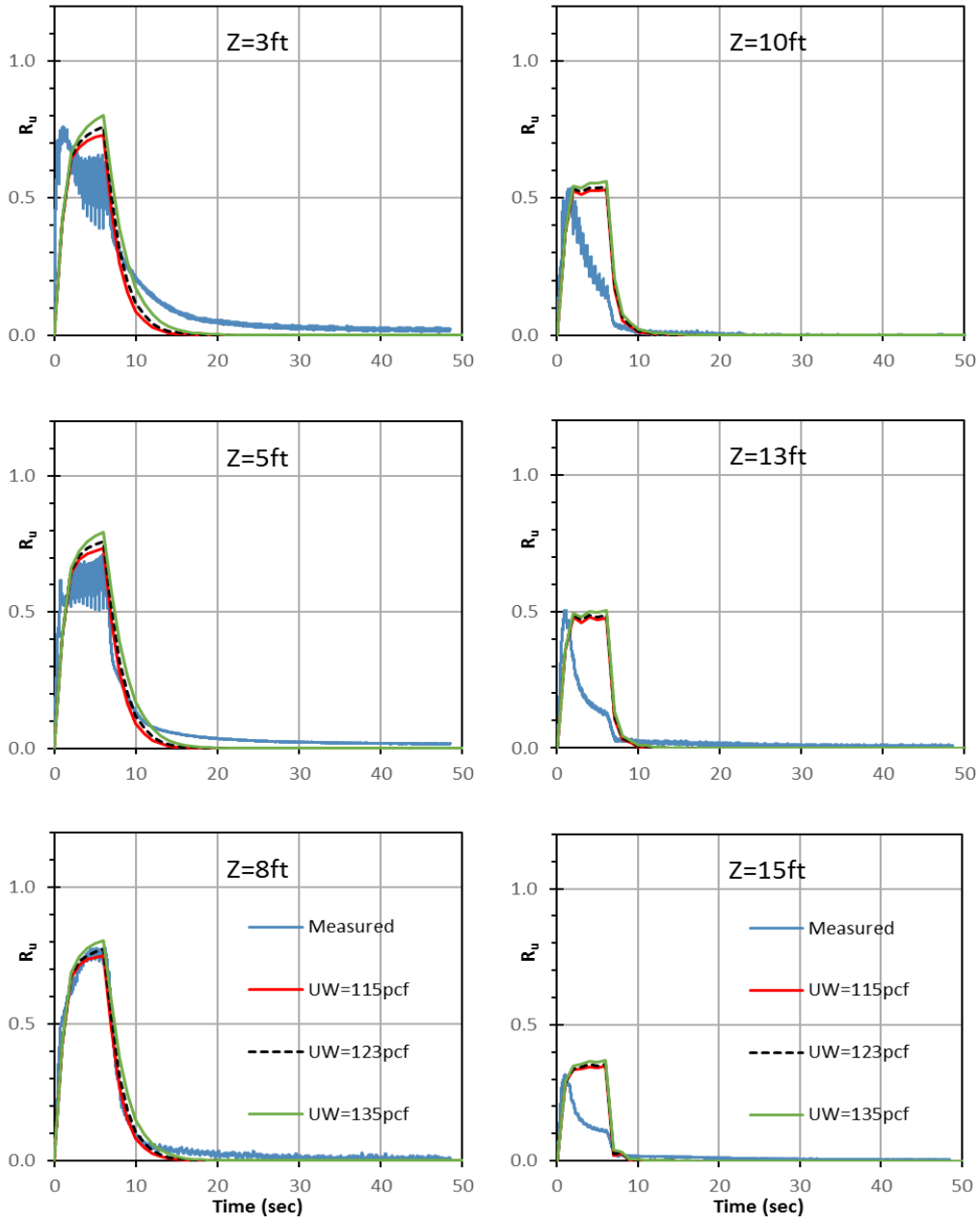

Figure 4-21 Effect of Varying Unit Weight (UW)/(γ) at Each Piezometer Level.

Results of the parametric study for the soil unit weight are shown in Figure 4-21 for each level where pore pressure transducers are located. Comparisons are provided with measured and back-calculated models as has been done previously. A review of the data in Figure 4-21 indicates that hardly any effect on the R_u vs time was noticeable from trying different soil unit weights. For soil unit weights below 66 lb/ft^3, a default value of 66 lb/ft^3 is automatically chosen by the program.

4.4 Effect of Variation in Drain Diameter

Drain diameter has a significant effect on the ability of water to escape from the soil and thus prevent excess pore pressures. Models were made to compare several sizes of drains, namely: no drain, a wick drain, and circular PV drains with diameters of 2", 3", 4" and 6".

Modeling of the 'no drain' case was not successful using the 'kopt' parameter (no drain/ constant m_v drain/ variable m_v drain). Instead a very small decimal value less than one was used for drain diameter, which produced the high R_u values expected from having no drain.

When using appropriate parameters for modeling wick drains, the program fails to run to completion. It appears that when vertical resistance in the drain becomes large, the calculations don't converge. For larger drains, the vertical head loss is a small decimal less than 1 (3" drain or bigger), but for wick drains and even 2"drains, the value is orders of magnitude larger. By using the maximum stable vertical resistance value and proportionally reducing the drain size to increase the head loss, the resulting R_u curves are reasonable. The values used to describe drain properties and head loss coefficients are shown in Table 4-4.

Modeling of 2" drains required a reduced head loss value and also needed a slight reduction to the drain size to reach convergence, while still accounting for the full head loss.

The 3" drains are the same size as those used in the laminar shear box and did not require any special adjustments. No special adjustments were needed for the 4" and 6" diameter drains.

Table 4-4 Values Used for Modeling Various Drain Sizes

Drain Type	Drain Radius (expected)	Drain Radius (modeled)	Drain Area	C1 (expected)	C1 (modeled)	Orifice	Permittivity
	ft	ft	ft^2			ft^2/ft	s^{-1}
No drain	**N/A**	**0.0001**	0.049	1.705	1.705	0.008	0.083
Wick drain	**0.110**	**0.003**	0.004	**200**	**6**	0.690	0.500
2" PVD	**0.108**	**0.046**	0.022	**14**	**6**	0.002	0.083
3" PVD	0.154	0.154	0.049	1.705	1.705	0.008	0.083
4" PVD	0.200	0.200	0.087	0.368	0.368	0.013	0.083
6" PVD	0.288	0.288	0.196	0.042	0.042	0.015	0.083

Results of the parametric study for the effect of drain diameter are shown in Figure 4-22 for each level where pore pressure transducers are located. Comparisons are provided with measured and back-calculated models as has been done previously. The presence of the wick drain clearly increases the rate of pore pressure dissipation at the conclusion of shaking; however, the peak R_u values are not significantly decreased relative to the curve for no drain. The 2" diameter drain further increases the rate of pore pressure dissipation relative to the wick drain curve, but does not decrease the peak R_u value significantly.

The 4" diameter drain reduces the peak R_u value by 20 to 25 percentage points at shallow depths (3 to 8 ft.), but only by about 10 percentage points at deeper depths (10 to 15 ft.) relative to the 3" diameter drain. The rate of dissipation following shaking decreases only marginally. Use of a 6" diameter drains has relatively little effect on the R_u vs time curve relative to the 4" diameter drain and may not be economically justifiable for clean sands such as those investigated in this study.

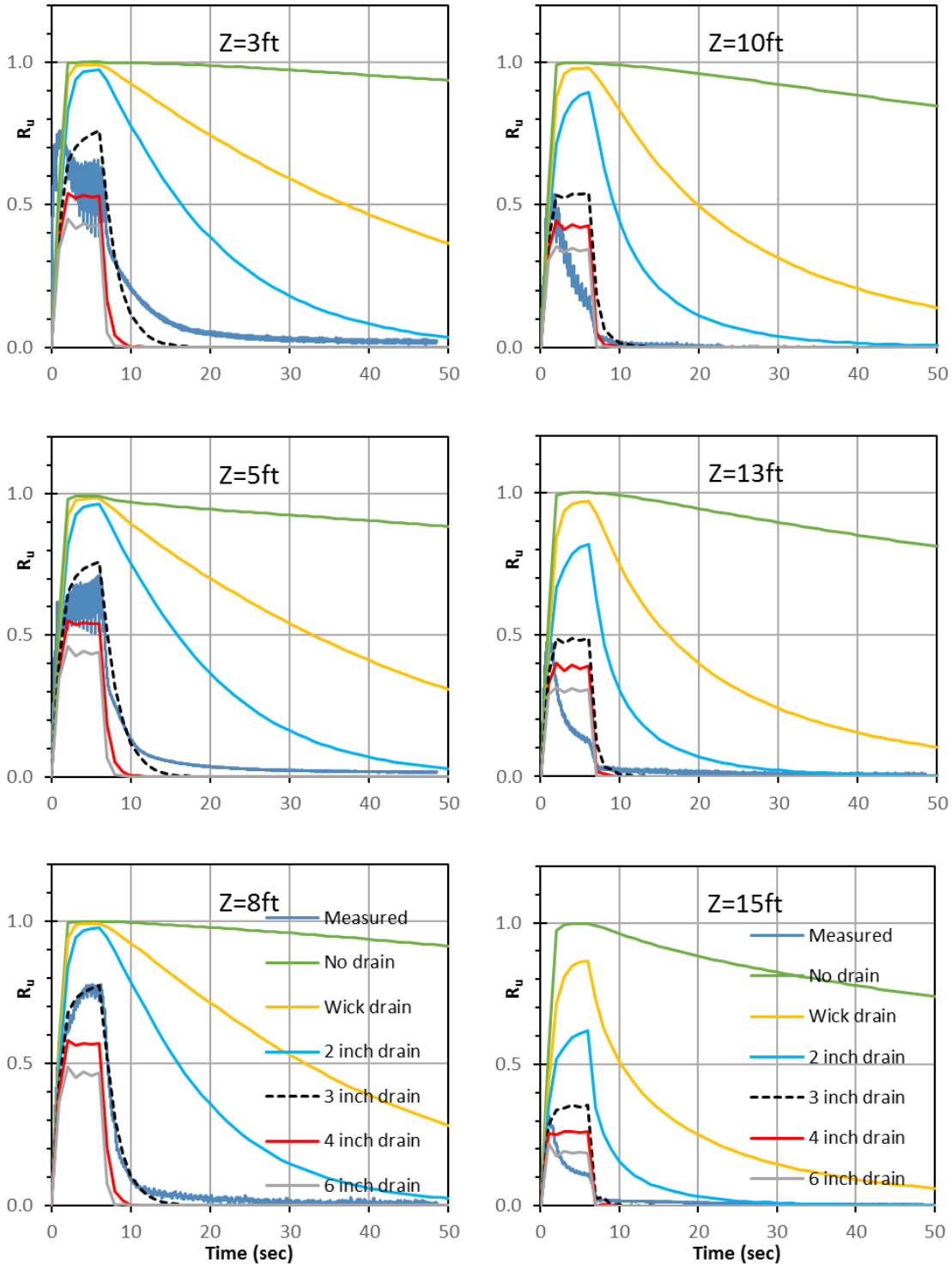

Figure 4-22 Effect of Drain Diameter on Excess Pore Pressure Response at Each Piezometer Level.

4.5 Effect of Variation in Earthquake Magnitude

The FEQDrain program uses the number of equivalent cycles and shaking duration to define the magnitude of a seismic event. Having a longer duration of shaking (t_d) with a greater number of equivalent cycles (N_{eq}) describes a higher magnitude earthquake which would last longer or have higher accelerations. The user's manual provides recommendations for the number of equivalent cycles (Seed & Idriss, 1982), and duration of shaking (Seed et al., 1975b) to correspond to different moment magnitudes(M_w), shown below in Table 4-5. The basis for the cycles and time combination is provided by research with undrained cyclic shear tests which showed it does not matter whether the shear cycles were applied at 1 Hz or 10 Hz. (Seed, Martin & Lysmer, 1976). Because the frequency of loading had no effect, it follows that only the number of cycles really matters. This is probably why Pestana et al. (1997) recommended the combination of number of cycles and duration to account for increasing magnitude.

Table 4-5 Equivalent Number of Stress Cycles and Duration for Modeling Specific Magnitude Ground Motions. (Neq)

Equivalent number of cycles due to earthquake loading (from Seed & Idriss, 1982)

Magnitude	N_{eq}
5 ¼	2 – 3
6	5 – 6
6 ¾	10
7 ½	15
8 ½	26

Duration of earthquake strong motions (from Seed et al., 1975b)

Magnitude	Duration (sec)
5 ½ - 6	8
6 ½	14
7	20
7 ½	40
8	60

However, for the situation involving PV drains, the frequency and duration of loading is relevant. For example, an intense, short duration earthquake would likely overwhelm the drains and liquefy the soil. But a similar number of cycles applied over a longer time period might suggest that the drains would be sufficient to prevent liquefaction. In fact, the application of 15 cycles of loading, typical of a 7.5 M_w earthquake, in 7.5 seconds during the laminar shear box testing, could represent a relatively severe loading for the drains in comparison with a 40 second duration that would be typical of a 7.5 M_w earthquake.

To investigate the effect of earthquake duration and number of cycles on pore pressure response, the computer program FEQDrain was used to analyze the soil profile for various magnitudes of earthquakes. Results of the parametric study for the effect of earthquake magnitude are shown in Figure 4-23, for each level where pore pressure transducers are located. It should be noted that this model represents one of the 4 ft drain spacing test, and as such its piezometers were at slightly different depths. Comparisons are provided with measured and back-calculated models as has been done previously.

As shown in Figure 4-23, the peak R_u values computed for all the different earthquake magnitude events are substantially lower in almost all cases than that observed with 15 uniform load cycles over a 7.5 second duration in the experimental testing. The primary pore pressure response includes an initial pore pressure rise, a plateau, and dissipation when the shaking stops. There is a noticeable difference in the plateau length of each curve, but none has a very high maximum value. Surprisingly, there is no progressive increase in peak pore pressure for higher magnitude events. Higher magnitude seismic events have more cycles (N_{eq}) and a longer duration (t_d) which results in a longer plateau, but with nearly the same pore pressure rise as for smaller quakes. This response occurs because the longer duration "dilutes" the energy of the shear cycles by allowing time for drainage and dissipation to occur while shaking continues, without overwhelming the drains. Similar pore pressure response among models for increasing earthquake magnitude agrees with the similarity in the ratio of shaking duration to equivalent uniform cycles (seconds/cycle) for each magnitude.

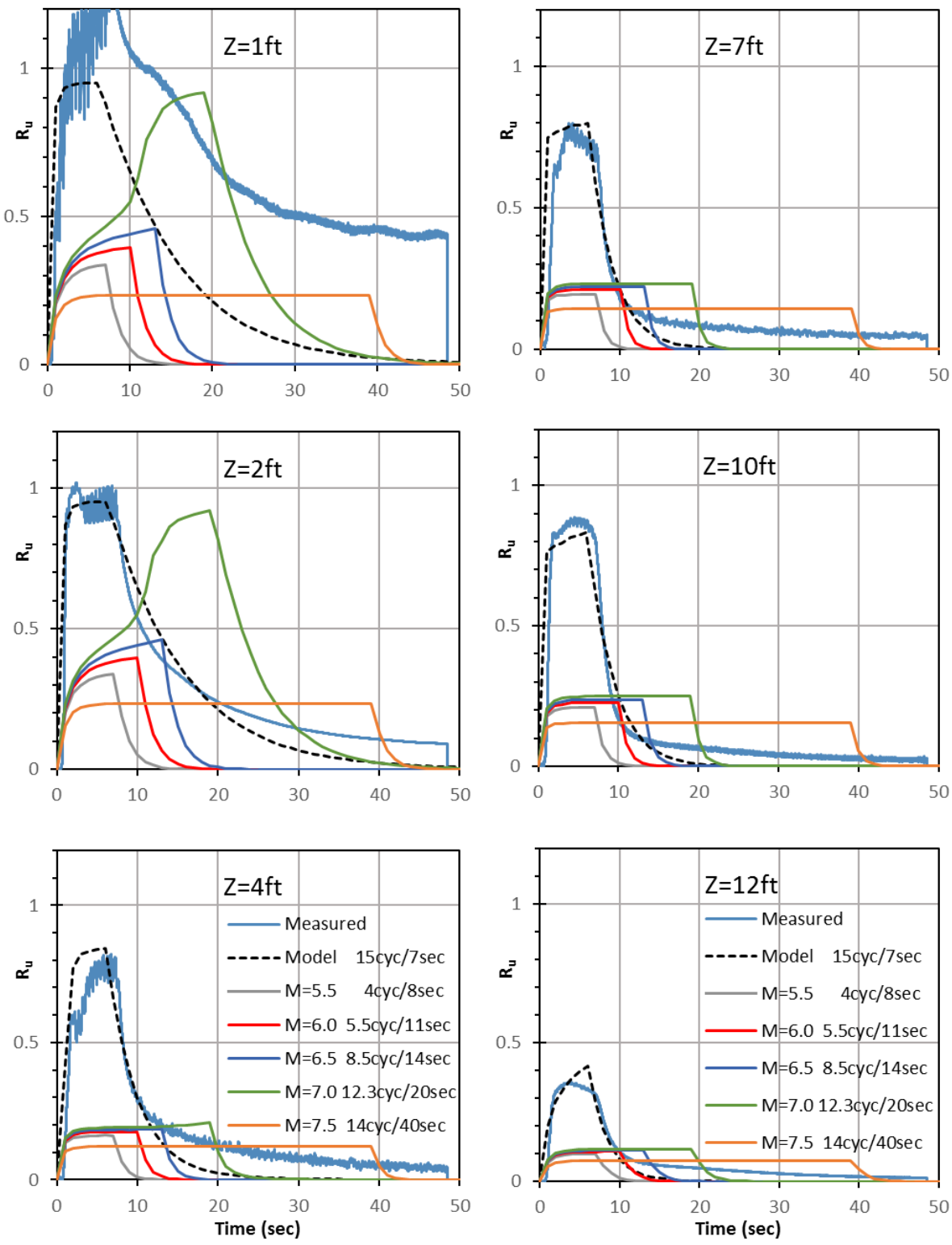

Figure 4-23 Effect of Number of Cycles and Shake Duration with Variations in Earthquake Magnitude Suggested by FEQDrain User Manual (Pestana et al. 1997).

Based on the recommendations in the FEQDrain user's manual (Pestana et al, 1997), typical seconds/cycle values range from about 2 to 2.67 seconds/cycle for M_w values ranging from 5.5 to 8.5. Of course, this loading rate is much slower than the 0.5 seconds/cycle loading rate actually used in the experimental testing. Therefore, the results from the laminar shear box testing likely represent a conservative estimate of the response that might be observed in a real earthquake. However, it should be recognized that earthquakes do not typically apply cycles at a uniform rate over the entire duration of shaking. Therefore, higher frequency shaking over a short portion of the total duration could still reduce the effectiveness of PV drains relative to the predictions in Figure 4-23.

4.6 Comparison to Vytiniotis et al. (2013)

The numerical modeling performed by Vytiniotis et al. (2013), was a full 2D model instead of a unit-cell axisymmetric model. The assessment of soil improvement measured by Vytiniotis et al. (2013) was horizontal soil deformations of a slope adjacent to the treated area, rather than excess pore water pressures in the treated area itself. The horizontal lateral deformations were found to be well correlated with peak ground acceleration (PGA). Also, no correlation was found with Arias Intensity (I_a), which implies that drain systems would be similarly effective under different acceleration time histories. Significant reductions in horizontal displacement were observed just as significant reductions in vertical displacement were observed in the laminar shear box testing.

Results from FEQDrain agree with some conclusions of Vytiniotis (2013) in that drain effectiveness is relatively independent of earthquake magnitude, but for different reasons. FEQDrain simplifies all earthquakes of a specific magnitude to a number of equivalent cycles over a specified duration and results from modeling show no increased pore pressure effects from larger magnitude events. Vytiniotis et al. (2013) used unique time histories and found no correlation between Arias intensity and improvement ratio, relative to the untreated case. FEQDrain showed pore pressures reaching a plateau within 1-2seconds, instead of 15seconds as suggested by Vytiniotis et al (2013), but this is likely related to differences in the duration of shaking and the density of the sands in the two studies.

4.7 Comparison to Howell et al. (2014)

The numerical modeling performed by Howell, Rathje, and Boulanger (2014), used computer models to match preexisting experimental data similar to what was done in this study. The three finite element model types were: a 2D model of the full centrifuge test, a 3D unit cell around a single drain, and a 2D unit cell. The study showed that finite element models predict excess pore pressure ratios consistent with the experiments. However, a few of the back calculated soil properties were not within the expected range, and had to be adjusted to achieve agreement. Also, the computer model most like the centrifuge test geometry gave the best prediction of horizontal displacements.

Howell et al. (2014) observed similar trends in the generation and dissipation of R_u versus time relative to basic soil properties as was noted in the modeling performed in this study with FEQDrain. The two most important input properties, hydraulic conductivity (k) and soil compressibility (m_v), were opposite between the two studies. However, the differences in both properties appear to be proportional and inverse, thus resulting in nearly the same modeled R_u values.

The compressibility (m_v) used by Howell et al. (2014) ranged from 0.7 $x10^{-5}$ to 1.5 $x10^{-5}$ m^2/kN, which is 3-14 times smaller than the values reported by Pestana et al. (1997), which means their model assumed a very stiff soil. Howell et al (2014) found their compressibility range by back-calculating from a constitutive model, for different levels of pore pressure generation. These compressibility figures followed the trend that the m_v increases as the pore pressure increases, but were noted as being very small compared to tests of Monterey sand by Lee and Albaisa (1974). The prototype conductivity measured in the centrifuge was k=0.03 cm/sec, but it was adjusted to satisfy the chosen constitutive model. Thus k=0.007cm/sec was used in the finite element models.

The compressibility (m_{vo}) used for FEQDrain models in this study ranged from 2 $x10^{-6}$ to 2 $x10^{-5}$ ft^2/lb, or (4.2 $x10^{-5}$ to 4.2 $x10^{-4}$ m^2/kN) which is 2-10 times larger than the values reported by Pestana et al. (1997), which represents a softer soil. The conductivity measured in the laminar shear box was k=0.028 - 0.07cm/sec. This is 4-9 times larger than the values used in the analysis by Howell et al. (2014). However, the actual measured values in both cases are very

similar. Therefore, based on the raw hydraulic conductivity values, it is likely that the hydraulic conductivity of the sand used in both experiments was similar.

Because the hydraulic conductivity and compressibility have inverse effects on R_u, then modeling in FEQDrain with the higher, but measured, k values and with high m_v produced similar R_u values to the Howell et al. (2104) 3D unit cell model which used lower k and lower m_v values.

Howell et al. (2014) chose to adjust the conductivity, within a range, until a best fit value was obtained; rather than deviate from suggested values of soil compressibility. This under prediction of volumetric compressibility inherent in the constitutive model produced an under-prediction of settlement. This under prediction suggests that the compressibility used by Howell et al. (2014) was far too low, and that higher compressibility values would be appropriate, such as was used in this modeling with FEQDrain, which allowed it to closely predict settlement. In any case, the sand in the centrifuge test and in the laminar box are both very young and would tend to have a higher than expected compressibility.

Both modeling efforts calculated a soil compressibility that differed, by up to one order of magnitude, from the values recommended by Pestana et al. (1997). Both parent experiments used artificially placed, saturated loose sand, in a freshly formed state, with no cementitious bonds. Both experiments had comparable levels of acceleration and some tests used sinusoidal input motions.

4.8 Comparison to Oakes (2015)

The findings of this numerical modeling study, shown in regular text, are described after each of Oakes (2015) conclusion points, shown in bold.

1. **Excess pore pressures dissipated rapidly after shaking, with higher density in later tests increasing the rate of dissipation.**

   Modeling of the 3 ft and 4 ft spacing tests had rapid dissipation for all shakes. Later test were modeled with higher relative density and somewhat lower m_v values. Therefore, later tests also had faster dissipation.

2. **Excess pore pressures dissipated significantly faster than previous laminar shear box testing without drains, taking seconds rather than minutes for pore pressures to fully dissipate.**

   Modeling showed pore pressures dissipated within seconds, and there was faster dissipation for closer drain spacing. A parametric study of drain size indicated faster pore pressure dissipation for larger drains and longer dissipation rates for very small drains.

3. **Higher acceleration caused more settlement and settlement deeper in the soil profile.**

   FEQDrain predicted settlement relatively well for all acceleration levels and both drain spacings. FEQDrain does not provide a way to specify higher acceleration levels, while keeping the number of cycles the same because the effect of acceleration is expressed by shortening the number of cycles to liquefaction.

4. **Settlement was reduced by 20-64% when compared to previous laminar shear box testing without drains. This matches previous results from centrifuge testing.**

   When modeled with very small drains (simulates having no drain) the computed settlement was one tenth as much. This settlement figure is based on the volume of water discharged, which was also one tenth of the treated case. In reality, the soil would still experience upward flow, though not in the drain, and thus even larger settlements would occur. Settlement predicted with FEQDrain was somewhat greater than measured in the experiments.

5. **Drains spaced closer together are more effective at reducing excess pore pressures, and may have slightly reduced settlement.**

   Models with drains spaced closer together were more effective at reducing excess pore pressure, but they increased the computed settlement somewhat, because more water was discharged. This was also true for the freshly placed laminar shear box sand. However, under field conditions during earthquakes, better drainage with longer durations helps keep R_u values below 0.4 or 0.5 and may lead to less settlement.

4.9 Suggestions for Practical Use of FEQDrain

Given the uncertainties encountered in performing this study of modeling excess pore pressure ratios via the program FEQDrain, a discussion is in order for practical use of the program in evaluating liquefaction prevention by large diameter vertical drains. General usage is described first, followed by a discussion of key parameters.

General Usage

This paragraph is a list of steps for using FEQDrain, but the primary reference should still be the FEQDrain user manual or Pestana et al. (1997). First, determine appropriate input values as discussed in sections 3.4, 3.5, and 3.6. Second, determine an appropriate number of equivalent cycles and shaking duration. Third, determine appropriate values for sensitive parameters of hydraulic conductivity (K), modulus of soil compressibility (m_{vo}), and cycles to liquefaction (N_{liq}). Fourth, run FEQDrain and change a few parameters within a reasonable range to determine if the model will run properly or if it will crash. Fifth, test a combination of input values to produce the highest, middle, and lowest expected R_u curves. Sixth, evaluate predictions, review and refine assumptions, model again.

Program troubleshooting-- Run FEQDrain and change a few different parameters within a reasonable range to determine if the model will run properly or if it will crash. If FEQDrain keeps crashing using normal input values, then try lengthening the total time of analysis as discussed in section 3.6. If the problem persists, try using the opposite system of units or attempt to duplicate a previous researcher's FEQDrain model, such as this study or Strand (2008). These actions may solve the issue or will help uncover the problem.

Key Parameters

Drain geometry-- Use standard diameters for which there is available flow property data. This should be based on data provided by a drain manufacturer, as shown in the Appendix, section A.2 Flow Properties of HDPE Corrugated Pipe. Also, assume a drain spacing interval. Many studies have used a drain spacing of 3-4 ft, which are good starting values.

Number of layers and model increments-- These are described in section 3.3 of this document, and are discussed more fully in Pestana et al. (1997).

Non-sensitive parameters— These properties usually can be measured, and have little effect on the R_u or settlement predictions.

Cycles to Liquefaction (N_{liq})-- For very loose soils use a value between 2 and 4, as seen in Figure 4-19. For denser soils, use the SPT and CPT correlations provided by Pestana et al. (1997), for natural soils. But, using a higher N_{liq} value will suppress the predicted pore pressures, even if the hydraulic conductivity and modulus of compressibility are high. Nevertheless, using a number from 2-4, in these cases is still recommended because it will be conservative.

Hydraulic Conductivity (K) -- Use an in-situ pump test to measure this value if possible. If pump testing is not possible, or not possible for a given soil layer, use the suggested conductivity values from Table 3-4, based on grain size.

Modulus of Soil Compressibility (m_{vo})-- Use either of two methods. Preferred method: Calculate modulus directly from expected strain (via liquefaction settlement predictions), this is the recommended method and is described in the next paragraph. Alternate method: Use the values suggested in Table 3-9, but note that the fairly wide range of compressibility values in the table can give noticeably different pore pressure predictions. Perhaps use a value in the middle of the range of m_{vo}. when using the table values.

One might select appropriate m_{vo} values for aged soils by using tables but m_{vo} values could be better estimated based on liquefaction settlement prediction equations. First, compute factor of safety against liquefaction for a given layer using a triggering curve such as Boulanger & Idriss (2014) based on CPT or SPT penetration resistance for an appropriate magnitude earthquake with a peak ground acceleration. Second, determine the relative density of the sand layer from the CPT or SPT penetration resistance. Third, use Ishihara & Yoshimine (1992) graph, Figure 4-24, to determine volumetric strain (ε_v) for the layer.

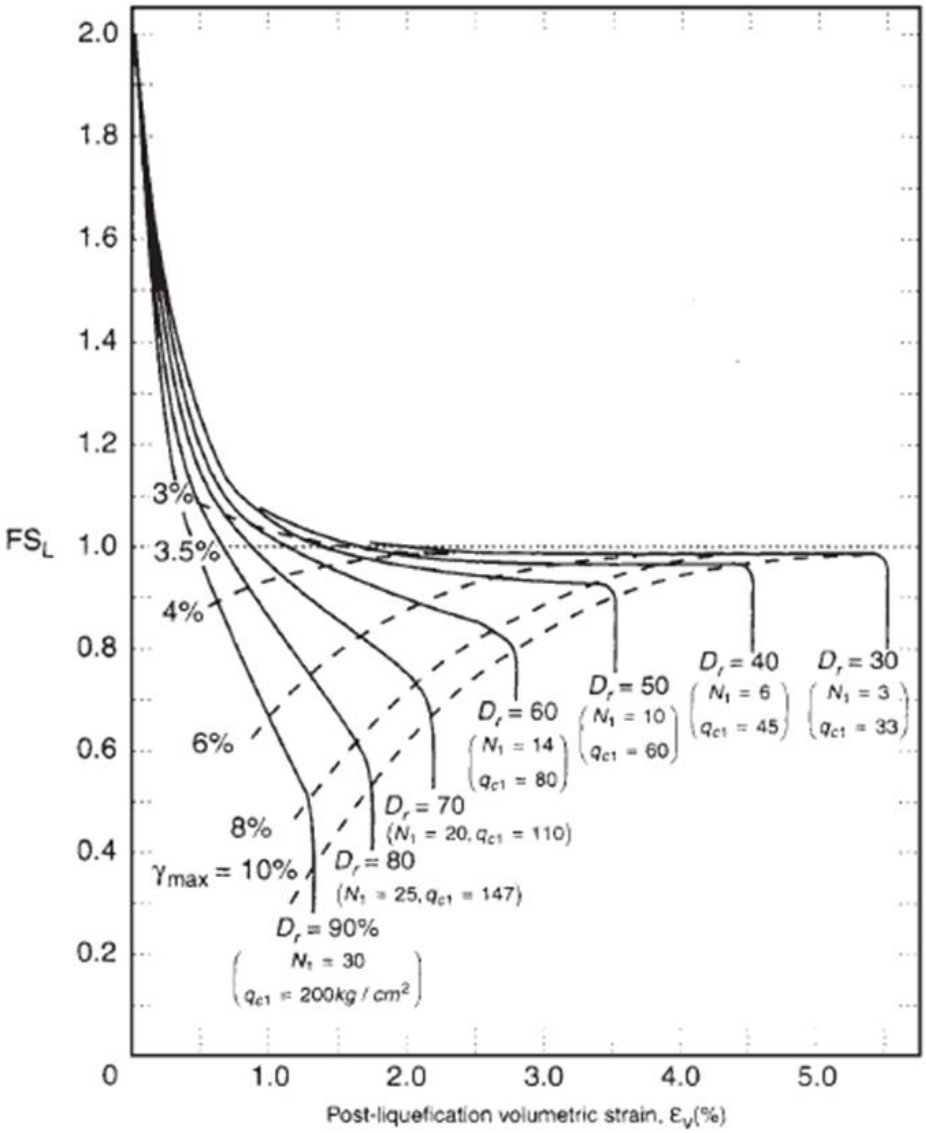

Figure 4-24 Graph of Post-Liquefaction Strain (ε_v %), Ishihara & Yoshimine (1992).

Fourth, compute the initial vertical effective stress (σ'_o) at the center of the sand layer. Fifth, compute m_v by using the equation ($m_v = \varepsilon_v / \sigma'_o$). Sixth, compute the initial (pre-liquefaction) modulus, m_{vo} using the equation ($m_{vo} = m_v (1 + Y + 0.5\ Y^2) / e^Y$) with ($y = a \cdot r_u^b$, where $a = 5(1.5\text{-}Dr)$, and $b = 3(4)^{-Dr}$), which are respectively, Equation **(8)** and Equation **(17)**.

Number of equivalent cycles and shaking duration-- Use the values provided in Table 4-5 based on the design earthquake. These combinations are perhaps appropriate in designing for a consistent long, uniform pattern of accelerations. But since seismic motions can manifest

different acceleration time-histories at various locations, it would be prudent to design for a shorter more intense version of the same earthquake. This can be done by leaving the number of cycles the same and using a fraction of the shake duration, perhaps half or a quarter as long.

5 SUMMARY AND CONCLUSIONS

In this study, numerical modeling was performed with the finite element program FEQDrain, using data from shake testing of large diameter prefabricated drains in the NEES@ Buffalo laminar shear box. Test results were reported by Oakes (2015) for drain spacings of 3ft and 4ft on centers. For each drain spacing, the physical testing was performed for three rounds of shake tests with three shake tests per round having peak acceleration levels, 0.05g, 0.1g, and 0.2g, respectively for a total of nine shake tests. For each successive shake test the soil became progressively denser with more resistance to liquefaction and lower hydraulic conductivity and compressibility. Results from drain spacings of 3ft and 4ft were both modeled and compared to the measured experimental data, and compared to modeling done by other researchers.

Numerical modeling used measured soil parameters and simplified input motions to match the measured pore pressure ratio time-histories. Each input parameter of the modeling program was systematically evaluated to determine its effect on the outcome. Parameters that were found to have the greatest effect were compared against the upper- and lower-bound measured values to ensure they were within the correct measured range.

The objective of this modeling effort was to examine the reliability of the existing computer modeling program, FEQDrain, designed specifically for use with prefabricated drains. By showing that this program can predict excess pore pressure ratios for a controlled full-scale shake table experiment, the program can then be used more confidently to predict the effects of prefabricated drains in natural soil, under real earthquake scenarios.

5.1 Conclusions

FEQDrain is capable of modeling the excess pore pressure ratio time-histories observed in the laminar shear box experiments, as long as an appropriate combination of ‘number of

equivalent cycles' and 'shake duration' is chosen and sensitive soil parameters are compatible with measured values. However, predicted settlement values are typically somewhat higher than measured settlements in almost all analyses.

Hydraulic conductivity, soil modulus of compressibility, and cycles to liquefaction are sensitive parameters in numerical evaluations of response. Conductivity can be measured in-situ, but soil modulus and cycles to liquefaction are more difficult to estimate. Higher conductivity results in lower R_u values, presumably because pore water can more easily flow to vertical drains. Vertical conductivity has minimal effect because horizontal flow to drains is more significant than vertical flow in the soil. Higher compressibility results in higher computed R_u values, presumably because for a given change in pressure there is a greater tendency of contraction which produces greater pore water pressure. In this study, back-calculated and experimentally derived compressibility values were typically about four times higher on average than those suggested by Pestana et al (1997). The higher compressibility is likely because the water-pluviated sand in the laminar box was very uniform, newly deposited, and did not have time to develop any significant micro-structure or bonding between the particles.

Similar R_u values can be modeled with different combinations of conductivity and compressibility. For example, Howell et al. (2014) in modeling centrifuge results used a lower k and lower m_v than suggested by Pestana et al. (1997) while in this study higher k values and higher m_v values were used than Pestana et al. (1997) recommended. Nevertheless, both studies yielded similar R_u values, because the differences generally offset each other.

The number of cycles to liquefaction (N-liq) is a somewhat ambiguous parameter defining the liquefaction susceptibility of the soil. N-liq decreases as acceleration increases and increases as relative density increases. For sands deposited by natural processes and aged for a reasonable time, N-liq can be estimated using liquefaction triggering curves based on the SPT $(N_1)_{60}$ or CPT (q_{c1N}) values along with the peak ground acceleration. However, for the newly deposited hydraulic fill used in this study, these correlations are not well calibrated. For these laminar shear box tests, liquefaction generally occurred within three cycles for shake tests without drains, thus N-liq was assumed to be equal to three; however, N-liq likely increased

somewhat with each round of shake tests. Nevertheless, parametric studies showed that the peak R_u and dissipation rate were not significantly affected for N-liq values less than about five.

The application of 15 uniform load cycles in 7.5 seconds (2 Hz frequency) during the laminar shear box testing represents a relatively severe loading case for the PV drains. In this study, parametric analyses investigated the effect of earthquake magnitude by considering the variation of earthquake duration and number of uniform cycles with M_w. Typically, the average frequency of loading for the earthquakes events was only about 0.4 Hz. As a result, in Figure 4-23, the peak R_u values computed for the different earthquake magnitude events were almost all substantially lower than computed with 15 uniform load cycles over a 7.5 second duration. This response occurs because the longer duration "dilutes" the energy of the shear cycles by allowing time for drainage and dissipation to occur while shaking continues, without overwhelming the drains. However, it should be recognized that earthquakes do not typically apply cycles at a uniform rate over the entire duration of shaking. Therefore, higher frequency shaking over a short portion of the total duration could still reduce the effectiveness of PV drains

Parametric analyses involving drain size suggest that wick drains are relatively ineffective for preventing liquefaction while 2" diameter PVDs are also fairly ineffective for the sand properties in this study. The 3" diameter drains were generally effective for keeping pore pressures low, but can be overwhelmed during very intense short duration seismic shaking. Drains which are 4" in diameter or larger are most effective at keeping pore pressures low and should be used whenever possible, if increased costs can be accommodated. Drains placed closer together (e.g. 3ft vs 4ft) also show improvement in R_u dissipation.

Soil parameter such as the unit weight, relative density, and the pore pressure generation coefficient were found to have minimal effect on the test results.

FEQDrain will fail to function properly when certain parameters are outside of an expected range. However, related parameters can sometimes be adjusted to have a similar effect while bringing the excessive parameter back into the stable range. The total time of analysis should be five to ten times the time of interest, not two times as suggested in the user's manual.

5.2 Recommendations for Future Research

In corresponding with industry professionals, it was suggested that an experiment be performed using the recommended combination of number of cycles and duration for different earthquake magnitudes, as given in the FEQDrain manual and developed by Seed & Idriss (1982) and Seed et al. (1975b). For example, M_w=7.5 corresponds to 12-14 cycles over 40 seconds. These tests would show if the pore pressures developed are similar for each combination as computer modeling suggests. Tests could also be used to show the effect of sinusoidal motions versus irregular earthquake motions.

It would also be useful to conduct laminar box testing of several recorded earthquake time histories, and several uniform shakes with different numbers of cycles. This would provide a better understanding of how induced R_u values correlate with FEQDrain's method of equivalent cycles. Modeling would be done to determine the relationship between time history characteristics and the appropriate combination of cycles and duration to use for predicting behavior of natural soils. Future experiments would also ideally be tested by CPT, before and after every shake test.

REFERENCES

Andrus, R.D. and Stokoe, K.H., II (2000). "Liquefaction resistance of soils from shear wave velocity." *Journal of Geotechnical and Geoenvironmental Engineering*, 126(11), 1015-1025.

Bethapudi, R., (2008). "Liquefaction induced lateral spreading in large-scale shake testing." *Master Thesis, State University of New York at Buffalo*.

Brennan, A. J. and Madabhushi, S.P.G. (2002). "Effectiveness of vertical drains in mitigation of liquefaction." *Soil Dynamics and Earthquake Engineering,* 22(9), 1059-1065.

Brennan, A. J. and Madabhushi, S.P.G. (2006). "Liquefaction Remediation by vertical drains with varying penetration depths." *Soil Dynamics and Earthquake Engineering,* 26(5), 469-475.

Chang, W. J., Rathje, E. M., Stokoe, K. H., and Cox, B. R. (2004). "Direct evaluation of effectiveness of prefabricated vertical drains in liquefiable sand." *Soil Dynamics and Earthquake Engineering*, 24, 723–731

Cubrinovski, M., Bradley, B., Wotherspoon, L., Green, R., Bray, J., Wood, C., Pender, M., Allen, J., Bradshaw, A., Rix, G., Taylor, M., Robinson, K., Henderson, D., Giorgini, S., Ma, K., Winkley, A., Zupan, J., O'Rourke, T., DePascale, G., and Wells, D. (2011). "Geotechnical aspects of the 22 February 2011 Christchurch earthquake." *Bulletin of the New Zealand Society for Earthquake Engineering*, 44(4), 205-226.

Dobry, R., Thevanayagam, S., Medina, C., Bethapudi, R., Elgamal, A., Bennett, V., Abdoun, T., Zeghal, M., El Shamy, U., Mercado, V. M., (2011). "Mechanics of lateral spreading observed in a full-scale shake test." *Journal of Geotechnical and Geoenvironmental Engineering*, 137(2), 115-129.

Dobry, R., Thevanayagam, S., Abdoun, T., Gonzalez, M. A., Elgamal, A., Zeghal, M., Mercado, V. M., and El Shamay, U., (2013). "Centrifuge and large-scale modeling of seismic pore pressures in sands: cyclic strain interpretation." *Journal of Geotechnical and Geoenvironmental Engineering*, 139(8), 1215-1234.

Elgamal, A., and Adalier, K., (2004). “Mitigation of liquefaction and associated ground deformations by stone columns.” *Engineering Geology*, 72, 275–291.

Ellington-Cross (2008). “Recent projects—Earthquake drains”. http://ellingtoncross.com/recent-projects-earthquake-drains-liquefaction-mitigation-systems-geotechnical-contractor-ground-imporvement-wick-drains.html (June 2016).

EQE (1995). “The January 17, 1995 Kobe earthquake, summary report,” http://www.absconsulting.com/es/resources/Catastrophe_Reports/Kobe,%20Japan%20EQ%201995.pdf (June 2016).

Gallagher, P.M., Conlee, C.T., and Rollins, K.M., (2007). “Full-scale testing of colloidal silica grouting for mitigation of liquefaction risk,” *Journal of Geotechnical and Geoenvironmental Engineering*, 133 (2), 186-196.

Gohl, B. (2002). “Report on gravel drain testing at south end of George Massey Tunnel.” *Prepared for Buckland & Taylor, Ltd. And British Columbia Ministry of Transportation, Pacific Geodynamics, Inc.*, Vancouver, BC, Canada.

Hayward Baker (2015). “Earthquake Drains”, *HB Wick Drains,* brochure W1-MAR-10002-JW (Rev 02/15)

Howell, R., Kamai, R., Conlee, C., Rathje, E., Boulanger, R., Marinucci, A., Rix, G., (2009). “Evaluation of the effectiveness of prefabricated vertical drains for liquefaction remediation –centrifuge data report for RLH01,” *Center for Geotechnical Modeling,* Data Report UCD/CGMDR-0801

Howell, R., Rathje, E. M., Kamai, R., and Boulanger, R. W., (2012). Centrifuge Modeling of Prefabricated Vertical Drains for Liquefaction Remediation.” *Journal of Geotechnical and Geoenvironmental Engineering*, 138(3), 262-271.

Howell, R., Rathje, E. M., and Boulanger, R. W., (2014). “Evaluation of Simulation Models of Lateral Spread Sites Treated with Prefabricated Vertical Drains,” *Journal of Geotechnical and Geoenvironmental Engineering*, 141 (1), -1—1

Kutter, B. L., (1995). “Recent advances in centrifuge modeling of seismic shaking,” *International Conferences on Recent Advances in Geotechnical Earthquake Engineering and Soil Dynamics*, Paper 4, 927-941.

Landers, J., (2012, May). “New Method for Alleviating Soil Liquefaction to Undergo Field Tests.” *Civil Engineering*, 38-39.

Lew, M., and Hudson, M. B., (2004, June). “Liquefaction Basics,” *Structure*, 10-12.

Marinucci, A., (2010). “Effect of prefabricated vertical drains on pore water pressure generation and dissipation in liquefiable sand,” *Doctoral Dissertation, The University of Texas at Austin*.

Nonaka, T., and Tashiro, M., (2016). “Numerical simulation of pore water pressure dissipation method based on a soil-water coupled analysis enhanced by macro element method,” *The 15th Asian Regional Conference on Soil Mechanics and Geotechnical Engineering*, 1996-2001.

National Research Council (1985). “Liquefaction of soils during earthquakes.” *National Academy Press*, 240 p.

Oakes, C. R. (2015). “Shaking table testing to evaluate effectiveness of prefabricated vertical drains for liquefaction mitigation.” *All Theses and Dissertations* Paper 6152. http://scholarsarchive.byu.edu/etd/6152/.

Onoue, A. (1988). "Diagrams considering well resistance for designing spacing ratio of gravel drains." Soils and Foundations, *Japanese Soc. of Soil Mechanics and Foundation Engineering*, 28(3), 160-168.

Pestana, J.M., Hunt, C.E. and Goughnour, KR. (1997). "FEQDrain: A finite element computer program for the analysis of the earthquake generation and dissipation of pore water pressure in layered sand deposits with vertical drains," *Earthquake Engineering Research Center*, Report No. \JCB/EERC 97-17

Rathje, E.M., Chang, W.-J, Cox, B.R., and Stoke, K.H.II (2004). "Effect of prefabricated vertical drains on pore pressure generation in liquefiable sand." *Proceedings, 11th International conference on soil dynamics and earthquake engineering*, Stallion Press, Vol. 2, 529-536.

Rollins, K. M., Anderson, J. K.S., McCain, A., and Goughnour, R.R (2003) “Vertical composite drains for mitigating liquefaction hazard.” *Proceedings of The Thirteenth (2003) International Offshore and Polar Engineering Conference, Honolulu, Hawaii, USA, May 25–30, 2003.* 498-505.

Rollins, K. M. and Anderson, J.K.S., (2004a). "Performance of vertical geocomposite drains based on full-scale testing at Massey Tunnel, Vancouver, B.C.", Final Report, NCHRP-IDEA Project 94, Transportation Research Board, Washington, D.C., 107 p

Rollins, K.M., Goughnour, R.R., Anderson J.K.S. and McCain, A. (2004b). "Liquefaction hazard mitigation using vertical composite drains." *Procs. 131th World Conf. on earthquake Engineering*, Earthquake Engineering Research Institute, Vancouver, B.C., 210-220.

Rollins, K.M., Lane, J.D., Dibb, E., Ashford, S.A., and Mullins, A. G. (2005). "Pore pressure measurement in blast-induced liquefaction experiments." Transportation Research Record 1936, "Soil Mechanics 2005", Transportation Research Board, Washington DC, p. 210-220.

Seed, H.B., Martin, P.P., and Lysmer, J. (1975a). "The generation and dissipation of pore water pressures during soil liquefaction." Earthquake Engineering Research Center, Report No. CB/EERC 75-26.

Seed, H.B., and Booker, J.R. (1977). "Stabilization of potentially liquefiable sand deposits using gravel drains," *Journal of Geotechnical Engineering Division,* ASCE, 103(GT7), 757-768.

Stover, C.W. and Coffman, J.L., (1993) "Seismicity of the United States, 1569-1980 (Revised)," *U.S. Geologic Survey Professional Paper 1527,* United States Government Publishing Office, Washington.

Strand, S. R. (2008). "Liquefaction mitigation using vertical composite drains and liquefaction induced downdrag on piles: implications for deep foundation design," *All Theses and Dissertations.* Paper 1648. http://scholarsarchive.byu.edu/etd/1648

Vytiniotis, A., and Whittle, A. J., (2013) "Effectiveness of PV Drains for Mitigating Earthquake-Induced Deformations in Sandy Slopes." *Geo-Congress 2013. American Society of Civil Engineers*, 908–917.

Yegian, M., Thevanayagam, S., Stokoe, K., and Youd, L., (2015). "Induced partial saturation method for soil liquefaction mitigation - large-scale shake testing." *Preliminary Project Report for NEESR: Induced Partial Saturation (LPS) Through Transport and Reactivity for Liquefaction Mitigation.*

Youd, T. L. and Idriss, I. M. (2001) "Liquefaction Resistance of Soils: Summary report from the 1996 NCEER and 1998 NCEER/NSF workshops on evaluation of liquefaction resistance of soils." *Journal of Geotechnical and Geoenvironmental Engineering*, Vol. 127(4), pp. 297-31

Zeghal, M., Elmagal, A. W. and Ender, P. (1996). "Analyses of site liquefaction using downhole array seismic records." *Eleventh World Conference on Earthquake Engineering*, Paper No. 371.

APPENDIX A. PARAMETER DESCRIPTIONS AND PROPERTIES

A.1 FEQDrain Parameter Descriptions

Filename: The name of the file generated (8 character max).

Title: A text description that appears in the main output file.

N layers: number of layers in the soil profile. This is how many different ranges of soil properties there are. i.e. different m_{vo} or K values. Strand had 6. I'm using 7.

Rad Increm: number of radial increments used in the math calcs (remember it's a finite element model). Between10-15 is usually appropriate. Use 10, that's what my macros are set for.

Unit weight of water: 62.4 pcf or the SI value. All values must match these units.

Depth to GWT: We will use 0 feet because our soil is all saturated.

Eff Vert Stress at surface: Use 0pcf (no surface load).

Drain allow: YES (water can escape from drains).

Initial PPR: Obviously not =0

Earthquake Loading Conditions

Equiv earthquake cycles (nq) or Neq: Refers to the magnitude of the EQ/ground accelerations, (see Tables 4&5). We are setting this as the number of acceleration cycles (14cycles) for the experiment. Neq, can be found by analyzing an earthquake stress history using the method proposed by Seed et al. (1975b). Values in Table 5 (Seed & Idriss, 1982), based upon the analysis of numerous earthquakes, may be used.

Equiv time of shaking (td), duration of strong motion or bracketed duration. It can be estimated from Table 6. Program will still run if td=0 (pore pressure dissipation only). We will use 7-7.5 seconds.

N time steps: number of distinct time-steps (see section 4.3.2 for example). We'll use 1.

Total analysis time: Use something longer than 7.5sec to see PPR dissipation rate. (Should be at least twice the duration of the earthquake). Use 15 seconds.

Time Integration Parameters

N iterations per time-step: (see Pestana et al (1997), section 4.3.2 for example).

Duration of time-step: controls accuracy of the integration scheme (see section 4.3.2 for example).

Print resolution: The frequency of results output, results printed every PRNSTEP seconds.

Drain and Reservoir Parameters

Symmetry: Axisymmetric (used for most drainage cases)

Compressibility: Variable or Constant, (constant for PP < 0.6)

Type of drain (kopt): Probably use "composite drain"

Out files: How many types of files will be created.

Additional Drainage Parameters

rw: outside radius of drain (3.7" for us) = 3.7/12/2 =0.15417ft

rout: tributary area radius (1.5ft and 2ft)

aread: Cross-sectional area of inside of drain (3" → 0.0491 ft^2)

arear: Cross-sectional area of inside of reservoir, (can't be less than that of drain).

depres: Depth to bottom of reservoir (0 for us, no res)

c1: constant, provided by the manufacturer, see data sheet (c1=1.7049). If c1=0→no vertical head loss.

c2: constant, provided by the manufacturer, see data sheet (c2=2)

c3: constant for reservoir, leave blank or use same value as c1.

c4: constant for reservoir, leave blank or use same value as c2.

corf: 1 or 0 depending on full head loss vs. no head loss.

orf: area of perforations per foot of pipe, provided by manufacturer, see email (0.0077 sq ft/ft).

permit: filter permittivity, provided by manufacturer, (Use 0.8325 ft3/sec/ft2/ft), fabric alone value is 4x higher but ¾ of it is against corrugations

Horizontal & vertical hydraulic conductivity: Kh was measured and reported in Caleb's Thesis. Kv can be obtained by dividing (see table below). But Kv is less important.

Number of cycles to cause liquefaction: See FEQ Manual Pg29-34.

Relative density, Dr: use adjusted Dr values from m_{vo} spreadsheet.

Total unit weight: Saturated unit weight of the soil. Caleb's thesis never specifies this. Try 100pcf.

Coeff of pore pressure generation: Uniform sand range 0.5-0.9, higher values for very loose deposits. 0.7 is often used for design.

Types of Output Files:

.out : Standard output file, summary at top, labeled results of each time-step are below.

.col: Unlabeled columns of data for importing into a spreadsheet (six columns). Time, node number, x-cord, y-cord, excess PP, PPR.

.sum: Summary data file, shows max PPR for each layer during the entire analysis (at each printed step).

.exr: PPR data file at time t, first row is x-coords, first column is y-coords, all rest are PPRs at that node. This can be used to make a 3D plot.

.exp: same format as .exr, but gives pressures not ratios.

.con: Consolidation Data File, only made when an initial excess PP is specified. Can be used w/o drain and w/o EQ to determine consolidation settlement as pore pressures redistribute and dissipate.

A.2 Flow Properties of HDPE Corrugated Pipe

CORRUGATED PLASTIC PIPI (eg ADS):

Manning equation

$$v = \frac{1.486}{n} R^{2/3} S^{1/2}$$

where

R is the hydraulic radius = Area/Wetted Perimeter
N is th Manning factor
S is equivalent to i (the hydraulic gradient)

For a circular conduit flowing full, Area = πr^2

$$R = \frac{\pi r^2}{2\pi r} = \frac{r}{2}$$

And

$$AR^{2/3} = \pi r^2 (r/2)^{2/3} = 1.9791 r^{2.667}$$

ADS (and Hancor) recommend:
n=0.015 for 2" to 6" pipe
n=0.016 for 8" pipe
n=0.017 for 10" pipe
n=0.018 for 12' to 15" pipe
n=0.020 for 18' to 24 pipe

Therefore for 2"corrugated pipe

$$Q = vA = \frac{1.486}{n} 1.9791 r^{2.667} S^{1/2} = 0.2598 i^{1/2}$$

or

$$I = 14.8198 Q^2$$

Therefore:

2"	C1=14.8198	C2=2
3"	C1=1.7049	C2=2
4"	C1=0.3676	C2=2
6"	C1=0.04229	C2=2
8"	C1=0.01037	C2=2
10"	C1=0.003562	C2=2
12"	C1=0.001510	C2=2
15"	C1=0.0004594	C2=2
18"	C1=0.0002145	C2=2
24"	C1=0.00004625	C2=2

Equivalent radius 4" = 0.1996 ft
Internal area = 0.1214 sq ft

Equivalent radius 3" = 0.1542 ft
Internal area = 0.0594 sq ft

Equivalent radius 2" = 0.1083ft
Internal area = 0.0264 sq ft

Orfice (slit) area:

For 4" = approx 1.90 sq in/foot pipe = 0.01319 sq ft/ft
For 3" = approx 1.1 sq in/ft pipe = 0.0077 sq ft/ft
For 2" = approx 0.325 sq in/ft = 0.0023 sq ft/ft

Fabric (Amaco CEF Style 4545)

Permitivity – 0.333 $ft^3/sec/ft^2/ft$ head
Reduce this to 0.333/4 = 0.08325 $ft^3/sec/ft^2/ft$ head because about ¾ of fabric rests against corrugations

APPENDIX B. FEQDRAIN OUTPUT FILE TYPES

This appendix contains examples of the five types of output files created by FEQDrain.

.COL—This file is far larger than any of the others. It has six columns showing (L-R): Time, Node number, X-coordinate, Y-coordinate, pore pressure, pore pressure ratio. This file is what gets imported and sorted in Excel. It would take hundreds of pages to show a full example of this file.

.EXP/.EXR—This file shows the calculated pore pressure (.exp) and pore pressure ratio (.exr) values for each node in the array, at each printed time. The values of each node are in a rectangular table which preserves the spatial organization of the nodes.

.OUT—This file shows all of the input parameters displayed in table form at the top. Below that is a table of coordinates and effective stress for each node, and a table of nodal connectivity. The remainder of the file are tables of pore pressure values (average and max), by layer, at the time interval specified for printing results.

.SUM—This file lists the values of several parameters, all in a single horizontal row. Each printed time is a new row. If print interval is 1sec, and time of analysis is 100sec, we get 100 rows.

.COL

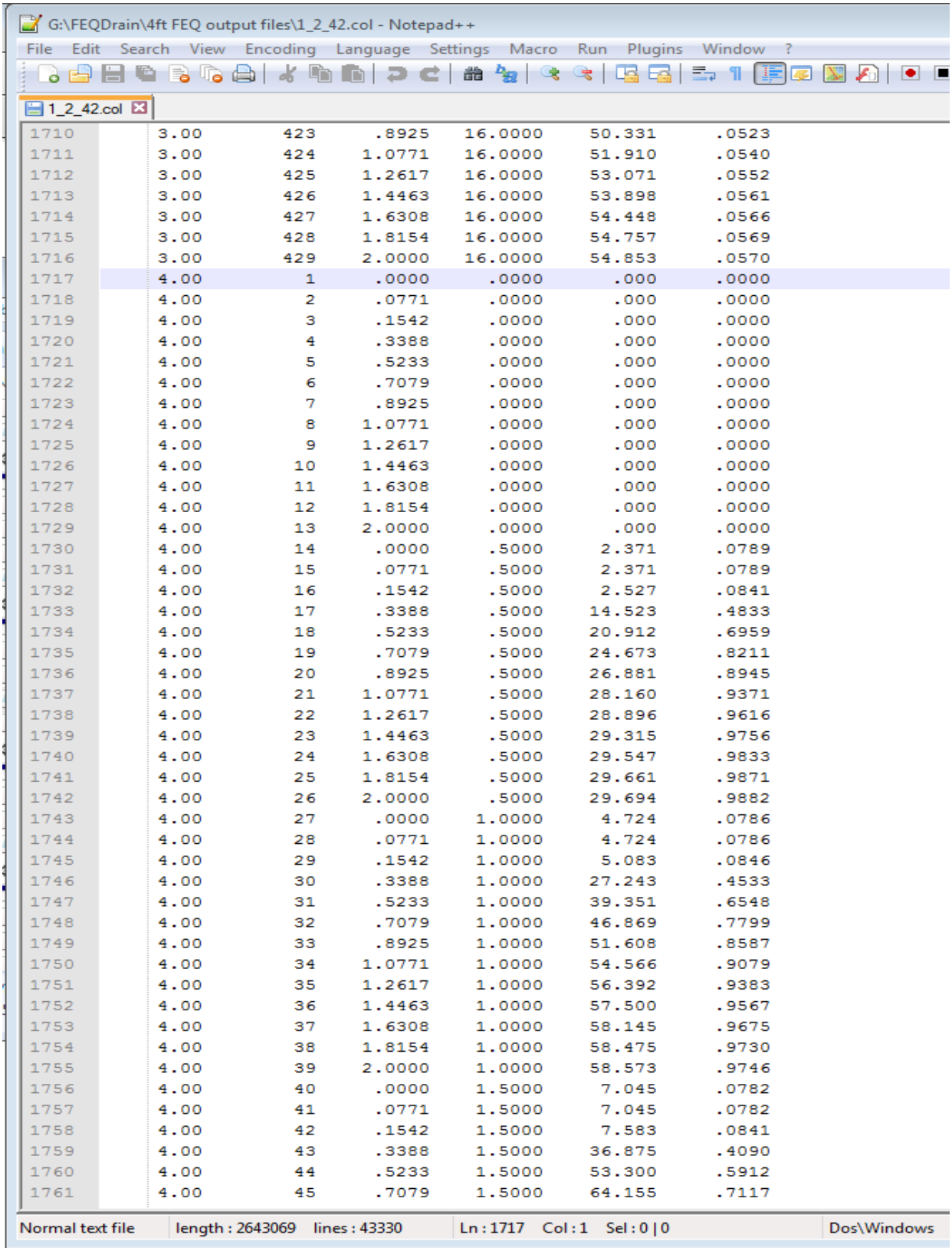
G:\FEQDrain\4ft FEQ output files\1_2_42.col - Notepad++
File Edit Search View Encoding Language Settings Macro Run Plugins Window ?
1_2_42.col
1710 3.00 423 .8925 16.0000 50.331 .0523
1711 3.00 424 1.0771 16.0000 51.910 .0540
1712 3.00 425 1.2617 16.0000 53.071 .0552
1713 3.00 426 1.4463 16.0000 53.898 .0561
1714 3.00 427 1.6308 16.0000 54.448 .0566
1715 3.00 428 1.8154 16.0000 54.757 .0569
1716 3.00 429 2.0000 16.0000 54.853 .0570
1717 4.00 1 .0000 .0000 .000 .0000
1718 4.00 2 .0771 .0000 .000 .0000
1719 4.00 3 .1542 .0000 .000 .0000
1720 4.00 4 .3388 .0000 .000 .0000
1721 4.00 5 .5233 .0000 .000 .0000
1722 4.00 6 .7079 .0000 .000 .0000
1723 4.00 7 .8925 .0000 .000 .0000
1724 4.00 8 1.0771 .0000 .000 .0000
1725 4.00 9 1.2617 .0000 .000 .0000
1726 4.00 10 1.4463 .0000 .000 .0000
1727 4.00 11 1.6308 .0000 .000 .0000
1728 4.00 12 1.8154 .0000 .000 .0000
1729 4.00 13 2.0000 .0000 .000 .0000
1730 4.00 14 .0000 .5000 2.371 .0789
1731 4.00 15 .0771 .5000 2.371 .0789
1732 4.00 16 .1542 .5000 2.527 .0841
1733 4.00 17 .3388 .5000 14.523 .4833
1734 4.00 18 .5233 .5000 20.912 .6959
1735 4.00 19 .7079 .5000 24.673 .8211
1736 4.00 20 .8925 .5000 26.881 .8945
1737 4.00 21 1.0771 .5000 28.160 .9371
1738 4.00 22 1.2617 .5000 28.896 .9616
1739 4.00 23 1.4463 .5000 29.315 .9756
1740 4.00 24 1.6308 .5000 29.547 .9833
1741 4.00 25 1.8154 .5000 29.661 .9871
1742 4.00 26 2.0000 .5000 29.694 .9882
1743 4.00 27 .0000 1.0000 4.724 .0786
1744 4.00 28 .0771 1.0000 4.724 .0786
1745 4.00 29 .1542 1.0000 5.083 .0846
1746 4.00 30 .3388 1.0000 27.243 .4533
1747 4.00 31 .5233 1.0000 39.351 .6548
1748 4.00 32 .7079 1.0000 46.869 .7799
1749 4.00 33 .8925 1.0000 51.608 .8587
1750 4.00 34 1.0771 1.0000 54.566 .9079
1751 4.00 35 1.2617 1.0000 56.392 .9383
1752 4.00 36 1.4463 1.0000 57.500 .9567
1753 4.00 37 1.6308 1.0000 58.145 .9675
1754 4.00 38 1.8154 1.0000 58.475 .9730
1755 4.00 39 2.0000 1.0000 58.573 .9746
1756 4.00 40 .0000 1.5000 7.045 .0782
1757 4.00 41 .0771 1.5000 7.045 .0782
1758 4.00 42 .1542 1.5000 7.583 .0841
1759 4.00 43 .3388 1.5000 36.875 .4090
1760 4.00 44 .5233 1.5000 53.300 .5912
1761 4.00 45 .7079 1.5000 64.155 .7117
Normal text file length : 2643069 lines : 43330 Ln : 1717 Col : 1 Sel : 0 | 0 Dos\Windows

.EXP/.EXR

1_2_42.exp

1	Numstep	Numx	Numy
2	101	13	33
3			
4	Time =	.000	Excess Pore Pressure Values

	.0000	.0771	.1542	.3388	.5233	.7079	.8925	1.0771	1.2617	1.4463	1.6308	1.8154	2.0000
.000	.000	.000	.000	.000	.000	.000	.000	.000	.000	.000	.000	.000	.000
.500	.000	.000	.000	.000	.000	.000	.000	.000	.000	.000	.000	.000	.000
1.000	.000	.000	.000	.000	.000	.000	.000	.000	.000	.000	.000	.000	.000
1.500	.000	.000	.000	.000	.000	.000	.000	.000	.000	.000	.000	.000	.000
2.000	.000	.000	.000	.000	.000	.000	.000	.000	.000	.000	.000	.000	.000
2.500	.000	.000	.000	.000	.000	.000	.000	.000	.000	.000	.000	.000	.000
3.000	.000	.000	.000	.000	.000	.000	.000	.000	.000	.000	.000	.000	.000
3.500	.000	.000	.000	.000	.000	.000	.000	.000	.000	.000	.000	.000	.000
4.000	.000	.000	.000	.000	.000	.000	.000	.000	.000	.000	.000	.000	.000
4.500	.000	.000	.000	.000	.000	.000	.000	.000	.000	.000	.000	.000	.000
5.000	.000	.000	.000	.000	.000	.000	.000	.000	.000	.000	.000	.000	.000
5.500	.000	.000	.000	.000	.000	.000	.000	.000	.000	.000	.000	.000	.000
6.000	.000	.000	.000	.000	.000	.000	.000	.000	.000	.000	.000	.000	.000
6.500	.000	.000	.000	.000	.000	.000	.000	.000	.000	.000	.000	.000	.000
7.000	.000	.000	.000	.000	.000	.000	.000	.000	.000	.000	.000	.000	.000
7.500	.000	.000	.000	.000	.000	.000	.000	.000	.000	.000	.000	.000	.000
8.000	.000	.000	.000	.000	.000	.000	.000	.000	.000	.000	.000	.000	.000
8.500	.000	.000	.000	.000	.000	.000	.000	.000	.000	.000	.000	.000	.000
9.000	.000	.000	.000	.000	.000	.000	.000	.000	.000	.000	.000	.000	.000
9.500	.000	.000	.000	.000	.000	.000	.000	.000	.000	.000	.000	.000	.000
10.000	.000	.000	.000	.000	.000	.000	.000	.000	.000	.000	.000	.000	.000
10.500	.000	.000	.000	.000	.000	.000	.000	.000	.000	.000	.000	.000	.000
11.000	.000	.000	.000	.000	.000	.000	.000	.000	.000	.000	.000	.000	.000
11.500	.000	.000	.000	.000	.000	.000	.000	.000	.000	.000	.000	.000	.000
12.000	.000	.000	.000	.000	.000	.000	.000	.000	.000	.000	.000	.000	.000
12.500	.000	.000	.000	.000	.000	.000	.000	.000	.000	.000	.000	.000	.000
13.000	.000	.000	.000	.000	.000	.000	.000	.000	.000	.000	.000	.000	.000
13.500	.000	.000	.000	.000	.000	.000	.000	.000	.000	.000	.000	.000	.000
14.000	.000	.000	.000	.000	.000	.000	.000	.000	.000	.000	.000	.000	.000
14.500	.000	.000	.000	.000	.000	.000	.000	.000	.000	.000	.000	.000	.000
15.000	.000	.000	.000	.000	.000	.000	.000	.000	.000	.000	.000	.000	.000
15.500	.000	.000	.000	.000	.000	.000	.000	.000	.000	.000	.000	.000	.000
16.000	.000	.000	.000	.000	.000	.000	.000	.000	.000	.000	.000	.000	.000

Time = 1.000 Excess Pore Pressure Values

	.0000	.0771	.1542	.3388	.5233	.7079	.8925	1.0771	1.2617	1.4463	1.6308	1.8154	2.0000
.000	.000	.000	.000	.000	.000	.000	.000	.000	.000	.000	.000	.000	.000
.500	1.984	1.984	2.163	14.377	20.254	23.606	25.653	26.944	27.768	28.288	28.602	28.767	28.817
1.000	3.952	3.952	4.361	26.775	37.948	44.584	48.815	51.599	53.447	54.656	55.406	55.810	55.933
1.500	5.891	5.891	6.475	35.713	51.153	60.876	67.433	71.979	75.137	77.284	78.656	79.409	79.640
2.000	7.788	7.789	8.684	47.649	68.012	80.744	89.297	95.217	99.331	102.131	103.923	104.908	105.211
2.500	9.634	9.634	10.892	59.446	84.864	100.767	111.451	118.843	123.976	127.467	129.701	130.927	131.304
3.000	11.416	11.416	13.125	71.302	101.723	120.743	133.516	142.351	148.488	152.661	155.332	156.798	157.249
3.500	13.122	13.123	15.176	82.299	117.486	139.544	154.397	164.697	171.867	176.753	179.885	181.606	182.136
4.000	14.746	14.746	17.140	93.107	133.059	158.187	175.160	186.966	195.205	200.831	204.444	206.432	207.044
4.500	16.281	16.281	19.232	104.655	149.544	177.762	196.817	210.068	219.317	225.632	229.688	231.920	232.607
5.000	17.718	17.719	21.240	116.088	165.949	197.296	218.464	233.183	243.454	250.467	254.970	257.447	258.210
5.500	19.052	19.052	23.197	127.393	182.089	216.438	239.616	255.726	266.966	274.640	279.568	282.279	283.114

Time = 100.000 Excess Pore Pressure Values

	.0000	.0771	.1542	.3388	.5233	.7079	.8925	1.0771	1.2617	1.4463	1.6308	1.8154	2.0000
.000	.000	.000	.000	.000	.000	.000	.000	.000	.000	.000	.000	.000	.000
.500	.000	.000	.000	.004	.007	.009	.010	.011	.012	.013	.013	.013	.013
1.000	.000	.000	.000	.005	.007	.009	.010	.012	.012	.013	.013	.014	.014
1.500	.000	.000	.000	.003	.005	.006	.007	.007	.008	.008	.009	.009	.009
2.000	.000	.000	.000	.002	.003	.004	.004	.005	.005	.005	.005	.006	.006
2.500	.000	.000	.000	.002	.002	.002	.003	.003	.003	.003	.004	.004	.004
3.000	.000	.000	.000	.001	.001	.001	.002	.002	.002	.002	.002	.002	.002
3.500	.000	.000	.000	.001	.001	.001	.001	.001	.001	.001	.001	.001	.001
4.000	.000	.000	.000	.001	.000	.000	.001	.001	.001	.001	.001	.001	.001
4.500	.000	.000	.000	.000	.000	.000	.001	.001	.001	.001	.001	.001	.001
5.000	.000	.000	.000	.000	.000	.000	.000	.000	.000	.000	.000	.000	.000
5.500	.000	.000	.000	.000	.000	.000	.000	.000	.000	.000	.000	.000	.000
6.000	.000	.000	.000	.000	.000	.000	.000	.000	.000	.000	.000	.000	.000
6.500	.000	.000	.000	.000	.000	.000	.000	.000	.000	.000	.000	.000	.000
7.000	.000	.000	.000	.000	.000	.000	.000	.000	.000	.000	.000	.000	.000
7.500	.000	.000	.000	.000	.000	.000	.000	.000	.000	.000	.000	.000	.000
8.000	.000	.000	.000	.000	.000	.000	.000	.000	.000	.000	.000	.000	.000
8.500	.000	.000	.000	.000	.000	.000	.000	.000	.000	.000	.000	.000	.000
9.000	.000	.000	.000	.000	.000	.000	.000	.000	.000	.000	.000	.000	.000
9.500	.000	.000	.000	.000	.000	.000	.000	.000	.000	.000	.000	.000	.000
10.000	.000	.000	.000	.000	.000	.000	.000	.000	.000	.000	.000	.000	.000
10.500	.000	.000	.000	.000	.000	.000	.000	.000	.000	.000	.000	.000	.000
11.000	.000	.000	.000	.000	.000	.000	.000	.000	.000	.000	.000	.000	.000
11.500	.000	.000	.000	.000	.000	.000	.000	.000	.000	.000	.000	.000	.000
12.000	.000	.000	.000	.000	.000	.000	.000	.000	.000	.000	.000	.000	.000
12.500	.000	.000	.000	.000	.000	.000	.000	.000	.000	.000	.000	.000	.000
13.000	.000	.000	.000	.000	.000	.000	.000	.000	.000	.000	.000	.000	.000
13.500	.000	.000	.000	.000	.000	.000	.000	.000	.000	.000	.000	.000	.000
14.000	.000	.000	.000	.000	.000	.000	.000	.000	.000	.000	.000	.000	.000
14.500	.000	.000	.000	.000	.000	.000	.000	.000	.000	.000	.000	.000	.000
15.000	.000	.000	.000	.000	.000	.000	.000	.000	.000	.000	.000	.000	.000
15.500	.000	.000	.000	.000	.000	.000	.000	.000	.000	.000	.000	.000	.000
16.000	.000	.000	.000	.000	.000	.000	.000	.000	.000	.000	.000	.000	.000

Normal text file length : 492944 lines : 3639

.OUT

1_2_41.out

```
                                FEQDRAIN
                ANALYSIS OF PORE PRESSURE GENERATION AND DISSIPATION
                DURING EARTHQUAKE LOADING FOR A SOIL PROFILE TREATED
                                WITH VERTICAL DRAINS
                             Version 2.1     December 1997



  ANALYSIS:

  SOIL PROFILE DATA:

Layer  Thick  Hydr. Conductivity   Volum.   Tot.Unit  Cycles  # of  Theta   Rel.
  #     ness      kx         ky    Compress  Weight     to    Vert.        Dens.
        feet    ft/sec     ft/sec  1/lb/ft^2 lb/ft^3   Liquef  Incr.         (%)
-------------------------------------------------------------------------------
  1    1.000  .1050E-02 .1050E-03 .200E-04  122.500      1.      2   .700   .500
  2    2.500  .1050E-02 .1050E-03 .800E-05  122.500      1.      5   .700   .500
  3    2.500  .1000E-02 .1000E-03 .700E-05  122.500      1.      5   .700   .500
  4    2.500  .1000E-02 .1000E-03 .600E-05  122.500      1.      5   .700   .500
  5    2.500  .1700E-02 .1700E-03 .800E-05  122.500      1.      5   .700   .500
  6    2.500  .1200E-02 .1200E-03 .800E-05  122.500      7.      5   .700   .500
  7    2.500  .2000E-03 .2000E-04 .100E-05  122.500    100.      5   .700   .700


   ANALYSIS TYPE:
         Axisymmetric case                  (iopt   = 2)
         Variable compressibility           (iopt   = 2)
         Composite drain                    (kopt   = 4)
         Output files created:              (noprint= 7)
               1) Main File                 (*.out)
               2) Columnar File             (*.col)
               3) Summary File              (*.sum)
               4) Pore Pressure Ratio File  (*.exr)
               5) Excess Pore Pressure File (*.exp)

   EARTHQUAKE DATA:
         Equivalent No of cycles    =    14.00
         Duration of shaking        =     7.00 seconds

   CONTROL DATA:
         Number of layers           =        7
         Radial soil increments     =       10
         Radial drain increments    =        2
         Vertical increments        =       32
         Effective Overburden       =     .000 lb/ft^2
         Depth to water table       =     .000  feet
         Unit weight of water       =   62.400 lb/ft^3
         Print results to a limit of=   100.00 seconds
         No of different time steps =     1
```

Normal text file | length : 144745 lines : 2324 | Ln : 1 Col : 1 Sel : 0 | 0 | Dos\Windows | ANSI as UTF-8

Number of steps	Step Size (seconds)	Print Resolution
100	1.000	1.000

DRAIN DATA:

Radius of tributary area = 2.0000 feet
Equivalent radius of drain = .1542 feet
Internal drain area = .0491 sq ft
Vertical head loss, dh/dz = C1*Q^C2 (Manning)
Coefficient C1 = 1.7049
Coefficient C2 = 2.0000
Horizontal head loss, dh/dx = corf*V^2/2g+V/permit
Coefficient of head loss,corf= 1.00000
Orifice Area,per unit length = .00770 sq ft / feet
Geotextile Permittivity = .83250 ft/sec / feet of head

RESERVOIR DATA:

Area of reservoir = .0491 sq ft
Depth to bottom of reservoir = .0000 feet
Vertical head loss, dh/dz = C3*Q^C4 (Manning)
Coefficient C3 = 1.7049
Coefficient C4 = 2.0000

NODAL COORDINATES AND EFFECTIVE STRESSES

Node	Coordinates x	Coordinates y	Vertical Stress	Node	Coordinates x	Coordinates y	Vertical Stress
1	.000	.000	.00	2	.077	.000	.00
3	.154	.000	.00	4	.339	.000	.00
5	.523	.000	.00	6	.708	.000	.00
7	.893	.000	.00	8	1.077	.000	.00
9	1.262	.000	.00	10	1.446	.000	.00
11	1.631	.000	.00	12	1.815	.000	.00
13	2.000	.000	.00	14	.000	.500	30.05
15	.077	.500	30.05	16	.154	.500	30.05
17	.339	.500	30.05	18	.523	.500	30.05
19	.708	.500	30.05	20	.893	.500	30.05
21	1.077	.500	30.05	22	1.262	.500	30.05
23	1.446	.500	30.05	24	1.631	.500	30.05
25	1.815	.500	30.05	26	2.000	.500	30.05
27	.000	1.000	60.10	28	.077	1.000	60.10
29	.154	1.000	60.10	30	.339	1.000	60.10
31	.523	1.000	60.10	32	.708	1.000	60.10
33	.893	1.000	60.10	34	1.077	1.000	60.10
35	1.262	1.000	60.10	36	1.446	1.000	60.10
37	1.631	1.000	60.10	38	1.815	1.000	60.10
39	2.000	1.000	60.10	40	.000	1.500	90.15
41	.077	1.500	90.15	42	.154	1.500	90.15

NODAL CONNECTIVITY NUMBER OF ELEMENTS = 384

Elem	Node Connectivity 1	2	3	4	Elem	Node Connectivity 1	2	3	4
1	1	2	15	14	2	14	15	28	27
3	27	28	41	40	4	40	41	54	53
5	53	54	67	66	6	66	67	80	79
7	79	80	93	92	8	92	93	106	105
9	105	106	119	118	10	118	119	132	131
11	131	132	145	144	12	144	145	158	157
13	157	158	171	170	14	170	171	184	183
15	183	184	197	196	16	196	197	210	209
17	209	210	223	222	18	222	223	236	235
19	235	236	249	248	20	248	249	262	261
21	261	262	275	274	22	274	275	288	287
23	287	288	301	300	24	300	301	314	313
25	313	314	327	326	26	326	327	340	339
27	339	340	353	352	28	352	353	366	365
29	365	366	379	378	30	378	379	392	391
31	391	392	405	404	32	404	405	418	417
33	2	3	16	15	34	15	16	29	28
35	28	29	42	41	36	41	42	55	54
37	54	55	68	67	38	67	68	81	80
39	80	81	94	93	40	93	94	107	106
41	106	107	120	119	42	119	120	133	132
43	132	133	146	145	44	145	146	159	158
45	158	159	172	171	46	171	172	185	184
47	184	185	198	197	48	197	198	211	210
49	210	211	224	223	50	223	224	237	236
51	236	237	250	249	52	249	250	263	262
53	262	263	276	275	54	275	276	289	288
55	288	289	302	301	56	301	302	315	314
57	314	315	328	327	58	327	328	341	340
59	340	341	354	353	60	353	354	367	366
61	366	367	380	379	62	379	380	393	392
63	392	393	406	405	64	405	406	419	418
65	3	4	17	16	66	16	17	30	29
67	29	30	43	42	68	42	43	56	55
69	55	56	69	68	70	68	69	82	81
71	81	82	95	94	72	94	95	108	107
73	107	108	121	120	74	120	121	134	133
75	133	134	147	146	76	146	147	160	159
77	159	160	173	172	78	172	173	186	185
79	185	186	199	198	80	198	199	212	211
81	211	212	225	224	82	224	225	238	237
83	237	238	251	250	84	250	251	264	263
85	263	264	277	276	86	276	277	290	289
87	289	290	303	302	88	302	303	316	315
89	315	316	329	328	90	328	329	342	341

```
  Current Time        =      1.00 sec
  Max. Pressure ratio=     .9580
  Max. Average ru     =     .8883              at elevation =      .500 feet
  Water level drain   =      .000 feet          Settlement   =     .0078 feet
  Volume Discharged   =     .0970 feet    ^3

            Current Values           *         Cummulative  Values
  Layer Maximum  Node  LayAvg DepAvg * Maximum  Node  LayAvg DepAvg    Time
-------------------------------------------------------------------------------
      1   .9580   26.   .6549  .8883 *   .9580   26.   .6549  .8883    1.00
      2   .9292   39.   .7957  .8543 *   .9292   39.   .7957  .8543    1.00
      3   .8636  104.   .7737  .7844 *   .8636  104.   .7737  .7844    1.00
      4   .8434  169.   .7459  .7646 *   .8434  169.   .7459  .7646    1.00
      5   .8059  234.   .6672  .7294 *   .8059  234.   .6672  .7294    1.00
      6   .5118  299.   .2330  .4644 *   .5118  299.   .2330  .4644    1.00
      7   .1513  364.   .0517  .1386 *   .1513  364.   .0517  .1386    1.00


  Current Time        =      2.00 sec
  Max. Pressure ratio=     .9873
  Max. Average ru     =     .9222              at elevation =      .500 feet
  Water level drain   =      .000 feet          Settlement   =     .0234 feet
  Volume Discharged   =     .2928 feet    ^3

            Current Values           *         Cummulative  Values
  Layer Maximum  Node  LayAvg DepAvg * Maximum  Node  LayAvg DepAvg    Time
-------------------------------------------------------------------------------
      1   .9873   26.   .6830  .9222 *   .9873   26.   .6830  .9222    2.00
      2   .9747   39.   .8477  .8994 *   .9747   39.   .8477  .8994    2.00
      3   .9288  104.   .8254  .8371 *   .9288  104.   .8254  .8371    2.00
      4   .9085  169.   .7923  .8154 *   .9085  169.   .7923  .8154    2.00
      5   .8598  234.   .6937  .7681 *   .8598  234.   .6937  .7681    2.00
      6   .6338  299.   .3150  .5631 *   .6338  299.   .3150  .5631    2.00
      7   .2207  364.   .0785  .1986 *   .2207  364.   .0785  .1986    2.00


  Current Time        =      3.00 sec
  Max. Pressure ratio=     .9913
  Max. Average ru     =     .9275              at elevation =      .500 feet
  Water level drain   =      .000 feet          Settlement   =     .0401 feet
  Volume Discharged   =     .5003 feet    ^3

            Current Values           *         Cummulative  Values
  Layer Maximum  Node  LayAvg DepAvg * Maximum  Node  LayAvg DepAvg    Time
-------------------------------------------------------------------------------
      1   .9913   26.   .6876  .9275 *   .9913   26.   .6876  .9275    3.00
      2   .9801   39.   .8604  .9068 *   .9801   39.   .8604  .9068    3.00
      3   .9377  104.   .8407  .8516 *   .9377  104.   .8407  .8516    3.00
      4   .9185  169.   .8094  .8318 *   .9185  169.   .8094  .8318    3.00
      5   .8689  234.   .7268  .7850 *   .8689  234.   .7268  .7850    3.00
      6   .7149  299.   .3695  .6408 *   .7149  299.   .3695  .6408    3.00
      7   .2498  364.   .0919  .2260 *   .2498  364.   .0919  .2260    3.00
```

```
  Current Time        =    100.00 sec
  Max. Pressure ratio=     .0017
  Max. Average ru     =     .0015             at elevation =      .500 feet
  Water level drain   =      .000 feet         Settlement   =     .1874 feet
  Volume Discharged   =    2.3413 feet   ^3

            Current Values          *        Cummulative  Values
  Layer Maximum  Node  LayAvg DepAvg * Maximum  Node  LayAvg DepAvg    Time
-------------------------------------------------------------------------------
      1   .0017   26.   .0009  .0015 *   .9917   26.   .6887  .9288    6.00
      2   .0009   39.   .0002  .0008 *   .9812   39.   .8636  .9087    6.00
      3   .0000  104.   .0000  .0000 *   .9427  104.   .8451  .8555    6.00
      4   .0000  169.   .0000  .0000 *   .9257  169.   .8156  .8369    6.00
      5   .0000  229.   .0000  .0000 *   .8823  234.   .7622  .7938    6.00
      6   .0000  298.   .0000  .0000 *   .8389  299.   .5174  .7546    6.00
      7   .0000  362.   .0000  .0000 *   .3102  364.   .1127  .2794    6.00


-------------------------------------------------------------------------------
  End of Run Statistics
-------------------------------------------------------------------------------


  Current Time        =    100.00 sec
  Max. Pressure ratio=     .9917
  Max. Average ru     =     .9288             at elevation =      .500 feet
  Water level drain   =      .000 feet         Settlement   =     .1874 feet
  Volume Discharged   =    2.3413 feet   ^3

            Current Values          *        Cummulative  Values
  Layer Maximum  Node  LayAvg DepAvg * Maximum  Node  LayAvg DepAvg    Time
-------------------------------------------------------------------------------
      1   .0017   26.   .0009  .0015 *   .9917   26.   .6887  .9288    6.00
      2   .0009   39.   .0002  .0008 *   .9812   39.   .8636  .9087    6.00
      3   .0000  104.   .0000  .0000 *   .9427  104.   .8451  .8555    6.00
      4   .0000  169.   .0000  .0000 *   .9257  169.   .8156  .8369    6.00
      5   .0000  229.   .0000  .0000 *   .8823  234.   .7622  .7938    6.00
      6   .0000  298.   .0000  .0000 *   .8389  299.   .5174  .7546    6.00
      7   .0000  362.   .0000  .0000 *   .3102  364.   .1127  .2794    6.00
```

.SUM

1_2_41.sum

Time	Time/td	Maximum	DepAvg	Wat_level	Settlem	Drain_Vol	Surf_Vol
.00	.0000	.0000	.0000	.0000	.0000	.0000	.0000
1.00	.1429	.9580	.8883	.0000	.0078	.0964	.0006
2.00	.2857	.9873	.9222	.0000	.0234	.2912	.0017
3.00	.4286	.9913	.9275	.0000	.0401	.4975	.0029
4.00	.5714	.9914	.9276	.0000	.0574	.7124	.0040
5.00	.7143	.9917	.9288	.0000	.0751	.9324	.0052
6.00	.8571	.9917	.9288	.0000	.0933	1.1592	.0064
7.00	1.0000	.9784	.8831	.0000	.1094	1.3592	.0075
8.00	1.1429	.9550	.8486	.0000	.1223	1.5188	.0086
9.00	1.2857	.9241	.8136	.0000	.1329	1.6505	.0096
10.00	1.4286	.8900	.7803	.0000	.1415	1.7573	.0106
11.00	1.5714	.8545	.7467	.0000	.1487	1.8454	.0116
12.00	1.7143	.8183	.7139	.0000	.1545	1.9176	.0125
13.00	1.8571	.7821	.6812	.0000	.1594	1.9773	.0134
14.00	2.0000	.7461	.6492	.0000	.1634	2.0268	.0142
15.00	2.1429	.7106	.6177	.0000	.1668	2.0681	.0150
16.00	2.2857	.6757	.5870	.0000	.1696	2.1026	.0158
17.00	2.4286	.6417	.5570	.0000	.1720	2.1316	.0165
18.00	2.5714	.6085	.5279	.0000	.1740	2.1561	.0172
19.00	2.7143	.5764	.4997	.0000	.1757	2.1769	.0178
20.00	2.8571	.5453	.4726	.0000	.1772	2.1946	.0184
21.00	3.0000	.5153	.4464	.0000	.1784	2.2097	.0190
22.00	3.1429	.4865	.4212	.0000	.1795	2.2227	.0196
23.00	3.2857	.4588	.3971	.0000	.1804	2.2338	.0201
24.00	3.4286	.4324	.3740	.0000	.1812	2.2435	.0206
25.00	3.5714	.4071	.3520	.0000	.1819	2.2518	.0210
26.00	3.7143	.3829	.3310	.0000	.1826	2.2591	.0214
27.00	3.8571	.3599	.3110	.0000	.1831	2.2654	.0219
28.00	4.0000	.3381	.2921	.0000	.1836	2.2709	.0222
29.00	4.1429	.3173	.2741	.0000	.1840	2.2757	.0226
30.00	4.2857	.2976	.2570	.0000	.1844	2.2800	.0229
31.00	4.4286	.2790	.2408	.0000	.1847	2.2837	.0232
32.00	4.5714	.2614	.2256	.0000	.1850	2.2870	.0235
33.00	4.7143	.2447	.2112	.0000	.1852	2.2898	.0238
34.00	4.8571	.2290	.1976	.0000	.1854	2.2924	.0241
35.00	5.0000	.2142	.1848	.0000	.1856	2.2946	.0243
36.00	5.1429	.2003	.1727	.0000	.1858	2.2966	.0245
37.00	5.2857	.1872	.1613	.0000	.1860	2.2984	.0247
38.00	5.4286	.1748	.1507	.0000	.1861	2.3000	.0249
39.00	5.5714	.1632	.1407	.0000	.1862	2.3014	.0251
40.00	5.7143	.1523	.1313	.0000	.1864	2.3026	.0253
41.00	5.8571	.1421	.1224	.0000	.1865	2.3037	.0254
42.00	6.0000	.1326	.1142	.0000	.1865	2.3047	.0256
43.00	6.1429	.1236	.1064	.0000	.1866	2.3056	.0257
44.00	6.2857	.1152	.0992	.0000	.1867	2.3064	.0259
45.00	6.4286	.1073	.0924	.0000	.1868	2.3071	.0260
46.00	6.5714	.1000	.0861	.0000	.1868	2.3077	.0261
47.00	6.7143	.0931	.0801	.0000	.1869	2.3083	.0262
48.00	6.8571	.0866	.0746	.0000	.1869	2.3088	.0263
49.00	7.0000	.0806	.0694	.0000	.1870	2.3093	.0264

65	62.00	8.8571	.0311	.0267	.0000	.1873	2.3124	.0271
66	63.00	9.0000	.0289	.0248	.0000	.1873	2.3125	.0272
67	64.00	9.1429	.0268	.0230	.0000	.1873	2.3126	.0272
68	65.00	9.2857	.0249	.0214	.0000	.1873	2.3127	.0272
69	66.00	9.4286	.0231	.0198	.0000	.1873	2.3128	.0272
70	67.00	9.5714	.0214	.0184	.0000	.1873	2.3129	.0273
71	68.00	9.7143	.0199	.0171	.0000	.1873	2.3130	.0273
72	69.00	9.8571	.0184	.0158	.0000	.1874	2.3130	.0273
73	70.00	10.0000	.0171	.0147	.0000	.1874	2.3131	.0273
74	71.00	10.1429	.0158	.0136	.0000	.1874	2.3132	.0273
75	72.00	10.2857	.0147	.0126	.0000	.1874	2.3132	.0274
76	73.00	10.4286	.0136	.0117	.0000	.1874	2.3133	.0274
77	74.00	10.5714	.0126	.0109	.0000	.1874	2.3133	.0274
78	75.00	10.7143	.0117	.0101	.0000	.1874	2.3133	.0274
79	76.00	10.8571	.0109	.0093	.0000	.1874	2.3134	.0274
80	77.00	11.0000	.0101	.0086	.0000	.1874	2.3134	.0274
81	78.00	11.1429	.0093	.0080	.0000	.1874	2.3134	.0274
82	79.00	11.2857	.0086	.0074	.0000	.1874	2.3135	.0274
83	80.00	11.4286	.0080	.0069	.0000	.1874	2.3135	.0274
84	81.00	11.5714	.0074	.0064	.0000	.1874	2.3135	.0275
85	82.00	11.7143	.0069	.0059	.0000	.1874	2.3135	.0275
86	83.00	11.8571	.0064	.0055	.0000	.1874	2.3136	.0275
87	84.00	12.0000	.0059	.0051	.0000	.1874	2.3136	.0275
88	85.00	12.1429	.0055	.0047	.0000	.1874	2.3136	.0275
89	86.00	12.2857	.0051	.0044	.0000	.1874	2.3136	.0275
90	87.00	12.4286	.0047	.0040	.0000	.1874	2.3136	.0275
91	88.00	12.5714	.0044	.0037	.0000	.1874	2.3136	.0275
92	89.00	12.7143	.0040	.0035	.0000	.1874	2.3136	.0275
93	90.00	12.8571	.0037	.0032	.0000	.1874	2.3137	.0275
94	91.00	13.0000	.0035	.0030	.0000	.1874	2.3137	.0275
95	92.00	13.1429	.0032	.0028	.0000	.1874	2.3137	.0275
96	93.00	13.2857	.0030	.0025	.0000	.1874	2.3137	.0275
97	94.00	13.4286	.0027	.0024	.0000	.1874	2.3137	.0275
98	95.00	13.5714	.0025	.0022	.0000	.1874	2.3137	.0275
99	96.00	13.7143	.0024	.0020	.0000	.1874	2.3137	.0275
100	97.00	13.8571	.0022	.0019	.0000	.1874	2.3137	.0275
101	98.00	14.0000	.0020	.0017	.0000	.1874	2.3137	.0275
102	99.00	14.1429	.0019	.0016	.0000	.1874	2.3137	.0275
103	100.00	14.2857	.0017	.0015	.0000	.1874	2.3137	.0275
104	100.00	14.2857	.0017	.0015	.0000	.1874	2.3137	.0275
105								

Cummulative Values

106	Layer	Maximum	Node	LayAvg	DepAvg	Time
107	1	.9917	26.	.6887	.9288	6.00
108	2	.9812	39.	.8636	.9087	6.00
109	3	.9427	104.	.8451	.8555	6.00
110	4	.9257	169.	.8156	.8369	6.00
111	5	.8823	234.	.7622	.7938	6.00
112	6	.8389	299.	.5174	.7546	6.00
113	7	.3102	364.	.1127	.2794	6.00

APPENDIX C. PARENT STUDY R_U PLOTS

These plots of applied acceleration and measured excess pore pressure ratio come from the laminar shear box testing done by Oakes (2015), and are the foundation of this modeling effort. The figures are presented in chronological order of when testing occurred.

C.1 4ft Spacing

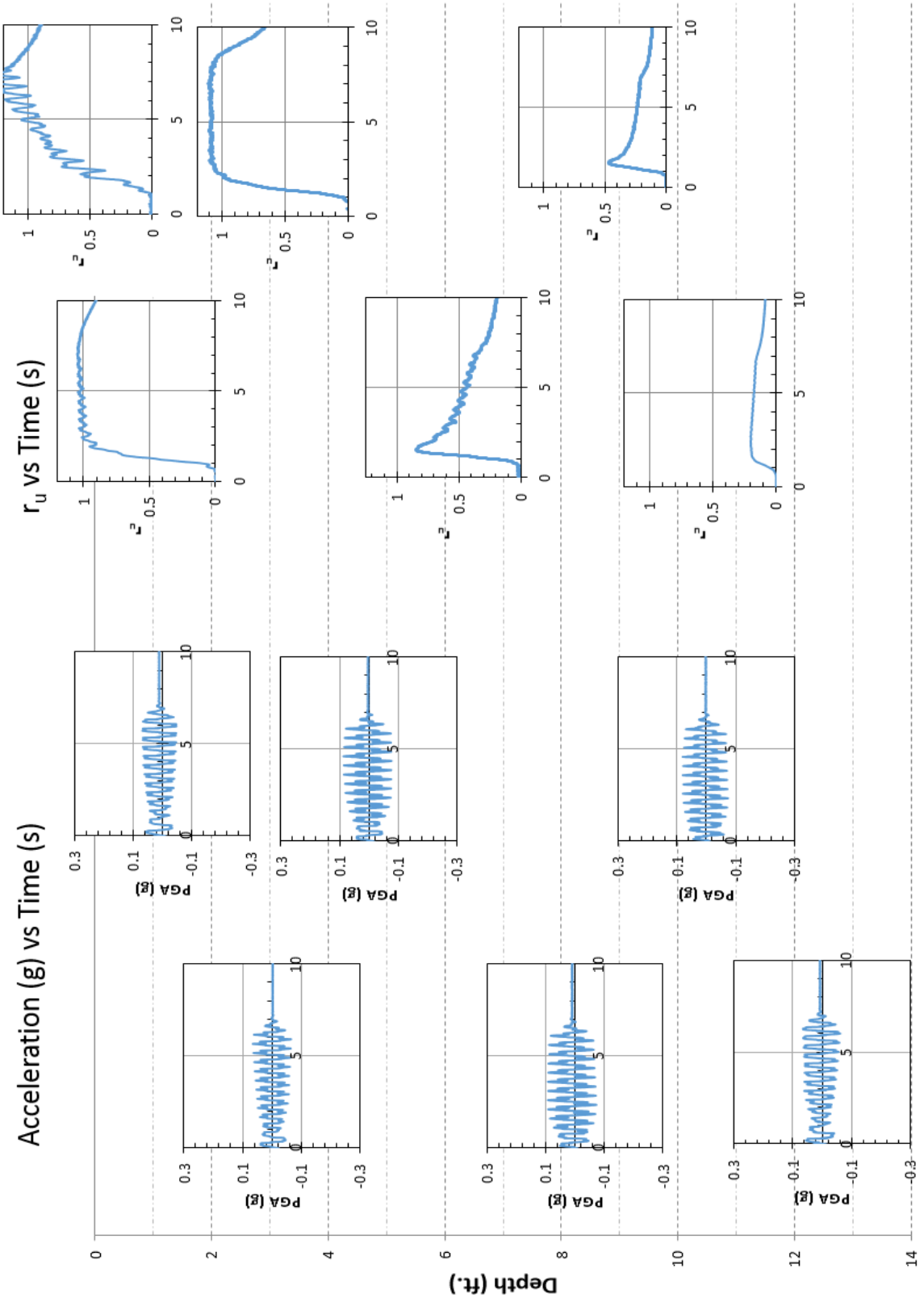

Figure C-1: Acceleration vs. Time Paired with Excess Pore Pressure Ratio vs. Time for Round 1, a_{max} = 0.05

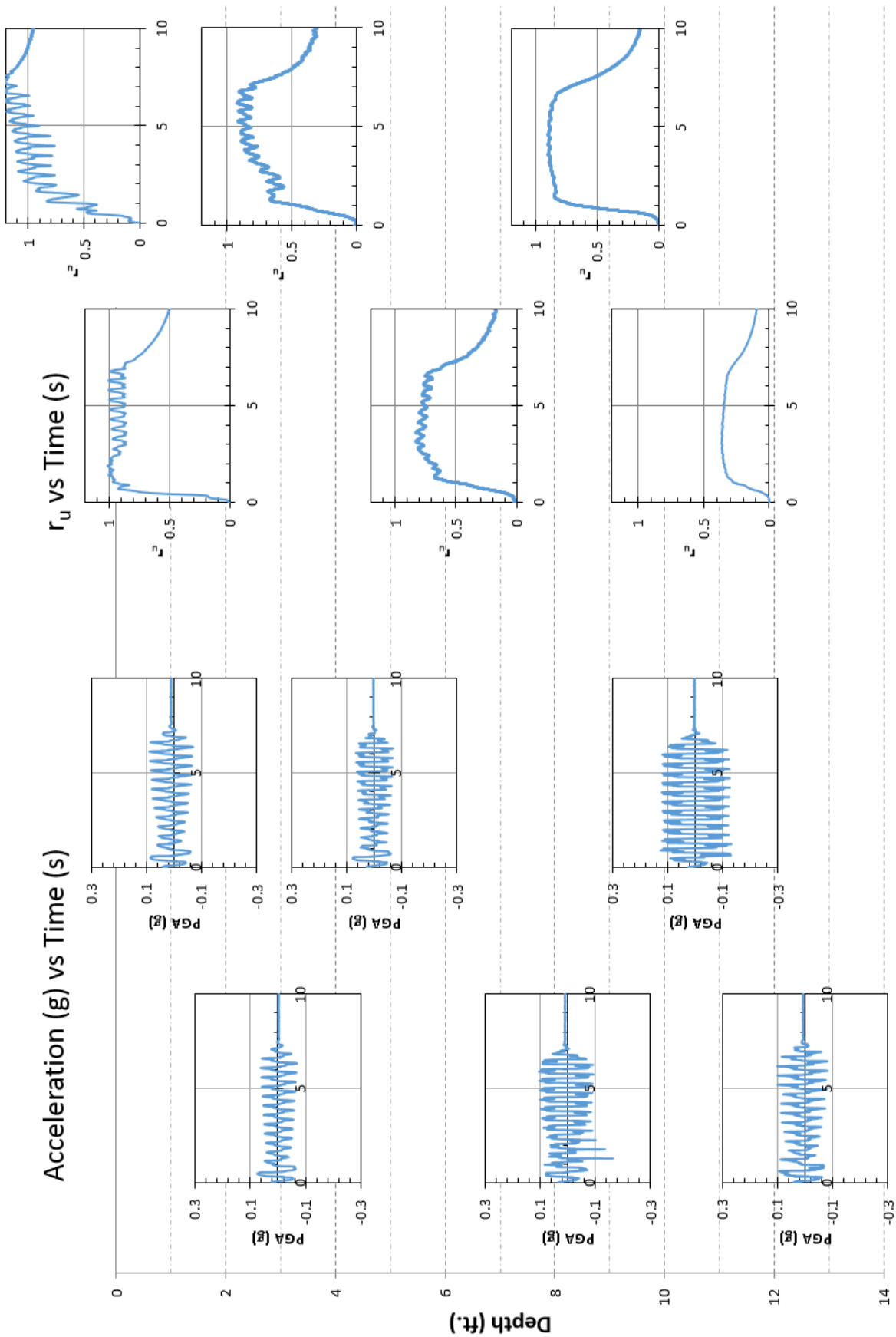

Figure C-2: Acceleration vs. Time Paired with Excess Pore Pressure Ratio vs. Time for Round 1, a_{max} = 0.1g

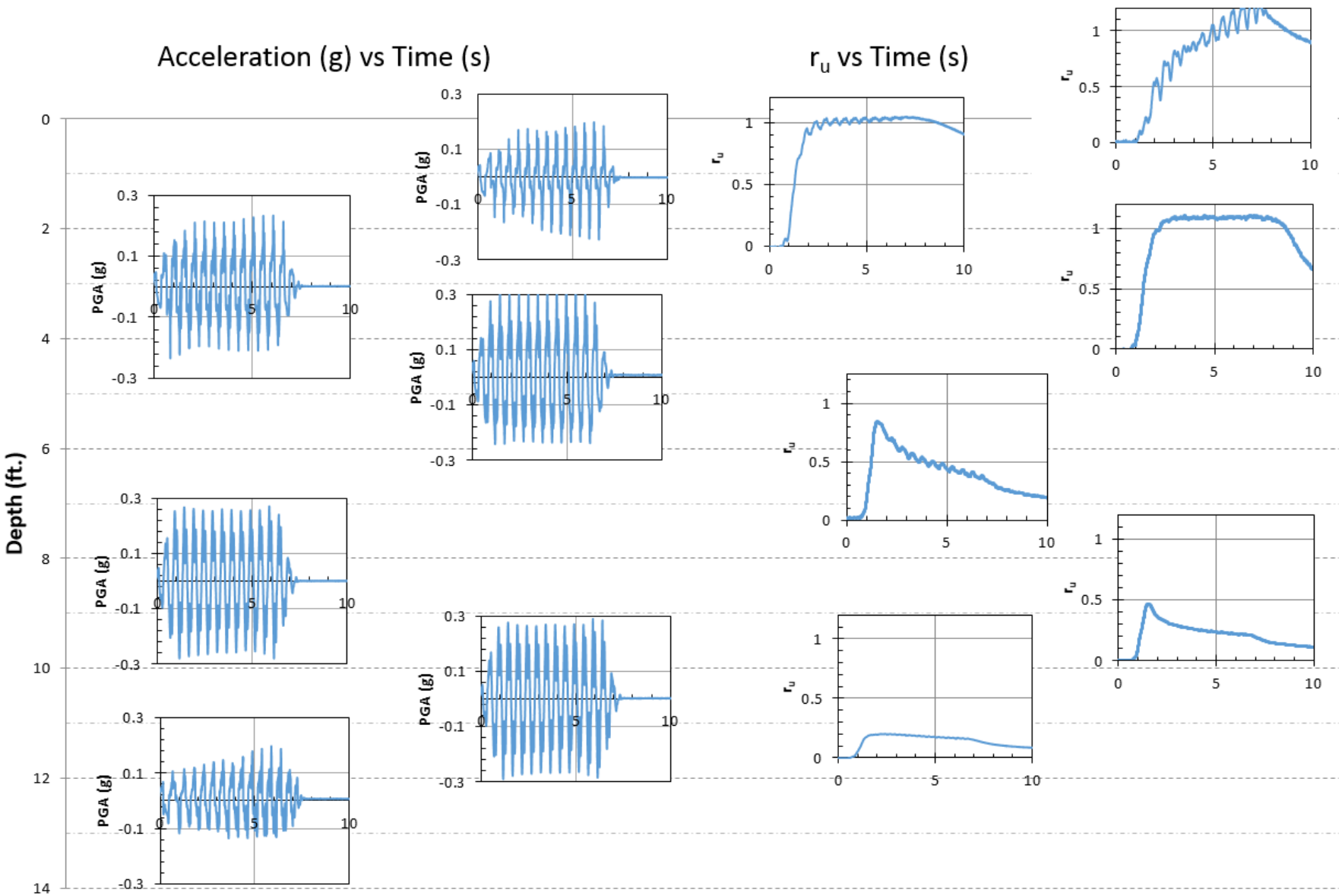

Figure C-3: Acceleration vs. Time Paired with Excess Pore Pressure Ratio vs. Time for Round 1, a_{max} = 0.2g

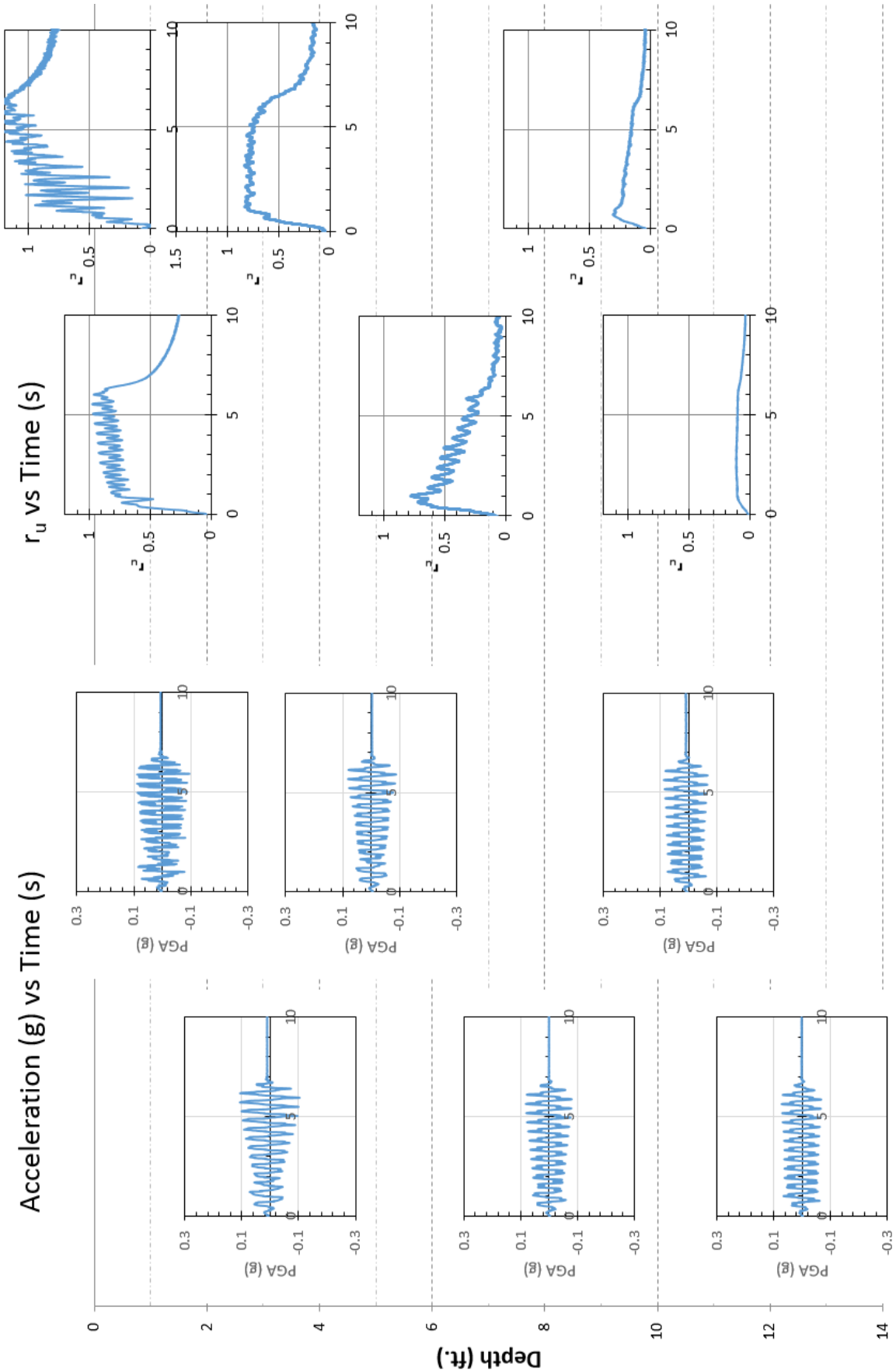

Figure C-4: Acceleration vs. Time Paired with Excess Pore Pressure Ratio vs. Time for Round 2, a_{max} = 0.05g

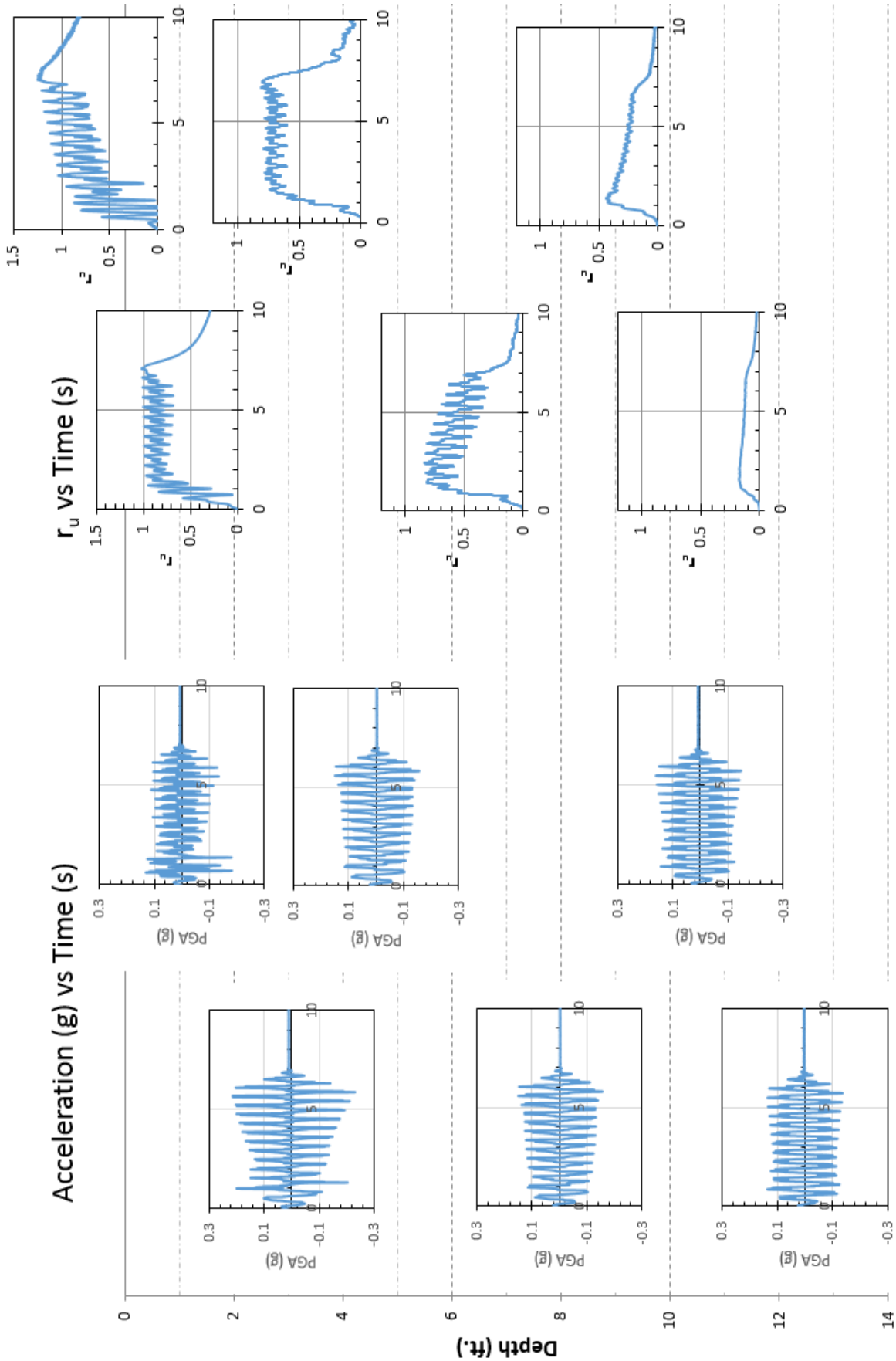

Figure C-5: Acceleration vs. Time Paired with Excess Pore Pressure Ratio vs. Time for Round 2, a_{max} = 0.1g

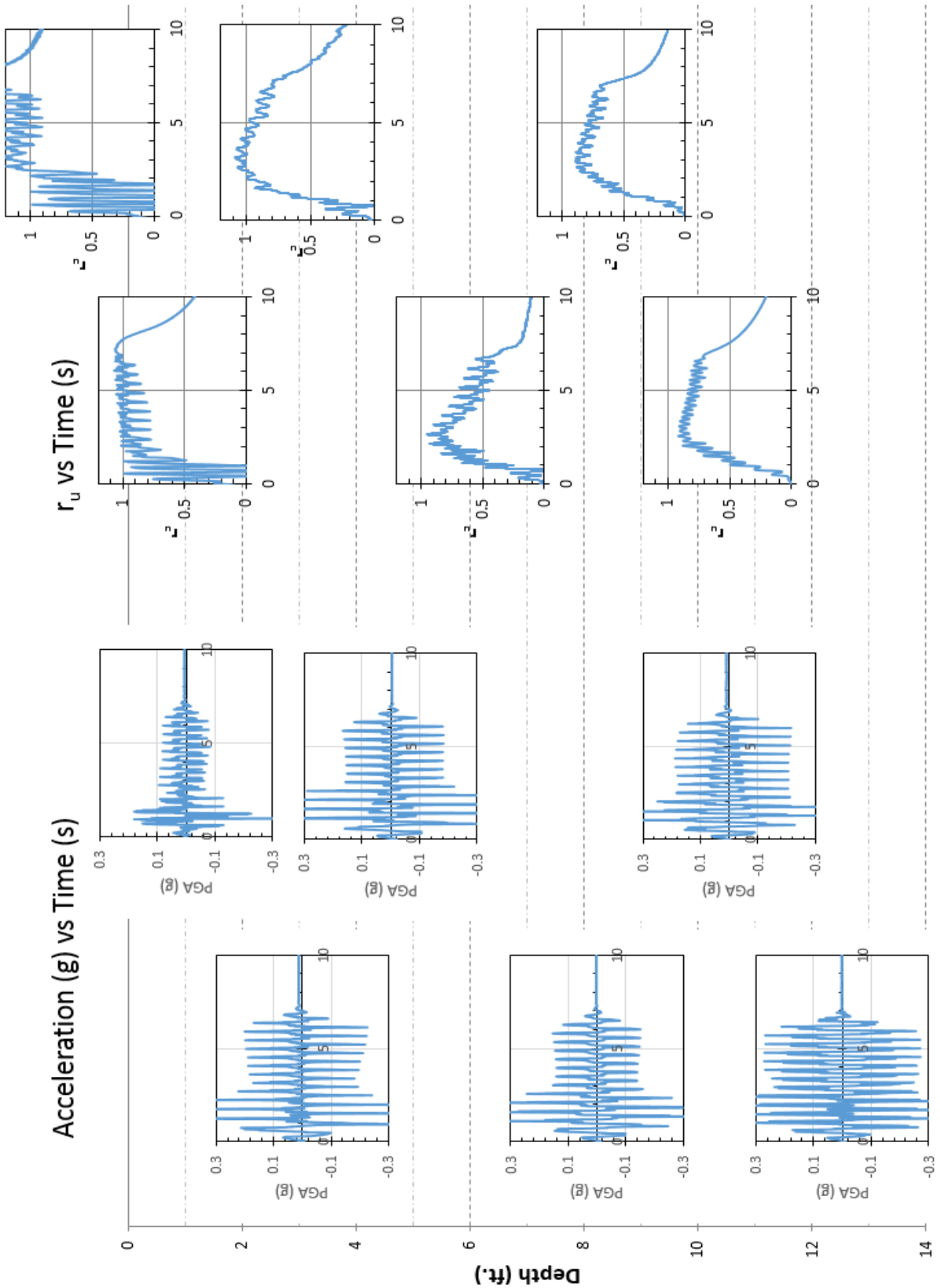

Figure C-6: Acceleration vs. Time Paired with Excess Pore Pressure Ratio vs. Time for Round 2, a_{max} = 0.2g

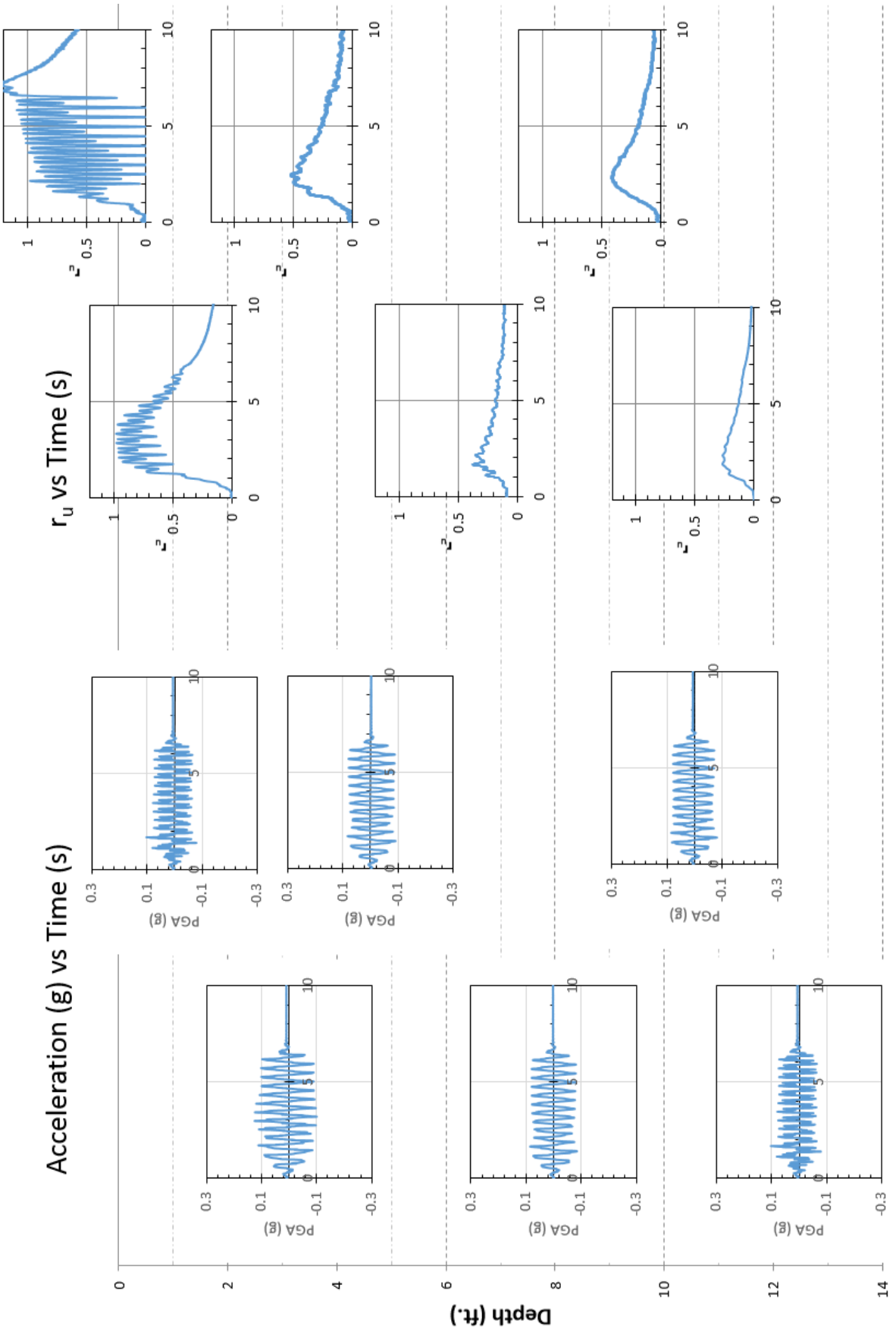

Figure C-7: Acceleration vs. Time Paired with Excess Pore Pressure Ratio vs. Time for Round 3, a_{max} = 0.05

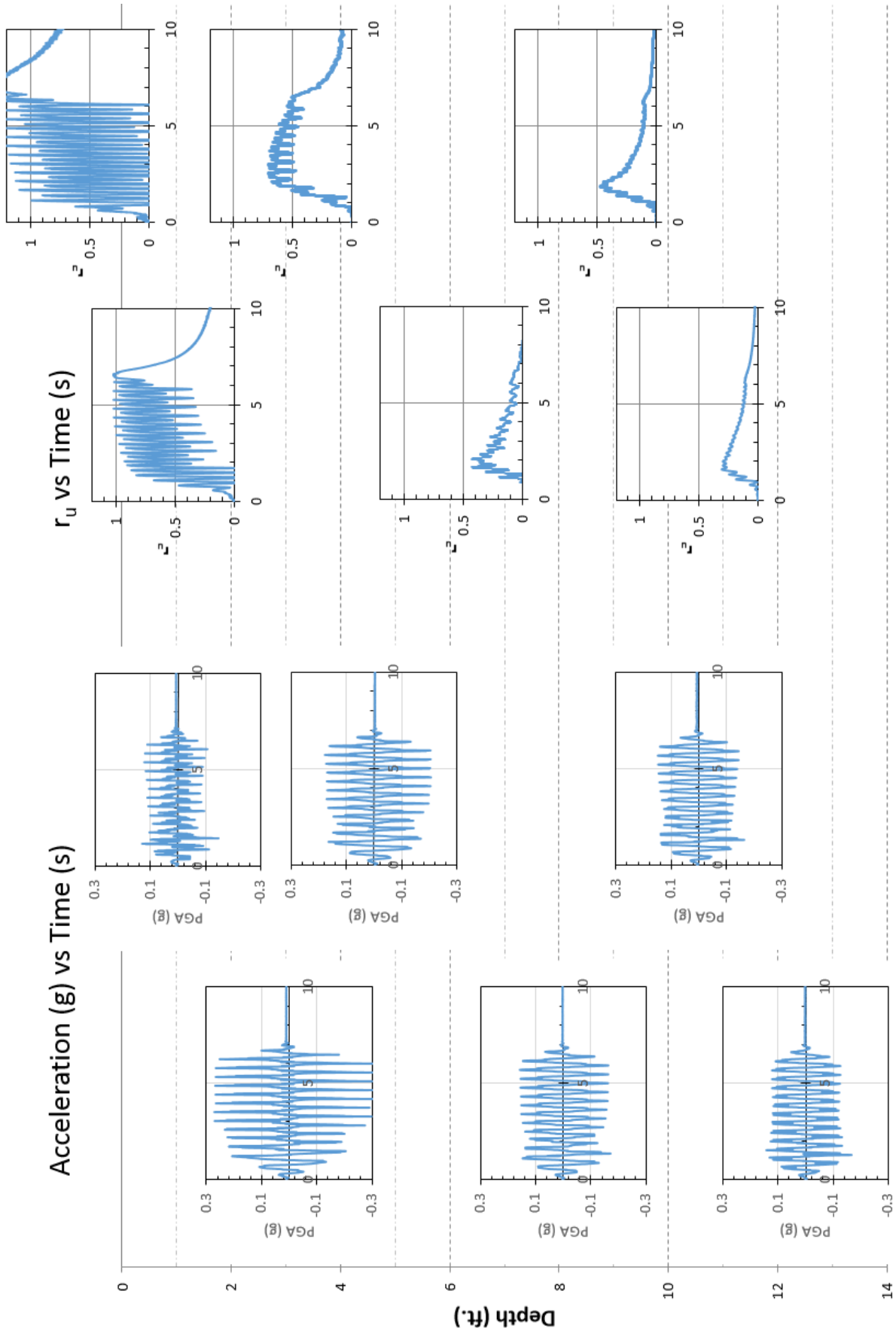

Figure C-8: Acceleration vs. Time Paired with Excess Pore Pressure Ratio vs. Time for Round 3, a_{max} = 0.1g

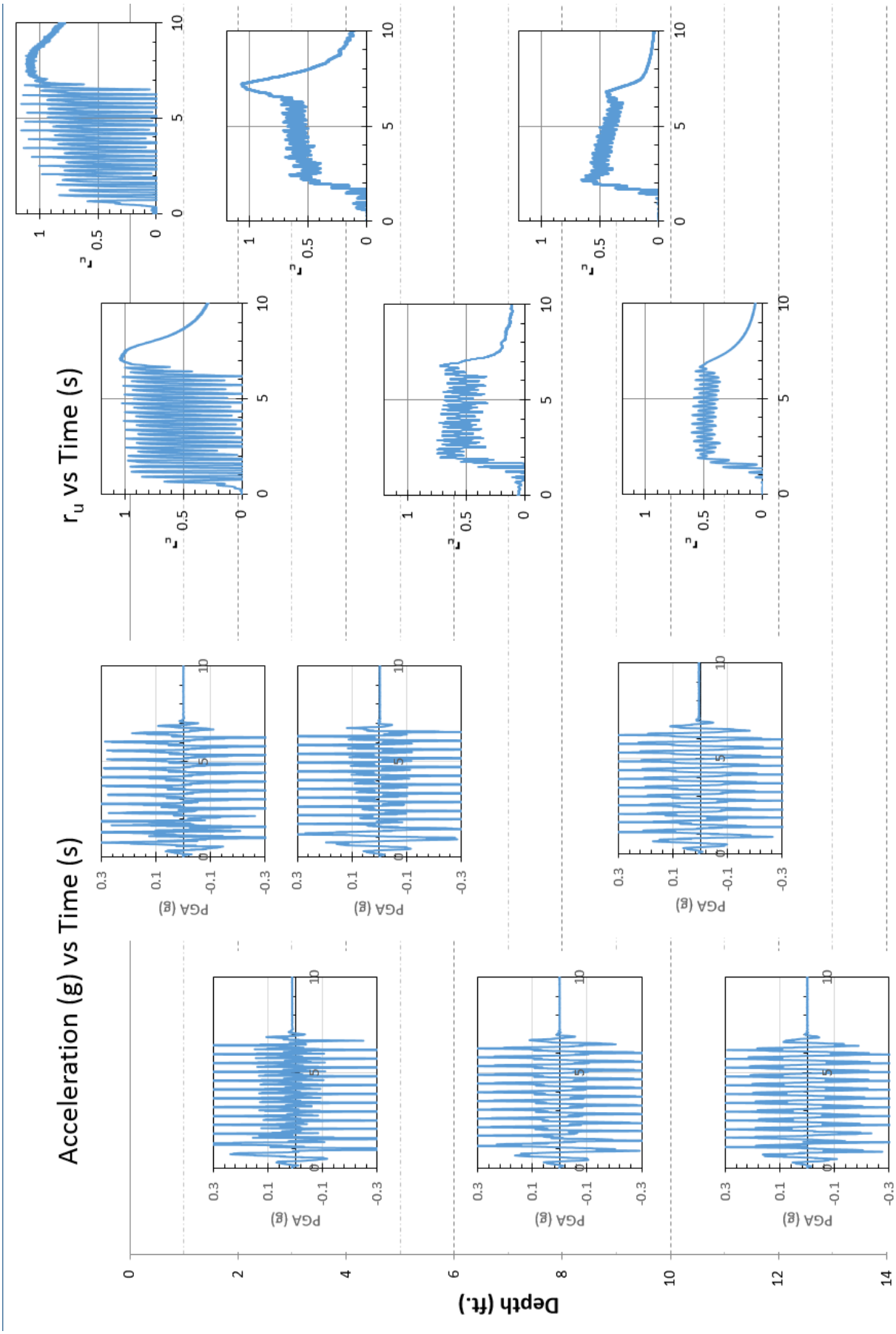

Figure C-9: Acceleration vs. Time Paired with Excess Pore Pressure Ratio vs. Time for Round 3, a_{max} = 0.2g

C.2 3ft Spacing

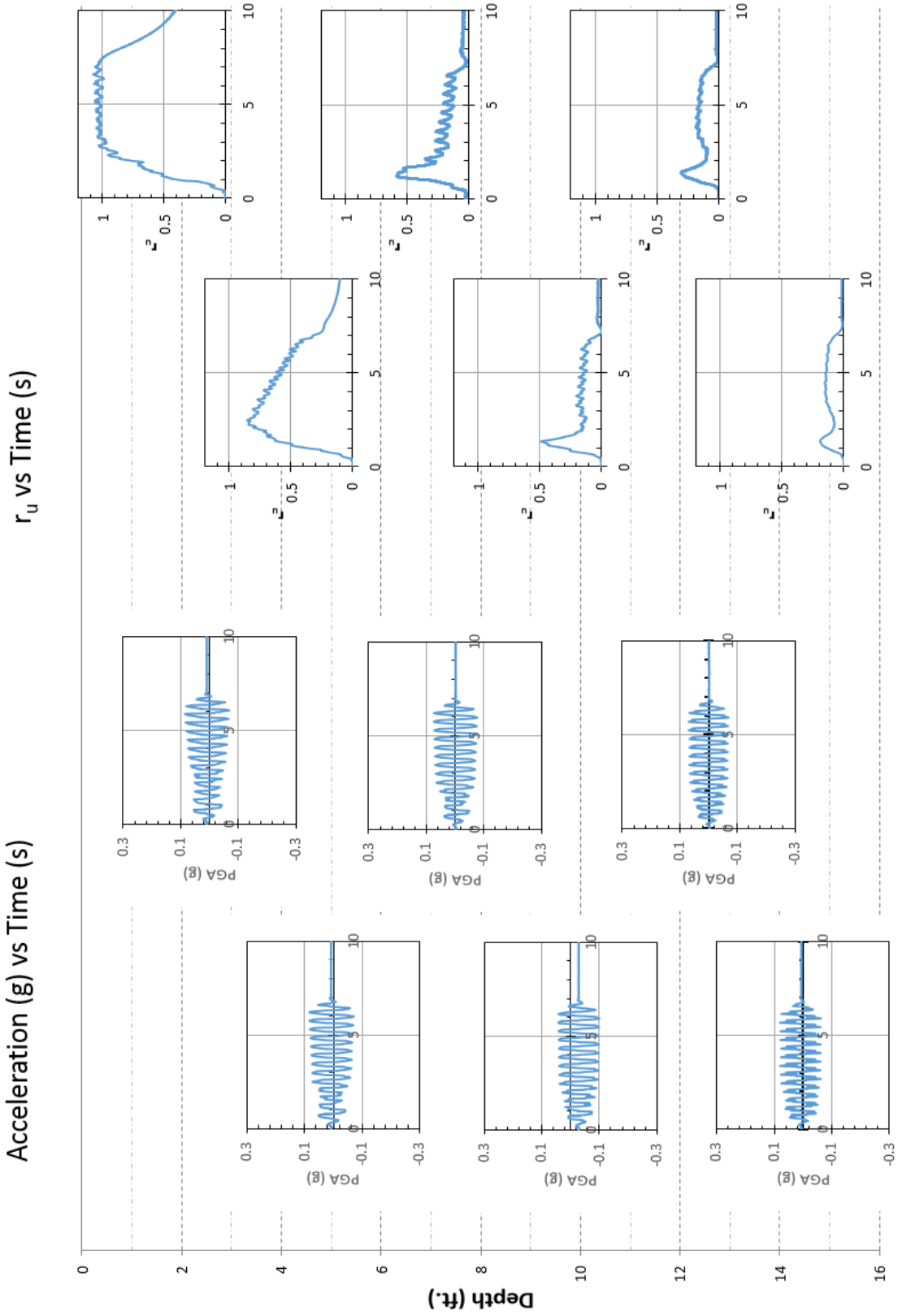

Figure C-10: Acceleration vs. Time Paired with Excess Pore Pressure Ratio vs. Time for Round 1, a_{max} = 0.05g

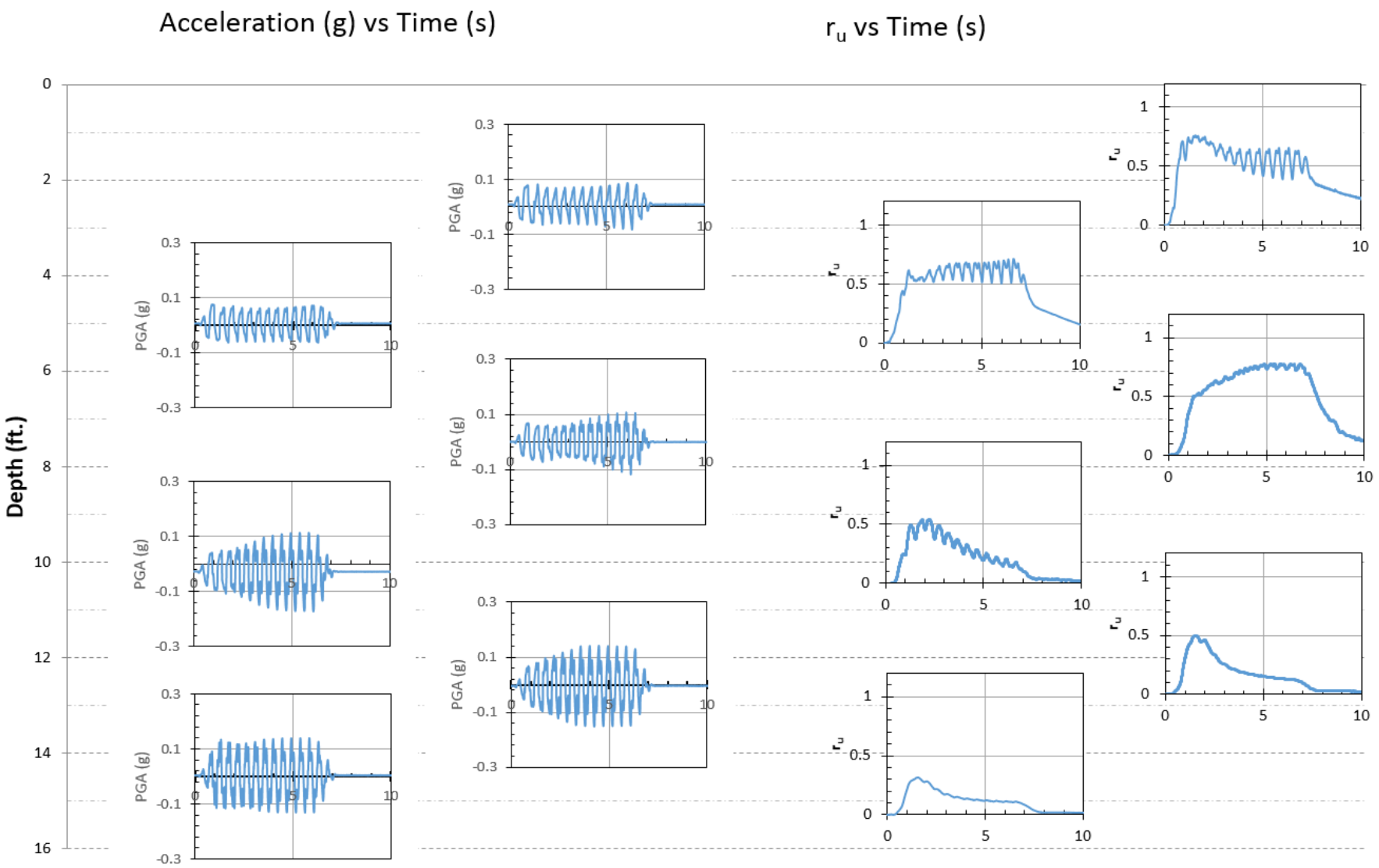

Figure C-11: Acceleration vs. Time Paired with Excess Pore Pressure Ratio vs. Time for Round 1, a_{max} = 0.1g

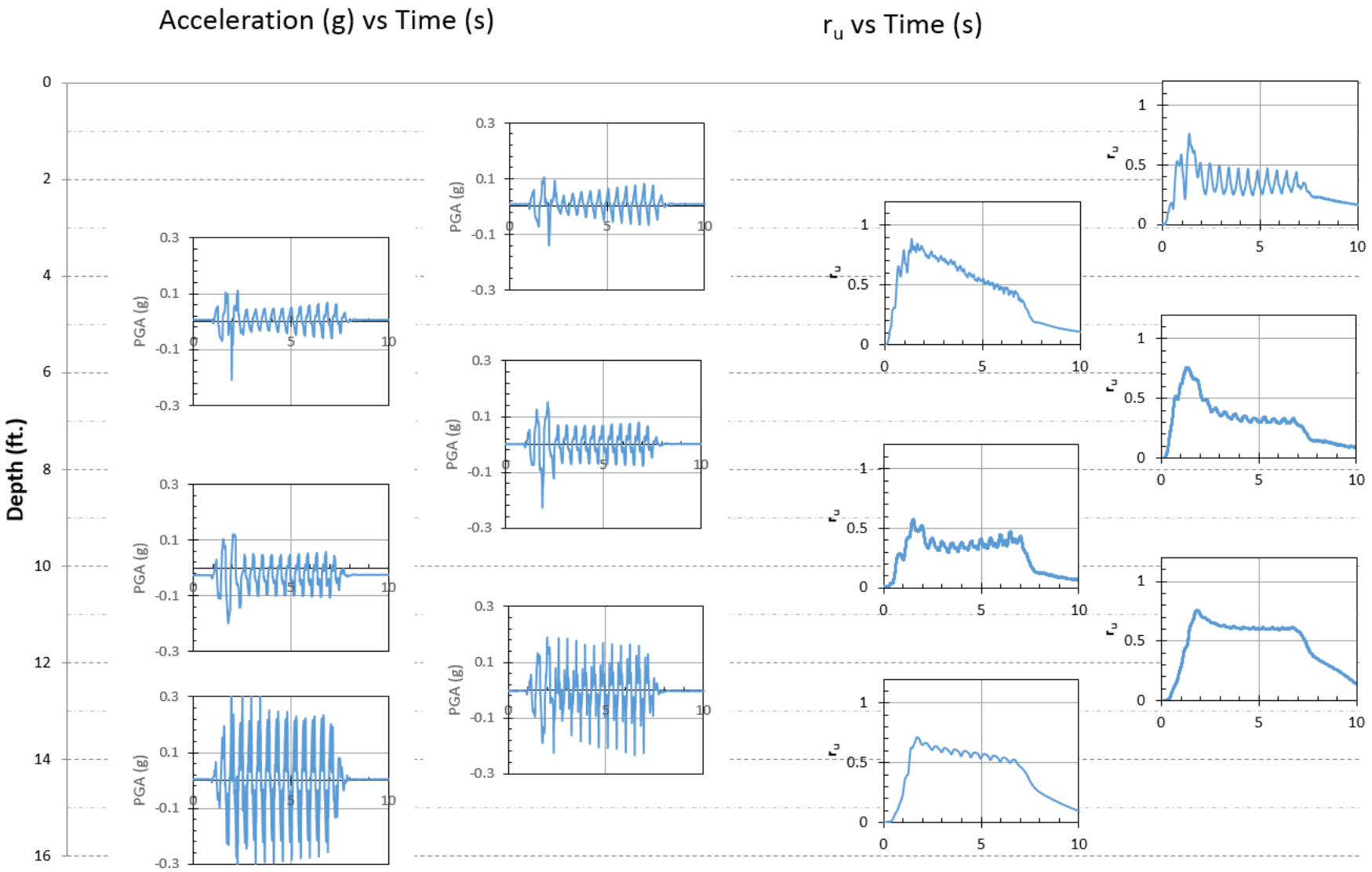

Figure C-12: Acceleration vs. Time Paired with Excess Pore Pressure Ratio vs. Time for Round 1, a_{max} = 0.2g

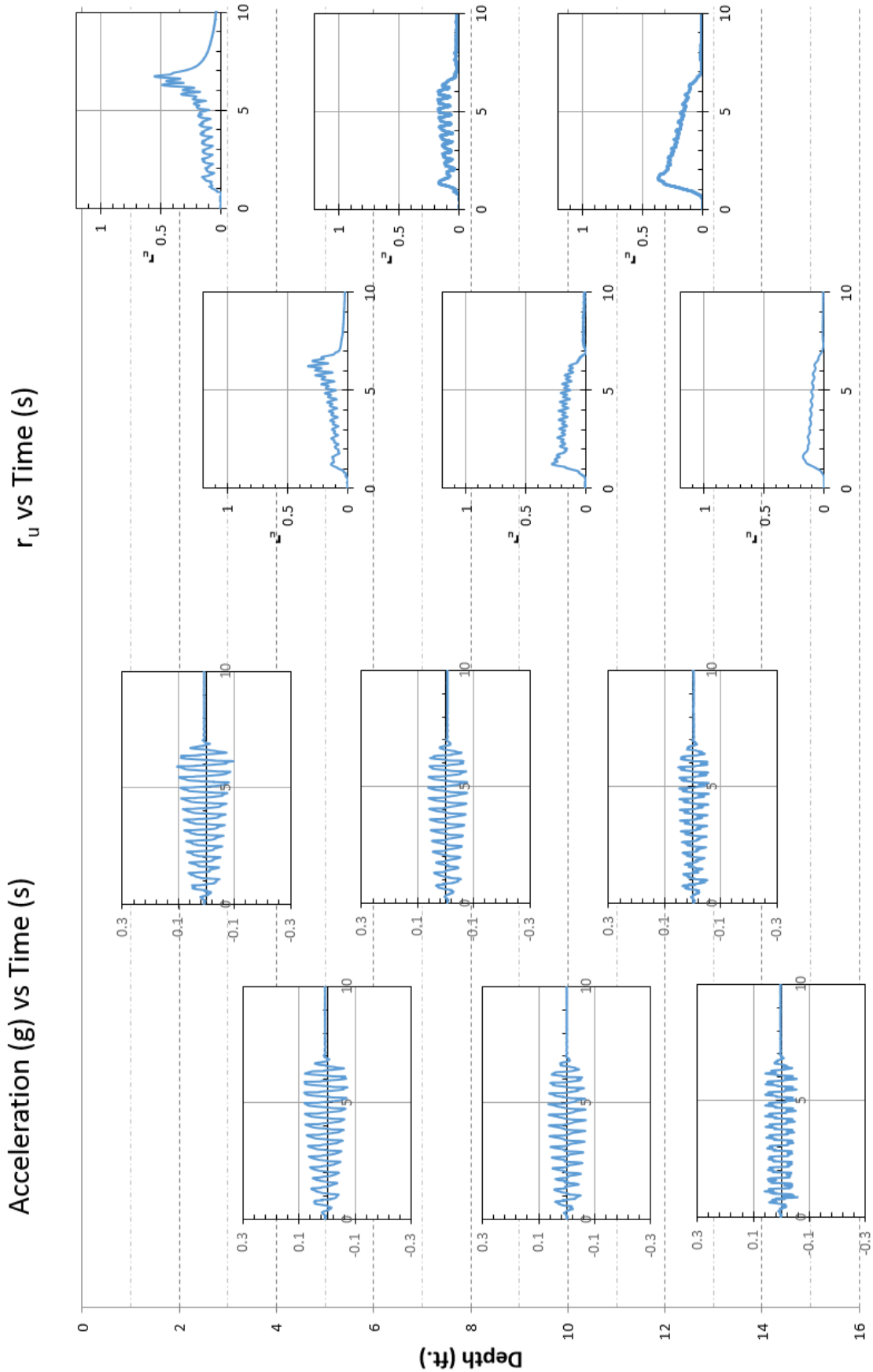

Figure C-13: Acceleration vs. Time Paired with Excess Pore Pressure Ratio vs. Time for Round 2, a_{max} = 0.05g

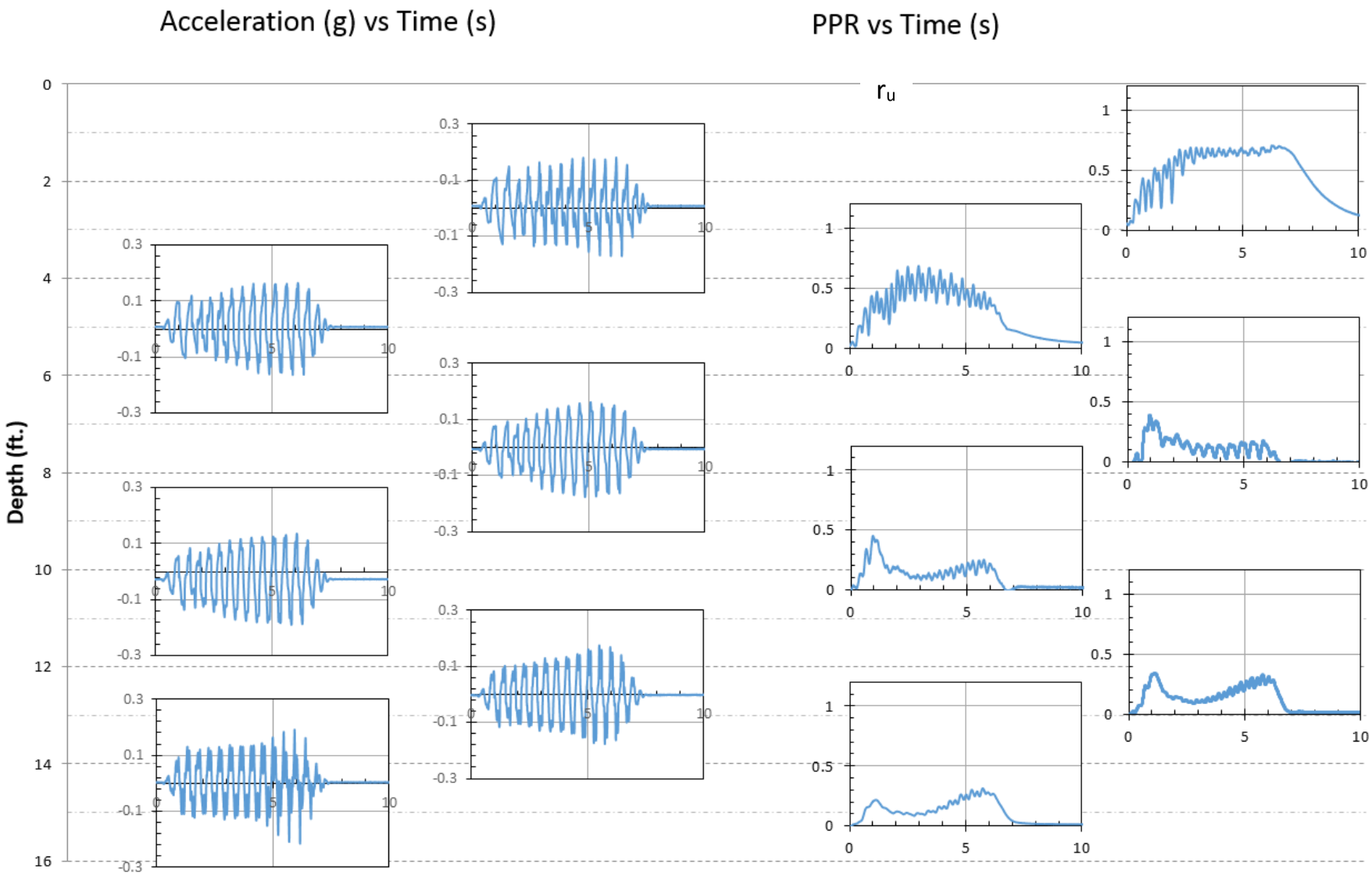

Figure C-14: Acceleration vs. Time Paired with Excess Pore Pressure Ratio vs. Time for Round 2, a_{max} = 0.1g

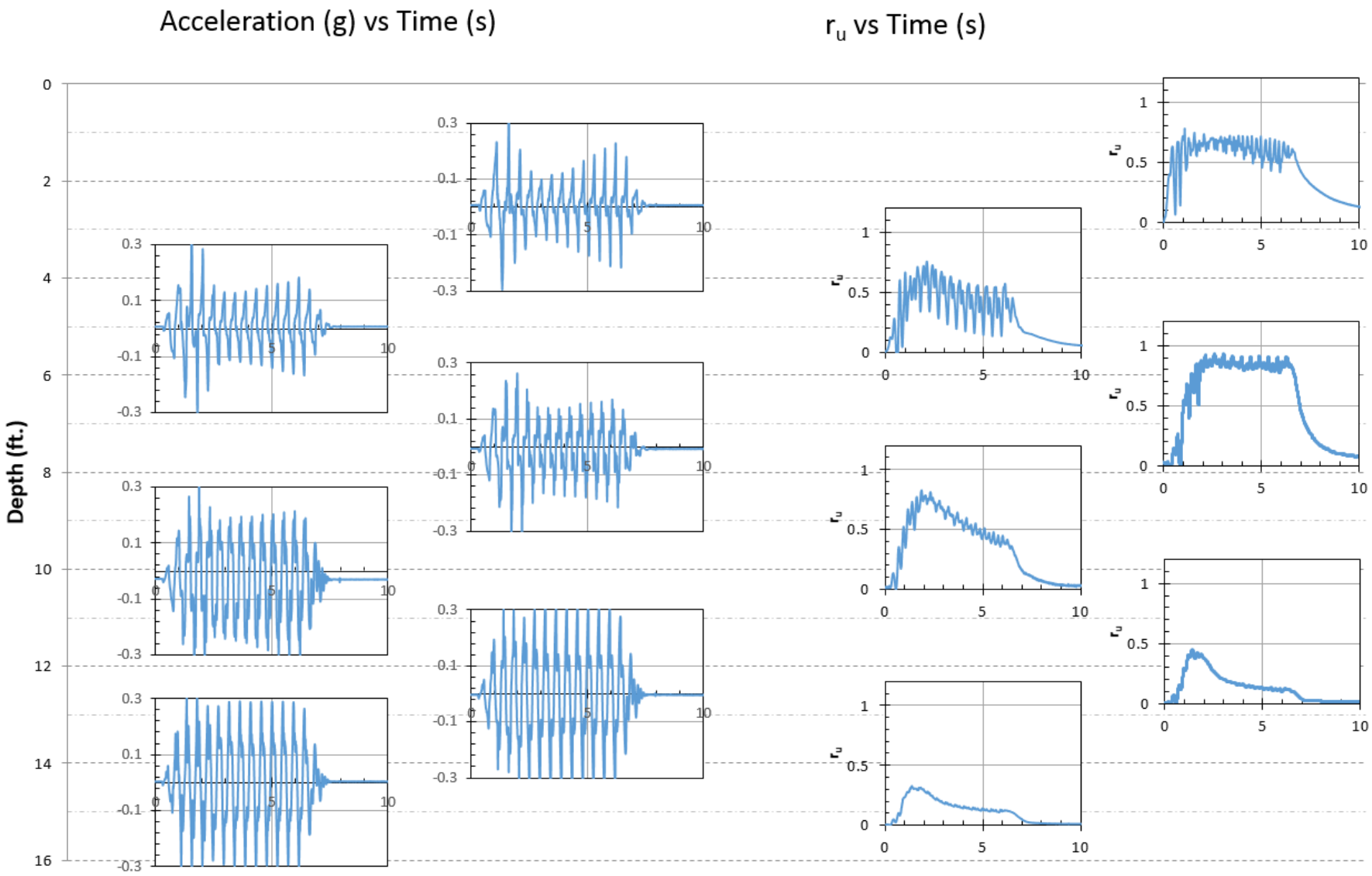

Figure C-15: Acceleration vs. Time Paired with Excess Pore Pressure Ratio vs. Time for Round 2, a_{max} = 0.2g

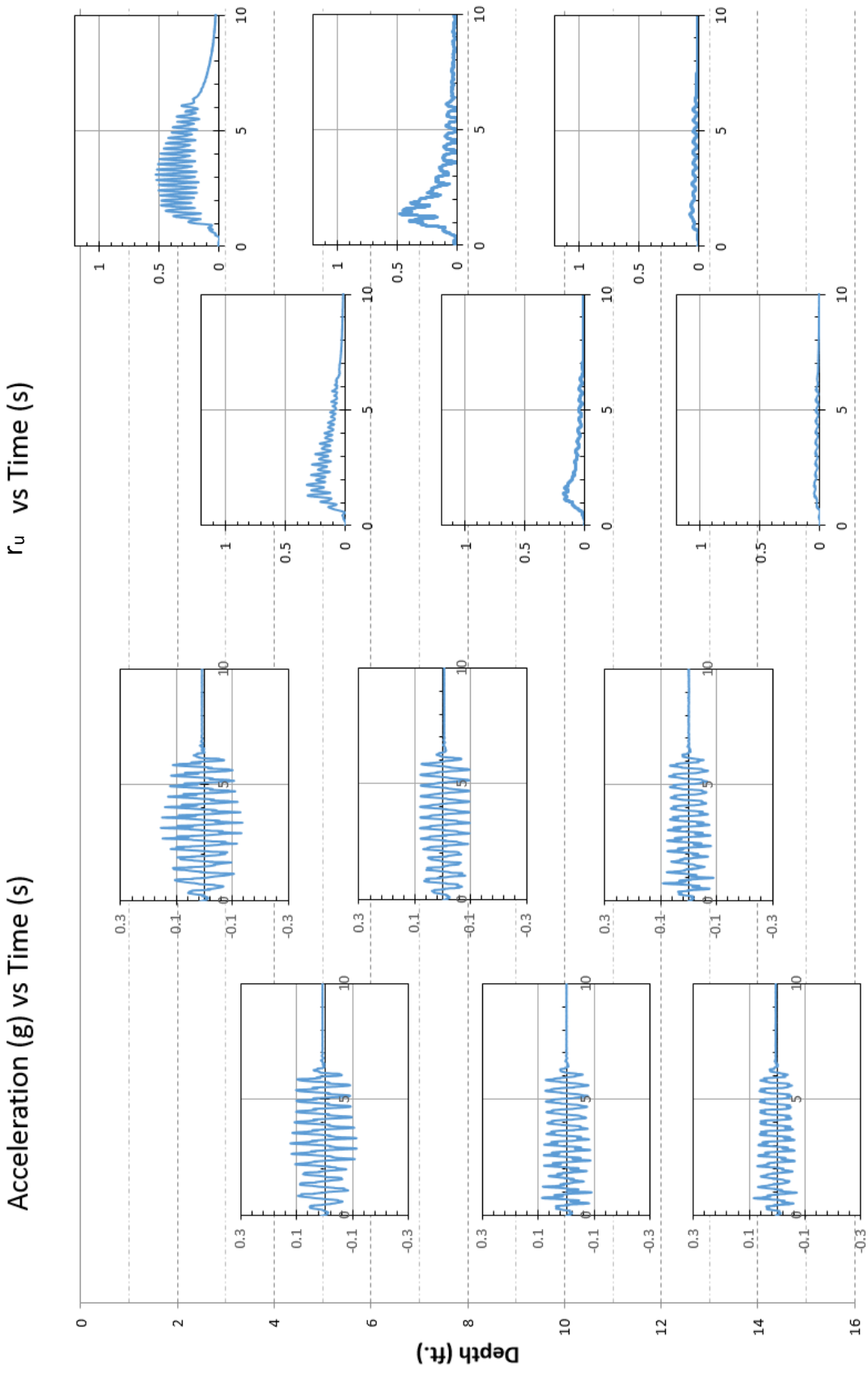

Figure C-16: Acceleration vs. Time Paired with Excess Pore Pressure Ratio vs. Time for Round 3, a_{max} = 0.05g

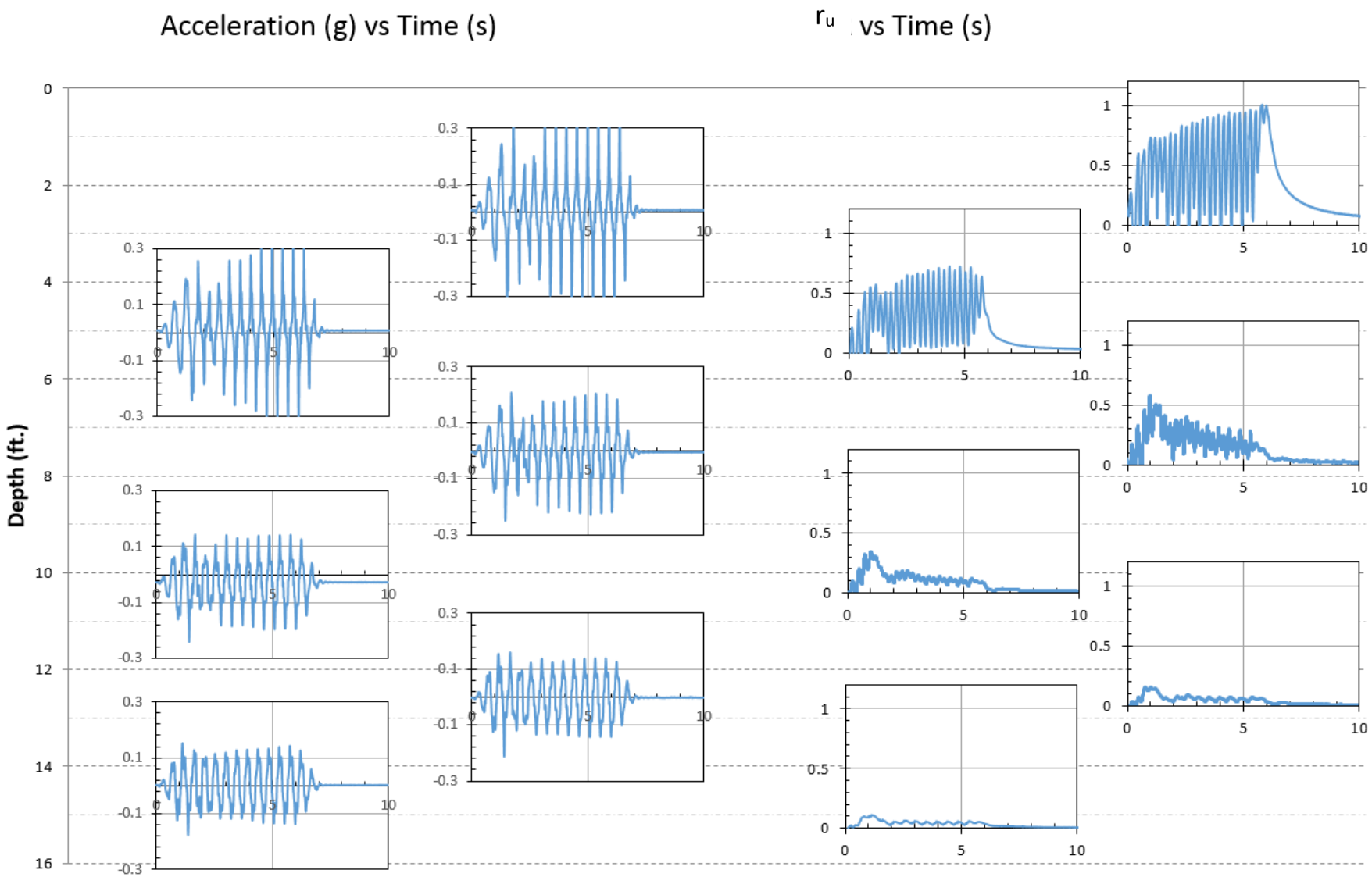

Figure C-17: Acceleration vs. Time Paired with Excess Pore Pressure Ratio vs. Time for Round 3, a_{max} = 0.1g

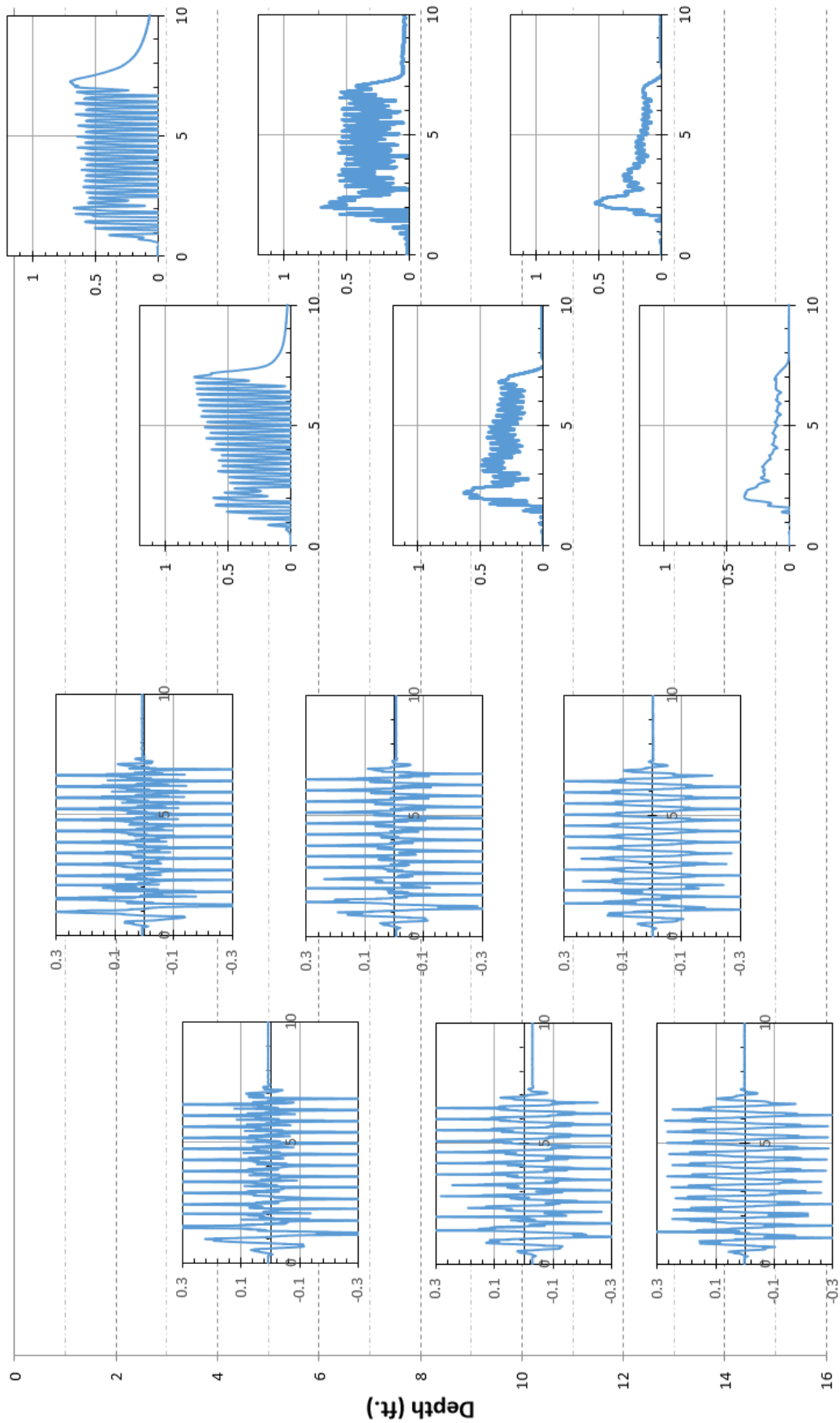

Figure C-18 Acceleration vs. Time Paired with Excess Pore Pressure Ratio vs. Time for Round 3, a_{max} = 0.2g

APPENDIX D. SOIL COMPRESSIBILITY

					H_{solids} (in)			0.0167344		
		Red in these columns indicate potential outliers.			101.5464					
Round	Depth (ft) (see Fig.38,39,40)	r_u (see_Fig.38, 39,40)	Volumetric Strain ($\Delta\varepsilon$) (see Fig.59,60,61)	Prior Settlement (in) (see Table.9)	H_{voids} (in) (portion of H_{total})	e_{new}	$\gamma_{sat\ new}$ (pcf) (from e_{new})	$D_{r\ new}$ (from e_{new})	$\Delta\sigma'$	$m_v = \Delta\varepsilon/\Delta\sigma'$
1.05	2.5	1	1.45	Prior					150.2	0.0097
	4.5	1	1.45	0	72.5	0.714	122.5	0.45	270.4	0.0054
	7.5	0.9	1.1						405.6	0.0027
	10	0.48	0.5	This round					288.4	0.0017
	12.5	0.2	0.3	1.89					150.2	0.0020
1.1	2.5	1	0.8	Prior					151.9	0.0053
	4.5	0.78	1.1	1.89	70.6	0.695	123.1	0.55	213.2	0.0052
	7.5	**0.57**	1.1						259.7	0.0042
	10	0.67	**1.8**	This round					407.0	0.0044
	12.5	0.27	1.4	2.03					205.0	0.0068
1.2	2.5	1	1.75	Prior					153.7	0.0114
	4.5	0.83	1.9	3.92	68.5	0.675	123.9	0.65	229.6	0.0083
	7.5	0.94	1.6						433.4	0.0037
	10	0.91	1.45	This round					559.4	0.0026
	12.5	0.56	1.4	2.64					430.3	0.0033
2.05	2.5	1	0.75	Prior					156.1	0.0048
	4.5	1	0.5	6.56	65.9	0.6489	124.8	0.79	281.0	0.0018
	7.5	0.96	0.75						449.6	0.0017
	10	0.55	0.4	This round					343.4	0.0012
	12.5	0.25	0.2	0.9					195.1	0.0010
2.1	2.5	1	1.05	Prior					156.9	0.0067
	4.5	1	0.85	7.46	65.0	0.64	125.2	0.83	282.5	0.0030
	7.5	0.98	1.3						461.4	0.0028
	10	0.65	0.2	This round					408.1	0.0005
	12.5	0.45	0.22	1.22					353.1	0.0006
2.2	2.5	1	0.2	Prior					158.1	0.0013
	4.5	1	0.4	8.68	63.8	0.628	125.6	0.90	284.6	0.0014
	7.5	1	0.25						474.3	0.0005
	10	0.97	1.25	This round					613.5	0.0020
	12.5	0.94	**3.4**	1.39					743.1	0.0046
3.05	2.5	0.96	0.4	Prior					153.1	0.0026
	4.5	0.55	0.1	10.07	62.4	0.614	126.2	0.97	157.9	0.0006
	7.5	0.42	0.2						200.9	0.0010
	10	0.43	0.1	This round					274.2	0.0004
	12.5	0.27	0.45	0.46					215.3	0.0021
3.1	2.5	0.94	0.28	Prior					150.3	0.0019
	4.5	0.69	0.2	10.53	61.9	0.610	126.4	0.99	198.6	0.0010
	7.5	0.58	0.35						278.2	0.0013
	10	0.52	**0.4**	This round					332.6	0.0012
	12.5	0.29	0.25	0.67					231.8	0.0011
3.2	2.5	1	0.6	Prior					160.6	0.0037
	4.5	0.94	0.5	11.2	61.3	0.603	126.6	1.02	271.7	0.0018
	7.5	0.83	0.7						399.8	0.0018
	10	0.69	0.9	This round					443.1	0.0020
	12.5	0.61	0.95	1.19					489.7	0.0019

				Duplicate from leftside		
$a=5(1.5-D_r)$	$b=3(4)^{-Dr}$	$y=a*r_u^{\ b}$	m_{vo}	Round	Depth (ft) (see Fig.38)	
		5.25	0.0010	1.05	2.5	
5.247	1.607	5.25	0.0006		4.5	
		4.43	0.0005		7.5	
		1.61	0.0014		10	
		0.40	0.0020		12.5	
		4.76	0.0008	1.1	2.5	
4.763	1.405	3.36	0.0018		4.5	
		2.16	0.0027		7.5	
		2.71	0.0022		10	
		0.76	0.0065		12.5	
		4.24	0.0023	1.2	2.5	
4.242	1.216	3.38	0.0028		4.5	
		3.93	0.0009		7.5	
		3.78	0.0007		10	
		2.10	0.0021		12.5	
		3.57	0.0015	2.05	2.5	
3.565	1.008	3.57	0.0005		4.5	
		3.42	0.0006		7.5	
		1.95	0.0008		10	
		0.88	0.0010		12.5	
		3.33	0.0024	2.1	2.5	
3.334	0.945	3.33	0.0011		4.5	
		3.27	0.0010		7.5	
		2.22	0.0003		10	
		1.57	0.0005		12.5	
		3.02	0.0005	2.2	2.5	
3.021	0.867	3.02	0.0006		4.5	
		3.02	0.0002		7.5	
		2.94	0.0009		10	
		2.86	0.0021		12.5	
		2.58	0.0014	3.05	2.5	
2.665	0.785	1.67	0.0005		4.5	
		1.35	0.0008		7.5	
		1.37	0.0003		10	
		0.95	0.0019		12.5	
		2.43	0.0010	3.1	2.5	
2.547	0.760	1.92	0.0007		4.5	
		1.68	0.0010		7.5	
		1.55	0.0010		10	
		0.99	0.0010		12.5	
		2.38	0.0022	3.2	2.5	
2.375	0.724	2.27	0.0011		4.5	
		2.08	0.0011		7.5	
		1.82	0.0015		10	
		1.66	0.0015		12.5